THE UNIVERSITY of TULSA

Department of Chemical Engineering

Fundamentals of Delayed Coking Joint Industry Project

ANNUAL REPORT

June 2002 through September 2003

Principal Investigators

Dr. Michael Volk, Jr. & Dr. Keith Wisecarver

600 S. College Tulsa, OK 74104

October, 2003

DOE Award DE-FC26-02NT15381

Table of Contents 2003 Annual Report
June 2002 – September 2003

Table of Figures

Table of Tables

1. Disclaimer

This report was prepared as an account of work sponsored by an agency of the United States Government. Neither the United States Government nor any agency thereof, nor any of their employees, makes any warranty, express or implied, or assumes any legal liability or responsibility for the accuracy, completeness, or usefulness of any information, apparatus, product, or process disclosed, or represents that its use would not infringe privately owned rights. Reference herein to any specific commercial product, process, or service by trade name, trademark, manufacturer, or otherwise does not necessarily constitute or imply its endorsement, recommendation, or favoring by the United States Government or any agency thereof. The views and opinions of authors expressed herein do not necessarily state or reflect those of the United States Government or any agency thereof.

2. Public Abstract

Delayed coking evolved steadily over the early to mid 1900s to enable refiners to convert high boiling, residual petroleum fractions to light products such as gasoline. Pound for pound, coking is the most energy intensive of any operation in a modern refinery. Large amounts of energy are required to heat the thick, poor-quality petroleum residuum to the 900 to 950 degrees F required to crack the heavy hydrocarbon molecules into lighter, more valuable products. One common misconception of delayed coking is that the product coke is a disadvantage. Although coke is a low valued (near zero economic value) byproduct, compared to transportation fuels, there is a significant worldwide trade and demand for coke as it is an economical fuel. Coke production has increased steadily over the last ten years, with further increases forecast for the foreseeable future. Current domestic production is near 111,000 tons per day. A major driving force behind this increase is the steady decline in crude quality available to refiners. Crude slates are expected to grow heavier with higher sulfur contents while environmental restrictions are expected to significantly reduce the demand for high-sulfur residual fuel oil. Light sweet crudes will continue to be available and in even greater demand than they are today. Refiners will be faced with the choice of purchasing light sweet crudes at a premium price, or adding bottom of the barrel upgrading capability, through additional new investments, to reduce the production of high-sulfur residual fuel oil and increase the production of low-sulfur distillate fuels. A second disadvantage is that liquid products from cokers frequently are unstable, i.e., they rapidly form gum and sediments. Because of intermediate investment and operating costs, delayed coking has increased in popularity among refiners worldwide. Based on the 2000 Worldwide Refining Survey published in the Oil and Gas, the delayed coking capacity for 101 refineries around the world is 2,937,439 barrels/calendar day. These cokers produce 154,607 tons of coke per day and delayed coking accounts for 88% of the world capacity. The delayed coking charge capacity in the United States is 1,787,860 b/cd.

Despite its wide commercial use, only relatively few contractors and refiners are truly knowledgeable in delayed-coking design, so that this process carries with it a “black art” connotation. Until recently, the expected yield from cokers was determined by a simple laboratory test on the feedstock. As a result of Tulsa University’s prior related research, a process model was developed that with additional work could be used to optimize existing delayed cokers over a wide range of potential feedstocks and operating conditions.

The objectives of this research program are to: utilize the current micro, batch and pilot unit facilities at The University of Tulsa to enhance the understanding of the coking process; conduct additional micro and pilot unit tests with new and in-house resids and recycles to make current optimization models more robust; conduct focused kinetic experiments to enhance the furnace tube model and to enhance liquid production while minimizing sulfur in the products; conduct detailed foaming studies to optimize the process and minimize process upsets; quantify the parameters that affect coke morphology; and to utilize the knowledge gained from the experimental and modeling studies to enhance the computer programs developed in the previous JIP for optimization of the coking process. These refined computer models will then be tested against refinery data provided by the member companies. Novel concepts will also be explored for hydrogen sulfide removal of furnace gases as well as gas injection studies to reduce over- cracking.

The following deliverables are scheduled from the two projects of the three-year JIP:

1. A novel method for enhancing liquid yields from delayed cokers and data that provide insight as to the optimum temperature to remove hydrogen sulfide from furnace gases.
2. An understanding of what causes foaming in coker drums and ways to minimize sulfur in the produced liquids.
3. An understanding of the HES impacts resulting from hot spots, poor drainage, and settling.
4. A screening model to quantify how other feedstocks and/or a combination of feedstocks will behave in a refinery, and kinetic/optimization models that can represent virtually any delayed coking unit across a wide range of process conditions and feedstocks.

Primarily graduate students, post-Doctoral Research Associates and faculty members, will conduct the research in this project.

This research project should find ways to reduce the amount of contaminants in coke, making it better suited for commercial use in the metals or chemistry industry, as well as ways to reduce the amount of sulfur in the gasoline and diesel fractions. Reducing foaming in the coke drum will also be studied in this project. Reducing the amount of antifoamant used in the coke drum by $0.10 per ton will save the refiners $5 million per year. During 2001, both production and consumption of petroleum coke has increased, and this trend is set to continue. Since 1992 world petroleum coke production capacity has increased by more than 40% to reach a peak of 154,607 tpd in 2001. This expansion is expected to continue with at least fifteen new coking units coming into production by 2003 providing new jobs and markets for the coke, such as a fuel source for kilns in the cement industry and for boilers in electric power plants or in the manufacture of electrodes to be consumed in carbon anodes for aluminum smelting and graphite electrodes of steel making.

Knowledge from this project will be transferred to the industry through semiannual advisory board meetings, graduate education of two Ph.D. students and two MS students and through the coordination of annual workshops for hands on experience of using computer programs that come out of the research.

3. Executive Summary

Eleven organizations are currently members of the Fundamentals of Delayed Coking Continuation JIP that started June 1, 2002: Baker-Petrolite, Chevron, ExxonMobil, Foster Wheeler, Great Lakes Carbon, KBC Advance Technologies, Marathon-Ashland, Petrobras, Shell, Suncor, and the U.S. Department of Energy. Discussions are ongoing with ConocoPhillips, Citgo, BP and Kuwait.

The Coking test facilities include three reactors (or cokers) and ten utilities. Experiments are being conducted using the micro coker, pilot unit and stirred batch reactor. Gas products are analyzed in-house using simulated distillation (HP 5880a), high temperature gas chromatography (6890), detailed hydrocarbon analysis, and ASTM distillation.

Facility Improvements were made to the micro reactor, batch reactor and the pilot unit to improve/enhance the quality of data obtained. For the micro reactor, the major improvements include Eurotherm temperature controls, pressure transducer to vapor line, thermocouples for reactor T's and Vapor T's, pulse meter for continuous gas volume readings, and Labview control and data acquisition system. These upgrades improved the assembly/disassembly time as well as increased the amount of data acquired and the process in which it was acquired. Increasing the amount of data acquired has improved the understanding of each run and improved the comparison of the micro reactor data to pilot unit data. The improvements to the batch reactor were made to remove operator error in system functions and data acquisition and to improve system functionality. Limiting operator error has improved data reproducibility as well as increased the time available for liquid sampling. The changes made were including higher wattage heaters, increasing the liquid sample receivers from 4 to 12, installing a larger sampling system to allow for SARA analyses, and a Labview control and data acquisition system. For the pilot unit, overhead and feedline injection capabilities were added for antifoams and a pump system that provided the ability to quench with large water volumes through the feedline and overhead.

In the second phase of study, 126 micro reactor tests have been conducted. 27 shakedown tests showed that the gas recoveries were excessively high when compared to the pilot unit. These runs resulted in the addition of a new pressure gauge on the vapor line, the addition of a carrier gas to remove the stagnant vapors and controlling the test using an internal thermocouple.

87 parametric tests were then conducted with the in-house resid samples at three temperatures and three pressures. Individual resid product and liquid sub-product yields were predicted fairly well using linear regression. Overhead temperature and pressure were the parameters used. A slight variation in experimental data was seen in the coke (0.93%), liquid (1.27%) and gas (0.92%) yields when the data was compared to the data predicted with the micro-screening model. The individual liquid sub-product yield predictions improved for the new runs when compared to the previous runs when the liquid sub-products were estimated in terms of total weight percent of feed instead of total weight percent of liquids. Liquid content was seen to increase with temperature for the paraffinic resids while the aromatic, napthenic, and intermediate resids showed and optimum at 930°F.

Thirteen tests were conducted with recycle. It is too early to draw any conclusions. Upon completion of these tests, tests will be conducted with the three new resids: Cerro Negro, the Heavy Canadian and the Rose pitch.

The Batch reactor was upgraded and is now generating high quality data. Nine tests have been conducted with the facility. These were shakedown tests with water, vacuum oil and with Marathon recycle. Parametric tests were begun with the Petrobras resid. Analytical measurements are being expanded to include SARA on reactor samples and PiONA on liquids so the kinetic model can be enhanced to include

olefin-producing reactions, napthene ring-opening and dehydrogenation reactions, and aromatic condensation reaction.

A batch reactor model was developed based on the model used in the literatures by different researchers (Raychaudhuri, Banerjee, & Ghar, 1994; Stangeland, 1974). This model uses the boiling points of the feed that is produced by the HTGC and the operating conditions of the batch reactor to predict the product distributions. A program has been built and compiled using FORTRAN to predict the kinetic parameters using a nonlinear least square method. The method used in the program was the known Levenberg-Marquardt method developed separately by Levenberg (Levenberg, 1944) and Donald Marquardt (Marquardt, 1963). The subroutines and functions were programmed using FORTRAN. There were two distinctive sections in the program. One section calculates the model and then passes it to the other to calculate the model parameters. The kinetic model program was developed and compiled. The program was run using literature data and it worked very well.

HTGC data, which is essential to the development of the kinetic model, was completed. These data along with SimDis and GC data will be used in our model to produce the kinetic parameters. The kinetic model is still in the testing stage for tuning it to the batch reactor produced data.

68 tests have been conducted with the pilot unit using the in-house resids. Studies were first conducted to determine the extent of antifoam carrying over during overhead injection using water. These studies indicated that some of the antifoam was carried over into the liquids when injected from overhead. However, the very low recovery of silicon indicates that most of the injected antifoam remained in the drum. More antifoam would be carried over during the coking process because the superficial velocity of the HC vapor is larger. Studies were also conducted to establish what was causing the fluctuations in the fluid in the furnace tube. By recording temperatures as a function of distance from coil inlet to outlet, it was hypothesized that an increase in vaporization of the fluid causes more irregularities in the flow pattern and temperature profile. When both recycle and antifoam were injected, it was noticed that the furnace had to be fired harder to achieve the desired operating temperature as compared to when only resid is injected.

Antifoam injection studies were run using both a low viscosity 100,000 cSt (0.3 ml AF/ 70 ml diesel) and a high viscosity 600,000 cSt (0.75 ml AF/ 70 ml diesel) antifoam. In some of the tests, antifoam was injected continuously (2 min ON and 8 min OFF) while in others it was injected on as-needed basis (observation of foam determines the injection time). Antifoams were injected in the drum overhead, through the feedline, and mixed with the resid in the feed bucket. During the experiments, temperatures at the inlet to furnace coil, the fluid temperature, the furnace skin temperature, the overhead temperature and the temperature inside the coke drum near the bottom were measured. From test to test, variations were seen in the overhead temperature and the furnace coil temperatures. In general, injecting antifoam on a continuous basis reduces the overhead temperature, while injecting antifoam in the feedline requires the furnace to be fired harder to get the fluid to the desired temperature.

A partitioning study was conducted on the samples taken during the pilot unit tests in which oil and water samples were collected from the lights and heavies tank. More analytical results are needed for silicon in the liquid products but the tentative conclusion is that silicon from the antifoam injected overhead tends to carry over to the hydrocarbon liquids, while the silicon injected from the feedline tends to break down and end up in the decant water.

A detailed liquid analyses study was initiated in June 2003. This study is looking at 160 liquid samples generated in the first phase of study and those currently being generated in the continuation phase. The samples are being distilled and simulated distillation, detailed hydrocarbon analyses and sulfur analyses are run on each cut. The overall outcome of the study is to be able to predict what type of PiONA component, sulfur, etc. would be dominant at a certain temperature and pressure, and how a change in the temperature and pressure would affect its production.

Foaming runs were begun in June 2002. The first series of foaming tests were conducted using the Suncor resid to establish the differences between overhead, feed and feed line injection. The second series of tests were run using six in-house resids to gain an understanding of how pressure and temperature affect foaming as well as the impact of feed rate. This data was integrated with the results obtained during the first phase of study.

The parametric studies with the six in-house resids were completed. These tests show that paraffinic structured resids made Sponge coke, Aromatic resids made Shot coke, Napthenic resids made a mixture of shot and sponge coke while Intermediate structured resids made a mixture of agglomerated and large BB's. Petrobras and Marathon resids made an entire drum of sponge coke, irrespective of the operating conditions, while the Suncor resid made shot coke irrespective of operating conditions, Equilon made a mix of sponge, agglomerated shot and different sized BB's while Chevron and Citgo made either sponge coke or shot coke depending on operating conditions.

For the resids which produce sponge coke, the thickness of the liquid layer decreased with an increase in temperature; the coke density increased with an increase in either temperature or pressure and decrease in feed rate, unless it was affected by excess antifoam injection which also increased the density of the coke. Sponge coke has a linear bed growth, where as in the case of agglomerated shot, the coke bed attains a certain height at which point the lower layers grow denser until break through occurs or the test was terminated due to pressure buildup. Increasing the temperature and feedrate made more shot coke and also more BB's whereas an increase in pressure decreased shot coke formation. Samples have been selected for permeability, porosity and CT scans. A Masters student will be added in the near future to continue this study.

In general, the lower the temperature and pressure, and the higher the feedrate, the worse the foaming. This was especially true for the Marathon, Petrobras, and Chevron resid. However, Equilon & Citgo foamed worse at higher pressure.

Nine antifoam optimization tests using the resid from Petrobras showed that injection of higher concentrations of antifoam/unit of carrier uses more antifoam than is required to effectively control foaming; however, the time between injection is longer and a denser coke is made. When large quantities of diesel are injected as the carrier, foaming appeared to be enhanced. Foaming resulted in uniform temperature profiles in the drum and when the temperatures in the drum were fairly uniform throughout, pure shot or a uniform sponge was made.

Continuous overhead and feed line injection are effective at controlling foaming throughout the run. Feed line injection with an antifoam/carrier concentration of 0.3/70 was only effective at controlling foaming on a continuous basis for the first 80 minutes whereas the 30/70 concentration was effective throughout the run. The 0.3/70 mixture was also the optimum AF concentration for controlling foaming overhead. It was also found that when 100,000 cSt and 600,000 cSt antifoams are used at equivalent concentrations, foam control is comparabl; however, the time to rise was longer for the 600,000 cSt antifoam..

Two approaches were developed to quantify foam, liquid and coke heights. These approaches are being compared to test data to determine which technique, or a combination the techniques, works best.

Tests with recycle and at refinery conditions were begun. Although early in the testing phase, it was observed that a denser coke was made and that the morphology was starting to change in the bottom portion of the drum. Coke density was also observed to change when increasing concentrations of antifoam were used.

A foaming model was developed based on work by Pelton and Goddard. The model predicts foam volumes both in the presence and absence of antifoam emulsions. The model was tested on three data sets, Citgo 9 and 11 and Petrobras 4. The predictions are very good for the 3 runs investigated. The model, apart from predicting foam volumes for various times during the run, predicts the foam collapse taking place at antifoam injection and thereafter. The model is able to predict possible foam over tendencies for

particular runs like Petrobras 4 and in general predicts a foam volume increase before an antifoam injection.

Gamma densitometer traces before and after steam stripping were used to show the loss of mass from the coke bed due to steam stripping. This loss of mass is due to the volatile matter that is stripped from the coke. Some of the runs had significant bed compaction from steam stripping while some had none. Bed slumping in some cases was as much as 10% of the bed height. In these cases, the slumping actually caused an increase in the coke bed density, mostly at the bottom of the bed, but to a lesser extent in the middle of the bed.

From the process studies it was observed that different coke morphologies have different cooling rates. Sponge coke seems to cool faster than shot coke. The density of the coke affects the way it cools; denser coke in general cools slower than a less dense coke morphology. Particle size and structure also have an effect on cooling rates. Large, loose BB shot coke pellets seem to take longer to cool than smaller, more clustered particles. Run pressure also seemed to have an effect on the way the produced coke bed cooled. The lower-pressure runs in general produced less dense coke morphologies, which in turn cooled faster than the denser morphologies produced by the higher-pressure runs.

Cooling temperature profiles of the coke revealed the cooling procedure used. Cooling the coke bed with nitrogen and with the furnace door opened is more effective than cooling it with the door shut. When cooling the coke bed with the furnace door opened a large temperature drop takes place in the first few hours and then the drop is more uniform and less dramatic until the bed is at approximately room temperature. When cooling the coke bed with the furnace door shut the cooling is very uniform and the coke bed is only at approximately at 170ºF after about 18 hours of cooling. For most of the runs the cooling profiles look similar as long as the coke bed is cooled by the same cooling procedure. The cooling rates however, are different for each run.

A lumped heat capacity model was developed for the cooling of the coke drum by free convection to the surrounding air with the furnace door open. The heat capacities estimated for the coke were around 0.5 Btu/ºF-hr for sponge coke and 0.6 Btu/ºF-hr for shot coke. These values are in agreement with a few literature values of approximately 0.45 Btu/hr-ºF. Plotting the predicted temperatures against the measured or real values showed that the method was satisfactory in roughly predicting how a certain coke morphology would cool as a function of time.

Convective cooling rates were also correlated by averaging the cooling rates of different runs that were operated under very similar conditions and that produced similar coke morphologies and then using a curve fit to model the experimental data. Using this procedure it was found that an exponential curve fit predicts the cooling of the coke bed well.

Water quenching is the most effective way to cool the coke bed over a relatively short period of time. Several factors such as water injection rate, injection time, total amount of water injected and injection point have an effect on the way a certain coke bed cools. Injecting the water from the bottom of the drum is more effective than injecting it overhead.

A quench model was developed to predict temperature profiles when the coke bed is cooled by flowing water from the bottom. The model divides the coke bed into one-inch segments of coke and performs energy balances over the coke and steam or water on each segment. The model uses literature values of heat capacity and thermal conductivity of the coke and adjusts the heat transfer coefficient and coke porosity to best fit the given data. The model works very well in predicting the temperatures as a function of injection time for each zone. Some slight differences between the model and experimental data are probably due to assuming the same coke properties (porosity, heat capacity, and thermal conductivity) throughout the coke bed.

Work is now underway to modify the existing bottom quench model to satisfactorily describe overhead quenching. Overhead quenching is by its nature much more difficult to model than bottom

quenching, because the water introduced does not initially flow through the bed, but will penetrate downward some distance into the bed before vaporizing and reversing direction to exit in the overhead line as steam. The key to successfully modeling this situation will be determining a heat transfer coefficient that will predict the rate of vaporization of the water and the rate of cooling of the coke in the top section of the bed.

The address for the Delayed Coking Web Site is http://www.tudcp.utulsa.edu. The web site has become a useful tool to welcome visitors and tell them about the JIP. It is segmented such that visitors can gain general information while the "Members Only" site contains confidential information generated in the JIP. There is a reading room, applications, a tour of the facility, a place to meet the personnel, JIP news, experimental data from the three cokers, models and correlations, and a discussion board. During the continuation phase of study, significant postings and updates were made to the web site. The web site was also modified to make it more user friendly.

A tentative date for the eleventh Advisory Board meeting is Wednesday and Thursday, May 19-20, 2004. The meeting will be held at the University of Tulsa in ACAC. The meeting on the 19th will begin at 1 pm and adjourn at 5 p.m. A social is planned that evening in the Presidents Lounge from 5 to 9 p.m. The meeting on the 20th will begin at 8 a.m. and adjourn at 2:30 p.m.

4. Experimental Methods

A. Scope of Problem

Three state-of-the-art test facilities were developed for use in the previous JIP. The facilities were used to generate high-quality data. These facilities, with some minor modifications to improve them, are now being utilized to gather large quantities of coking related data to enhance the capabilities of the predictive models developed during the first three years of the Fundamentals of Delayed Coking Joint Industry Project (JIP). The work plans for this Joint Industry Project show the work being conducted with two major projects:

Project 1 – Small Scale Reactor Studies - conducts studies with the micro and batch reactors to generate sufficient data to enhance the robustness of the screening model and to better understand the reaction kinetics in the furnace tube and coke drum. Methods for removing sulfur, for enhancing liquid production, as well as ways to reduce sulfur in the liquids to help refiners meet the upcoming stringent sulfur requirements will also be studied.

Project 2 – Pilot Unit Studies - conducts detailed studies to enhance the robustness of the process optimization model and to better understand the foaming process thereby minimizing or eliminating process upsets as well as optimizing the use of antifoams thereby increasing refinery margins. Concurrent studies on the produced coke will provide a better understanding as to what parameters affect coke morphology as well as provide insight as to why settling, poor drainage and hotspots occur in coke drums minimizing health and safety hazards.

Results from these Projects will be used to further develop correlations for product yields and properties, as well as to develop mechanistic models for the furnace tube and coke drum that account for reaction kinetics and energy effects (i.e., heats of reaction, heats of vaporization, and heat transfer effects).

B. Program Chronology

The schedule for completing the complex and interrelated tasks over a three year period is shown in Table 1 and Table 2. Table 1 and Table 2 also show when significant deliverables in the form of report, models, and data will be provided to the participants. Those items colored blue are complete while those in red show when the task is scheduled for completion.

Table 1 - Pilot Unit/Foaming Studies

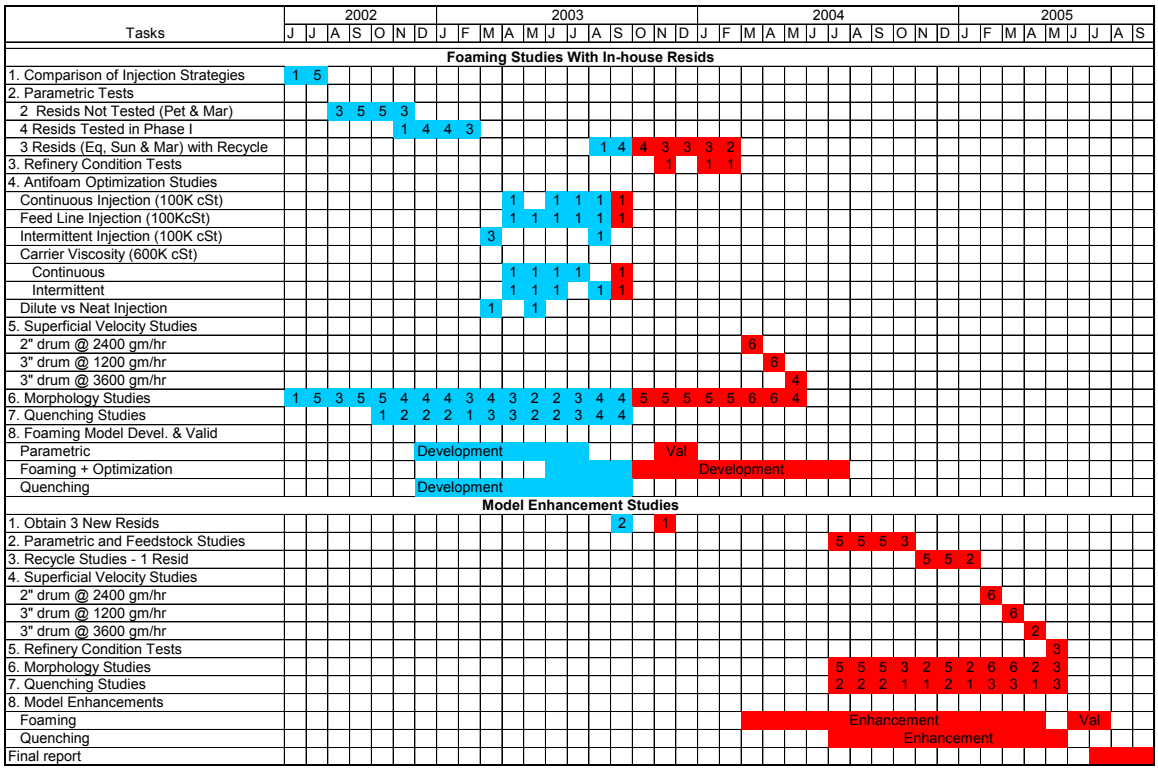

Table 2 - Small Scale Reactor Studies

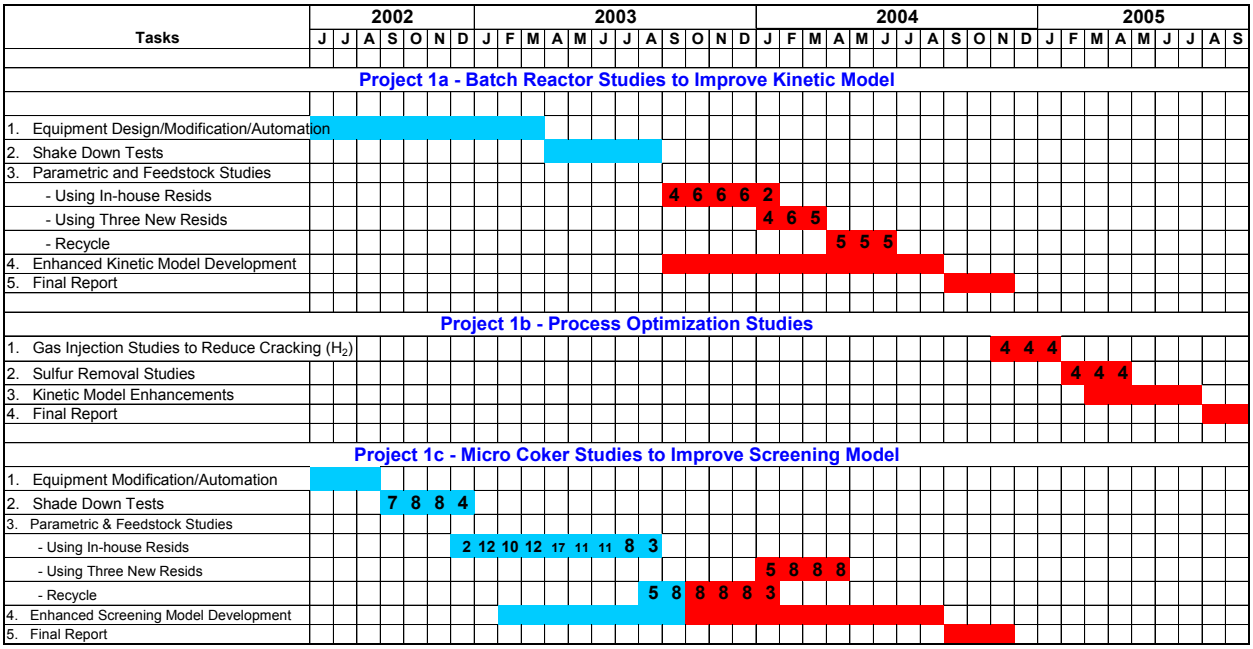

1. Pilot Unit/Foaming Studies:

While conducting parametric studies in the previous JIP, runs were made with and without antifoams. Contrary to refinery experience, antifoams were successfully injected with the feed. Runs were made with and without foaming; however no technique was available to measure foam height. In the continuation study, a gamma densitometer is utilized for this purpose. The tests shown below are being conducted to gain a better understanding of the foaming process to minimize or eliminate process upsets as well as optimize the use of antifoams to increase refinery margins. In all studies, analyses will be conducted to quantify the amount of Silicon going into the quench water and hydrocarbon liquids. The test conditions for the pilot unit will include temperatures of 900, 930 and 950 °F; pressures of 15, 30, 40 and 50 psig, carrier viscosities of 100,000 and 600,000 cSt; feed rates of 2400 and 3600 gm/hr; and recycle rates of 5 and 10%. The proposed test matrix includes 179 tests as shown in Table 3.

Table 3 - Test to be Conducted for Foaming Studies

Type of Test	Temperature	Pressure	Resids	Feed Rates	Recycle Rates	Viscosity	Drum Sizes	Injection Points	Total
General Tests									
1. Parametric and Feedstock									
3 New Resids	3	3	3	1					27
Old Resids Not Tested	2	2	2	2					16
Resids Tested in Foaming	2	2	4	1					16
Recycles	3	2	3	1	2				36
2. At Refinery Conditions	1	1	9	1	?				9
3. Superficial Velocity	3	3	1	1			3		27
Focused Tests									
1. Continuous vs Feed Injection	1	1	6	1		1		2	12
2. Continuous vs Intermittent	1	1	6	1		1		1	6
3. Carrier Viscosity	1	1	9	1		2	1	1	18
4. Dilute vs Neat Injection	1	1	3	1		2		1	12
Total									179

2. Batch Reactor Studies

In the prior JIP, 30 tests were run with six resids. All of these tests, except for the three that were run at 15 psig, were run at a pressure of 40 psig. These tests were not sufficient to adequately define the wide range (15 to 50 psig) of pressures that refinery furnaces and coke drums operate at. The batch reactor tests using the old and the new resid samples will generate the additional data needed to establish a robust kinetic model, especially over the wide range of pressures that commercial furnaces and coke drums operate at. Parametric studies will be conducted using the six resids that were utilized in the parametric studies in the prior JIP. Additional runs will be made with recycle. In addition, three new resids will also be run. These tests will be conducted at pressures of 15 and 40 psig. The analytical program will be enhanced to include other tests on the reactor resid samples that were not conducted in the previous JIP. An experimental program will be established, possibly using the visbreaking column, to quantify the amount of vaporization taking place in the furnace tube. The Delayed Coking Model that was developed in the previous Joint Industry Project was a lumping model based on boiling point distributions. It assumed that any material that is cracked into components light enough to become vapor will leave the drum without further cracking, while any cracked material that is heavy enough to stay in the drum will become heavier

(through condensation or polymerization reactions) to eventually form coke. With additional data obtained from the continuation study, we will have a larger database of kinetic studies, so we will be able to better determine how feedstock properties affect the kinetics. We will also expand the analytical measurements for the batch reactor experiments to include SARA analyses on the reactor samples and PiONA analyses on the product liquids, which will allow us to enhance our kinetic model to include olefin-producing reactions, naphthene ring-opening and dehydrogenation reactions, and aromatic condensation reactions. These principles will expand modeling beyond correlated data available from this Joint Industry Project. The model should be able to represent virtually any delayed coking unit, commercial or pilot scale, across a wide range of process conditions and feedstocks. Thirty tests are planned with the six resids used in the prior JIP and thirty tests with three new resids as shown in Table 4 and Table 5.

Table 4 - Batch reactor tests to be conducted with in-house resids

	Pressure				Heating Rate			
Resid	15	30	40	Total	Low	Medium	High	Total
Chevron	2	1	2	5	3		2	5
Citgo	2	1	2	5	3		2	5
Equilon	2	1	2	5	3		2	5
Suncor	2	1	2	5	3		2	5
Marathon	2	1	2	5	3		2	5
Petrobras	2	1	2	5	3		2	5
Total	12	6	12	30	18		12	30

Table 5 - Batch reactor tests to be conducted with new resids

	Pressure				Heating Rate			
Resid	15	30	40	Total	Low	Medium	High	Total
Resid 7	2	1	2	5	3		2	5
Resid 8	2	1	2	5	3		2	5
Resid 9	2	1	2	5	3		2	5
Recycle 1	2	1	2	5	3		2	5
Recycle 2	2	1	2	5	3		2	5
Recycle 3	2	1	2	5	3		2	5
Total	12	6	12	30	18		12	30

3. Micro Reactor Studies

A screening model is a useful tool to quantify how other feedstocks and or combination of feedstocks will behave in a refinery. Results from the prior JIP show the micro reactor produced results that were scaleable to industry. However, this model was built using only three feedstocks and the range of several key parameters such as asphaltene content, MCR, recycle and metals (Ni, V) were not broad enough for a robust model. The micro reactor tests using the old and the new resid samples will generate new data for making enhancements to the existing screening model. They will provide a better understanding of the effects of metals, MCR, recycle and asphaltene content on the coking process. Parametric studies will be conducted using the three resids (Citgo, Chevron and Petrobras) that were not utilized in the parametric studies in the prior JIP. In addition, three new resids will also be run. These tests will be conducted at three temperatures (900, 910, 930 and 950 °F) and at pressures of 6, 15 and 40 psig. The analytical program will be the same as in the previous JIP. The tests to be conducted are shown in Table 6 and Table 7 below.

Table 6 - Micro reactor test conducted with in-house resid

	6 PSIG			15 PSIG			40 PSIG			
Resid	910 °F	930 °F	950 °F	900 °F	930 °F	950 °F	900 °F	930 °F	950 °F	Total
Chevron	1	1	1	1		1	1	1	1	8
Citgo	1	1	1		1	1	1	1	1	8
Equilon				1		1	1		1	4
Suncor	1		1				1		1	4
Marathon	1		1				1		1	4
Petrobras	1		1	1		1	1		1	6
Total	5	2	5	3	1	4	6	2	6	34

Table 7 - Micro reactor tests conducted with new resids

	6 PSIG			15 PSIG			40 PSIG			
Resid	910 °F	930 °F	950 °F	900 °F	930 °F	950 °F	900 °F	930 °F	950 °F	Total
Resid 7	1	1	1	1	1	1	1	1	1	9
Resid 8	1	1	1	1	1	1	1	1	1	9
Resid 9	1	1	1	1	1	1	1	1	1	9
Recycle 1	1	1	1	1	1	1	1	1	1	9
Recycle 2	1	1	1	1	1	1	1	1	1	9
Recycle 3	1	1	1	1	1	1	1	1	1	9

C. ACTIVITY SUMMARY – YEAR 1

The Gantt chart for the studies conducted with the small scale reactors were shown in Table 2 while the Gantt chart for the studies conducted with the pilot unit were shown in Table 1. The events colored in blue are complete while those in red are scheduled completions. The numbers in each cell tell you how many tests are planned or were completed that month.

During the first year, a batch reactor facility was modified. Testing began in September. One hundred and twenty six tests were conducted with the micro reactor. Twenty seven were shakedown in nature; Eighty six were parametric and feedstock while thirteen were with recycle. Additional details of these tests are provided below. Sixty two tests were conducted with the pilot unit.

Analytical analyses were conducted by TU, Baker-Petrolite and GLC on all the coke and liquid products produced from the three facilities. The analyses conducted included the following: distillation, SimDis, Detailed Hydrocarbon Analysis, Metals, Sulfur, Ash, Volatiles, HGI, RON, CHN, Permeability, Porosity, and CT Scans.

Equipment Modifications: To better monitor the micro-coker and improve its functionality, upgrades to the system were made. These upgrades have shortened the assembly/disassembly time as well as increased the amount of data acquired and the process in which it is acquired. Increasing the amount of data acquired has improved the understanding of each run and will allow for comparison of micro data to pilot unit data. The upgrades implemented to the micro reactor are listed below:

1. Temperature control – Four new Eurotherm temperature controllers were installed to control the reactor heater, pre-heater, mantle and the heat tape before the pre-heater – this upgrade will eliminate fluctuations in the temperature profiles from run to run
2. A pressure transducer and digital pressure gauge were installed to measure the vapor line pressure for improving gas yield calculations
3. Thermocouples – to improve correlations and comparisons to pilot unit data
    a. Thermocouple well installed in reactor head to hold thermocouple that reads top, middle and bottom reactor temperature
    b. Thermocouple installed that reads temperature of the vapors leaving reactor
    c. Thermocouple installed that reads temperature of the vapors leaving primary liquid trap
4. Pulse meter installed on wet test meter for computer data acquisition
5. Labview is used for system controls and data acquisition (T's, P's and flows)

In addition to the above mentioned modifications/upgrades, a new syringe pump housing was machined to eliminate the stirrer – there were no apparent benefits to keeping the stirrer while its presence extended clean-up time and added error to mass balances due to the feed leaking around the seals. Multiple housings improve turn around time. A second reactor was manufactured to improve turn around time.

One hundred and twenty-six tests were conducted with the microreactor facility. As a result of the changes to the apparatus, the microreactor generates data that is much more in line with that observed with the pilot unit. This data was utilized to further modify/enhance the screening model, especially at higher temperatures and with the recycle. When the liquid sub-product yields were estimated in terms of total wt%

of feed instead of taking them as wt% of liquids, the correlations improved for gasoline, diesel and gas oils and are predicted as good as the correlations for the main products (gas, liquid and coke).

The batch reactor facility was modified to increase the number of liquid samples taken from 4 to 12. A photograph of the modified facility is shown in Figure 1. Shakedowns of the test facility were conducted. These tests showed that ball valve that controlled the nitrogen flow was not sufficient. It was replaced with a flow meter. A thermocouple was also installed to monitor the temperature of the liquids/vapors leaving the condenser. A less cumbersome and larger capacity sampling system was designed and installed as shown in Figure 2. Four tests were conducted with water to test the heating capabilities and the heat loss of the system. One run was made with vacuum oil that showed the separation system was working properly. Several tests with Marathon recycle were made to optimize the switching controls and heating regime. Tests with the Petrobras Resid were begun.

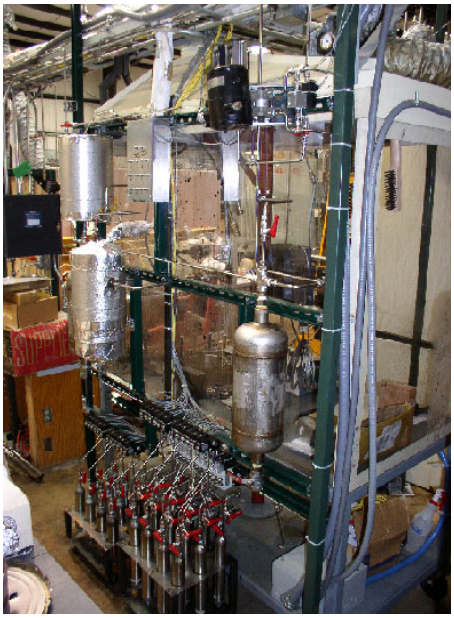

Figure 1 - Modified Batch Reactor Facility

A model of the batch reactor was built based on Herbst and Fuerstenau (1968), and other researcher's studies (Stangeland, 1974; and Raychaudhuri, Banerjee, and Ghar, 1994). The model has three parameters and can predict the boiling point curve of a given feed under different experimental conditions. A FORTRAN program was built to solve the model parameter using Levenberg-Marquadt method which is widely used to solve nonlinear equations. Two different packages, namely LINPACK and ODRPACK, were used to solve for the model parameters. The packages could not predict the parameters correctly as given by Raychaudhuri et al. (1994). The program was tested with other linear and nonlinear functions and confirmed its functionality. However, the program cannot solve singular matrix which is the case for the least square problem. Least square problems are always close to singularity, however; in our model, the problem is the number of equations are more than the parameters (overdetermined) and combinations of parameters that exist (underdetermined). The solution for this problem was to use singular value decomposition (SVD). A subroutine for SVD was compiled to solve for the least square problem to determine the model parameters.

Foaming data from the parametric and antifoam optimization tests run in the Pilot Unit were analyzed to quantify the foam, liquid and coke volumes. A plot of the type of data generated is shown in Figure 3. A model of foam growth in the presence of antifoam emulsions developed by Robert Pelton was found in the literature. Using the different model correlations, foam volume vs. time plots for the runs conducted, both in the presence and absence of antifoam, were made. The plots developed were compared with actual run findings to determine the efficacy of the model. For input parameters, the majority are obtained from actual run data whereas for the remaining, necessary assumptions were being made. This effort is confirming whether high antifoam concentrations prevent foam growth until the antifoam concentration in the liquid phase is depleted and whether antifoam is active for a longer time when treating larger bubbles. Figure 4 shows a comparison between actual and predicted results.

Figure 2 - New Batch Sample Tube Assembly

During the first year of study sixty-two pilot unit foaming runs were made. The coke morphology produced from each run was described and the samples analyzed for metals content. The contents in drum from many of the runs were quenched with water. The waters are analyzed for trace metals. A Gantt chart for this study was shown Table 1.

Figure 3 - Foam Height Quantification

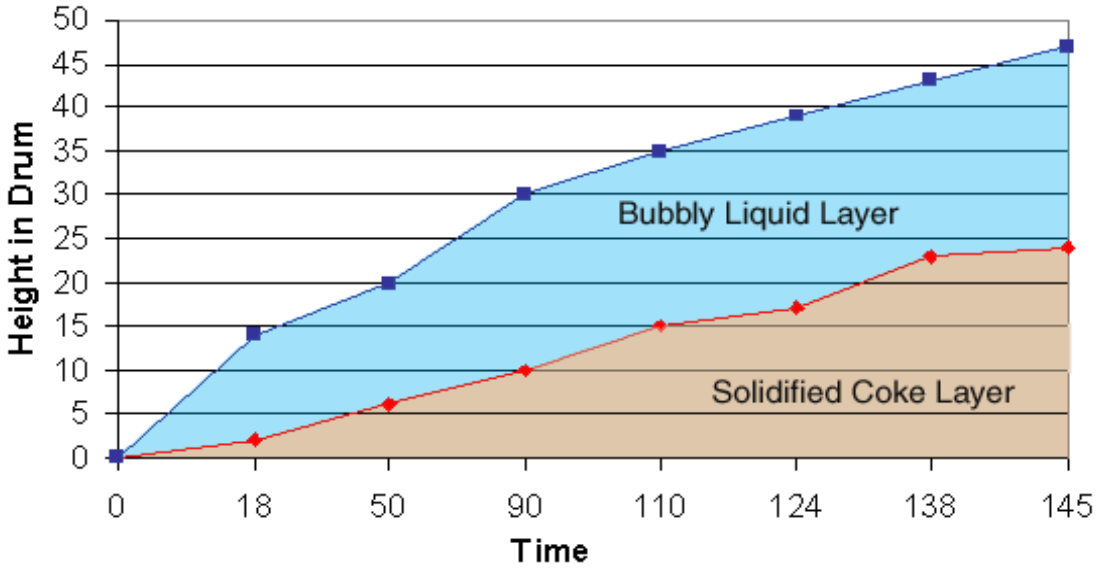

Figure 4- Comparison between Foam Volumes, Model Predicted & Actual Run Data for PETR 4

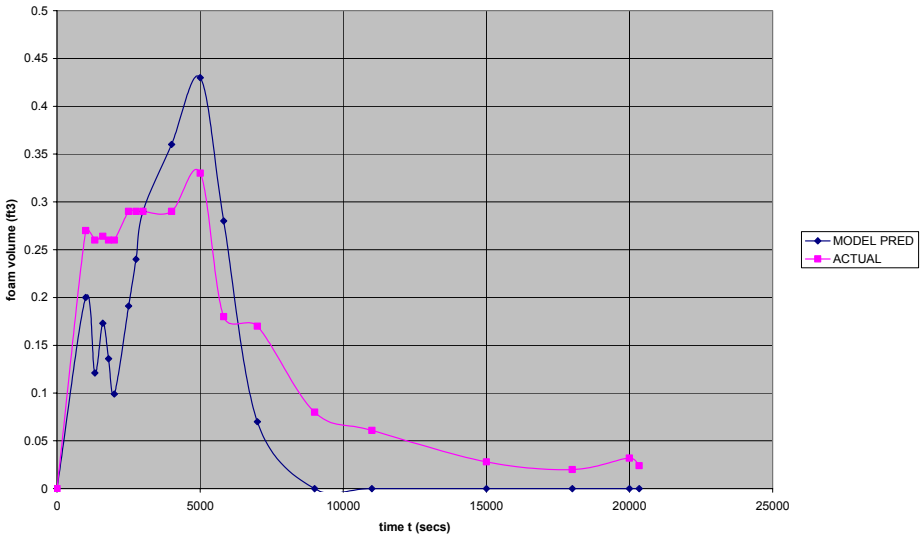

Foam optimization studies were conducted that demonstrated that feed line injection of antifoam is as effective as overhead injection.

Gamma densitometer traces before and after steam stripping showed that some resids have a loss of mass from the coke bed due to steam stripping and that in some cases the bed slumps causing an increase in coke bed density. The feed properties responsible for this observation were quantified.

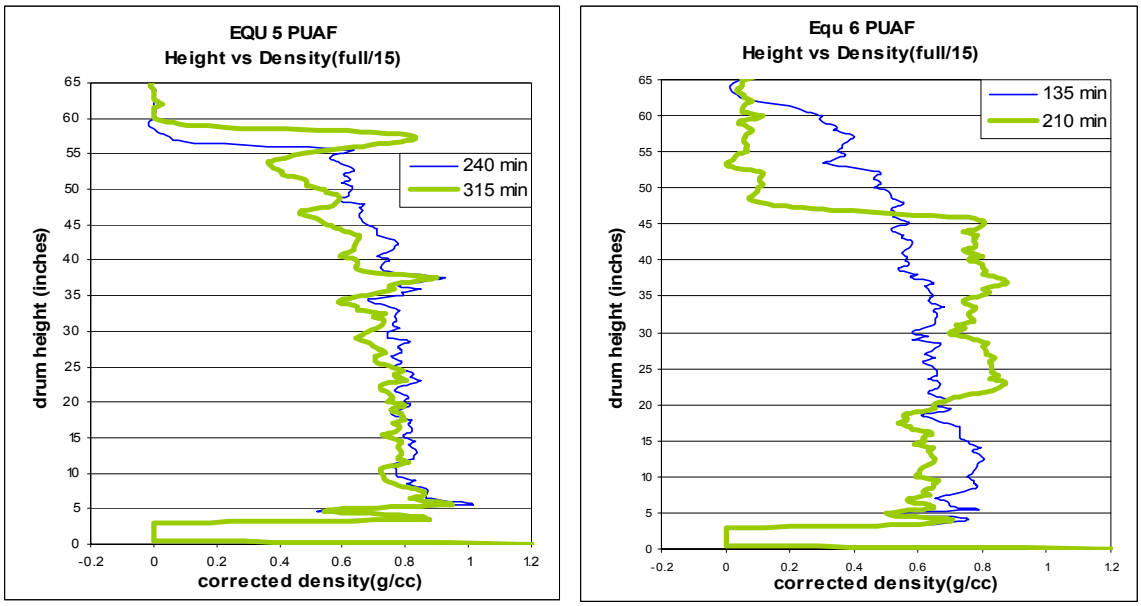

Figure 5 - Steam Strip plots for EQU 5 PUAFI and EQU 6 PUAFI runs

Additional resid samples used from the start of the study in 1999 were obtained from Suncor, Marathon and Petrobras. Two new Resid samples were also received from Exxon Mobil: the Heavy Canadian Resid and Cerro Negro Resid.

A lumped heat capacity model was developed for the cooling of the coke drum by free convection to the surrounding air with the furnace door open. The heat capacities estimated for the coke were around 0.5 Btu/ºF-hr for sponge coke and 0.6 Btu/ºF-hr for shot coke. These values are in agreement with a few literature values of approximately 0.45 Btu/hr-ºF. Plotting the predicted temperatures against the measured or real values showed that the method was satisfactory in roughly predicting how a certain coke morphology would cool as a function of time.

A quench model was developed to predict temperature profiles when the coke bed is cooled by flowing water from the bottom. The model divides the coke bed into one-inch segments of coke and performs energy balances over the coke and steam or water on each segment. The model uses literature values of heat capacity and thermal conductivity of the coke and adjusts the heat transfer coefficient and coke porosity to best fit the given data. The model works very well in predicting the temperatures as a function of injection time for each zone. Some slight differences between the model and experimental data are probably due to assuming the same coke properties (porosity, heat capacity, and thermal conductivity) throughout the coke bed. A quench model is also being developed to predict the profiles when the coke bed is cooled using top injection.

D. FACILITIES

The coking test facilities consist of 3 reactors or cokers and eleven utilities. The micro-coker was supplied by the U.S. Department of Energy (U.S. DOE). The batch-coker reactor, also supplied by U.S. DOE, required construction of the heating, control, and product gathering systems. The operational pilot-coker, that utilizes a 3 foot drum, was obtained from Equilon in exchange for membership. The University expanded this facility to a six foot drum with a gamma densitometer to study foaming. The utilities include an on-line gas chromatograph and caustic scrubber from Equilon; house air and nitrogen; a University of Tulsa glycol chiller, purchased steam generator, hydrogen sulfide monitors and sample storage refrigerators; and donated vent hood and oven. The three cokers and associated utilities are described below.

1. Micro Reactor

The micro-reactor is shown in Figure 6. It consists of a syringe pump with stirrer, preheater, (corresponding to the commercial furnace), a coke drum with liner, three cooled liquid traps, a wet-gas test meter, and an on-line GC. The first cooled liquid trap is metal and the following two are glass. The first trap collects the majority of the liquid. Potential leaking between the glass joints limited the operating pressure of the micro-reactor as described and shown. Higher pressure is desirable to match refinery-operating conditions. Also foaming occurred in the pilot-coker coke drum when processing Equilon feed at the low pressure. For these two reasons and since the majority of the liquid was captured in the metal trap, a modified micro-coker set-up was developed. In this modified set-up the glass traps were removed and replaced by a single piece of metal tubing.

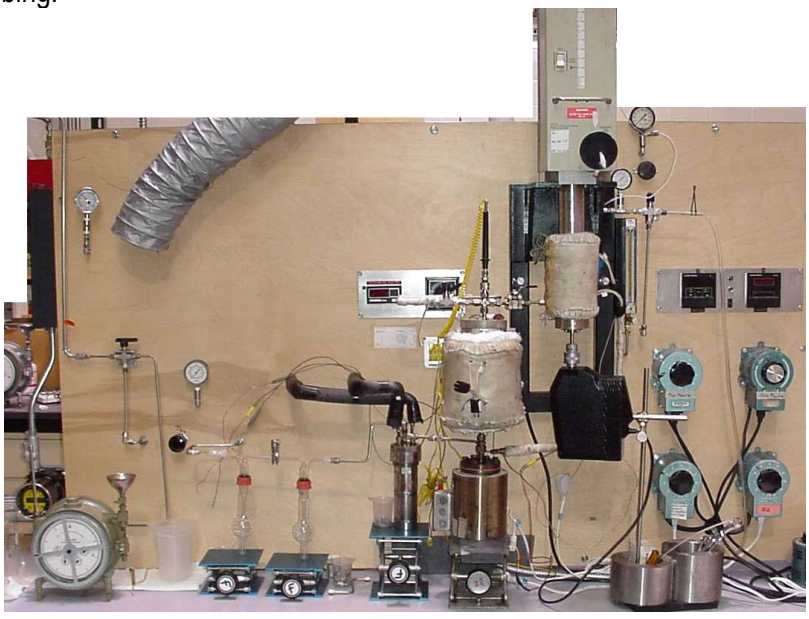

Figure 6 - Picture of Micro-Coker

The main objectives for utilizing this reactor are to:

1. Reproducibly mimic commercial operation for a very short time, producing small quantities of coke, liquids and gases for testing,
2. Investigate and correlate the effect of feedstock composition and to a lesser extent pressure, temperature and residence time on product rates and compositions and on coke morphology,
3. Develop and validate a model(s), and
4. Investigate scale-up issues.

2. Micro Reactor Upgrades

To better monitor the micro-reactor and improve its functionality, upgrades to the system were made. These upgrades improved the assembly/disassembly time as well as the amount of data acquired and the process in which it is gathered. A picture of the modified micro-coker is shown in Figure 7.

During the first facility-testing phase of the micro-reactor, it was found that the gas recoveries were excessively high compared to pilot runs. The cause is considered in three phases. The vapor line pressure gauge was giving false (high) readings; this resulted in a high-standardized volume of gas. The absence of a carrier gas caused the vapors to become virtually stagnant at the beginning and end of each run, resulting in over cracking. The micro-reactor operating temperature was the furnace temperature, instead of an internal liquid temperature used in the pilot unit. This meant that the internal liquid temperature was lower. The lower internal temperature allows the liquids that are produced to sit in the reactor longer, extending cracking time. In response to these problems, a pressure transducer and digital pressure gauge was installed to measure the gas pressure more precisely, carrier gas flow is maintained even during the run to push off the stagnant vapors out of the reactor, and the run temperature is now controlled by an internal thermocouple at the bottom of the reactor. All the upgrades implemented are listed below:

1. New syringe pump housing is used to eliminate the stirrer. There were no apparent benefits to keeping the stirrer while its presence extends clean-up time and adds error to the mass balance due to the feed leaking around the seals-multiple housings has improved turn around time,
2. Temperature control- Four new Eurotherm temperature controllers were installed to control the reactor heater, pre-heater, mantle and the heat tape before the pre-heater-this upgrade eliminated the fluctuations in the temperature profiles from run to run,
3. A pressure transducer and digital pressure gauge was installed to measure the gas pressure more precisely. Helium is being injected into the top of the reactor to increase the flow rate of the hydrocarbon vapors out of the reactor. Pre-run helium flow data is recorded and an average flow rate is backed out of the final wet test meter reading. It has since been determined that the helium carrier which was left running over night was causing the evaporation of some of the liquids in the primary trap. The helium is now turned off at the end of each run and the system is being isolated to prohibit this evaporation. As a result the gas yields made a sizable decrease and were more consistent and comparable to the gas yields seen in the pilot unit.
4. Thermocouples- to improve correlations and comparisons to pilot unit data.

a) Thermocouple well was installed in reactor head to hold thermocouple that reads top, middle and bottom reactor temperature,
b) Thermocouple was installed to read temperature of the vapors leaving the reactor,
c) Thermocouple was installed to read temperature of the vapors leaving the primary liquid trap,

A typical temperature profile inside the drum for the new runs using modified micro-coker equipment is shown in Figure 8.

5. Pulse meter installed on wet test meter for computer data acquisition, and
6. Labview software for system controls and data acquisition (T's, P's and flows).

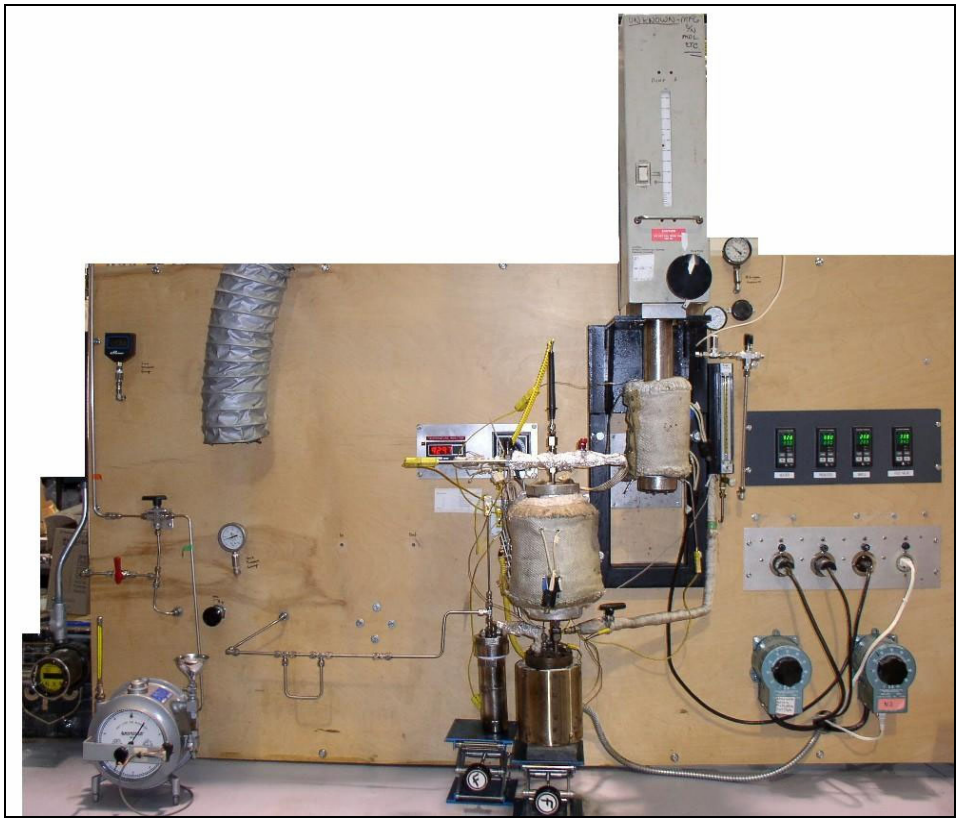

Figure 7 - Picture of Modified Micro-Coker

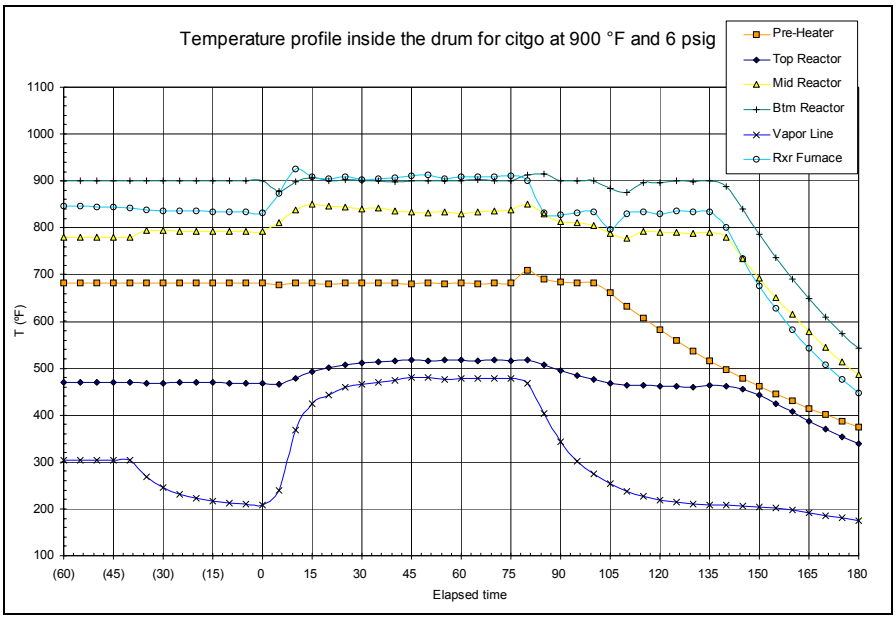

Figure 8 - Temperature profiles inside the drum

3. Stirred Batch Reactor

The stirred batch reactor unit is shown in Figure 9. It consists of a stainless steel cylinder, 13 inches tall and 11 inches outside diameter, with flanged lid. An 8"x 9.5" stainless steel liner that holds the feed and the coke product is placed inside the reactor. In addition, an impeller, for mixing and better heat transfer, is mounted on an overhung shaft and is situated two inches from the bottom. The shaft is driven by a 3-phase motor, which is controlled by an AC inverter for variable speed. The reactor is heated from the outside by two Mica band heaters. Other auxiliary equipment include: two gas-liquid separators, a blowdown tank, a cooler, a gas flowmeter, temperature controllers, and a back-pressure regulator.

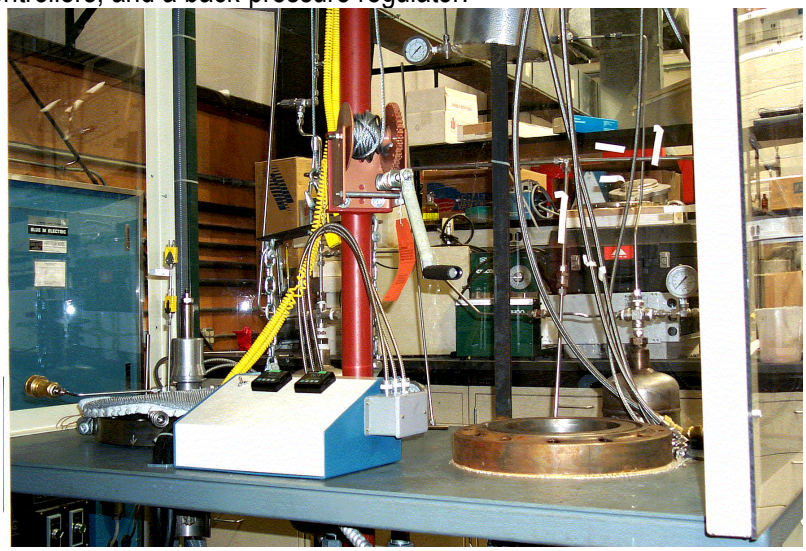

Figure 9 - Stirred Batch Reactor Unit

The main objectives for utilizing this reactor are to:

1. Identify the coke precursors,
2. Study heat rate effect on yields (simulate furnace tube), and
3. Study the kinetics of the thermal cracking reactions.

A hot resid sample is placed inside the liner. The band heaters heat this reactor and liner. To homogeneously heat the feed, the stirrer is rotated at a predetermined shaft speed. Unless there are two phases that cannot be mixed, the mixing effect also helps obtain a homogeneous composition of the contents of the reactor. The system is purged and pressurized with nitrogen to the desired test pressure. Also, the nitrogen displaces the vapor and gases remaining in the system at the end of the run.

During the test, processed resid samples are drawn from the reactor to identify the coke precursors. Since the samples are viscous or solid at room temperature or at a temperature lower than their sampling temperatures, they have to be set in the oven overnight and collected in a 20 ml sample jar. These samples then are analyzed using the high temperature gas chromatograph (HTGC) that can cover up to n-C100-n-C110 (~1330 °F).

The vapor from the reactor flows to the gas-liquid separator that is wrapped with a steam coil. Approximately 80 # steam, 250 °F, is used to cool the hot vapor. Gas that is not condensed flows to a cooler, which uses 37 °F water as a coolant. Liquid from this cooling process is collected in a second gas-liquid separator. The liquid samples are collected using eight receivers (4 for the lights and 4 for the heavies) with quick disconnect fittings. Using the quick disconnect fittings eliminated the need to close the valves during the test. The receivers are connected and disconnected during the test to collect the different condensate batches. The gas trapped with the liquid is taken into account. The liquid and the gas are weighed in the receiver, then the liquid is weighed alone and the differences in weights, i.e. receiver, liquid, and gas, give the mass of the gas. This gas is assumed to have the same composition as the gas analyzed in the GC during the liquid collection period. This system is shown in Figure 10.

Figure 10 - Liquid collection system with Hoke cylinders and quick disconnect valves

The remaining gas flows to a gas flowmeter and then to the online GC. A back- pressure regulator before the flowmeter maintains the system at the desired pressure.

4. Stirred Batch Reactor Upgrades – Quarter 4, 2002 & Quarter 1, 2003

Upgrades to the batch reactor were made. The upgrades were focused on removing operator error in system functions and data acquisition and improving the system functionality. Limiting operator involvement will improve data reproducibility as well as increase time available for liquid sampling. The revised list of upgrades and the status of each upgrade is listed below.

1. The band heaters used in the old runs were run at the upper limits of voltage input causing early failure and limiting control. A new 11 kW ceramic heater was installed to eliminate this problem, see Figure 11,
2. The reactor was machined down from a 1.2 inch wall thickness to a 0.6 inch wall thickness to improve temperature control,
3. Thermocouples – see Figure 12
    a. A thermocouple was installed to read temperature of vapors leaving reactor,
    b. Thermocouples were installed to monitor reactor process temperature,
    c. Thermocouples were installed to monitor furnace element temperature for the purpose of a high temperature shutoff,
    d. Four thermocouples were installed in the reactor head at various heights from the bottom of the reactor. This gives a temperature profile inside the drum.
4. The hydrocarbon liquid collections system was automated, see Figure 13
    a. The light and heavy hydrocarbon liquids are split into 12 tanks each (increased from 4 each)
    b. The heavy tanks were fitted with dip tubes that allow a pressure differential indicator to measure the height of the liquid in the drums.
    c. Labview software is used to control two separate solenoid/pilot actuated manifold systems that step through the series of tanks as they fill. The tank stepping is controlled by the height of the liquids in the heavies tanks, the temperature of the resid in the reactor and time elapsed,
5. A computer bypass switching system was installed for emergency and cleaning purposes, see Figure 14,
6. A pressure transducer was installed to measure the vapor line pressure for improving gas yield calculations,
7. A pulse meter was installed on the wet test meter for acquisition of gas volume, see Figure 15,
8. Labview software that is used for system controls and data acquisition(T's, P's and flows), see Figure 16 and Figure 17

The Labview tank switching controls and data acquisition functions are in working order. The three variables for switching - time, temperature and liquid level - have all been tested. Each variable was tested individually by adjusting the set points for each tank and visually verifying that the next tank in sequence was activated. All three variables were then turned on simultaneously to verify that any of the three variables reaching its set point would cause a tank switch. For the case where an inadvertent switch occurs during operation, a tank increment and decrement switch was installed on the tank switching page in Labview, see Figure 17. For emergency and cleaning purposes a computer bypass switching system was installed. This switching system allows the operator to manually step through the series of tanks, see Figure 14 and Figure 18.

Figure 11 - Batch Reactor Furnace

Figure 12 - Batch Reactor Head

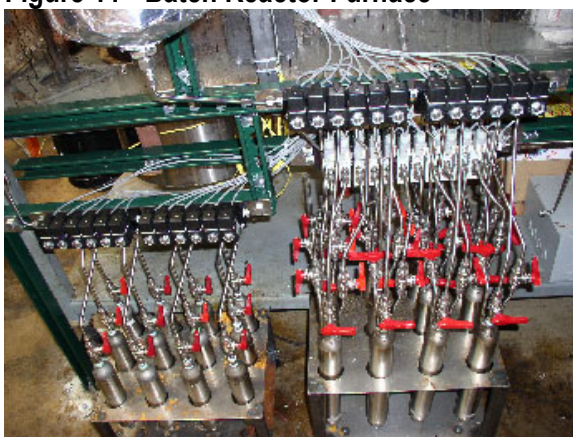

Figure 13 - Batch Reactor Manifold

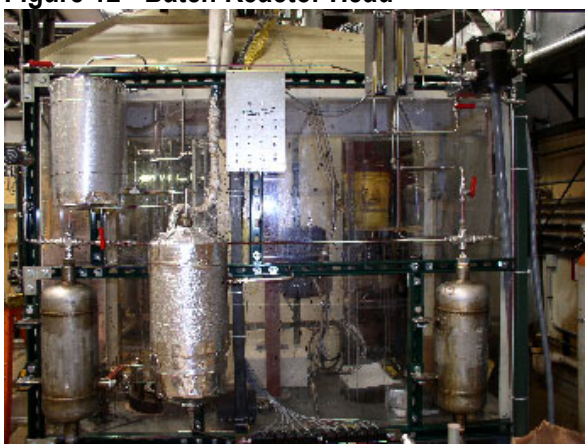

Figure 14 - Batch Reactor Tanks and Bypass Switching System

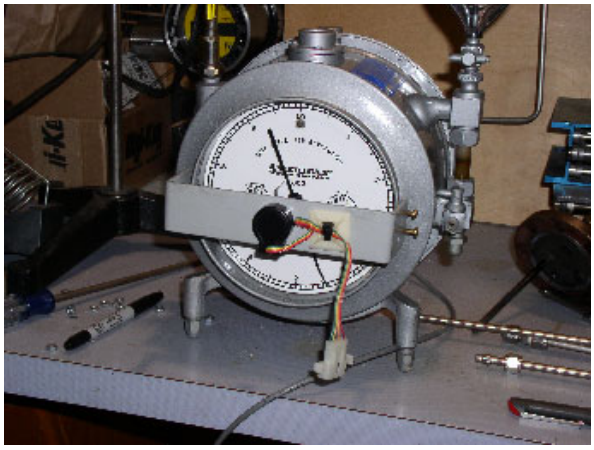

Figure 15 - Batch Reactor Wet Test Meter

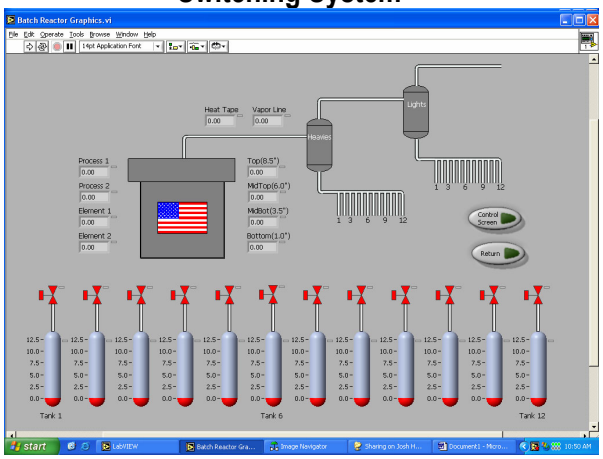

Figure 16 - Batch Reactor Labview

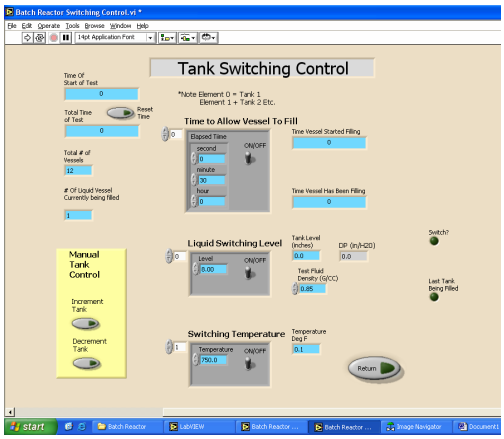

Figure 17 - Batch Reactor Labview

Figure 18 - Batch Reactor Back Side View

Sample Tube Upgrades

The old sampling tube was very cumbersome. It required many valves, attached nitrogen lines to purge resid from inserted tube and time to take each sample. The old sample tube can be seen in Figure 19. The new sample tube consists of a ½" diameter compression chamber between two valves and a collection tube that is inserted into the reactor, see Figure 20. The sample tube uses the pressure in the system to force the feed into the sample tube, compressing the gases above. The size of the compression chamber was calculated using a desired sample size of 30 mL. The pressure of most of the batch runs will be approximately 3.72 atmospheres (40 psig). The gases in the compression chamber before the bottom valve on the sample tube is opened are assumed to be one atmosphere. Thus, the compression chamber volume must be approximately 1.27 times the desired sample volume.

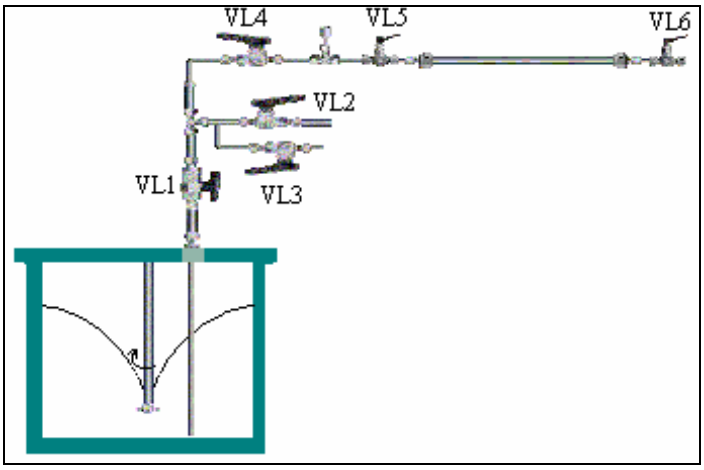

Figure 19 – Old Batch Sample Tube Assembly

The collection tube was designed in two pieces. The bottom portion is ¼" tubing and the top portion is 3/8" tubing. The two piece design was used because the 3/8" tubing holds more sample, minimizing the length of the assembly. The collection tube was oversized to allow a small head space between the sample and the bottom valve. Thus, the losses from each tube are limited to approximately $10 worth of tubing and ferrules.

Figure 20 – New Batch Sample Tube Assembly

The new sample tube assembly was first tested with ambient water and hot oil. The tubes consistently drew 25-30 ml of sample, over a series of eight attempts. A vent line has since been added to the new sample tube assembly above the valve at the bottom of the compression chamber. It was added to prevent any compressed gases above the sample from forcing the sample out of the tube after it is removed from the reactor. The new sample assembly has since been tested in the Marathon recycle facility testing runs. In a series of three facility testing runs, 20+ grams of sample was taken in each attempt.

5. Pilot Unit Equipment

The pilot coker can be viewed as two main pieces: the process equipment and the control system. In the section below each piece is described.

a. Process Equipment Description

The pilot-coker obtained from Equilon Enterprises, LLC is shown in Figure 21. It consists of a feed tank and circulation system, and a furnace with both the preheater and the coke drum. The feed drum holds approximately 15 gallons and is mounted on a scale. Feed passes from the outlet of the drum, goes to a Zenith pump (see Figure 22) with some return flow back to the feed drum. All the lines are steam traced. From the pump, the resid can flow back to the feed tank, to a slop tank or to the furnace. Initially the flow is back to the feed tank to circulate feed and stabilize the temperature. Once the unit is lined out the feed can be switched to a slop tank to check the flow rate (based upon the loss of weight measured by the scale).

When the rate is correct, flow is sent to the furnace. In the furnace are first a preheater coil (mimicking the commercial furnace) followed by a coke drum. The coke drum, with dimensions of 3" x 40" and a volume of ~4,750 cc, is located in the furnace to prevent heat loss. Commercial coke drums are well insulated and have a high volume-to-surface area ratio, making them adiabatic. To simulate commercial steam injection water is injected upstream of the preheater coil. Operating variables include temperature, pressure, steam injection rate, and charge flow rate. The latter two variables affect residence time and Reynolds number.

Figure 21 - Picture of Pilot-Coker Unit

The main objectives for utilizing this reactor are to:

1. Reproducibly mimic commercial operation producing sufficient quantities of coke, liquids and gases for testing,

2. Investigate and correlate the effect of feedstock composition and reactor conditions on product rates & compositions and coke morphology,
3. Maximize distillate product production and minimize coke and gas production,
4. Find ways to reduce tube fouling,
5. Develop and validate a model(s), and
6. Investigate scale-up issues.

This reactor is the workhorse in this Joint Industry Project (JIP) experimental investigation.

b. Control System Description

The control system includes an electrical control box, a cabinet that houses the Foxboro field bus modules (FBM's), a Foxboro µ-IA controller, and Foxboro's Softpack 6.1 control software for NT installed on a 450 MHz Pentium 2 computer (see Figure 23 & Figure 24). The control logic is built on top of the Softpack utilities. The University bought the µ-IA from Foxboro and Foxboro donated the Softpack 6.1 software.

Figure 22 - Zenith pump for pilot-coker

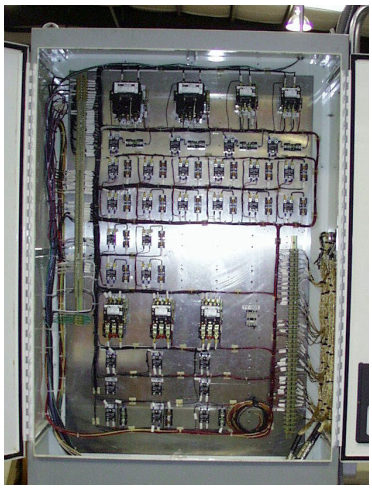

Figure 23 - Electrical control box

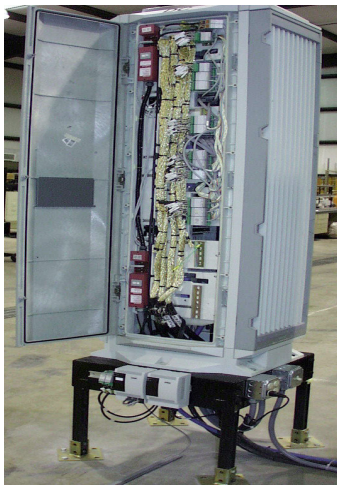

Figure 24 - Foxboro field bus module cabinet and a Foxboro I-IA controller mounted on the bottom

6. Foaming Studies Apparatus

As shown in Figure 25, the pilot unit was modified to study foaming by adding a larger furnace, a gamma densitometer and a lift. The gamma densitometer is used to measure the density of the gas, foam, liquid layer, and coke columns in the drum. The data, as a function of height is displayed on the control monitor for each scan. Time, drum location and the corresponding density are recorded in an Excel spreadsheet. A Macro was built that plots the data as height vs. density as a function of time and density as a function of time vs. height in the drum. This set up allows the researchers to establish and track, via the forklift, the interfaces and densities as a function of time. The system was automated with a Labview control system.

Figure 25 - New foaming studies apparatus

To obtain a continuous flow of steam, the pulsating pump used in the parametric study was replaced with the HPLC pump that injects continuously. The antifoam is injected using an Eldex Metering Piston pump.

a) *Facilities to inject carrier fluids and antifoaming agent*

As shown in Figure 26, the carrier fluid and antifoam are stored in a calibrated burette to measure the amount of fluid being feed to the antifoam pump. The system is manifolded with a valving system such that the antifoam can be injected overhead or into the feed line. The pump can inject the antifoam/carrier mixture from very low rates to a rate of 600 cc/hr.

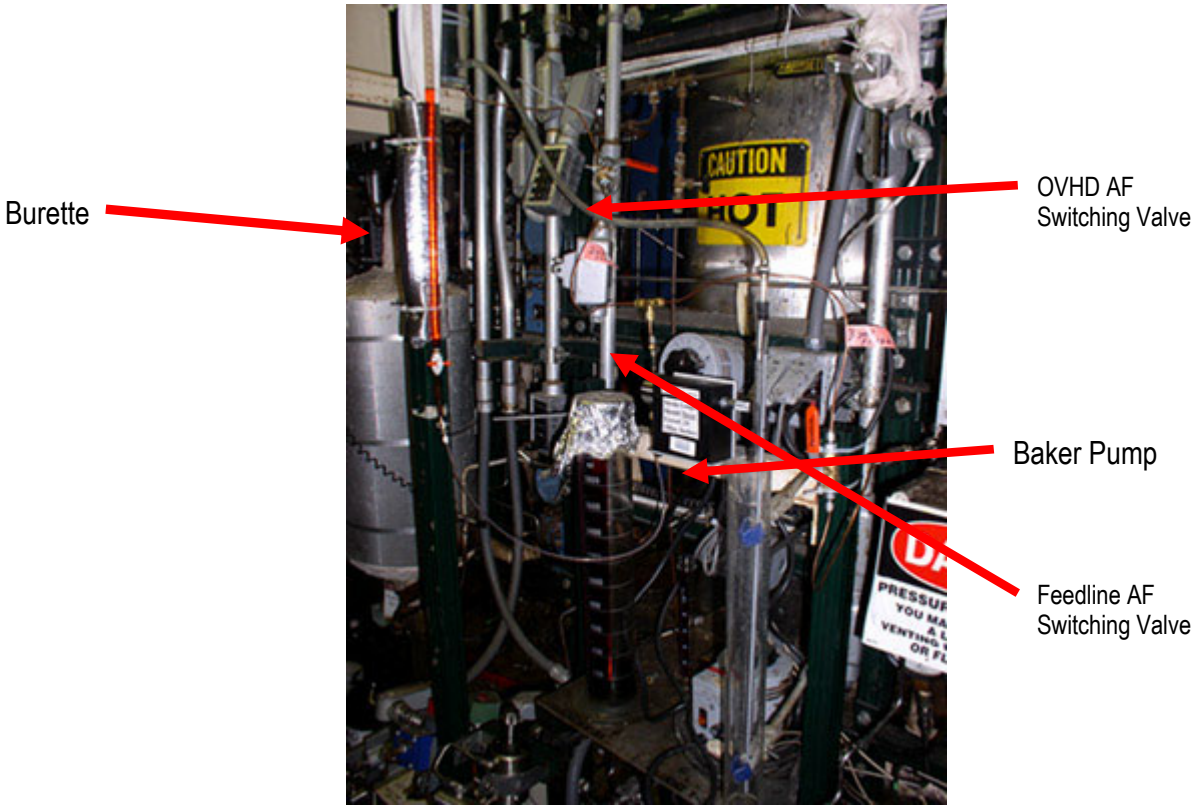

Figure 26 - Injection Antifoam

The objectives of this system are:

1. Quantify foam heights for model development,
2. Compare overhead injection of antifoam versus injection with feed,
3. Determine how antifoam partitions in the products,
4. Establish whether injection of antifoam in the feed alters the coke density, and
5. Longer coking runs (10 to 15 hours at feed rates used in the prior JIP).

b) Quench Water Injection Facilities

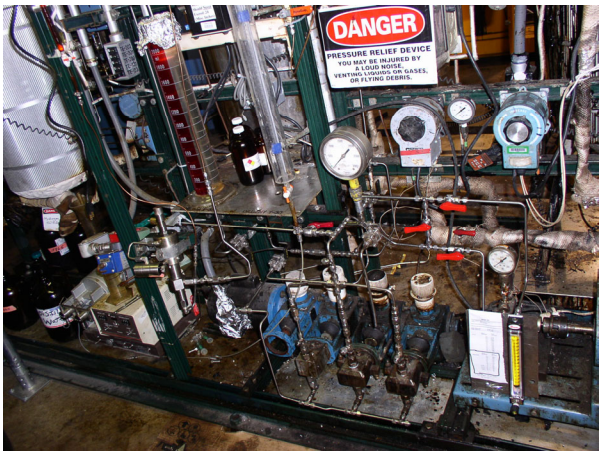

Figure 27 - Water Injection Facilities

7. Utilities

The utilities include an on-line gas chromatograph and caustic scrubber from Equilon, plus an ASTM distillation unit, a HP 5890, HP 6890 HTGC, house air and nitrogen; a University of Tulsa glycol chiller, purchased steam generator, hydrogen sulfide monitors, two freezer; and donated vent hood and oven.

5. Micro Reactor Studies

A. SHAKEDOWN TESTS

During the first facility testing phase of the micro coker, it was found that the gas recoveries were excessively high compared to pilot runs. The cause is considered three phase.

1. The vapor line pressure gauge was giving false (high) readings; this resulted in a high standardized volume of gas.

2. The absence of a carrier gas caused the vapors to become virtually stagnant at the beginning and end of each run, resulting in over cracking.

3. The micro-coker operating temperature was the furnace temperature, instead of an internal liquid temperature used in the pilot unit. This meant that the internal liquid temperature was much lower. The lower internal temperature allows the liquids that are produced to sit in the reactor longer, extending cracking time.

In response to these problems, the run temperature is now controlled by an internal thermocouple at the bottom of the reactor. A pressure transducer was installed to measure the gas pressure more precisely and helium was injected into the top of the reactor to increase the flow rate of the hydrocarbon vapors out of the reactor. Pre-run helium flow data was recorded and an average flow rate was backed out of the final wet test meter reading. It was then determined that the helium carrier which was left running over night was causing the evaporation of some of the liquids in the primary trap. The helium is now being turned off at the end of each run and the system is being isolated to prohibit this evaporation. The gas yields have since made a sizable decrease and are more consistent and comparable to the gas yields seen in the pilot unit. The shakedown runs are listed in Table 8.

The majority of these runs were completed with the old temperature control system and no helium carrier. These runs were rerun with the internal thermocouple as the run temperature controller. The results are presented in the next section.

Table 8 - Micro Coker Yields

Test		T	P		Feed rate			
Number	Date	T(F)	P(psig)	CCR values	(g/min)	liquid%	coke%	gas%
PETMR-4	9/19/2002	910	6	20.7	1.82	60.92%	26.39%	12.69%
PETMR-5	9/24/2002	950	6	20.7	2.01	61.41%	25.00%	13.59%
PETMR-6	9/26/2002	900	15	20.7	2.18	58.10%	29.54%	12.36%
PETMR-10	10/31/2002	930	6	20.7	2.16	64.01%	23.98%	12.01%
PETMR-11	11/5/2002	930	6	20.7	2.06	64.51%	24.59%	10.90%
PETMR-12	11/7/2002	930	6	20.7	2.13	64.20%	24.71%	11.10%
PETMR-14	11/14/2002	930	6	20.7	2.17	61.33%	25.54%	13.13%
PETMR-18	12/4/2002	930	6	20.7	1.96	60.67%	26.16%	13.16%
PETMR-21	12/16/2002	900	40	20.7	2.04	57.07%	29.55%	12.98%
PETMR-22	12/18/2002	900	15	20.7	2.07	61.09%	27.13%	11.78%
PETMR-23	12/19/2002	900	6	20.7	2.10	62.51%	25.62%	11.87%
PETMR-26	1/7/2003	900	15	20.7	2.17	61.99%	27.85%	10.16%
SUNMR-15	9/4/2002	910	6	20.2	2.14	54.40%	31.60%	14.00%
SUNMR-16	9/10/2002	950	6	20.2	1.77	55.63%	27.59%	16.79%
SUNMR-17	9/12/2002	910	40	20.2	2.07	49.62%	33.79%	16.59%
SUNMR-18	9/17/2002	950	40	20.2	1.70	48.95%	33.61%	17.43%
SUNMR-19	10/10/2002	910	40	20.2	1.75	51.68%	32.93%	15.40%
SUNMR-20	10/15/2002	930	40	20.2	2.27	48.42%	34.07%	17.51%
SUNMR-21	10/17/2002	930	40	20.2	1.92	48.12%	33.38%	18.50%
SUNMR-22	10/22/2002	930	40	20.2	1.79	47.42%	33.38%	19.20%
SUNMR-23	10/29/2002	930	6	20.2	1.93	53.31%	29.29%	17.40%

B. PARAMETRIC TEST & RECYCLE RESTS WITH IN-HOUSE RESIDS

1. Test Results for In-house Resids:

Tests were conducted at two temperatures (900ºF and 930 °F) and at pressures of 6, 15 and 40 psig. A summary of the tests to be conducted with the In-house Resids is shown in Table 9 below.

Table 9: Micro Reactor test completed with In-house Resid

Resid	900°F			930°F			950°F		Total
	6 psig	15 psig	40 psig	6 psig	15 psig	40 psig	15 psig	40 psig	
Chevron	1	1	1	1	1	1	1	1	8
Citgo	1	1	1	1	1	1	1	1	8
Equilon	1	1	1	1	1	1	1	1	8
Marathon	1	3	1	1	1	1	1	1	10
Petrobras	1	1	1	1	1	1	1	1	8
Suncor	1	1	1	1	1	1	1	1	8
Total	6	8	6	6	6	6	6	6	50

Due to the minimum effects that residence time had on the product distributions in past runs, it was eliminated as a variable in the test matrix. In order to improve the comparison of micro unit data to pilot unit data, all runs will be made at medium residence times.

2. New Micro-Coker Recoveries

The reproducibility of the micro-coker data was established by using the Marathon resid at 15 psig and 40 psig at a constant temperature of 900 °F. The results are shown in and Figure 29. Good reproducibility was obtained for both the 15 and 40 psig runs.

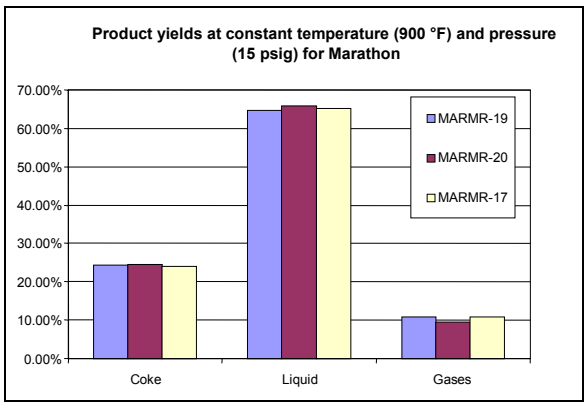

Figure 28 Product Yields at constant Temp. and Pressure for Marathon

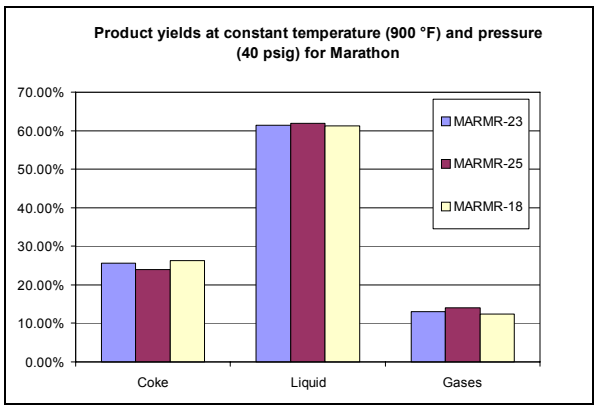

Figure 29 Product Yields at constant Temp. and Pressure for Marathon

Summary of unnormalized product recoveries for all the runs completed in the modified micro-coker is provided in Table 10.

Table 10: Micro-Coker yields for all six resids: Unnormalized and normalized yields:

		CONDITIONS			
Test		T	P	Feed rate	%
Number	Date	T(°F)	P(psig)	(g/min)	Total%
CHVMR-4	3/5/2003	930	6	2.31	96.42%
CHVMR-10	3/25/2003	900	40	2.15	97.21%
CHVMR-11	3/26/2003	930	15	1.21	98.86%
CHVMR-15	6/9/2003	930	40	2.04	97.12%
CHVMR-17	7/10/2003	950	15	2.09	98.38%
CHVMR-18	7/15/2003	950	40	2.07	98.96%
CHVMR-19	7/30/2003	900	6	2.20	97.20%
CHVMR-20	7/31/2003	900	15	2.13	99.15%
CITMR-2	3/28/2003	900	6	2.13	96.92%
CITMR-3	3/31/2003	900	15	2.18	100.04%
CITMR-4	4/2/2003	900	40	2.19	100.36%
CITMR-6	4/3/2003	930	6	2.19	98.92%
CITMR-8	4/8/2003	930	15	2.23	98.96%
CITMR-10	6/10/2003	930	40	1.85	99.14%
CITMR-11	6/19/2003	950	15	1.93	97.02%
CITMR-12	6/24/2003	950	40	1.99	99.32%
BQMR-14	2/13/2003	900	6	2.18	99.53%
BQMR-16	2/18/2003	900	15	2.01	96.91%
BQMR-17	2/19/2003	900	40	1.94	98.12%
BQMR-18	2/20/2003	930	6	1.85	98.73%
BQMR-22	4/23/2003	930	40	2.16	97.51%
BQMR-23	5/13/2003	930	15	2.05	95.75%
BQMR-24	7/16/2003	950	15	2.00	98.43%
BQMR-25	7/22/2003	950	40	1.91	100.26%
MAYMR-16	1/13/2003	900	6	2.02	96.04%
MAYMR-17	1/16/2003	900	15	2.18	96.59%
MAYMR-19	1/23/2003	900	15	1.97	98.17%
MAYMR-20	1/24/2003	900	15	1.99	100.84%
MAYMR-21	1/28/2003	930	6	1.85	98.14%
MAYMR-22	1/30/2003	930	15	2.15	96.47%
MAYMR-31	6/4/2003	900	40	2.17	97.39%
MAYMR-32	6/12/2003	930	40	2.1	96.71%
MAYMR-33	6/13/2003	950	15	2.09	98.61%
MAYMR-36	8/5/2003	950	40	2.28	98.50%
MAYMR-38 (5% rec)	8/13/2003	900	6	2.24	95.98%
MAYMR-39 (5% rec)	8/21/2003	930	6	2.21	98.24%
MAYMR-40 (5% rec)	8/25/2003	900	15	1.86	97.43%
MAYMR-41 (5% rec)	8/26/2003	930	15	2.22	96.05%
MAYMR-42 (5% rec)	8/27/2003	900	40	2.27	94.37%
MAYMR-43 (5% rec)	9/2/2003	930	40	2.22	98.71%
MAYMR-44 (5% rec)	9/3/2003	950	15	2.19	97.78%
MAYMR-48 (10% rec)	9/16/2003	900	6	2.1	99.25%
MAYMR-49 (10% rec)	9/18/2003	900	15	2.06	97.25%
MAYMR-50 (10% rec)	9/22/2003	900	40	2.16	96.09%
MAYMR-51 (10% rec)	9/24/2003	930	6	2.09	95.45%
PETMR-26	1/7/2003	900	15	2.17	97.87%
PETMR-27	1/10/2003	930	15	2.06	98.13%
PETMR-28	2/3/2003	900	6	2.13	97.84%
PETMR-31	2/11/2003	930	40	2.08	98.34%
PETMR-33	4/17/2003	900	40	2.1	103.68%
PETMR-35	4/24/2003	930	6	2.17	100.20%
PETMR-36	6/17/2003	950	15	2.06	98.12%
PETMR-37	6/18/2003	950	40	1.86	97.64%
SUNMR-25	4/30/2003	900	15	2.19	98.61%
SUNMR-26	5/1/2003	900	40	2.23	97.46%
SUNMR-27	5/5/2003	930	6	2.16	96.93%
SUNMR-29	5/8/2003	930	40	2.05	99.85%
SUNMR-30	5/12/2003	930	15	2.22	99.18%
SUNMR-31	5/15/2003	930	15	2.19	101.62%

3. Comparison to Phase One Runs

In order to compare old data to new data, the old data was adjusted using a new correction and normalization procedure. The Old vs. New runs comparisons are listed in Table 11. The lower interior temperature and the absence of carrier gas caused higher coke and lower liquid yields in the old runs. High

gas readings for the old runs were due to overcracking of stagnant vapors inside the reactor. A comparison of the yields was done for three resids; Marathon, Equilon and Petrobras at the same temperature and pressure. The comparisons for coke, liquid and gas yields are shown in Figure 30 through Figure 32.

Table 11: Micro Reactor Yields – Old vs. New Runs Comparison

RUN	Test Number	Date	T(ºF)	P (psig)	Coke%	Liquids%	Gases%
OLD RUN	EQMR-7b-PM	10/13/1999	930	6	33.60%	52.54%	13.87%
NEW RUN	EQMR-18	2/20/2003	930	6	32.81%	55.17%	12.02%
OLD RUN	EQMR-13	12/8/1999	930	40	39.78%	43.30%	16.92%
NEW RUN	EQMR-22	4/23/2003	930	40	37.89%	48.86%	13.25%
OLD RUN	MARMR-2-BT	12/13/1999	930	40	26.8%	55.8%	17.4%
NEW RUN	MARMR-24	4/11/2003	930	40	23.47%	63.00%	13.53%
OLD RUN	MARMR-7	1/14/2000	900	15	27.1%	58.9%	14.0%
NEW RUN	MARMR-19	1/23/2003	900	15	24.39%	64.77%	10.84%
OLD RUN	MARMR-9	1/21/2000	930	15	24.1%	58.2%	17.7%
NEW RUN	MARMR-22	1/30/2003	930	15	22.57%	66.18%	11.25%
OLD RUN	MARMR-13	2/8/2000	930	6	22.5%	64.9%	12.6%
NEW RUN	MARMR-21	1/28/2003	930	6	21.51%	67.70%	10.79%
OLD RUN	PETMR-2B-FS	6/5/2000	930	15	26.88%	61.26%	11.86%
NEW RUN	PETMR-27	1/10/2003	930	15	26.93%	61.35%	11.73%
OLD RUN	PETMR-3	2/21/2000	930	40	29.83%	53.98%	16.19%
NEW RUN	PETMR-31	2/11/2003	930	40	29.63%	57.70%	12.66%

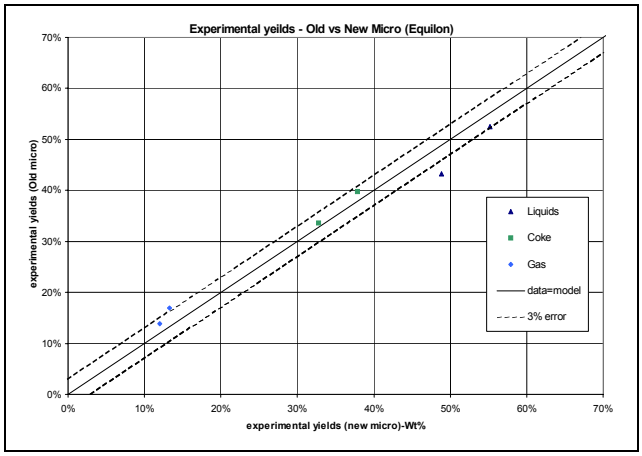

Figure 30 Experimental Yields – Old vs. New runs for Equilon

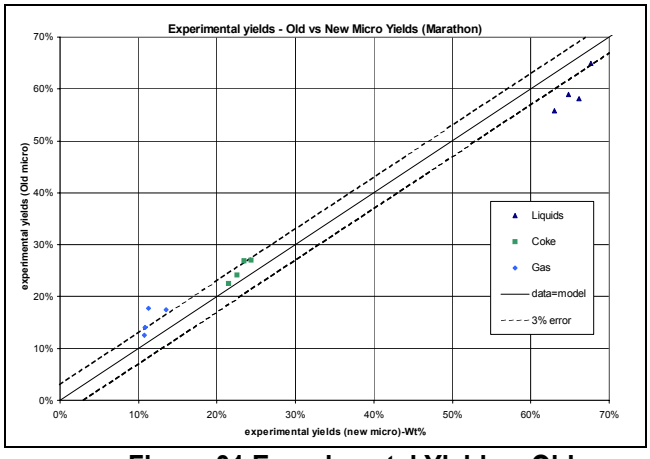

Figure 31 Experimental Yields – Old vs. New runs for Marathon

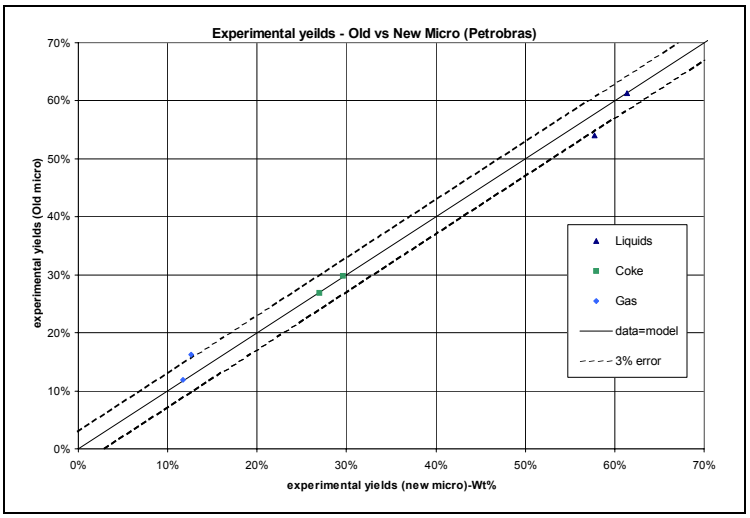

Figure 32 Experimental Yields – Old vs. New runs for Petrobras

Comparison of Liquid sub-product yields for the Marathon resid was done because more test runs were available to compare between old and new micro test runs. Old vs. New liquid sub-product yields are listed in Table 12. The gasoline yields were high for the old runs when compared with new runs because of the overcracking of heavy diesels and gas oils at low interior temperature.

Table 12 Micro Old vs. New Liquid Sub-product Comparisons for Marathon

						Liquid Sub-Products		
RUN	Test Number	Date	T(°F)	P (psig)	% Gas	In terms of wt% of feed		
						Gasoline%	Diesel%	Gas Oils%
OLD RUN	MARMR-2-BT	12/13/1999	930	40	3.00%	27.32%	18.40%	8.92%
NEW RUN	MARMR-24	4/11/2003	930	40	2.00%	24.57%	19.53%	17.64%
OLD RUN	MARMR-7	1/14/2000	900	15	2.00%	23.56%	20.62%	14.14%
NEW RUN	MARMR-19	1/23/2003	900	15	1.00%	18.78%	25.26%	20.08%
OLD RUN	MARMR-9	1/21/2000	930	15	3.00%	23.27%	18.03%	15.71%
NEW RUN	MARMR-22	1/30/2003	930	15	2.00%	19.19%	23.16%	22.50%
OLD RUN	MARMR-13	2/8/2000	930	6	2.00%	18.18%	20.77%	25.32%
NEW RUN	MARMR-21	1/28/2003	930	6	0.00%	16.25%	23.02%	28.44%

Comparison of the Gas Compositions for the old and new runs for Marathon MARMR-7 & MARMR-19 test runs were made. The results are plotted in **Error! Reference source not found.** through **Error! Reference source not found.**. The gas recoveries were high for the old runs when compared to the new runs because of the overcracking of stagnant vapors inside the reactor. The Gases for new runs are collected in less time due to the presence of carrier gas during the run. In all the comparisons, the gas recoveries for the old runs were higher when compared to the new runs except Hydrogen, which showed an opposite trend.

4. Pilot vs. Micro Comparisons:

Comparisons of the Pilot unit to the Micro unit were completed for six resids at the same temperature and pressure. The comparisons in overall and liquid sub-product yields along with temperature profiles inside the drum are shown in Figure 33.

The major difference in the coker tests was that the Pilot unit had liquid temperature controlling and Micro unit had bottom reactor temperature controlling. Micro-Coker test runs showed high coke and low liquid yields when compared to Pilot unit test runs. When the temperature profiles inside the drum were compared, the top reactor temperature for Pilot unit was higher when compared to Micro unit. This resulted in high liquid yields for Pilot unit. The gas yields for the Micro unit were higher when compared to Pilot unit because the vapors overcrack in the Micro unit due to the lower top reactor temperature.

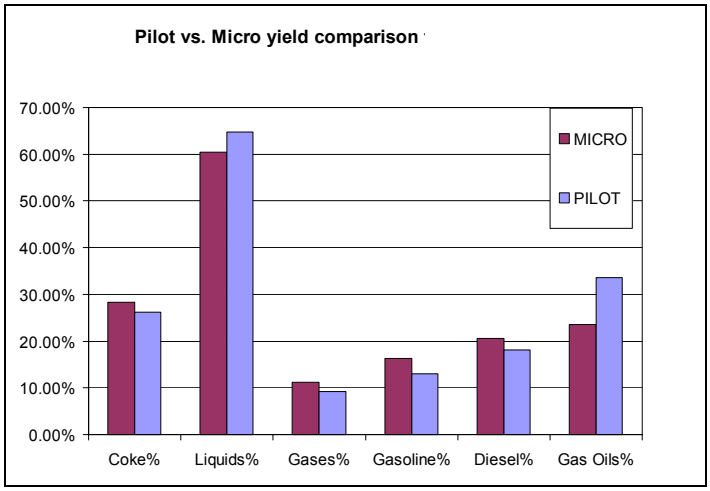

Figure 33 - Pilot vs. Micro

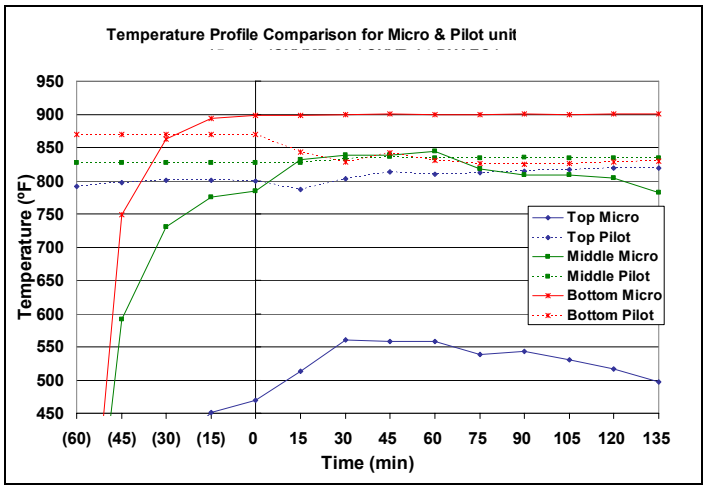

Figure 34 - Temperature Profile for Chevron at 900ºF & 15 psig

When the liquid sub-product yields are compared between the Micro unit and the Pilot unit runs, the Micro unit had high gasoline and high diesels. The heavy hydrocarbon vapors are staying inside the reactor for longer times in the Micro unit, which causes the vapors to overcrack and result in high gasoline and diesels. The gas oil yields were lower for the micro unit when compared to Pilot unit because of low vaporization resulting in more cracking.

5. Confirmation of Known Effects

Results from the micro-coker confirm the expected trends of temperature and pressure on coke and liquid product distributions.

a) *Effect of Temperature on Main and Liquid sub-product yields:*

At a constant pressure of 15 psig, the yield trends were compared at three different temperatures 900ºF, 930ºF and 950ºF respectively. The coke yields decreased for all six resids used when the temperature was increased from 900ºF to 930ºF. When the temperature was increased from 930ºF to 950ºF only Marathon and Petrobras resids showed a further decrease in coke yields whereas the remaining four resids showed an increase. Marathon and Petrobras being paraffinic showed different behavior in the yield trends for coke when compared to other four resids Chevron, Citgo, Equilon and Suncor. The liquid yields increased when the temperature was increased from 900ºF to 930ºF but there was a decrease in liquid yields when the temperature was further increased to 950ºF. This trend clearly shows that the optimum temperature to get maximum liquid yields is 930ºF for four resids Chevron, Citgo, Equilon and Suncor. The paraffinic resids, Marathon and Petrobras, showed maximum liquid yields at 950ºF. The gas yields increased for all six resids when the temperature was increased from 900ºF to 930ºF. When the temperature is further increased to 950ºF, Marathon and Petrobras resids showed a decrease in the gas yields whereas the remaining four resids showed an increase in the gas yields.

When the liquid sub-product yields are compared, gasoline followed no definite trend as the temperature increases from 900ºF to 930ºF. Marathon, Equilon and Chevron resids showed an increase and, Citgo, Petrobras and suncor resids showed a decrease in gasoline yields. However, the majority of the gasoline yields increased when the temperature was increased from 930ºF to 950ºF. The diesel yields decreased and the gas oils yeilds increased consistently for all six resids when the temperature was increased from 900ºF to 930ºF. Some variations in trends were seen when the temperature is further increased to 950ºF.

Despite the new temperature controllers, small fluctuations in the recoveries were seen in product yields for few a runs. The fluctuations may be caused from different temperature profiles inside the drum or because of measuring and operational errors. However these minor fluctuations have little effect on yield correlations in predicting the product yields.

b) *Effect of Pressure on Overall and Liquid sub-product yields:*

At a constant temperature of 900ºF, the coke yields decreased consistently with an increase in pressure from 6 psig to 40 psig and the liquid yields decreased with an increase in pressure following the expected trend. An increase in gas yields was observed when the pressure was increased. When the liquid sub-product yields were compared, the gasoline yields increased and the gas oil yields decreased with pressure. There was no definite trend for diesel.

Small variations in the liquids yields for the Citgo runs at a constant temperature of 900 °F were due to the differences in temperatures profiles inside the drum. Despite the pressure increase, the liquid yields increased. In this situation the effect of temperature dominated the effect of pressure. As shown in the temperature profile plots in Figure 35 and Figure 36, the average top reactor temperature for the 15-psig run was 8°F higher than that of the 6 psig run causing a higher liquid yield.

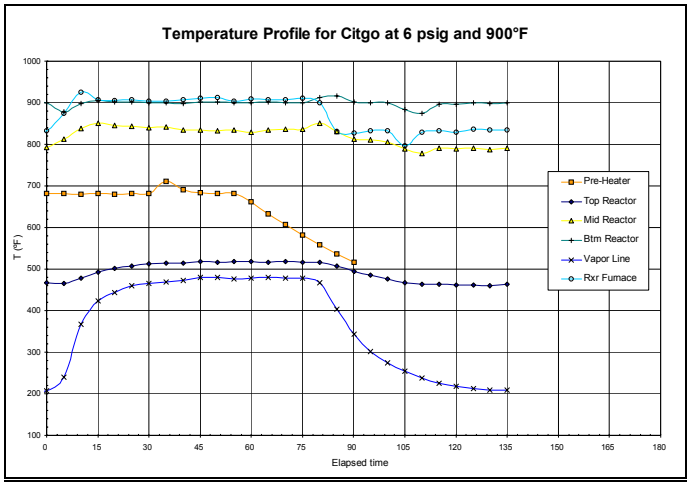

Figure 35 - Temp. profile for Citgo at 6 psig and 900 °F

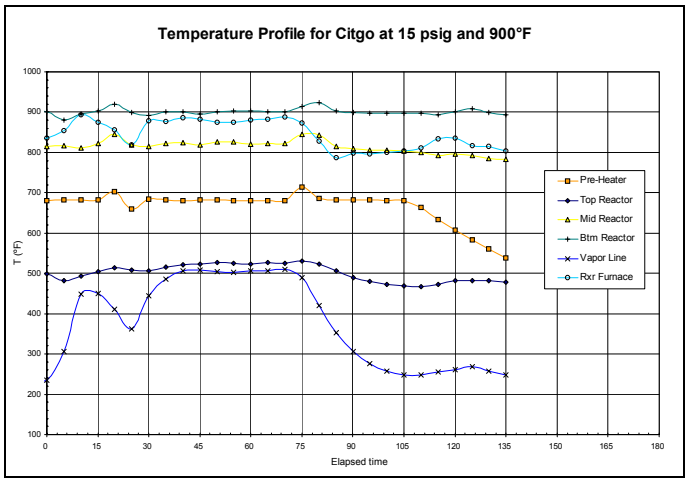

Figure 36 - Temperature profile for Citgo at 15 psig and 900 °F

6. Gas Analysis:

The gas analyses for the Equilon resid to show the effect operating conditions have on gas composition.

a) *Effect of Temperature on Gas Composition:*

Effects of temperature on gas composition were studied at a constant pressure of 15 psig. Hydrogen increased when the temperature was increased from 900°F to 930°F but decreased when the temperature was raised to 950°F. H_2S, Methane, Ethane, C4's and C5's showed a decrease when temperature was increased from 900°F to 930°F but increased when temperature was increased from 930°F to 950°F. Propane, Hexane and olefins showed an increase in composition with temperature. It was also observed that toward the end of the run (after the feed is complete) the gas composition for hydrogen increases.

b) *Effect of Pressure on Gas Composition:*

Hydrogen, ethane and propane increased with an increase in pressure. Methane, H_2S, Hexane, C4's and C5's showed a decrease when the pressure was increased from 6 to 15 psig but showed an increase with pressure from 15 to 40 psig. Olefins increased from 6 to 15 psig and decreased on further increase in pressure to 40 psig.

C. ENHANCED SCREENING MODEL

1. Feedstock Correlations:

Correlations to predict the product yields were developed for six resids. All the correlations developed using the data from the new runs showed considerable improvement in adjusted R square values when compared to the previous correlations using the old run data. Tomas Zambrano's micro-screening model was developed using the old data where the coefficients obtained in these correlations had to be multiplied by constants to minimize error and better match the industrial yields. Since the Modified Micro-Coker has internal temperature control, the yields are comparable to the Pilot unit and to the industrial units. Therefore, no corrections are needed. When the liquid sub-product yields are estimated in terms of total weight percent of feed instead of taking them as weight percent of liquids, the correlations improved for gasoline, diesel and gas oils and are predicted as good as the overall products. The correlations were developed using the steady overhead temperature and pressure as parameters.

.

2. Correlations for Liquid Sub-Product Yields:

Correlations for liquid sub-product yields were done for six resids (Chevron, Citgo, Equilon, Marathon, Petrobras and Suncor). All the yields for the resids lie within 3% error for individual liquid sub product correlations, which is a significant change that has been observed for the new runs when compared to the old runs.

Gasoline predictions were the best for Equilon with 88% of gasoline within 0.5% error when compared to remaining five resids. The best predictions for diesel were for Citgo and for gas oils Petrobras. All of the predictions were within 3% error.

Liquid sub-product yield correlations are listed in **Error! Reference source not found.** through **Error! Reference source not found.**. Gasoline is predicted well for all the resids when compared to diesel and gas oil. Micro recovery comparisons for sub-product yields are listed in **Error! Reference source not found.** through **Error! Reference source not found.**.

3. Overall Correlations for liquid sub-product yields-

Micro recovery comparison-Actual minus Predicted (Model)

The micro-coker screening model uses overhead temperature, pressure and MCR of the resid to predict the overall yields. Using this model, the recoveries for all the new runs were predicted. A slight variation in experimental data was seen in the coke (0.93%), liquid (1.27%) and gas (0.92%) yields when the experimental data was compared to the data predicted with the new micro-screening model.

4. Effect of recycle on product yields:

The recycle runs with 5% recycle and 10% recycle are being tested in the upgraded Micro-Coker equipment using Marathon, Equilon and Suncor resids at temperatures of 900°F, 930°F and 950°F and pressures of 6 psig, 15 psig and 40 psig. Seven micro tests with 5% recycle and four micro tests with 10% recycle were completed using the Marathon resid. A majority of the tests showed an increase in coke yields and a decrease in liquid yields with the addition of recycle. There was no definite trend observed for the gas yields. However, the gasoline and diesel cuts showed an increase and the gas oil cut showed a decrease in the recycle runs except in two of the comparisons. The variation in yields could be because of different temperature profiles inside the drum. The specific reasons behind variations in the recycle effect still need to be verified. This effort will be conducted during the next quarter.

D. CONCLUSIONS:

New thermocouples installed in the micro-coker proved helpful in explaining the discrepancies in product yields with variation in parameters: overhead temperature and pressure.

Individual resid product and liquid sub-product yields were predicted fairly well using linear regression. Overhead temperature and pressure were the parameters used. A slight variation in experimental data was seen in the coke (0.93%), liquid (1.27%) and gas (0.92%) yields when the data was compared to the data predicted with the new micro-screening model. The Micro-Coker tests give high coke and low liquid yields when compared to Pilot unit tests because of low top reactor temperature inside the drum.

Liquid content increased with temperature for the paraffinic resids while the aromatic, Napthenic and intermediate resids showed an optimum at 930°F. The individual liquid sub-product yield predictions improved for the new runs when compared to the previous runs when the liquid sub-product yields are estimated in terms of total weight percent of feed instead of total weight percent of liquids.

E. FUTURE WORK:

The remaining micro-coker recycle runs using the in-house resids will be completed for Marathon, Equilon and Suncor. Tests with the three new resids will then begin. The test matrix for the recycle runs and the new resids is shown in Table 7. The liquid and gas products data will also be analyzed and correlations developed. The product yields follow a curved path with variation in operating conditions for some of the resids. A model will be developed using a polynomial fit for these resids to more accurately predict the yields.

Gas analyses will be done to show the effect of operating conditions on the composition of the gas for the other five resids (Chevron, Citgo, Marathon, Petrobras and Suncor). The effect of recycle on gas composition will also be analyzed. Correlation for recycle will be developed.

6. Batch Reactor Studies

A. FACILITY TESTING

The first runs in the batch reactor were used to test the heating capabilities and the heat loss of the system. The first four runs were made with water. The first run was a system check. It proved the proper function of the data acquisition and controls systems and the new furnace. The three remaining H_2O runs were all operated at similar conditions. Due to the lag time of the heat entering the system, the system cannot be controlled directly by the internal liquid temperature. A high temperature cutoff system was integrated into the controls system. If either of the elements of the split furnace surpasses the set temperature, the power to the furnace is cut. The output to the furnace is set at 100% for each run. The computer records the times when the limit switch is tripped. This allows for an exact measurement of the percentage of time the furnace is on and the wattage that is supplied to the system. This will allow for future calculations of the heat losses of the system.

The system was preheated to an element temperature of 400ºF, see Figure 37. At the start of the run, the element cutoff temperature is set to 1400ºF. The element temperature cycles between 1375ºF and 1425ºF throughout the run, see Figure 38. The furnace continues to cycle until all of the water is vaporized. This can be seen when there is a significant increase in the temperatures throughout the reactor, see Figure 39.

One oil run has been made to date. This run was the first run used to test the liquid separations system. The water runs would have only tested the separation of the lights because the heavy liquids tank is maintained at 300+ºF. The oil used was a vacuum pump oil. The boiling point curve for this oil was made available via the internet. Its IBP was approximately 720ºF and 100% boiling was around 1004ºF, see Figure 40. For the oil run, the warm up and run element temperatures were set at 600ºF and 1400ºF, see Figure 41 and Figure 42. The separations system successfully stepped through each of the tanks using level and temperature limits.

Three runs have been completed using 100% Marathon recycle. The data obtained from these runs is shown in Table 13. The data includes recoveries and cut weights for each of the liquid tanks. The three runs showed very comparable recoveries, see Figure 43. The simulated distillation for each of the liquid fractions has not been completed. The completion of the SimDis could result in an increase in the gas recoveries and a decrease in the liquid recoveries. This is due to the normalization procedure; the masses of all C_3 and C_4 compounds are subtracted from the liquids and added to the gases. The mass of the C_5 and C_6 compounds in the gases have been added to the liquid cut.

The operating procedure used in the old batch reactor runs was used as a guide for the operation of the new batch reactor recycle runs. For warm-up, the furnace element cutoff temperature was set to 700ºF. This correlated to an internal temperature, 1” from the bottom of the drum, between 300ºF and 400ºF. Figure 44 shows the last 60 minutes of the warm-up and the internal temperature profile during the run of MARBR-FT-2.

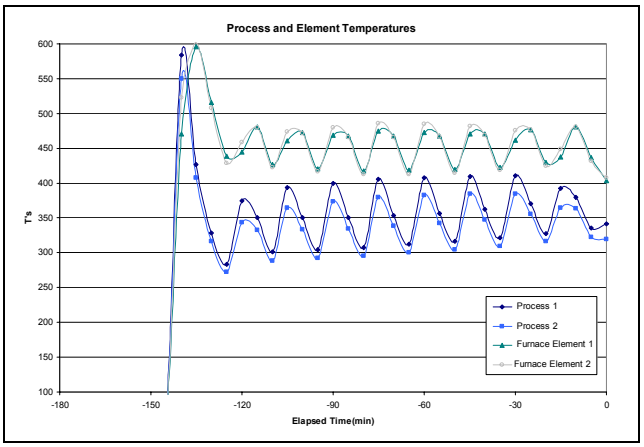

Figure 37 – Batch Element Warm-up Temperature Profile(H2O #4)

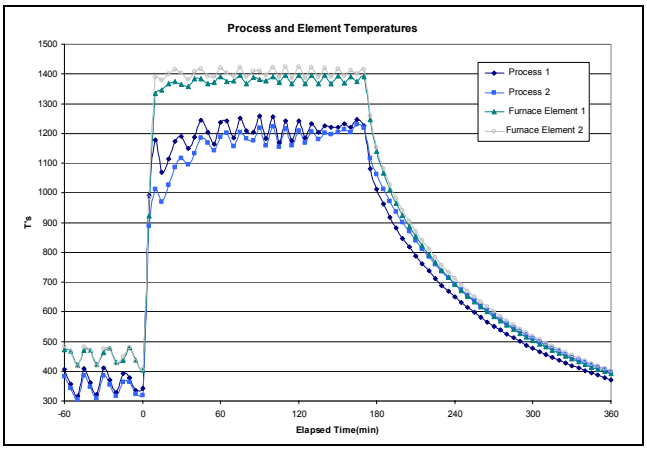

Figure 38 – Batch Element Run Temperature Profile(H2O #4)

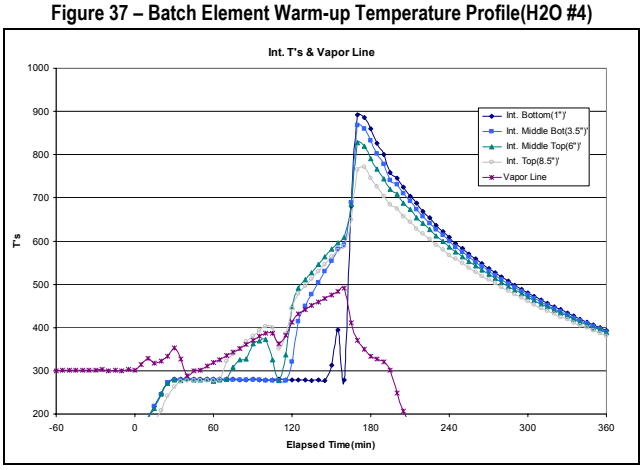

Figure 39 – Batch Internal Run Temperature Profile(H2O #4)

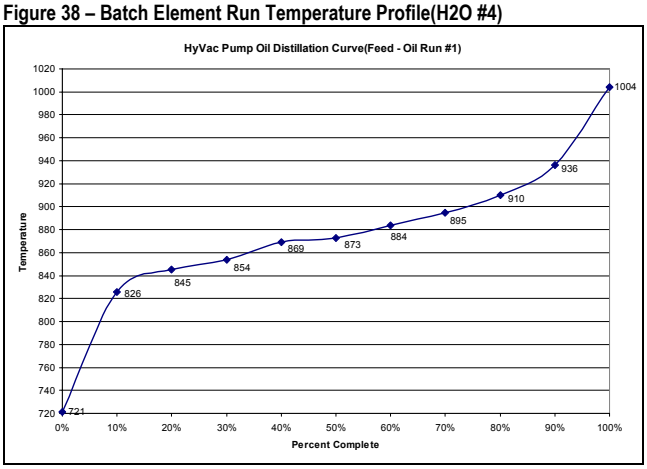

Figure 40 – Batch Vacuum Oil BP Curve(Manufacturer Supplied)

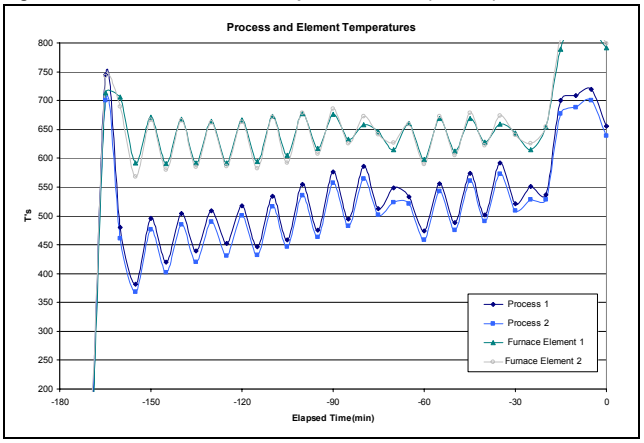

Figure 41 – Batch Element Warm-up Temperature Profile(Oil #1)

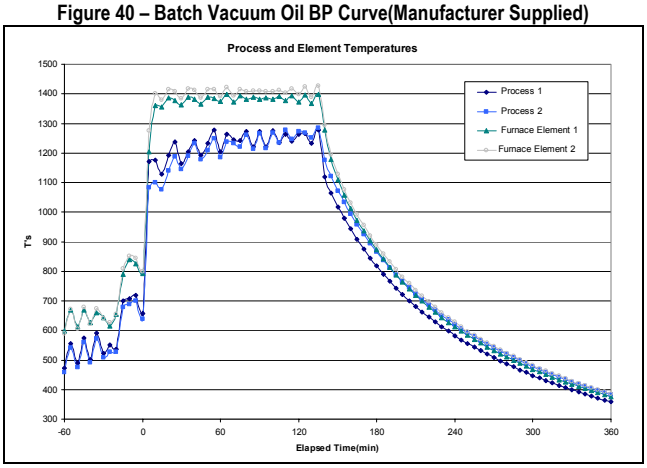

Figure 42 – Batch Element Run Temperature Profile(Oil #1)

During the run the furnace element temperature was set at 1400ºF until the internal temperature 1" from the bottom reached approximately 950ºF. The element limit was then set to 100ºF and the power cut to the elements. The internal temperatures continue to rise during the end of these runs; this will have an affect on the liquid composition and the overall product yields. The temperature profile inside the drum for MARBR-FT-2 can be seen in Figure 44. The next stage of testing will be the shakedown tests. In the

shakedown tests, there will be attempts to maintain the internal temperatures at the bottom of the reactor near 930ºF until the resid has had ample time to react.

Table 13 – Batch Reactor Facility Testing Data – 100% Recycle Runs

		Normalized Recoveries - No C5/C6 Adjustment				
	Run ID	**Coke%**	**Liquids%**	**Gases%**	**Samples**	**Total%**
	MARBR-FT-1	16.95%	73.66%	8.17%	1.23%	100.00%
	MARBR-FT-2	17.18%	73.75%	9.07%	0.00%	100.00%
	MARBR-FT-3	15.56%	74.01%	9.01%	1.42%	100.00%

RunID	MARBR-FT-1		MARBR-FT-2		MARBR-FT-3		Int. Temp(1")
Tank	Lights	Heavies	Lights	Heavies	Lights	Heavies	Temp. Cutoff
Tank 1	2.1	1.7	4.1	6.9	2.0	6.8	750
Tank 2	0.7	7.0	2.6	7.7	0.0	7.6	775
Tank 3	1.3	50.8	2.0	111.6	1.1	123.7	800
Tank 4	0.8	275.4	1.9	208.8	1.3	308.3	825
Tank 5	8.9	327.2	4.5	249.9	4.4	291.1	850
Tank 6	5.0	332.9	5.7	249.4	9.6	282.9	862.5
Tank 7	4.2	334.5	13.1	273.0	7.3	304.6	875
Tank 8	15.8	114.5	18.8	252.5	16.9	302.5	887.5
Tank 9	10.0	51.0	20.3	181.4	20.8	206.8	900
Tank 10	15.3	63.2	12.4	48.0	14.7	53.3	915
Tank 11	12.6	57.0	12.9	14.9	12.1	38.1	930
Tank 12	86.1	307.1	60.0	310.9	38.6	126.9	1000
Main	131.0	5.0	10.3	124.2	21.7	33.9	
Total	293.8	1927.3	168.6	2039.2	150.5	2086.5	

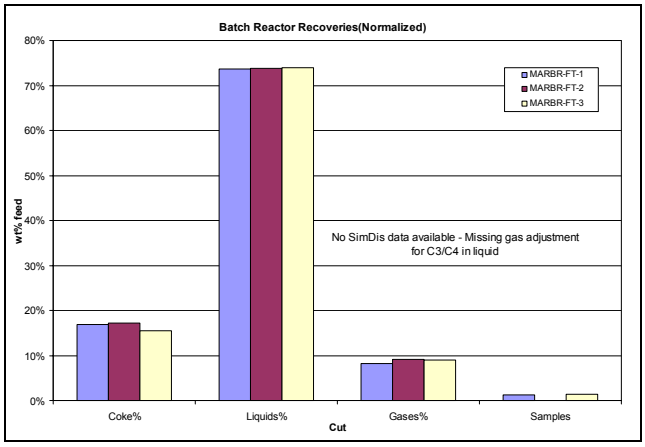

Figure 43 - Batch Facility Testing Recoveries – 100% Recycle Runs

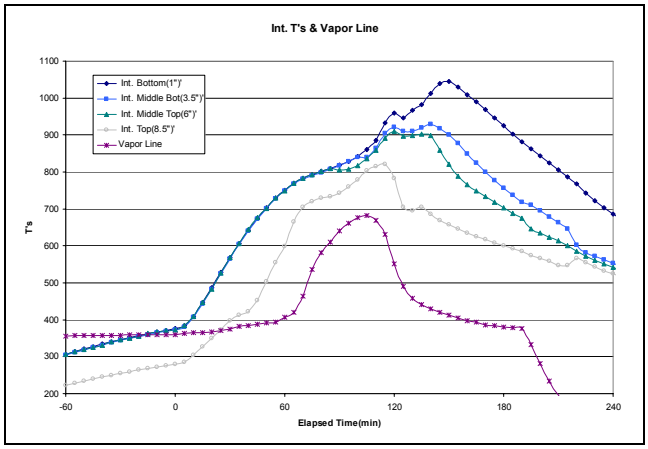

Figure 44 - Batch Facility Testing Recoveries – 100% Recycle Runs – MARBR-FT-2

B. KINETIC MODEL

1. Status of Model

A batch reactor model is developed based on the model used in the literatures by different researchers (Raychaudhuri, Banerjee, & Ghar, 1994; Stangeland, 1974). This model uses the boiling points of the feed that is produced by the HTGC and the operating conditions of the batch reactor to predict the product distributions. A program was written and compiled using FORTRAN to predict the kinetic parameters using a nonlinear least square method. The method used in the program was the known Levenberg-Marquardt method developed separately by Levenberg (Levenberg, 1944) and Donald Marquardt (Marquardt, 1963). The program is still in the testing stage to check its ability to produce the kinetic parameters for the batch reactor.

HTGC data, which is essential to the development of the kinetic model, is completed. These data along with SimDis and GC data will be used in our model to produce the kinetic parameters.

2. Theory of the Kinetic Model

A study of comminution in batch ball milling done by Herbst and Fuerstenau (1968) has led to the development of a phenomenological model. Two primary functions were used to characterize and predict the grinding particle sizes. These two functions are, as called in the comminution field, the selection and breakage functions (Herbst and Fuerstenau, 1968; Reid, 1965). Herbst and Fuerstenau (1968) developed equations (1) through (6) which are the basic equations of their model. These equations were the starting point for other authors (Stangeland, 1974; and Raychaudhuri, Banerjee, and Ghar, 1994) to develop their models for hydrocracking reactions.

Equation (1) is the mass balance equation which describes the behavior of the material of a system. This differential equation can be written in a matrix form as given in equation (2). If the reaction rate, K, is time-independent, an analytical solution can be obtained (Herbst and Fuerstenau, 1968).

$$\frac{dM_i(t)}{dt} = -k_i(t)M_i(t) + \sum_{j=1}^{i-1} v_{ij}k_j M_j(t) \qquad (1)$$

$$\frac{d\underline{M}(t)}{dt} = -\left[\underline{\underline{I}} - \underline{\underline{V}}\right]\underline{\underline{K}}(t)\underline{M}(t) \qquad (2)$$

For the case where no two cracking rates are equal, a solution (Herbst and Fuerstenau, 1968) for the above equation can be obtained as the following,

$$\begin{bmatrix} M_1(t) \\ M_2(t) \\ . \\ . \\ . \\ M_n(t) \end{bmatrix} = \begin{bmatrix} D_{11} & 0 & 0 & . & 0 \\ D_{21} & D_{22} & 0 & . & 0 \\ . & . & . & . & . \\ . & . & . & . & . \\ . & . & . & . & 0 \\ D_{n1} & . & . & . & D_{nn} \end{bmatrix} \begin{bmatrix} e^{-k_1 t} \\ e^{-k_2 t} \\ . \\ . \\ e^{-k_{n-1} t} \\ 1 \end{bmatrix} \quad (3)$$

where the elements of the jth eigenvector, D_{ij}, are given as follow.

$$D_{ij} = \sum_{h=j}^{i-1} \frac{v_{ih} k_h}{k_i - k_j} D_{hj} \qquad i > j \quad (4)$$

$$D_{ij} = M_i(0) - \sum_{h=1}^{i-1} D_{ih} \qquad i = j \quad (5)$$

$$D_{ij} = 0 \qquad i < j \quad (6)$$

To solve the above equations, one has to determine v_{ij} and k_i. Stangeland (1974) and Raychaudhuri et al. (1994a, 1994b) used three adjustable parameters to determine these values. It is worthwhile to mention that these authors used the same equations, equations (10) through (14); originally developed by Stangeland (1974), to determine the model parameters with only different units for the temperature and, subsequently, adjusting the constants. However, Raychaudhuri et al. (1994b) correlated the parameters with temperature in three simple equations as the following.

$$A = \frac{887.4}{(T + 459.67)} - \frac{194656}{(T + 459.67)^2} \quad (7)$$

$$B = \frac{(T - 32)}{240} - 4.0 \quad (8)$$

$$C = 7.50486 \times 10^{-24} (T + 459.67)^{7.5} \quad (9)$$

Equations (7), (8), and (9) when combined with equations (10) through (14) form the complete model for hydrocracking cracking reactions.

$$k_i = \frac{TBP_i}{TBP_f} + A\left[\left(\frac{TBP_i}{TBP_f}\right)^3 - \frac{TBP_i}{TBP_f}\right] \quad (10)$$

$$[C_4] = C \times \exp[-0.00693(TBP_j - 250)] \quad (11)$$

$$x = \frac{TBP_i - 50}{TBP_j - 150} \quad (12)$$

$$V_{ij} = x^2[1 + B(x-1)](1 - [C_4]) \quad (13)$$

$$y_{ij} = V_{ij} - V_{i-1\,j} \quad (14)$$

Stangeland (1974) suggests that an extension of his model could describe the yield from thermal cracking and coking reactions. In our research, we are interested in both reactions especially what is happening in the furnace tube of the delayed coker. To achieve this, the stirred batch reactor is being modeled using the above equations, mainly the one developed by Herbst and Fuerstenau (1968).

Although the theoretical model is complete, it still needs an algorithm to find the model parameters, equations (7), (8), and (9), for hydrocracking applications. A nonlinear least-squares method was developed by Marquardt (1963) and Levenberg (1944) which we are utilizing in our model to find the model parameters.

The problem to be solved is as the one given by Marquardt (1963) as in equation (15).

$$y = f(x_1, x_2, ..., x_m; \alpha_1, \alpha_2, ..., \alpha_k) \quad (15)$$

In the above equation, the dependent variable y_i is produced by the independent variable x_i and the model parameters α. A solution of the problem is reached when we find the parameters that will minimize the squared difference between the observed and the predicted variable as given in equation (16).

$$\Phi = \sum_{i=1}^{n} \left[Y_i - \hat{Y}_i \right]^2 \quad (16)$$

Because of the nonlinearity of the model, other methods such as the Gauss method or the Gauss-Newton method will not work. This led Marquardt (1968) to develop an algorithm which benefits from the speed of the Newton-Raphson method and the power of convergence found in the gradient methods.

3. Batch Reactor Modeling

The proceeding section describes the kinetic model that was originally developed for comminution ball milling and then modified for hydrotreating and hydrocracking processes. The assumptions that were used in developing this model, i.e. reaction rates are independent of time, facilitated the integration of the mathematical equations; however, it limited the models usefulness to constant reaction rates with respect

to time. To work around this assumption, Stangeland (1974) used relative reaction rates which are based on the heaviest pseudo component in the feed. Again, the relative reaction rates are time-independent.
The batch reactor data were obtained under nonisothermal conditions; thus, the model should account for changes of the reaction rates with time. For example, in Figure 45 the weight fraction of the heaviest pseudo component is decreasing exponentially with time. If we use equation (1) with a subscript 1 we get equation (17).

$$\frac{dM_1(t)}{dt} = -k_1(t)M_1(t) \qquad \textbf{(17)}$$

Equation (17) cannot be integrated unless k_1 is constant or it has a known form that can be integrated. If we integrate equation (17) assuming a constant k_1, this will give an average k_1 which is not representative of each reaction rate.

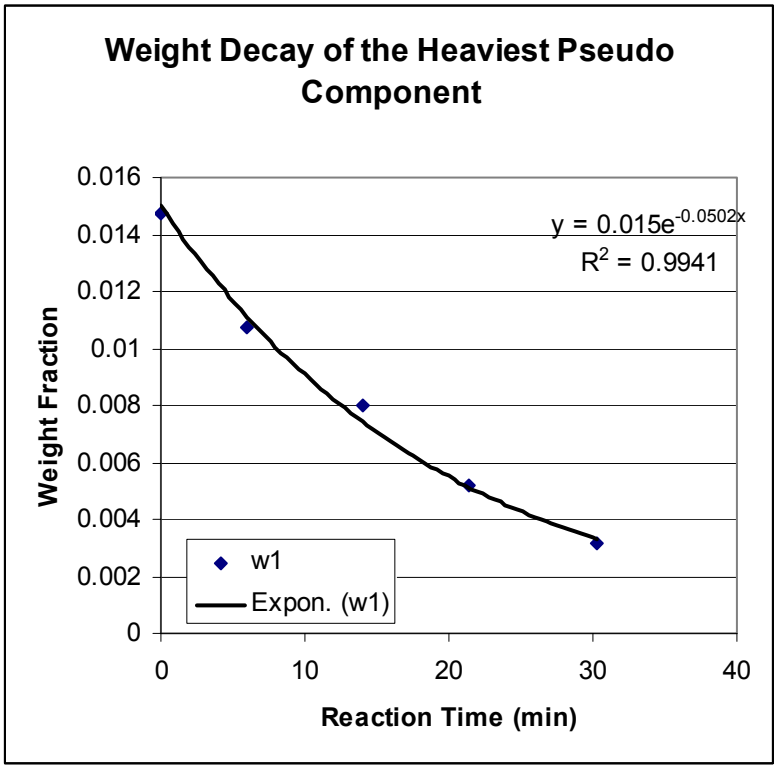

Figure 45 - Reaction rate for the heaviest pseudo component (CHVBR-20)

To overcome this problem we introduce the reaction rate equation we derived before, namely the Coats-Redfern equation.

$$\ln\left(-\frac{\ln[(M_i)]}{T^2}\right) = \ln\left[\left(\frac{A_{i0}R}{E_i}\right)\left(1-2\frac{RT}{E_i}\right)\right] - \frac{E_i}{RT} \qquad \textbf{(18)}$$

Differentiating equation (18) with respect to time leads to the following equation;

$$\frac{dM_i(t)}{dt} = -\left[A_i \left(1 - 6\left(\frac{RT}{E_i} \right)^2 \right) e^{\left(-\frac{E_i}{RT} \right)} \right] M_i(t) \qquad \textbf{(19)}$$

By comparing equation (17) and equation (19) we reach to equation (20) which is the form of k_1 as a function of time since temperature is a function of time.

$$k_1(t) = A_1 \left(1 - 6\left(\frac{RT}{E_1} \right)^2 \right) e^{\left(-\frac{E_1}{RT} \right)} \qquad \textbf{(20)}$$

Application of equation (18) gives us the values for the activation energy and frequency factor as given in Table 14.

Table 14 - Activation energy and frequency factor for the heaviest pseudo component (CHVBR-20)

E =	17474	A0 =	1.57E+09
t (min)	T (K)	k by Arrhenius	k by equ. (20)
0.0	674.8	8.92E-03	8.84E-03
6.0	685.9	1.36E-02	1.34E-02
14.0	699.8	2.25E-02	2.23E-02
21.3	713.7	3.66E-02	3.62E-02
30.3	727.6	5.84E-02	5.78E-02

4. Programming of Kinetic Model

A FORTRAN program for the Levenberg-Marquardt algorithm was obtained from the website of Argonne National Laboratory (ANL) to use in our model. As shown in Figure 1, the program is divided into separate sections. Each block in the flow diagram represents a subroutine or a function that is essential for the algorithm to be successful. Fortunately, this program is well documented which makes it easy to be read and understand. The subroutine LMDIF is the main subroutine in ANL's program. Its purpose is to minimize the squares of *m* nonlinear equations in *n* parameters using the Levenberg-Marquardt algorithm. A brief description is given at the end of the modeling section for each subroutine and function in this flow diagram.

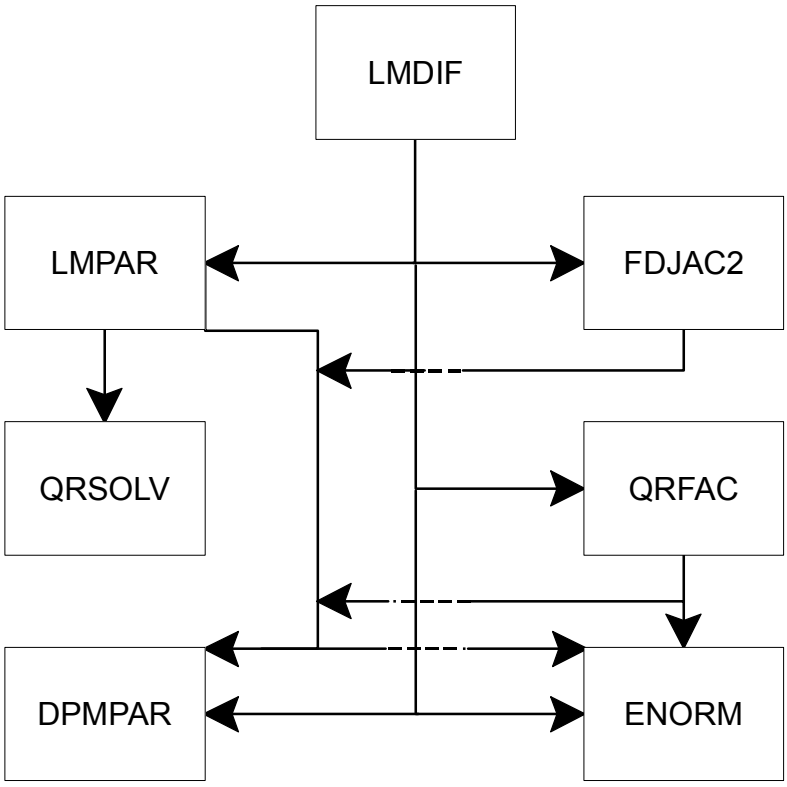

Figure 46 - Flowchart for the Levenberg-Marquardt algorithm built by LAN

The Levenberg-Marquardt algorithm given in Figure 46 is connected with the kinetic model in Figure 47 that we are developing at TU. Each block in Figure 47 represents a subroutine or a function written in FORTRAN. The connection between the program in Figure 46 and the program in Figure 47 is shown in Figure 48. The program was tested and verified to work properly.

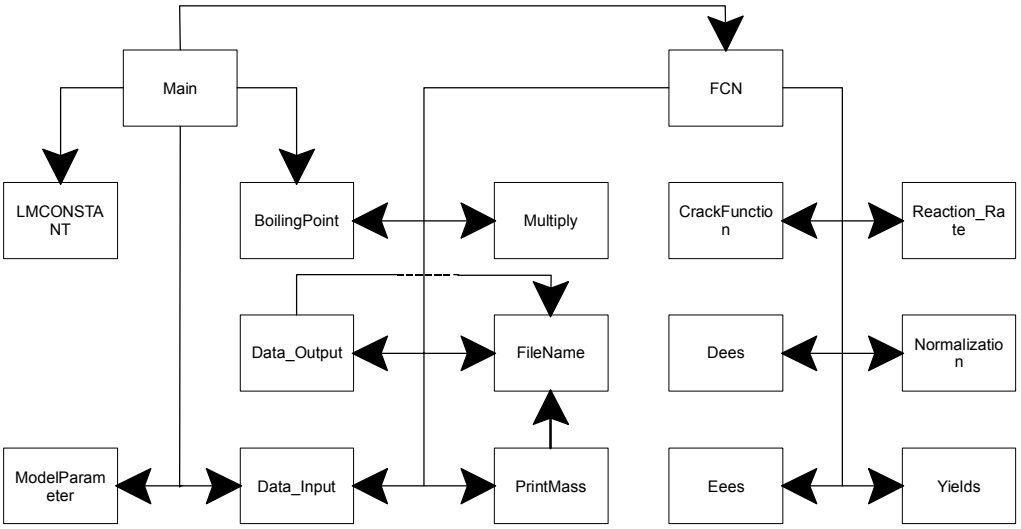

Figure 47 - Flow Diagram for the Kinetic Model Programmed in FORTRAN

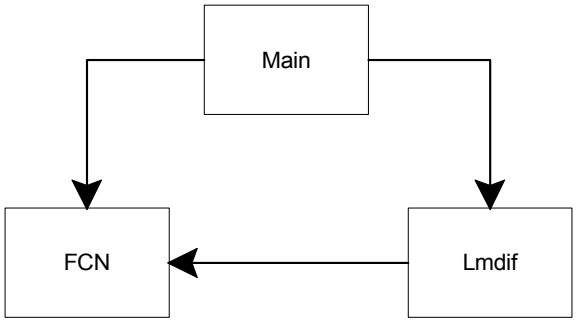

Figure 48 - Connection of the Levenberg-Marquardt Algorithm and the Kinetic Model

The subroutine and function names used in Figure 46 are described below.

- DPMPAR: A function that specifies the double precision machine parameters.
- ENORM: A function that calculates the Euclidean norm of x.
- FDJAC2: A subroutine that calculates the forward difference approximation for the m by n jacobian matrix.
- LMDIF: A subroutine that minimizes the sum of the squares of m nonlinear functions in n variables by a modification of the Levenberg-Marquardt algorithm. It calculates the jacobian of the functions by the forward-difference estimation.
- LMPAR: A subroutine that determines the parameters of the model.
- QRFAC: A subroutine that uses householder transformation to determine an orthogonal matrix q and an upper trapezoidal matrix r.
- QRSOLV: A subroutine that solves for the matrices provided by QRFAC.

The subroutine and function names used in Figure 47 are listed below alphabetically with a brief description.

- BoilingPoint: A subroutine that produces the pseudo components using the TBP curve.
- CrackFunction: A subroutine to calculate the stoichiometric coefficients of the pseudo components.
- Data_Input: A subroutine that gets the data from a text file.
- Data_Output: A subroutine that prints the output into a text file.
- Dees: A subroutine to calculate the matrix elements in equation (3) using equations (4), (5), and (6).
- Eees: A subroutine to calculate the elements of the column matrix on the right side of equation (3).
- FCN: A subroutine that calculates the matrices and provides them to other subroutines to calculate the model parameters.
- FileName: A subroutine that chooses the names of the output files.
- LMCONSTANT: A subroutine that reads the constants used in LMDIF from a text file, otherwise it will give a preset values if there is no text file.
- Main: The main driver of the FORTRAN program used for the kinetic model.
- ModelParameter: a subroutine that initializes the model parameter to start the calculation.
- Multiply: A subroutine that multiplies two matrices together and find a column matrix.
- Normalization: A subroutine to normalize the pseudo components to the heaviest feed component.
- PrintMass: A subroutine to print the masses to an output file.
- Reaction_Rate: A subroutine to calculate the reaction rate coefficients of the pseudo components.
- Yields: A subroutine to calculate the weights for the pseudo components.

C. CONCLUSIONS

1. Modeling Conclusions

A model developed for comminution in batch ball milling by Herbst and Fuerstenau (1968) has proven its usefulness in refining fields. It was shown by Stangeland (1974) then Raychaudhuri et al. (1994) that the same model could by used for hydrocracking reactions. Moreover, Stangeland (1974) has suggested an extension of the model to predict and describe the yields of thermal cracking and coking reactions. Therefore, the model is a good candidate to describe the thermal or coking reactions or both that was studied in the batch reactor to simulate the delayed coker furnace tubes. However, the model is developed based on the assumption of time-independent reaction rates. Thus, we have to account for a variable reaction rate with time. Nevertheless, the model is very attractive for the flexibility of its parameters to describe the TBP shapes, the operating conditions, and the severity of the operations. Moreover, the model can be programmed using a computer program to analyze the data which are usually large and can't be calculated by hand anyway. This will give a kinetic model which may be used to simulate a process, i.e. furnace tube, possibly online.

Most of the subroutines and functions were programmed using FORTRAN. There were two distinctive sections in the program. One section calculates the model and then passes it to the other to calculate the model parameters.

The kinetic model program was developed and compiled. However, it is still in the testing stage for tuning it to the batch reactor produced data. Nevertheless, the program has been tried with literature data and it works nicely.

2. Batch Reactor

The water and oil runs were helpful in determining the functionality of the system. The original changes made to the sample tube worked very well with the water runs because they were tested at room temperature. The assembly then proved to be inadequate for the hot oil runs due to the head pressure that builds above the liquid sample, forcing a portion of the sample out of the bottom of the tube. The vent line was then added to relieve the pressure and contain the sample in the tube. Early testing shows that the pressure problem has been alleviated.

The three facility testing runs were completed successfully. The liquid separation system worked as planned and detailed records of the rate of liquid production was recorded. The recovery data was fairly reproducible. Small changes in the overall products were seen and were expected due to the changes in the heating profile. The internal temperatures greatly exceeded the target temperature of 930ºF. The element temperature limit is set at 1400ºF, this corresponds to a process temperature (temperature of the air directly outside the reactor walls) of approximately 1200ºF. Thus, in the future, the power to the elements will be shut off when the internal temperature approaches 900ºF. The heat from the elements will be sufficient to continue heating the resid to the target temperature. Tests with the Petrobras resid will be used to determine the most appropriate time for the power to be turned off.

D. FUTURE WORK

1. Modeling

Development and tuning of the program for the batch reactor data will continue. This will include a subroutine and probably a model parameter to include the heating rate as a variable. When this is done, the model parameters for all feedstock and operating conditions used in the batch reactor will be produced. This model will then serve as a prediction tool to generate the product distribution and the yields for the thermal cracking reaction in the delayed coker.

2. Batch Reactor

The next set of runs will be a series of 4-6 shakedown tests using Petrobras resid. The purpose of these runs is to refine the control settings for liquid tank switching and heating. They will also be used to improve the sample taking procedures and verify reproducibility of the data produced. At the finish of the shakedown runs, a predetermined test matrix will be used as a guideline for future testing, see Table 2. The heat input data has been gathered and organized for the purpose of calculating the heat loss of the system. This is expected to improve the understanding of future kinetic studies.

7. Pilot Unit Studies

A. Discussion of Test Matrix

The pilot unit was modified in the fall of 2001 and then utilized to study foaming. The objectives of the continuation study are:

- To make additional runs to quantify foam heights for model development. Runs will also be made at refinery conditions for scale-up comparisons,
- To quantify the effects of operating variables, such as, pressure, temperature, feed rate, steam velocity over a broader range of feedstocks,
- To compare different antifoam injection schemes such as in the feed, the feed line and overhead using different carriers and dilution rates,
- To determine how the anti-foam partitions in products, and
- To establish whether injecting anti-foam in the feed alters the coke density.

The test matrix for these studies is shown in Table 15. It consists of general tests that are designed to gather as much data as possible from each test on foaming tendencies, the impact of superficial velocity, the impact of parametric and feedstock properties and coke morphology studies and focused tests to gain an understanding of how different injection procedures behave.

Table 15 - Foaming Studies Test Matrix

Type of Test	Temperature	Pressure	Resids	Feed Rates	Recycle Rates	Viscosity	Drum Sizes	Injection Points	Total
General Tests									
1. Parametric and Feedstock									
3 New Resids	3	3	3	1					27
Old Resids Not Tested	2	2	2	2					16
Resids Tested in Foaming	2	2	4	1					16
Recycles	3	2	3	1	2				36
2. At Refinery Conditions	1	1	9	1	?				9
3. Superficial Velocity	3	3	1	1			3		27
Focused Tests									
1. Continuous vs Feed Injectio	1	1	6	1		1		2	12
2. Continuous vs Intermittent	1	1	6	1		1		1	6
3. Carrier Viscosity	1	1	9	1		2	1	1	18
4. Dilute vs Neat Injection	1	1	3	1		2		1	12
Total									179

The continuation studies began June 1, 2002. The test matrix for the first year of study, June 1, 2002 through September 30, 2003, is shown in Table 16 through Table 20.

Table 16 - Focused Tests for Antifoam Optimization

Run #	Resid	Pressure Psig	Temp. °F	Feed Rate Gm/hr	AF Inject Location	Type of Injection	Date Run
Chev 7 PUAF	Chevron	15	900	1200	Ovhd	100L Inter	6/5/02
Sun 9 PUAF	Suncor	15	930	3600	Ovhd	100L Cont	6/20/02
Sun 10 PUAF	Suncor	15	930	3600	Ovhd	100H Cont	7/17/02
Sun 11 PUAF	Suncor	15	930	3600	Ovhd	100H Cont	7/24/02
Sun 12 PUAF	Suncor	15	930	3600	Ovhd	600H Cont	7/30/02
Sun 13 PUAF	Suncor	15	930	3600	Feedline	100H Cont	8/7/02

Table 17 - Pressure & Temp. Runs with Resids not Used in Phase I Foaming Studies

Run #	Resid	Pressure Psig	Temp. °F	Feed Rate Gm/hr	AF Inject Location	Type of Injection	Date Run
Pet 1 PUAF	Petrobras	15	900	2400	Feedline	100H INT	8/15/02
Pet 2 PUAF	Petrobras	15	930	2400	Ovhd	100H INT	8/21/02
Pet 3 PUAF	Petrobras	15	900	3600	Ovhd/FL	100H INT	8/27/02
Pet 4 PUAF	Petrobras	15	930	3600	Ovhd/FL	100H INT	9/5/02
Pet 5 PUAF	Petrobras	40	900	2400	Feedline	100H INT	9/10/02
Pet 6 PUAF	Petrobras	40	930	2400	Feedline	100H INT	9/12/02
Pet 7 PUAF	Petrobras	40	900	3600	Feedline	100H INT	9/17/02
Pet 8 PUAF	Petrobras	40	930	3600	Feedline	100H INT	9/24/02
Mara 1 PUAF	Marathon	15	900	3600	Feedline	100H INT	10/02/02
Mara 2 PUAF	Marathon	15	930	3600	Feedline	100H INT	10/11/02
Mara 3 PUAF	Marathon	15	930	2400	Feedline	100H INT	10/16/02
Mara 4 PUAF	Marathon	15	930	4800	Feedline	100H INT	10/18/02
Mara 5 PUAF	Marathon	15	900	2400	Feedline	100H INT	10/29/02
Mara 6 PUAF	Marathon	40	900	2400	Feedline	100H INT	11/05/02
Mara 7 PUAF	Marathon	40	930	2400	Feedline	100H INT	11/12/02

Table 18 - Pressure & Temp. Runs at Higher Feed Rates for Resids Used in Phase I Foaming Studies

Run #	Resid	Pressure Psig	Temp. °F	Flow Rate Gm/hr	AF Inject Location	Type of Injection	Date Run
CIT 9 PUAF	Citgo	15	900	3600	Feedline	100H INT	11/22/02
CIT 10 PUAF	Citgo	15	930	3600	Feedline	100H INT	12/03/02
CIT 11 PUAF	Citgo	40	900	3600	Feedline	100H INT	12/06/02
CIT 12 PUAF	Citgo	40	930	3600	Feedline	100H INT	12/17/02
CHEV 8 PUAF	Chevron	15	900	3600	Feedline	100H INT	01/07/03
CHEV 9 PUAF	Chevron	15	930	3600	Feedline	100H INT	01/10/03
CHEV 10 PUAF	Chevron	40	900	3600	Feedline	100H INT	01/15/03
CHEV 11 PUAF	Chevron	40	930	3600	Feedline	100H INT	01/23/03
	Suncor	15	900	3600	Feedline	100H INT	Can't Run
	Suncor	15	930	3600	Feedline	100H INT	Can't Run
	Suncor	40	900	3600	Feedline	100H INT	Can't Run
	Suncor	40	930	3600	Feedline	100H INT	Can't Run
EQ 2 PUAF	Equilon	15	930	3600	Feedline	100H INT	03/19/02
EQ 4 PUAF	Equilon	15	900	3600	Feedline	100H INT	02/06/03
EQ 5 PUAF	Equilon	40	930	3600	Feedline	100H INT	02/13/03
EQ 6 PUAF	Equilon	40	900	3600	Feedline	100H INT	02/19/03

Recycle tests with resids from Marathon and Equilon were scheduled to begin in March. However, due to insufficient quantities of these resids to conduct the planned tests, the antifoam optimization studies were begun while additional samples were obtained from Shell and Marathon. The test matrix for these studies is shown in Table 19. The test with Recycle and at refinery conditions began in August 2003. The test matrix is shown in Table 20.

Table 19 - Antifoam Optimization Studies

Antifoam Optimization Studies

Run	T	P	F	Type of AF	Method	Date
	^{O}F	psig	gm/hr			
CHEV 12 PUAFI	900	15	3600	100,000 cSt (0.3 AF/70 D)	O	7/16/2003
CHEV 13 PUAFC	900	15	3600	100,000 cSt (0.3 AF/70 D)	O	7/20/2003
CHEV 14 PUAFC	900	15	3600	100,000 cSt (0.3 AF/70 D)	F	7/29/2003
CHEV 15 PUAFC	900	15	3600	600,000 cSt (0.75 AF/70 D)	F	8/1/2003
CHEV 16 PUAFI	900	15	3600	600,000 cSt (0.75 AF/70 D)	O+F	8/6/2003
PETR 9 PUAFI	900	15	3600	100,000 cSt(30 ml/ 70 ml sun diesel)	O	3/13/2003
PETR 10 PUAFI	900	15	3600	100,000 cSt(3 ml/ 70 ml sun diesel)	O	3/21/2003
PETR 11 PUAFI	900	15	3600	100,000 cSt(0.3 ml/ 70 ml sun diesel)	O	3/26/2003
PETR 12 PUAFI	900	15	3600	None		4/1/2003
PETR 13 PUAFC	900	15	3600	100,000 cSt (0.3 AF/70 D)	O	4/9/2003
PETR 14 PUAFC	900	15	3600	100,000 cSt (0.3 AF/70 D)	O+F	4/15/2003
PETR 15 PUAFC	900	15	3600	600,000 cSt (0.12 AF/70 D) VARIOUS	O+F	4/18/2003
PETR 16 PUAFI	900	15	3600	600,000 cSt (0.75 AF/70 D) VARIOUS	O	4/23/2003
EQU 7 PUAFI	900	15	3600	100,000 cSt (0.3 AF/ 70 D)	O	6/4/2003
EQU 8 PUAFC	900	15	3600	100,000 cSt (0.3 AF/ 70 D)	F	6/11/2003
EQU 9 PUAFI	900	15	3600	100,000 cSt (0.3 ml AF/ 70 ml D)	O	8/29/2003
SUNC 14 PUAFI	900	15	2400	100,000 cSt (0.3 AF/ 70 D)	O	9/10/2003
SUNC 15 PUAFI	900	15	2400	100,000 cSt (0.3 AF/ 70 D)	O	9/17/2003
SUNC 16 PUAFI	900	15	2400	100,000 cSt (0.3 AF/ 70 D)	O	9/25/2003
SUNC 17 PUAFI	928	38	2400	100,000 cSt (0.3 AF/ 70 D)	O	10/1/2003

Table 20 - Test Matrix with Recycle and Refinery Conditions

Resid	T	P	Recycle	Feed Rate	AF	Inj Scheme	Inj Rate	Inj Conc
Marathon	900	15	None	2400	100,000	Overhead	As Needed	0.3 AF/70 cc Dies
Marathon	930	15	None	2400	100,000	Overhead	As Needed	0.3 AF/70 cc Dies
Marathon	900	15	5	2400	100,000	Overhead	As Needed	0.3 AF/70 cc Dies
Marathon	930	15	5	2400	100,000	Overhead	As Needed	0.3 AF/70 cc Dies
Marathon	900	15	10	2400	100,000	Overhead	As Needed	0.3 AF/70 cc Dies
Marathon	930	15	10	2400	100,000	Overhead	As Needed	0.3 AF/70 cc Dies
Marathon	900	15	5	3600	100,000	Overhead	As Needed	0.3 AF/70 cc Dies
Marathon	930	15	5	3600	100,000	Overhead	As Needed	0.3 AF/70 cc Dies
Marathon	900	15	10	3600	100,000	Overhead	As Needed	0.3 AF/70 cc Dies
Marathon	930	15	10	3600	100,000	Overhead	As Needed	0.3 AF/70 cc Dies
Marathon	**Refinery Conditions**							
Equilon	900	15	1	3600	100,000	Overhead	As Needed	0.3 AF/70 cc Dies
Equilon	900	15	5	3600	100,000	Overhead	As Needed	0.3 AF/70 cc Dies
Equilon	900	15	10	3600	100,000	Overhead	As Needed	0.3 AF/70 cc Dies
Eq/Slurry Mix	900	15	As Mixed	3600	100,000	Overhead	As Needed	0.3 AF/70 cc Dies
Eq/Slurry Mix	930	15	As Mixed	3600	100,000	Overhead	As Needed	0.3 AF/70 cc Dies
Eq/Slurry Mix	**Refinery Conditions**							
Suncor	900	15	None	2400	100,000	Overhead	As Needed	0.3 AF/70 cc Dies
Suncor	900	15	None	3600	100,000	Overhead	As Needed	0.3 AF/70 cc Dies
Suncor	900	15	5	2400	100,000	Overhead	As Needed	0.3 AF/70 cc Dies
Suncor	900	15	10	2400	100,000	Overhead	As Needed	0.3 AF/70 cc Dies
Suncor	900	15	5	3600	100,000	Overhead	As Needed	0.3 AF/70 cc Dies
Suncor	900	15	10	3600	100,000	Overhead	As Needed	0.3 AF/70 cc Dies
Suncor	**Refinery Conditions**							

COMPLETED

B. TEST SEQUENCE

The purpose of this section is to give the reader insight as to why the tests were conducted in the sequence listed in Table 16 through Table 20. A detailed discussion of the data collected from these tests will be provided later in this section.

The first set of foaming tests was run using the resid from Suncor June through July 2002. Five tests were conducted at a temperature of 930 °F and a pressure of 15 psig. The objective of this set of tests was to establish the difference between overhead, feed and feed line injection. Tests with carrier viscosities of 100,000 and 600,000 cSt were also conducted and compared. These tests revealed that feed line injection knocked the foam back almost instantaneously, whereas previous tests with overhead injection show the knock down of the foam to be a more gradual process. This finding led to studies that showed the antifoam was being carried out of the drum. An alternate approach for injecting antifoam overhead for higher viscosity carrier fluids was implemented. A pump to inject at higher rates was also added. These results were presented in the October 2002 report.

The second set of foaming tests, parametric studies, was run using the resids from Petrobras. Eight tests were conducted in August and September, 2002. The objective of this set of tests was to gather initial data for one of the two untested resids to provide additional understanding of how each resid is behaving for a given set of operating conditions. This data was used to classify the resids from the worst foamer to the one that foams the least.

The Petrobras tests were run at two feed rates (2400 gm/hr and 3600 gm/hr). The objective of this set of tests was to get an understanding of the effect of superficial vapor velocity and steam velocity on foaming. These tests would also help verify the drum velocity calculations that show the major component of the drum velocity is due to the hydrocarbon vapors.

The Petrobras tests were also used to establish the effects of operating conditions, mainly pressure and temperature, on foaming. Four tests were conducted at two temperatures (900 and 930°F) and two pressures (15 and 40 psig) and a flow rate of 2400 gm/hr and four tests were conducted at two temperatures (900 and 930°F) and two pressures (15 and 40 psig) and a flow rate of 3600 gm/hr. These results were also reported in the October 2002 report. A similar suite of tests were conducted with the Marathon resid during the months of October through November 2002.

To understand how the other in-house resids (Citgo, Chevron, Equilon and Suncor) are behaving as a function of operating conditions, tests were conducted at 3600 gm/hr because tests with these resids were conducted in the prior JIP at 2400 gm/hr. Four tests were conducted at two temperatures (900 and 930 °F) and two pressures (15 and 40 psig) for each of the four resids. The Citgo runs were completed in December 2002. The results were presented in the October – December 2002 quarterly report. During the first quarter of 2003, these tests continued with resids from Chevron and Equilon. The conditions these test were run under as well as recoveries are presented in Table 18. We were not able to conduct tests with the Suncor resid because insufficient quantities were available at that time.

During the first quarter of 2003, antifoam optimization studies were started. The first series of tests were conducted with the resid from Petrobras at a temperature of 900 °F and a pressure of 15 psig. The first set of tests was run with antifoam/carrier rates of 30/70, 3/70, 0.3/70 (near industry standards) and 0.03/70 to determine if an optimum existed. The optimum concentration was found to be 0.3/70 which is near the industrial standard. Injection of higher antifoam concentrations (3/70 and 30/70) resulted in an increase in the coke density but it also resulted in lower temperatures in the coke drum. The second set of tests was conducted with the 100,000 cSt antifoams to compare continuous overhead injection to continuous feedline injection. At the lower concentration, 0.3/70, feedline injection was not as effective in

controlling foam as it was in the Suncor run where the antifoam/carrier mixture of 30/70 was used. The third set of tests were conducted with the 600,000 cSt antifoam were conducted at two antifoam/carrier concentrations, 0.12/70 and 0.75/70, the first below industry standards and the second near industry standards. Similar results as to those obtained with the 100,000 cSt antifoam were observed.

Optimization tests were also conducted with the Equilon and Chevron resids. Similar findings as those observed with Petrobras were observed. It was noted for these runs especially at lower pressure and temperatures that a significant amount of unconverted resid was extracted during steam strip resulting in major cleanup and repair. Very little foaming, if any, was seen for the Equilon resid. On average, this foam height for the chevron resid was 7" while Petrobras was 20".

Test with recycle and at refinery conditions were begun late August 2003. Increasing rates of Recycle required firing the furnace harder to achieve the desired operating temperature. Recycle resulted in a dense coke and appeared to change the morphology. However, it is too early in the test program to draw any conclusions.

In the sections below, the results from all the studies conducted from January 2002 through September 2003 will be discussed.

C. OPERATING ISSUES

1. Silicon Partitioning Studies

a) *Overhead Antifoam Injection - Silicon Carry Over Study*

A study was conducted to determine the extent of the antifoam blowing over during overhead injection due to the vaporization of the carrier (diesel) and the high vapor velocity in the drum. The system was purged overnight with 20 ml/hr distilled H_2O and 0.25 SCFH nitrogen with no antifoam injected. The water was collected at the end of this period. Analyses showed it contained 86.8 ppm Si. Previous analysis of Tulsa tap water indicated a silicon content of 4.2 ppm. It seems likely that the purging process stripped out silicon that may have previously deposited in the drums or tubing.

The system was then run for the next two hours at the same steam and nitrogen flow rate with 0.2 ml/min 100,000 cSt antifoam injected; a total of 24.5 ml was injected. The antifoam was diluted in diesel: 70 ml diesel to 30 ml antifoam. The water and antifoam were then turned off for one hour to allow for the system to be purged of the previous antifoam and water injections. All of the water was removed at the end of each of the sampling periods. The drum vapor flow rates were then increased to mimic run conditions. The nitrogen was increased to 4.50 SCFH, the steam was increased to 60 ml/hr and the antifoam remained at 0.2 ml/min for one hour. The water was removed from the liquid tanks and the system was purged with steam and nitrogen overnight to remove all remaining silicon. Only about 5% of the silicon was accounted for. When comparing the blank (H_2O) silicon levels to the silicon levels in all the other samples, a noticeable increase in the silicon level can be noticed. If samples 2 and 3 were combined, the silicon levels would be 102 ppm (a 20% increase). If samples 3 and 4 were combined, the silicon levels would be 108 ppm (a 25% increase). These calculations indicate that some of the antifoam is carried over into the liquids when injected from overhead. However, the very low recovery of silicon indicates that most of the injected antifoam remained in the drum. More may be carried over during the coking process because the superficial velocity of the HC vapor is the largest.

b) *Lights & Heavy Analysis*

During the pilot unit tests, oil and water are collected in the lights and heavies tank. The oil and water in these samples are separated and samples taken for partitioning analyses. Silicon enters the drum from three possible sources: antifoam, feedstock, and feed water injected (both process steam and stripping steam). Silicon is recovered in the coke, the hydrocarbon liquids, and the decant water. Estimates of the silicon input from the feed water were made using a value of 4.2 ppm silicon in Tulsa tap water (measured in 2001). It should be noted that the silicon numbers in the coke tended to vary wildly between the top and bottom of the drum; some runs had nearly the same amount of silicon throughout the drum, while other runs showed up to forty times more silicon at the bottom of the drum than the top.

Several results are notable. First, note that the silicon entering the drum is dominated by the feedstock rather than the antifoam for most of the runs. This is especially true for the Suncor runs, since the Suncor feedstock has a very high silicon content.

The silicon content of the hydrocarbon liquids can be expected to increase if there is a foamover, as the liquids will be contaminated with resid and/or heavy gas oils containing the feed silicon. This appears to be the case for run SUNC 8 PUAF, for example, which has a very high silicon content in the hydrocarbon liquids but no antifoam was used.

It is assumed that silicon in the antifoam is insoluble in the water, but that the antifoam breakdown products may be water soluble and thus may show up in the decant water. This is illustrated by runs SUN 3 PUAF and SUN 4 PUAF, in which the antifoam was injected overhead and in the feed stream, respectively. SUN 3 PUAF has a higher concentration of silicon in the hydrocarbon liquid than does SUN 4 PUAF, perhaps due to carry-over of the antifoam, but SUN 4 PUAF has considerably more silicon in the water, apparently due to the breakdown of the antifoam. More analytical results are needed for silicon in the liquid products to form a firm conclusion (since SUN 4 PUAF is the only anti-foaming run with antifoam added to the feedline for which we have received the water analysis back), but the tentative conclusion is that silicon from antifoam injected overhead tends to carry over to the hydrocarbon liquids, while silicon from antifoam injected in the feedline tends to break down and end up in the decant water.

2. Coil Fluid Temperature Profiles

For the foaming tests conducted in the previous JIP, it was noted that the fluid temperature in the coil was fluctuating. To ascertain why, thermocouples were inserted in the coil at different locations. The results from these studies are discussed below.

Thermocouples were inserted into the furnace coil at various positions in order to study the rate at which the feed temperature changes. The data was collected from three consecutive runs. All the runs had a thermocouple at the inlet of the feed into the furnace (TI_131) and at the drum inlet/coil outlet (TI_107). The first run had a third thermocouple in the second loop of the coil – approximately 7 feet from the inlet, see Figure 49. The second run had a thermocouple approximately 13 feet from the inlet (4^{th} loop), see Figure 50. The third run had a thermocouple in the 3^{rd} and 5^{th} loop – approximately 10 and 16 feet from the inlet, see Figure 51. The equation, $(T-T_0)/(T_f-T_0)$, was used to calculate the percentage of the heating accomplished by that point of the coil. Table 21 shows the results of these calculations. Looking at the steady state portion of the runs, approximately 41% of the total heating is accomplished in the first 7

feet of the coil and 23% of the heating is done in the last 4 feet of the coil. Only 36% of the heating is accomplished in the middle 9 feet of the coil.

Table 21 - Percent Heating in Furnace Coil

Loop 2(7')	Loop 3(10')	Loop 4(13')	Loop 5(16')	Time
$(T-T_0)/(T_f-T_0)$	$(T-T_0)/(T_f-T_0)$	$(T-T_0)/(T_f-T_0)$	$(T-T_0)/(T_f-T_0)$	(min)
58.41%	67.30%	76.00%	77.97%	Prerun to 15
39.58%	53.45%	63.53%	75.07%	16 to 90
40.19%	54.96%	64.38%	75.89%	91 to 165
39.96%	54.90%	63.93%	76.24%	166 to 240
43.27%	67.32%	64.43%	81.15%	241 to 315
64.22%	67.57%	64.43%	79.54%	316 to 390
40.75%	57.66%	64.07%	77.09%	Steady-state
*T_0 = TI_131(Coil Inlet)				
**T_f = TI_107(Drum Inlet)				

Large fluctuations in the thermocouple readings have caused problems in controlling the fluid/furnace temperature. Figure 52 and Figure 53 show the fluctuations seen in the thermocouple readings during this study. It can be seen that the fluctuations increase as the fluid flows through the tube. As seen in Figure 53, the average fluctuation in the temperature of the fluid at the entrance of the coil is only +/-3ºF while the average fluctuation at the exit of the coil is +/-7ºF. It is believed that increase in vaporization of the fluid causes more irregularities in the flow pattern and the temperature profile.

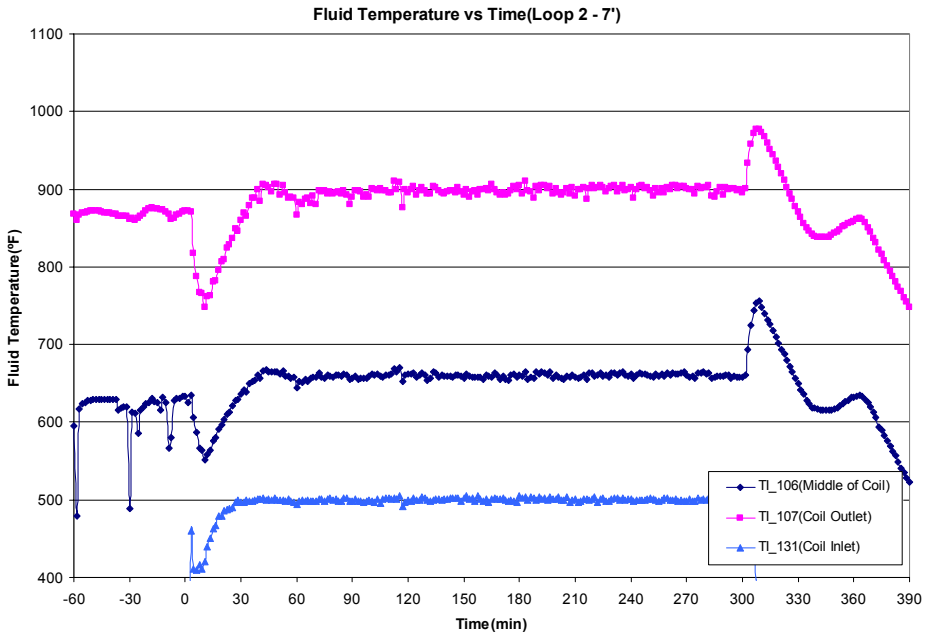

Figure 49 - Furnace Coil Heating – Loop 2

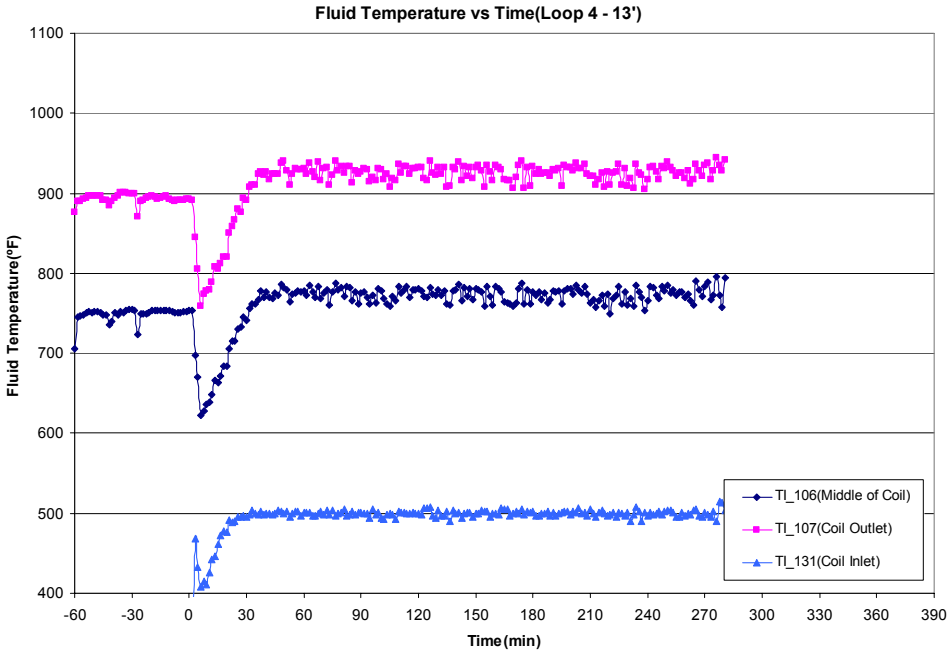

Figure 50 - Furnace Coil Heating – Loop 4

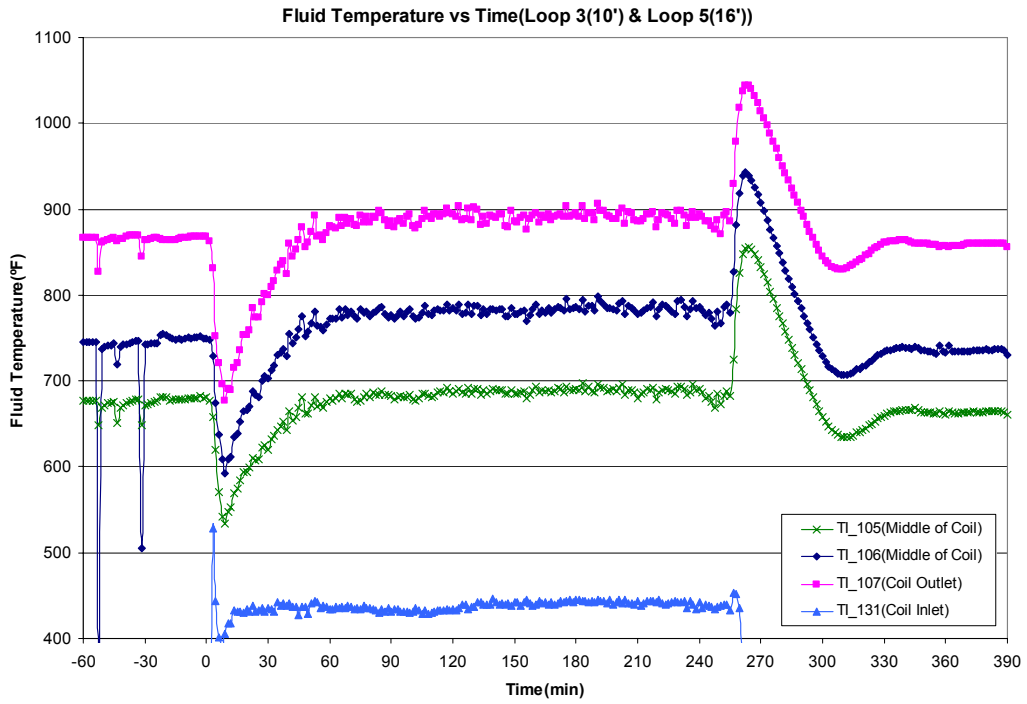

Figure 51 - Furnace Coil Heating – Loop 3 & 5

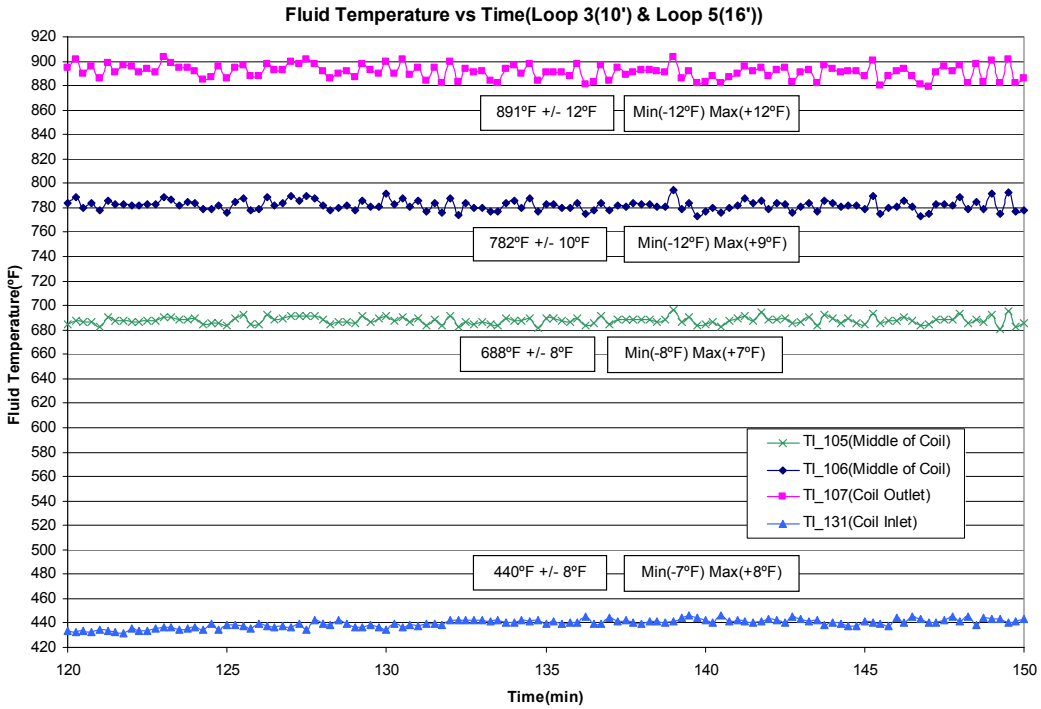

Figure 52 - Furnace Coil Temperature Profiles – Loop 3 & 5

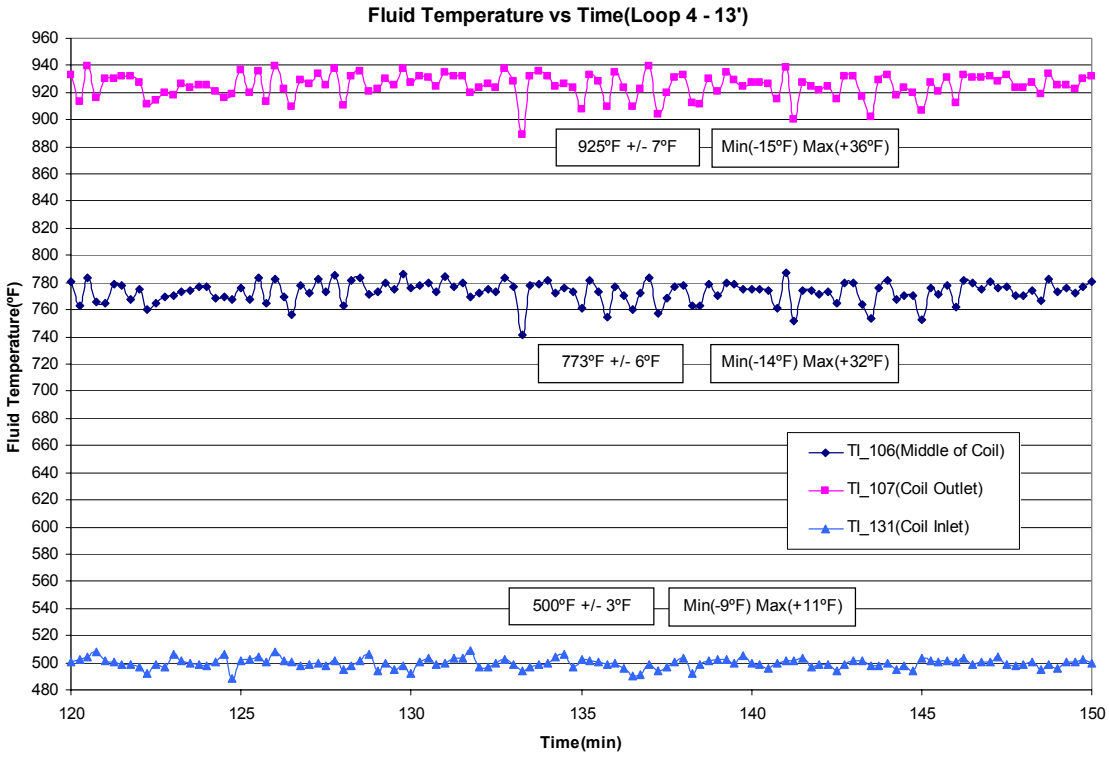

Figure 53 - Furnace Coil Temperature Profiles – Loop 4

3. Drum/Coil Velocity Calculations

Table 22 shows the effects of feed flow rates and drum diameter on superficial velocities at the drum outlet. These values were estimated assuming 72 wt% of the feed exits the drum as vapor (an approximate average from our experimental results) and assuming a vapor molecular weight of 108. Values of 0.3 to 0.7 ft/s, which would approximate commercial units, can be attained using a 1 inch or 2 inch drum, but cannot be attained with the 3 inch drum using reasonable feed rates.

The effects of feed flow rates and drum diameter on the superficial velocities in the coil and at the drum inlet are shown in Table 23. These values assume that 17 wt% the feed is vaporized in the furnace. The steam flow rate is seen to have little effect on overall vapor velocities for the ranges we are considering.

Table 22 - Effect of feed flow rate and drum diameter on superficial velocity at drum outlet

	Drum Diameter								
	1"			2"			3"		
Feed rate (gems/hr)	1200	3000	4800	1200	3000	4800	1200	3000	4800
Steam flow = 10 g/hr, N2 = 0.25 SCFH									
Superficial Velocity of Vapor at Drum Outlet (ft/s)	0.46	1.08	1.71	0.12	0.27	0.43	0.05	0.12	0.19
Steam flow = 20 g/hr, N2 = 0.25 SCFH									
Superficial Velocity of Vapor at Drum Outlet (ft/s)	0.49	1.11	1.74	0.12	0.28	0.43	0.05	0.12	0.19
Steam flow = 40 g/hr, N2 = 0.25 SCFH									
Superficial Velocity of Vapor at Drum Outlet (ft/s)	0.55	1.17	1.79	0.14	0.29	0.45	0.06	0.13	0.20
Steam flow = 40 g/hr, N2 = 0.5 SCFH									
Superficial Velocity of Vapor at Drum Outlet (ft/s)	0.56	1.19	1.81	0.14	0.30	0.45	0.06	0.13	0.20
Steam flow = 100 g/hr, N2 = 0.25 SCFH									
Superficial Velocity of Vapor at Drum Outlet (ft/s)	0.72	1.34	1.97	0.18	0.34	0.49	0.08	0.15	0.22
Steam flow = 200 g/hr, N2 = 0.25 SCFH									
Superficial Velocity of Vapor at Drum Outlet (ft/s)	1.01	1.63	2.25	0.25	0.41	0.56	0.11	0.18	0.25

Table 23 - Effect of feed flow rate and drum diameter on superficial velocity in coil and at drum inlet

	Drum Diameter								
	1"			2"			3"		
Feed rate (gms/hr)	1200	3000	4800	1200	3000	4800	1200	3000	4800
Steam flow = 10 g/hr, N2 = 0.25 SCFH									
Superficial Velocity of Vapor at Drum Inlet (ft/s)	0.15	0.29	0.44	0.04	0.07	0.11	0.02	0.03	0.05
Superficial Velocity of Vapor in Coil (ft/s)	2.35	4.71	7.06	2.35	4.71	7.06	2.35	4.71	7.06
Superficial Velocity of VR in Coil (ft/s)	0.03	0.08	0.12	0.03	0.08	0.12	0.03	0.08	0.12
Steam flow = 20 g/hr, N2 = 0.25 SCFH									
Superficial Velocity of Vapor at Drum Inlet (ft/s)	0.18	0.33	0.47	0.04	0.08	0.12	0.02	0.04	0.05
Superficial Velocity of Vapor in Coil (ft/s)	2.86	5.21	7.56	2.86	5.21	7.56	2.86	5.21	7.56
Superficial Velocity of VR in Coil (ft/s)	0.03	0.08	0.12	0.03	0.08	0.12	0.03	0.08	0.12
Steam flow = 40 g/hr, N2 = 0.25 SCFH									
Superficial Velocity of Vapor at Drum Inlet (ft/s)	0.24	0.39	0.54	0.06	0.10	0.13	0.03	0.04	0.06
Superficial Velocity of Vapor in Coil (ft/s)	3.86	6.21	8.56	3.86	6.21	8.56	3.86	6.21	8.56
Superficial Velocity of VR in Coil (ft/s)	0.03	0.08	0.12	0.03	0.08	0.12	0.03	0.08	0.12
Steam flow = 40 g/hr, N2 = 0.5 SCFH									
Superficial Velocity of Vapor at Drum Inlet (ft/s)	0.26	0.41	0.55	0.06	0.10	0.14	0.03	0.05	0.06
Superficial Velocity of Vapor in Coil (ft/s)	4.14	6.49	8.85	4.14	6.49	8.85	4.14	6.49	8.85
Superficial Velocity of VR in Coil (ft/s)	0.03	0.08	0.12	0.03	0.08	0.12	0.03	0.08	0.12

Table 24 shows the inches of coke that would deposit in the drum in a 5 hour run for various drum diameters and feed rates. This table shows that we cannot use the 1 inch drum, due to the extremely large drum height that would be required. Comparison of Table 22 with Table 24 shows that a 2 inch drum would allow us to achieve velocities approaching commercial values while maintaining a reasonable drum height. A 2 inch drum with a feed rate of 2400 g/hr, for example, would fill up about 65 inches of coke in a 4 hour run. If a steam flow rate of 60 g/hr and a N2 flow rate of 0.5 SCFH are used, the outlet drum velocity would be approximately 0.26 ft/s, which is on the low end of commercial values. Other runs can be carried out with the 3 inch drum and1200 g/hr feed, 40 g/hr steam, and 0.25 SCFH N2, for an overhead velocity of 0.06 ft/s, and 3600 g/hr feed, 40 g/hr steam, and 0.25 SCFH N2, for an overhead velocity of 0.15 ft/s.

Table 24 - Estimated coke level for 1", 2" and 3" drums (inches of coke formed in 5 hrs)

Drum Diameter		1"			2"			3"		
Feed rate (gms/hr)		1200	2400	3600	1200	2400	3600	1200	2400	3600
% of feed assumed deposited as coke	Density of coke									
22.5	0.65	161.3	322.6	483.9	40.3	80.76	121.0	17.9	35.8	53.8
22.5	0.70	149.8	299.6	449.4	37.4	74.9	112.3	16.6	33.3	49.9
25	0.65	179.2	358.5	537.7	44.8	90.0	134.4	19.9	39.8	59.7
25	0.70	166.4	332.9	499.3	41.6	83.2	124.8	18.54	37.09	55.5

4. Impact of Antifoam on Coil & Overhead Temperature

Antifoam injection studies were run using both a low viscosity 100,000 cSt (0.3 ml AF/ 70 ml diesel) and a high viscosity 600,000 cSt (0.75 ml AF/ 70 ml diesel) antifoam. In some of the tests, antifoam was injected continuously (2 min ON and 8 min OFF) while in others it was injected on as-needed basis (observation of foam determines the injection time). Antifoams were injected in the drum overhead, through the feedline, and mixed with the resid in the feed bucket. During the experiments, temperatures at the inlet to furnace coil (TIC131), the fluid temperature (TI107), the furnace skin temperature (TI200), the overhead temperature (TI208) and the temperature inside the coke drum near the bottom (TI214) are measured. From test to test, variations were seen in the overhead temperature and the furnace coil temperatures. In general, injecting antifoam on a continuous basis reduces the overhead temperature, while injecting antifoam in the feedline requires the furnace to be fired harder to get the fluid to the desired temperature. Discussed in the following section are the observations for the tests run using the Chevron and Equilon resids.

The CHEV 13 and CHEV 14 runs were carried out at a temperature of 900°F, a pressure of 15 psig and a feed rate of 3600 gm/hr. CHEV 13 used continuous overhead injection of 100,000 cSt (0.3/70) antifoam, whereas CHEV 14 used continuous feedline injection of 100,000 cSt (0.3/70) antifoam. As can be seen from the plot in Figure 54 the CHEV 13 run required less heat input to the feedline, had better control of fluid temperature and a cooler overhead. CHEV 14 required more heat input to the feedline, was harder to maintain the fluid temperature and had a comparatively warmer overhead.

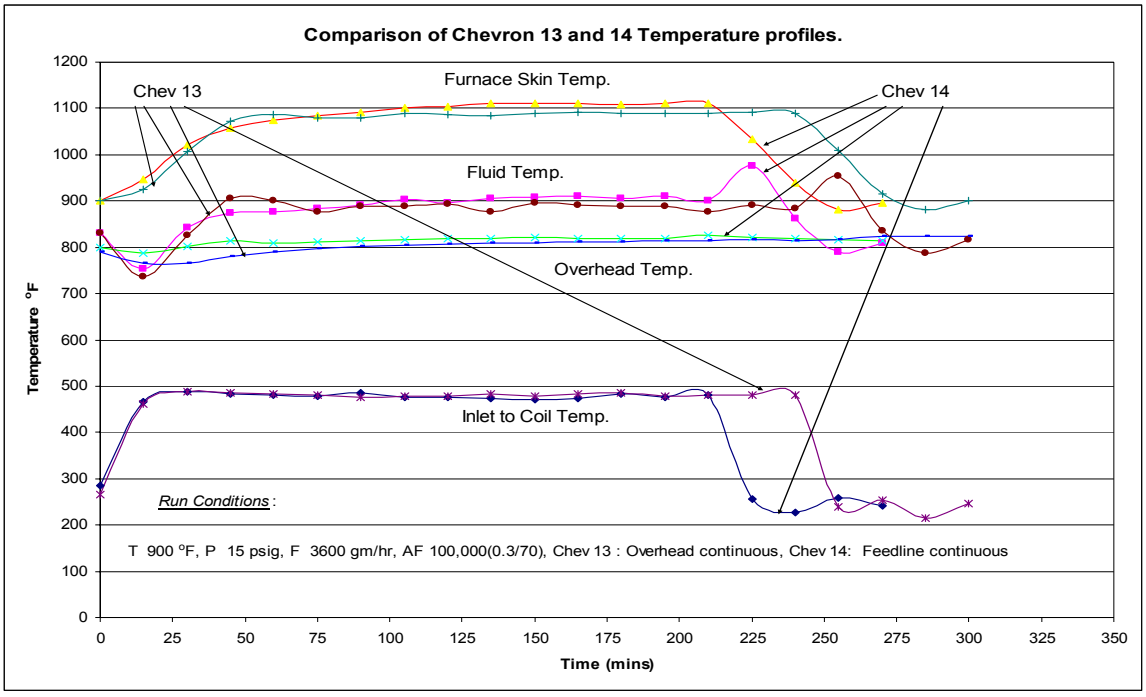

Figure 54 - Temperature profiles for CHEV 13 PUAFC and CHEV 14 PUAFC runs

The CHEV 12 and CHEV 14 runs were carried out at a temperature of 900°F, a pressure of 15 psig and a feed rate of 3600 gm/hr. CHEV 12 was an as-needed overhead injection of 100,000 cSt (0.3/70) antifoam, whereas CHEV 14 was a continuous feedline injection of 100,000 cSt (0.3/70) antifoam. As can be seen in Figure 55, CHEV 12 required less heat in feedline, was harder to maintain fluid temperature and the overhead was warmer. CHEV 14 required more heat in the feedline, had better control of fluid temperature and the overhead was comparatively cooler.

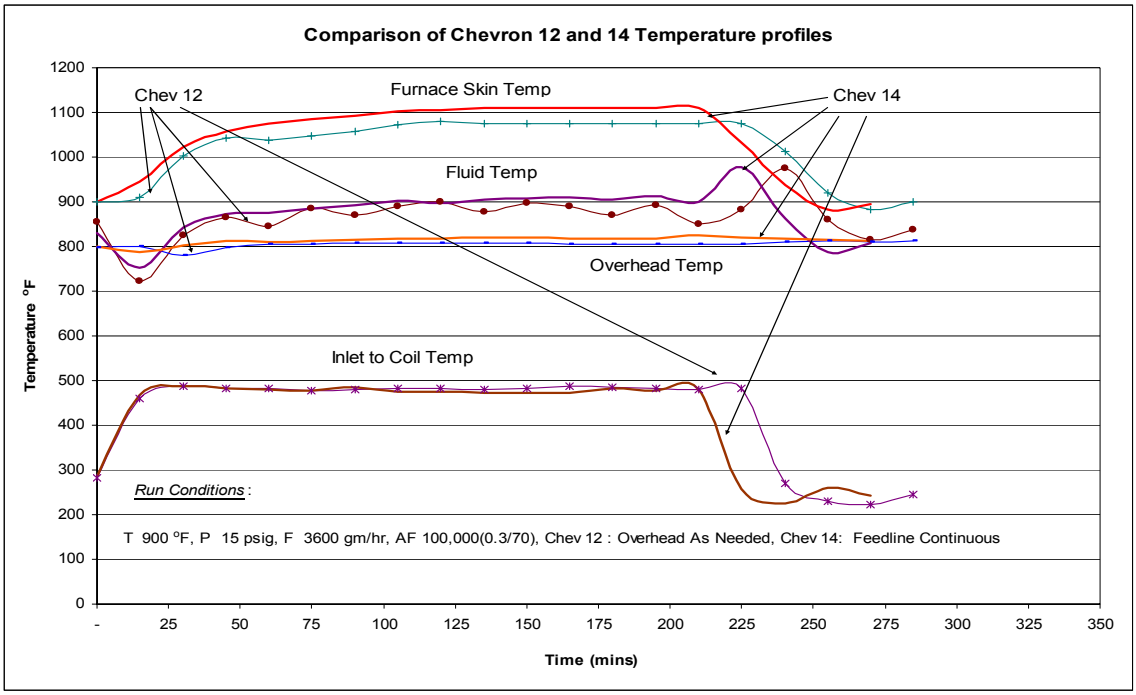

Figure 55 - Temperature profiles for CHEV 12 PUAFI and CHEV 14 PUAFC runs

The CHEV 12 and CHEV 16 runs were carried out at a temperature of 900°F, a pressure of 15 psig and a feed rate of 3600 gm/hr. CHEV 12 was an as-needed overhead injection of 100,000 cSt (0.3/70) antifoam, whereas CHEV 16 was an as-needed feedline+overhead injection of 600,000 cSt (0.75/70) antifoam. As can be seen in Figure 56 CHEV 12 required less heat in the feedline, was harder to maintain the fluid temperature, and had a cooler overhead. CHEV 16 required more heat input to the feedline, had average control of fluid temperature and a comparatively warmer overhead.

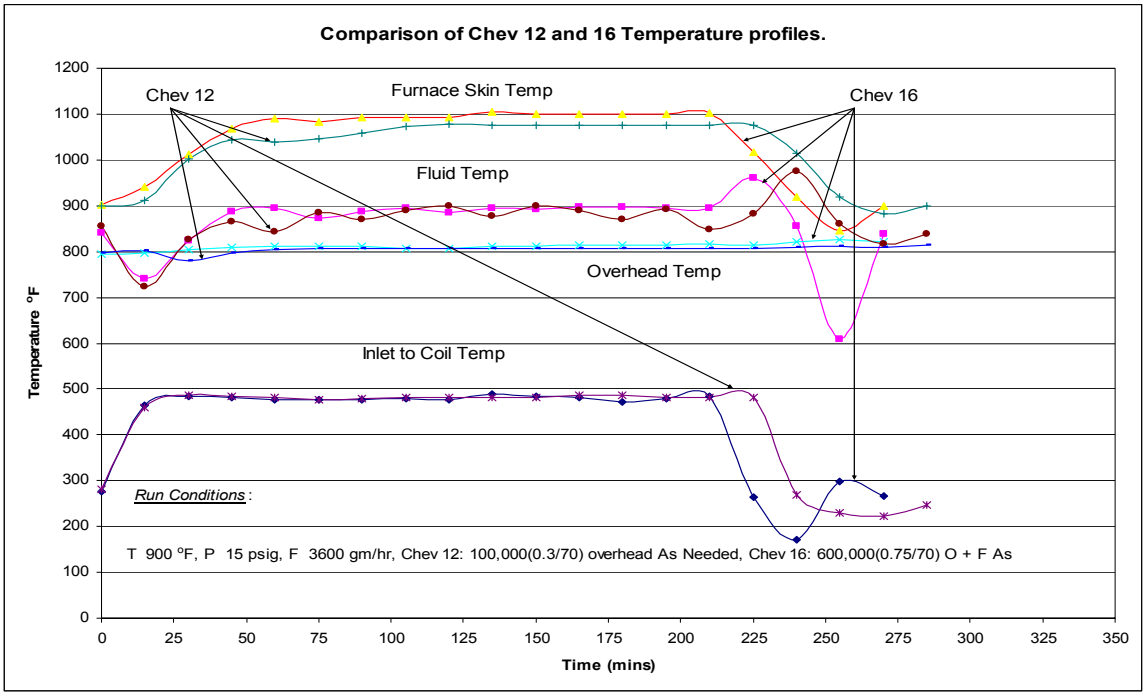

Figure 56 - Temperature profiles for CHEV 12 PUAFI and CHEV 16 PUAFI runs

The CHEV 14 and CHEV 16 runs were carried out at a temperature of 900°F, a pressure of 15 psig and a feed rate of 3600 gm/hr. CHEV 14 was a continuous feedline injection of 100,000 cSt (0.3/70) antifoam, whereas CHEV 16 was an as-needed feedline+overhead injection of 600,000 cSt (0.75/70) antifoam. As can be seen in Figure 57, CHEV 14 required more heat input to the feedline and the overhead was warmer. CHEV 16 on the other hand required less heat input to the feedline, had average control of fluid temperature and the overhead was comparatively cooler.

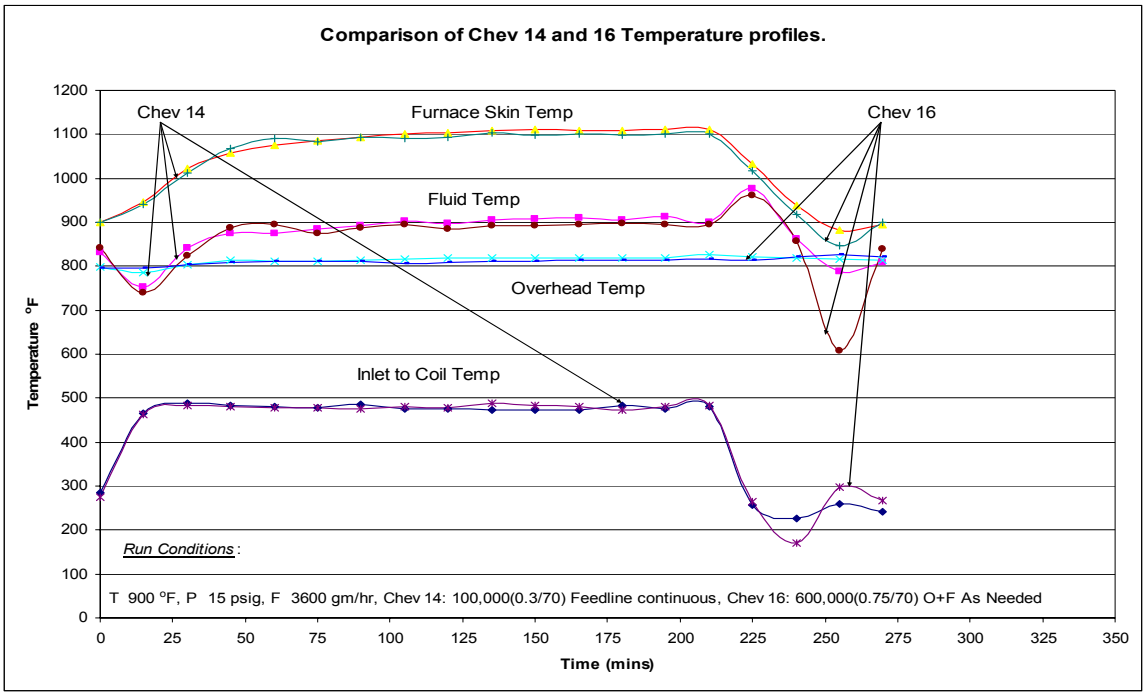

Figure 57 - Temperature profiles for CHEV 14 PUAFC and CHEV 16 PUAFI runs

The CHEV 8 and CHEV 12 runs were carried out at a temperature of 900°F, a pressure of 15 psig and a feed rate of 3600 gm/hr. CHEV 12 was an as-needed overhead injection of 100,000 cSt (0.3/70) antifoam, whereas CHEV 8 was an as-needed overhead injection of 100,000 cSt (30/70) antifoam. As can be seen in Figure 58, CHEV 8 required less heat input to the feedline, had higher fluid temperature and a warmer overhead temperature. CHEV 12 had a better control of the feedline temperature and substantially cooler overhead temperature.

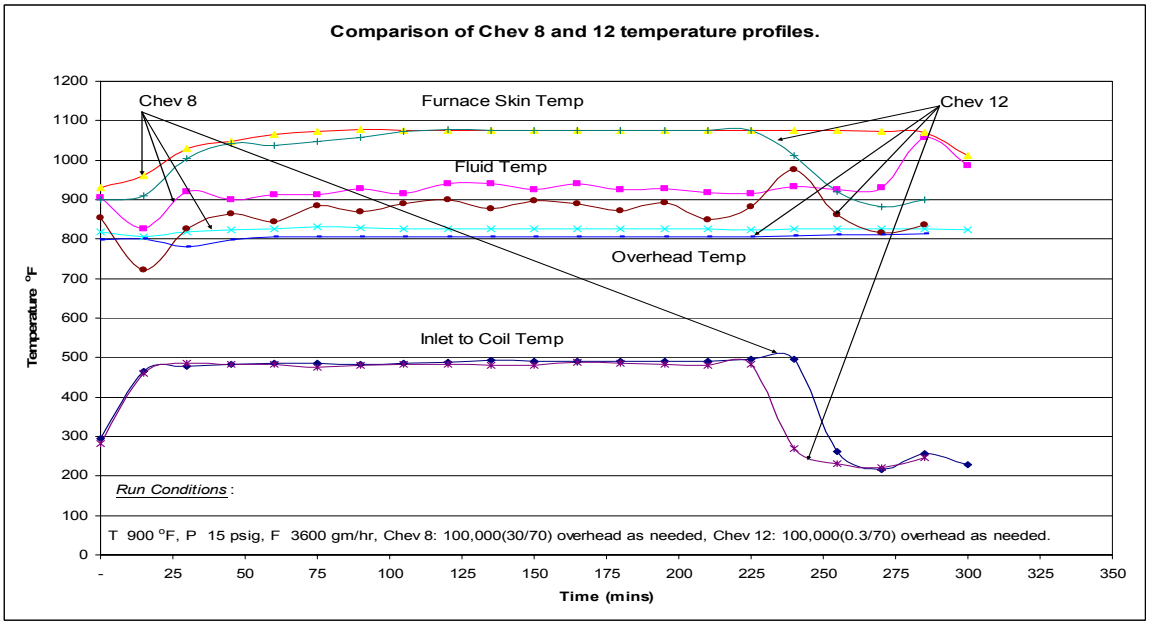

Figure 58 - Temperature profiles for CHEV 8 PUAFI and CHEV 12 PUAFI runs

The CHEV 8 and CHEV 13 runs were carried out at a temperature of 900°F, a pressure of 15 psig and a feed rate of 3600 gm/hr. CHEV 13 was a continuous overhead injection of 100,000 cSt (0.3/70) antifoam, whereas CHEV 8 was an as-needed overhead injection of 100,000 cSt (30/70) antifoam. As can be seen in Figure 59 that CHEV 8 required less heat input to the feedline, was harder to maintain fluid temperature and had a higher overhead temperature. CHEV 13 required more heat input to the feedline, had better control of fluid temperature and had a cooler overhead temperature.

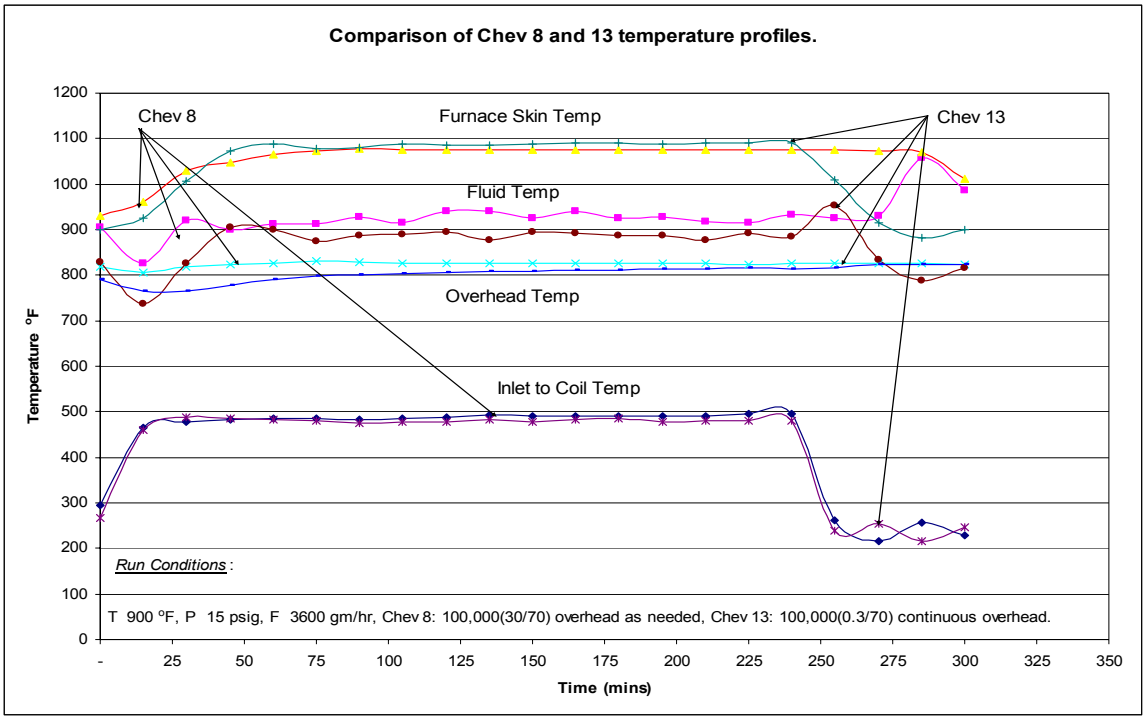

Figure 59 - Temperature profiles for CHEV 8 PUAFI and CHEV 13 PUAFC runs

The CHEV 8 and CHEV 14 runs were carried out at a temperature of 900°F, a pressure of 15 psig and a feed rate of 3600 gm/hr. CHEV 14 was a continuous feedline injection of 100,000 cSt (0.3/70) antifoam, whereas CHEV 8 was an as-needed overhead injection of 100,000 cSt (30/70) antifoam. As can be seen in Figure 60, CHEV 8 required less heat input to the feedline, was harder to maintain the fluid temperature and had a warmer overhead temperature. CHEV 14 on the other hand required more heat input to the feedline, had better control of fluid temperature and a comparatively cooler overhead temperature.

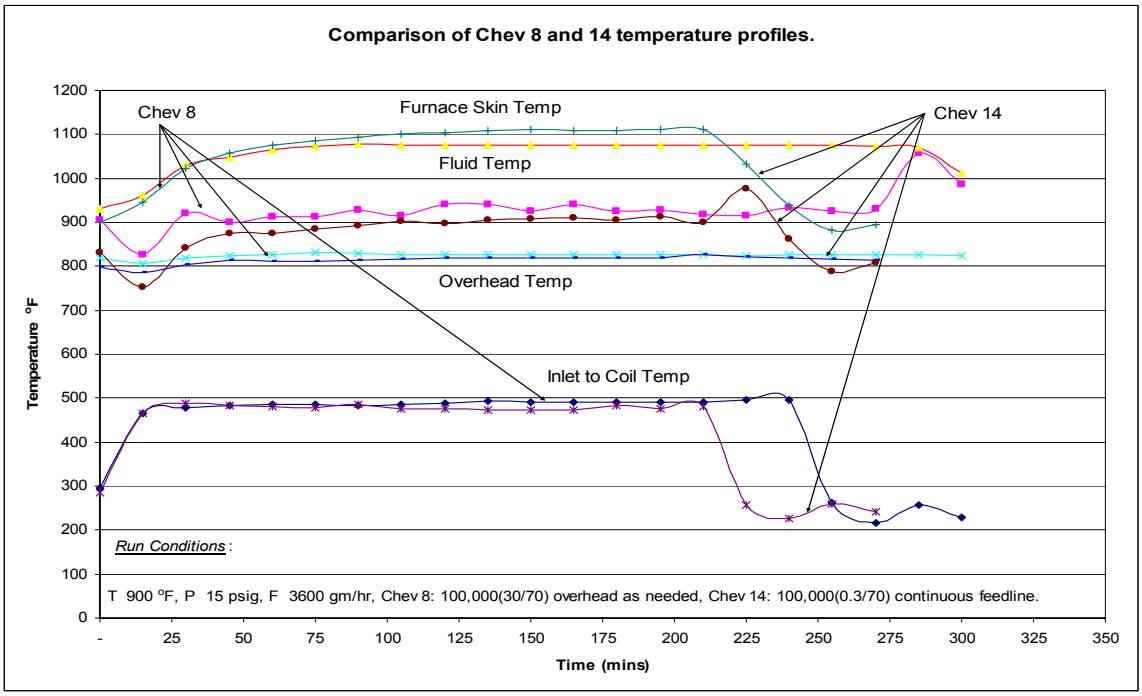

Figure 60 - Temperature profiles for CHEV 8 PUAFI and CHEV 14 PUAFC runs

EQU 5 run was carried out at a temperature of 930°F, a pressure of 40 psig and a feed rate of 3600 gm/hr, whereas EQU 6 run was carried out at a temperature of 900°F, a pressure of 40 psig and a feed rate of 3600 gm/hr. EQU 5 was an as-needed overhead injection of 100,000 cSt (30/70) antifoam and EQU 6 was an as-needed feedline injection of 100,000 cSt (30/70) antifoam. As can be seen in Figure 61, Equilon required more heat input to the feedline to attain the higher temperature and the overhead temperature was very high compared to EQU 6. EQU 6 required less heat input to the feedline but the overhead temperature dropped remarkably.

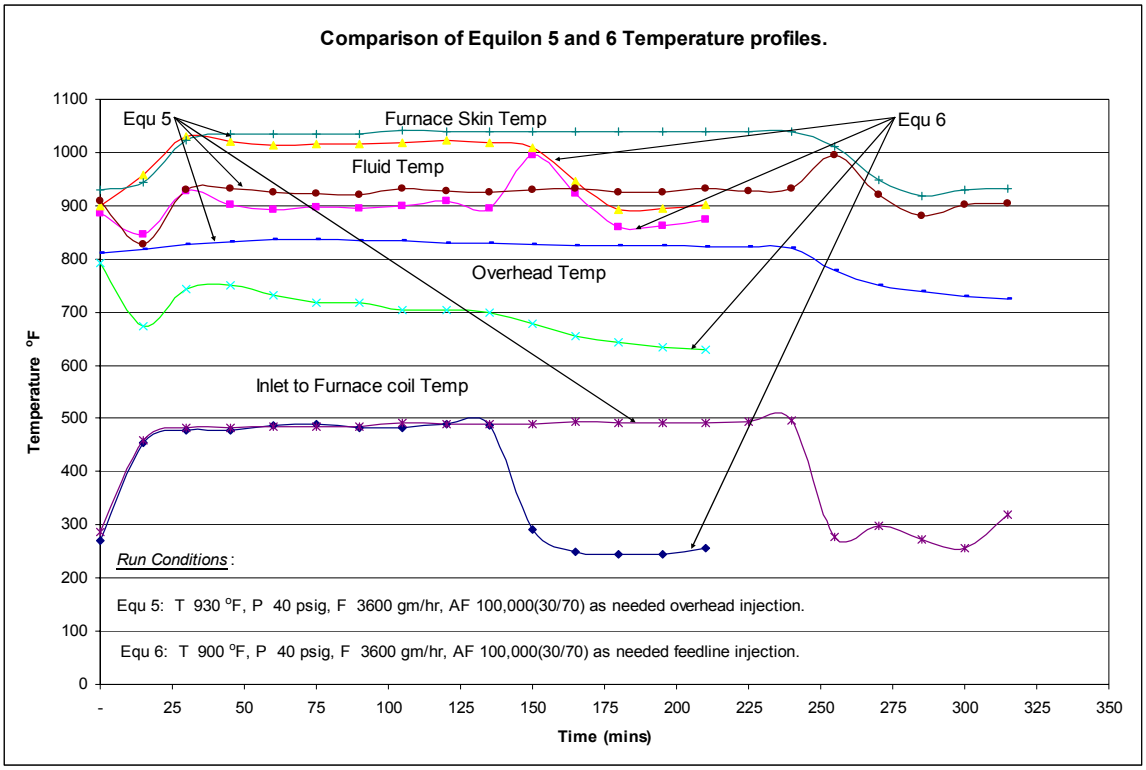

Figure 61 - Temperature profiles for EQU 5 PUAFI and EQU 6 PUAFI runs

The EQU 7 and EQU 8 runs were carried out at a temperature of 900°F, a pressure of 15 psig and a feed rate of 3600 gm/hr. EQU 7 used as-needed overhead injection of 100,000 cSt (0.3/70) antifoam, whereas EQU 8 used continuous feedline injection of 100,000 cSt (0.3/70) antifoam. As can be seen in Figure 62, EQU 7 required more heat input to the feedline, was difficult to control the fluid temperature and had a cooler overhead temperature. EQU 8 had better control of feedline temperatures.

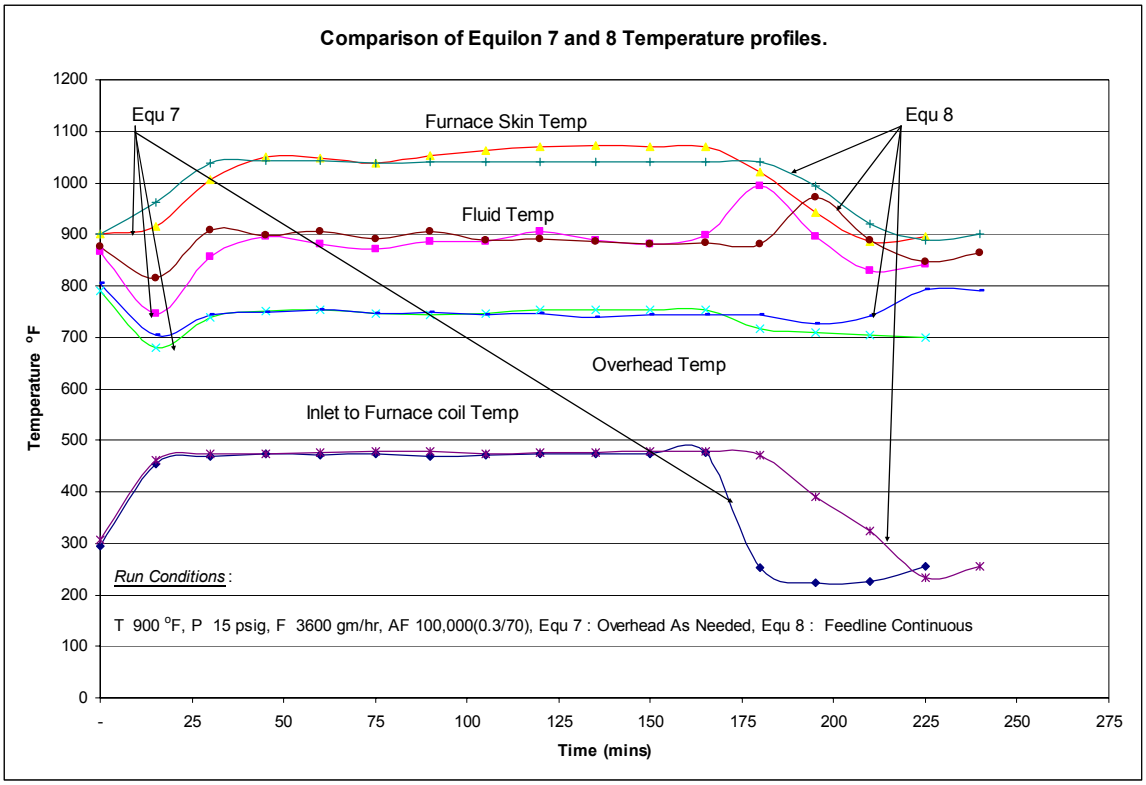

Figure 62 - Temperature profiles for EQU 7 PUAFI and EQU 8 PUAFC runs

The EQU 8 and EQU 9 runs were carried out at a temperature of 900°F, a pressure of 15 psig and a feed rate of 3600 gm/hr. EQU 8 was a continuous feedline injection of 100,000 cSt (0.3/70) antifoam, whereas EQU 9 was an as-needed feedline injection of 100,000 cSt (0.3/70) antifoam. For EQU 9, observations during the run showed no foam and hence antifoam was not injected. As can be seen in Figure 63, EQU 9 required more heat input to the feedline, was difficult to maintain fluid temperature and the overhead temperature was much higher than EQU 8 was. EQU 8 required less heat input to the feedline, had a better control of the fluid temperature and the overhead temperature was remarkably lower.

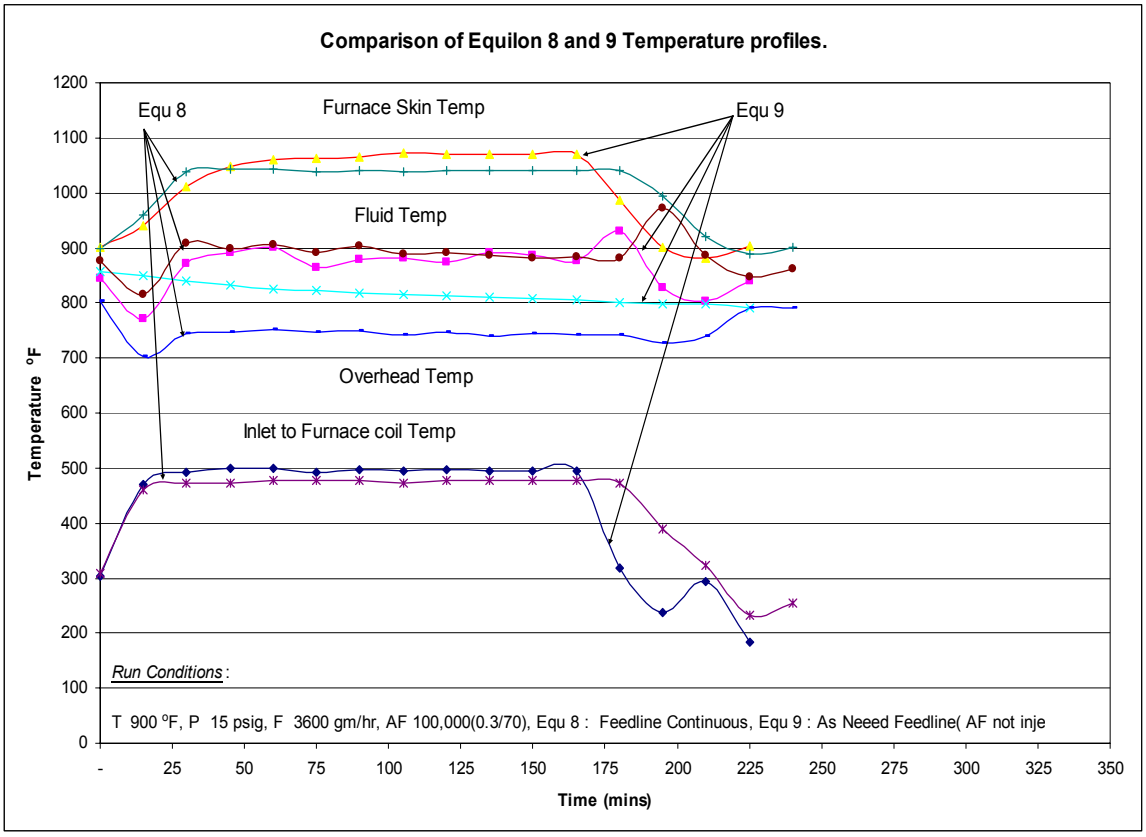

Figure 63 - Temperature profiles for EQU 8 PUAFC and EQU 9 PUAFI runs

The PETR 3 and PETR 13 runs were carried out at a temperature of 900°F, a pressure of 15 psig and a feed rate of 3600 gm/hr. PETR 3 was an as-needed overhead+feedline injection of 100,000 cSt (30/70) antifoam, whereas PETR 3 was a continuous overhead injection of 100,000 cSt (0.3/70) antifoam. As can be seen in Figure 64, PETR 3 required less heat input to the inlet coil, and had a warmer overhead temperature. PETR 13 on the other hand required more heat input to the inlet coil and had a comparatively cooler overhead temperature. The fluid and the furnace skin temperature were the same for both the runs.

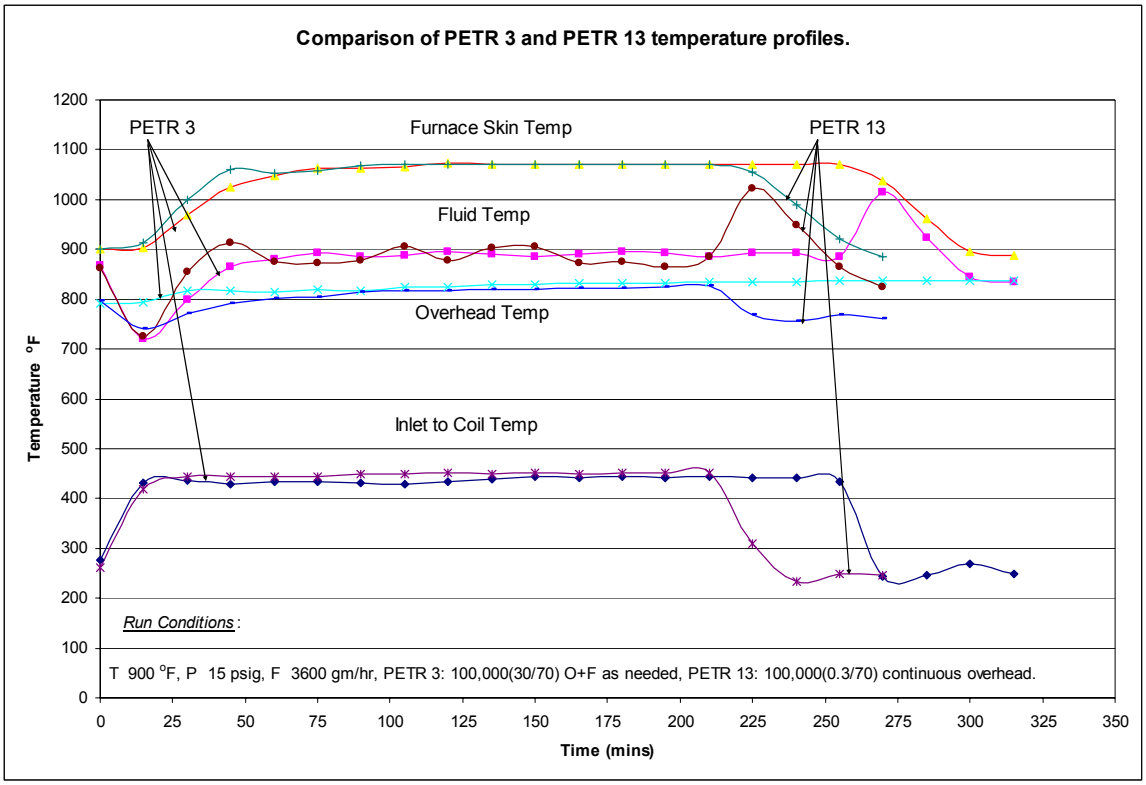

Figure 64 - Temperature profiles for PETR 3 PUAFI and PETR 13 PUAFC runs

The PETR 14 and PETR 15 runs were carried out at a temperature of 900°F, a pressure of 15 psig and a feed rate of 3600 gm/hr. PETR 14 used continuous overhead+feedline injection of 100,000 cSt (0.3/70) antifoam, whereas PETR 15 used continuous overhead+feedline injection of 100,000 cSt (0.3/70), 100,000 cSt (3/70), 600,000 cSt (0.12/70) and 600,000 cSt (0.75/70) antifoam. As can be seen in Figure 65, PETR 15 had a higher fluid and overhead temperature, whereas PETR 14 had a lower fluid and overhead temperature.

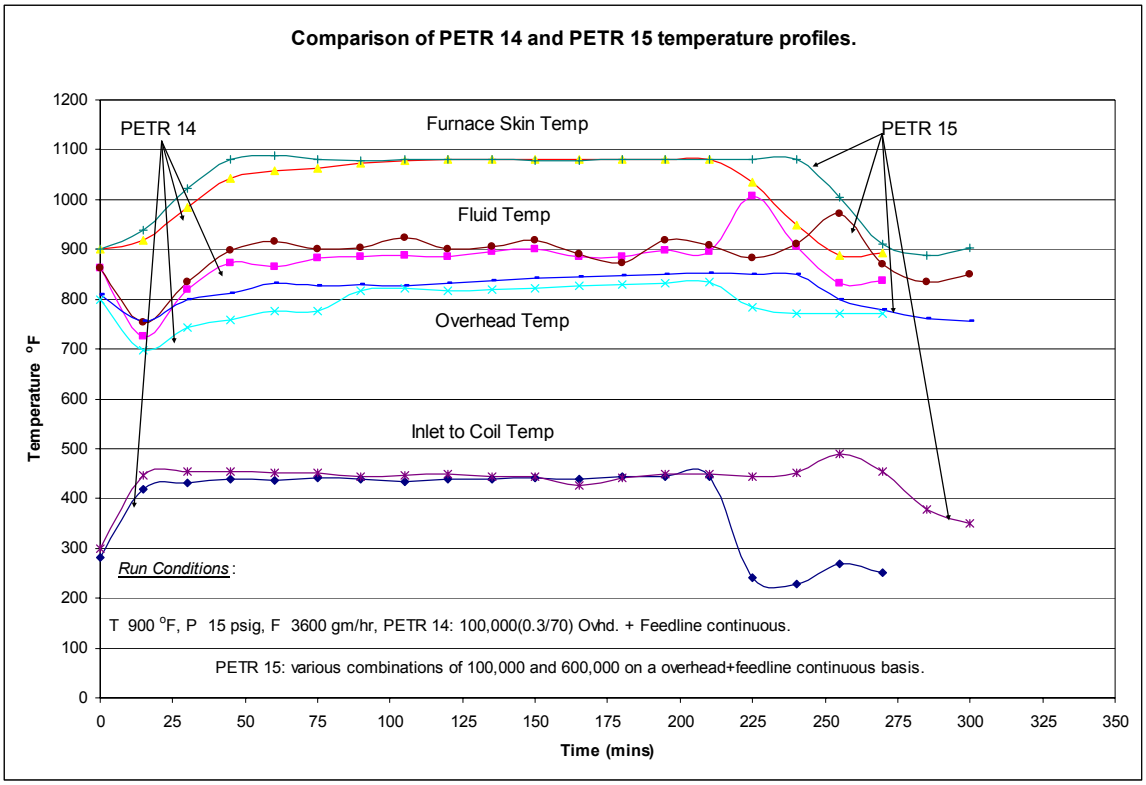

Figure 65 - Temperature profiles for PETR 14 PUAFC and PETR 15 PUAFC runs

D. DETAILED LIQUID ANALYSES

1. Scope of work:

This study analyzes the liquid products from Chevron, Marathon, Petrobras, Citgo, Equilon and Suncor resids for both the 3ft drum pilot unit (PU) and the 6ft drum pilot unit (PUAF).

In the previous report, the only available data were the distillation and detailed hydrocarbon analysis (DHA) data for the PU runs. These PU runs were performed without the use of antifoaming agents. In the second phase of studies, a 6ft drum with a 0.25 inch furnace coil were used. The use of antifoaming agents (PUAF) were also incorporated into the study.

The distillation plots of the weight percent (%) of the feed versus the bottom and overhead temperatures have been generated using the available PUAF resids. These plots were also repeated using the simulation distillation data, Sim Dis, from the 6ft pilot unit. The distillation data trends exhibited by both the 3ft and 6ft pilot units will be compared and discussed.

The PiONA contents of the resids have been analyzed at the boiling point ranges IBP-113^{o}F, 113-430^{o}F, and 400-430^{o}F. Plots evaluating the individual PiONA components based on the data from the 0.25 inch coiled 3ft pilot unit will be compared with that of the 0.25 inch coiled the 6ft (PUAF) drums. The overall outcome of the DHA analysis is to be able to predict what type of PiONA component would be dominant at a certain temperature and pressure, and how a change in the temperature and pressure would affects its production.

The sulfur analysis has only been conducted on the PU resids. When the DHA analysis of the PUAF liquids have been completed, then the sulfur analysis will begin. The weight percent (%) of sulfur in the different PU resids have been plotted against the fluid temperatures and pressures, at the different cuts. The resulting trends will be discussed.

Finally the densities, API, of the resids have been correlated to the different temperature cuts. The effects of temperature and pressure on the density, API, will be discussed.

Liquids Obtained Using 3 ft Coke Drum Pilot Unit Runs

In the first phase of study, coking runs were made using a 3ft pilot unit drum, PU, with both 0.25 and 3/8 inch furnace coils. These PU runs were performed without the use of antifoaming agents. Table 25 through Table 30 show the PU runs available in the compiled database. All analysis in the report is based solely on the available sample runs. A key has been provided to interpret the data.

Key

	0.25 inch
	0.375 inch
	Data is available
NO	No data is available
NO 650+	No data is available for the 650+ cut

In general, there was no sulfur analysis conducted for all the resids using the 0.375 inch coil.

	Data Type				Detailed Hydrocarbon Analysis		
CHEVRON	**Distillation**	**Sim Dis**	**Density**	**Sulfur**	**IBP - 113**	**113 - 400**	**400 - 430**
CHVPU 1 FS1				NO			
CHVPU 2 PT1	NO			NO			
CHVPU 2A PT1A				NO			
CHVPU 3 PT2				NO			
CHVPU 4 PT3				NO			
CHVPU 5 PT4				NO			
CHVPU 6 PT5				NO			
CHVPU 10 FS2							
CHVPU 11 PT11							
CHVPU 12 PT12				NO			
CHVPU 13 PT13							
CHVPU 14 PT14							

Table 25: Pilot Unit Chevron Resids

	Data Type				Detailed Hydrocarbon Analysis		
MARATHON	Distillation	Sim Dis	Density	Sulfur	IBP- 113	113 - 400	400 - 430
MARPU 8	NO	NO	NO	NO	NO		
MARPU 9 BT1				NO			
MARPU 9A BT1A				NO			
MARPU 10 BT2				NO			
MARPU 10A BT2A				NO			
MARPU 11 BT3				NO			
MARPU 11A BT3A				NO			
MARPU 12 PT2				NO	NO	NO	NO
MARPU 14 PT4				NO			
MARPU 15 PT5				NO			
MARPU 16 PT6				NO			
MARPU 17A PT7A				NO			
MARPU 18 PT8				NO			
MARPU 19 PT9				NO			
MARPU 19A PT9A				NO			
MARPU 21 PT11				NO			
MARPU 22 FS3							
MARPU 23 PT23							
MARPU 24 PT24							
MARPU 25 RS10							
MARPU 26 RS20							
MARPU 27 PT27				NO	NO	NO	NO
MARPU 28 PT28				NO	NO	NO	NO

Table 26: Pilot Unit Marathon Resids

	Data Type				Detailed Hydrocarbon Analysis		
SUNCOR	Distillation	Sim Dis	Density	Sulfur	IBP- 113	113 - 400	400 - 430
SUNPU1 PT1							
SUNPU2 FS1							
SUNPU 3 PT3							
SUNPU 4 PT4							
SUNPU 6 SO2							
SUNPU 7 PT7							

Table 27: Pilot Unit Suncor Resids

	Data Type				Detailed Hydrocarbon Analysis		
PETROBRAS	Distillation	Sim Dis	Density	Sulfur	IBP- 113	113 - 400	400 - 430
PETPU 1 PT1				NO			
PETPU 2B PT2B	NO			NO			
PETPU 3 *		NO		NO			
PETPU 4 PT4				NO			
PETPU 5 PT5				NO			
PETPU 6 PT6				NO			
PETPU 7 BT1				NO			
PETPU 8 PT8				NO			
PETPU 9 PT9				NO			
PETPU 10 PT10							
PETPU 12 FS							
PETPU 13 PT13	NO						

Table 28: Pilot Unit Petrobras Resids

*No Overhead Temperatures

	Data Type				Detailed Hydrocarbon Analysis		
CITGO	Distillation	Sim Dis	Density	Sulfur	IBP- 113	113 - 400	400 - 430
CITPU 1 PT1	NO		NO	NO	NO	NO	NO
CITPU 2A PT2A			NO	NO			
CITPU 3 PT3			NO 650+	NO			
CITPU 4 PT4			NO	NO	NO	NO	NO
CITPU 5 PT5	NO		NO	NO	NO	NO	NO
CITPU 6 PT6			NO 650+	NO			
CITPU 7 PT 7			NO 650+	NO			
CITPU 8 PT8				NO			
CITPU 10 PT10			NO 650+	NO			
CITPU 15 PT15			NO 650+	NO			
CITPU 16 PT16							
CITPU 17 PT17							
CITPU 18 PT18			NO 650+				
CITPU 19 PT19							
CITPU 20 PT20							
CITPU 21 PT21							

Table 29: Pilot Unit Citgo Resids

	Data Type				Detailed Hydrocarbon Analysis		
EQUILON	Distillation	Sim Dis	Density	Sulfur	IBP- 113	113 - 400	400 - 430
EQPU 8 PT8							
EQPU 9 PT9	NO	NO		NO	NO	NO	NO
EQPU 10 PT10							
EQPU 12 FS1							
EQPU 13 SO1	NO	NO		NO	NO	NO	NO
EQPU 14 SO2							

Table 30: Pilot Unit Equilon Resids

Liquids Obtained Using 6 ft Coke Drum Pilot Unit Runs

Tables 7-12 show the PUAF runs available in the compiled database. All analysis in the report is based solely on the available sample runs. Table 31 through Table 36 show the PUAF runs available in the compiled database. All analysis in the report is based solely on the available sample runs.

Key

	0.25 inch
	Data is available
NO	No data is available

No sulfur analyses have been conducted on any of the PUAF runs and detailed hydrocarbon analysis is still in progress.

	Data Type				Detailed Hydrocarbon Analysis		
CHEVRON	**Distillation**	**Sim Dis**	**Density**	**Sulfur**	**IBP- 113**	**113 - 400**	**400- 430**
CHEV 1 PUAF				NO	NO	NO	NO
CHEV 2 PUAF Rst				NO	NO	NO	NO
CHEV 3 PUAF				NO	NO	NO	NO
CHEV 4 PUAF *	NO	NO	NO	NO	NO	NO	NO
CHEV 5 PUAF				NO	NO	NO	NO
CHEV 6 PUAF				NO	NO	NO	NO
CHEV 7A PUAF				NO	NO	NO	NO
CHEV 8 PUAF				NO			
CHEV 9 PUAF				NO			
CHEV 10 PUAF				NO			
CHEV 11 PUAF	NO		NO	NO		NO	NO

Table 31: PUAF Chevron Resids ***No Normalized wt% (overhead) temperatures**

	Data Type				Detailed Hydrocarbon Analysis		
MARATHON	**Distillation**	**Sim Dis**	**Density**	**Sulfur**	**IBP- 113**	**113 - 400**	**400 - 430**
MARA 1 PUAF				NO			
MARA 2 PUAF				NO			
MARA 3 PUAF				NO			
MARA 4 PUAF				NO	NO		
MARA 5 PUAF				NO	NO		
MARA 6 PUAF		NO		NO			
MARA 7 PUAF				NO	NO		

Table 32: PUAF Marathon Resids

	Data Type				Detailed Hydrocarbon Analysis		
SUNCOR	Distillation	Sim Dis	Density	Sulfur	IBP- 113	113 - 400	400 - 430
SUN 1 PUAF				NO	NO	NO	NO
SUN 2 PUAF				NO	NO	NO	NO
SUN 3 PUAF				NO	NO	NO	NO
SUN 4 PUAF				NO	NO	NO	NO
SUN 5 PUAF				NO	NO	NO	NO
SUN 6 PUAF				NO	NO	NO	NO
SUN 7 PUAF				NO	NO	NO	NO
SUN 8 PUAF				NO	NO	NO	NO
SUN 9 PUAF				NO	NO		
SUN 10 PUAF				NO	NO		
SUN 11 PUAF	NO		NO	NO	NO	NO	NO
SUN 12 PUAF				NO	NO		
SUN 13 PUAF				NO			

Table 33: PUAF Suncor Resids

	Data Type				Detailed Hydrocarbon Analysis		
PETROBRAS	Distillation	Sim Dis	Density	Sulfur	IBP- 113	113 - 400	400 - 430
PETR 1 PUAF				NO			
PETR 2 PUAF				NO			
PETR 3 PUAF				NO			
PETR 4 PUAF				NO	NO		
PETR 5 PUAF				NO			
PETR 6 PUAF				NO			
PETR 7 PUAF				NO			
PETR 8 PUAF				NO			
PETR 9 PUAF I				NO			
PETR 10 PUAF I	NO		NO	NO			
PETR 11 PUAF I	NO		NO	NO	NO	NO	NO
PETR 12 PUAF I	NO		NO	NO	NO	NO	NO
PETR 13 PUAF C	NO		NO	NO	NO	NO	NO
PETR 14 PUAF C	NO	NO	NO	NO	NO	NO	NO
PETR 15 PUAF C	NO	NO	NO	NO	NO	NO	NO
PETR 16 PUAF I	NO	NO	NO	NO	NO	NO	NO

Table 34: PUAF Petrobras Resids

	Data Type				Detailed Hydrocarbon Analysis		
EQUILON	Distillation	Sim Dis	Density	Sulfur	IBP- 113	113 - 400	400 - 430
EQ 1 PUAF			NO	NO	NO	NO	NO
EQ 2 PUAF				NO	NO	NO	NO
EQ 3 PUAF				NO	NO	NO	NO
EQ 4 PUAF				NO			
EQ 5 PUAF				NO	NO		
EQ 6 PUAF				NO			
EQ 7 PUAF I	NO	NO	NO	NO	NO	NO	NO
EQ 8 PUAF C	NO	NO	NO	NO	NO	NO	NO
EQ SO1 PUAF				NO	NO	NO	NO

Table 35: PUAF Equilon Resids

	Data Type				Detailed Hydrocarbon Analysis		
CITGO	Distillation	Sim Dis	Density	Sulfur	IBP- 113	113 - 400	400 - 430
CIT 1 PUAF				NO			
CIT 2 PUAF				NO			
CIT 3 PUAF				NO			
CIT 4 PUAF				NO			
CIT 5 PUAF				NO			
CIT 6 PUAF				NO			
CIT 7 PUAF				NO			
CIT 8 PUAF				NO			
CIT 9 PUAF				NO	NO		
CIT 10 PUAF				NO	NO		
CIT 11 PUAF				NO			
CIT 12 PUAF				NO			

Table 36: PUAF Citgo Resids

2. *Distillation:*

The pilot unit runs were conducted at bottom feed temperatures of 900oF and 930oF, and the average overhead temperature was monitored. To ensure that the average overhead temperature can be substituted with the feed temperatures, the effects of the temperatures on the weight percent of the feed had to be investigated.

Using the data obtained from the 3ft pilot unit runs, the weight percent (%) of the feed for the boiling point ranges IBP-113°F, 113-400°F, 400-430°F, 430-650°F, and 650°F+ were plotted against the bottom temperatures (900°F and 930°F) at 15psig and 40psig, respectively (Figure 66 and Figure 67). These plots were also constructed using the average overhead temperature in place of the bottom temperature (Figure 68 and Figure 69).

All four plots were repeated using the Sim Dis data for the 3ft pilot unit and is illustrated in Figure 70 through Figure 73.

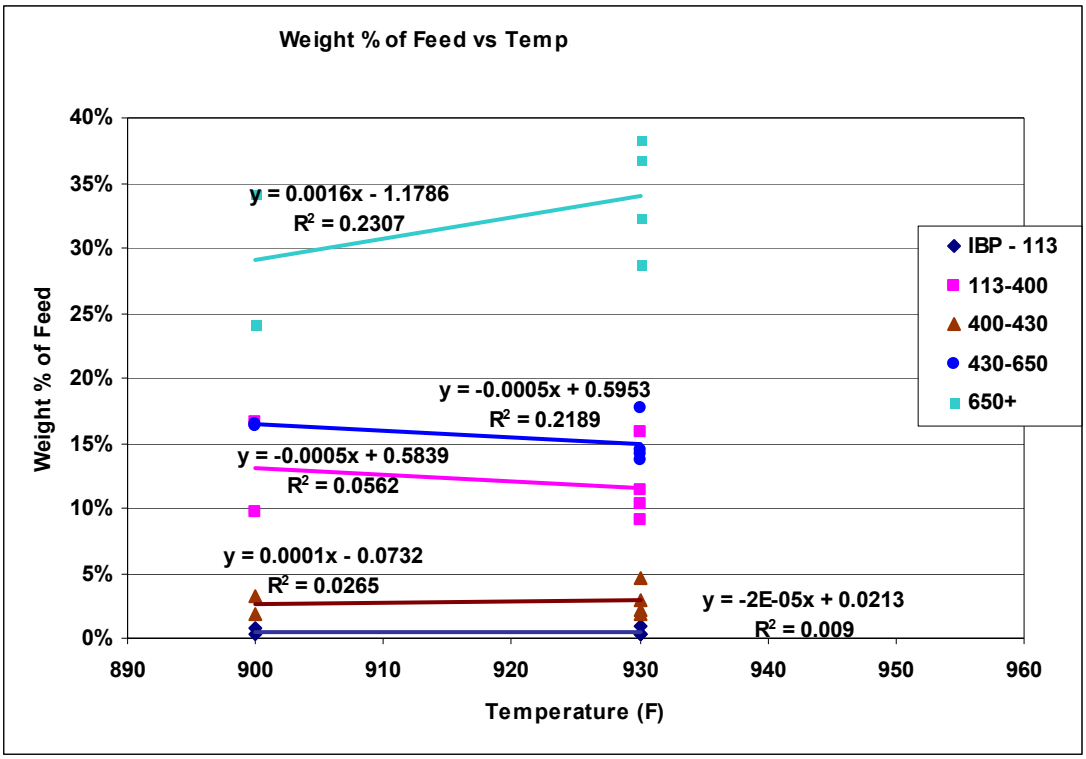

Figure 66: PU Distillation at 15psig with bottom temperatures of 900F and 930F

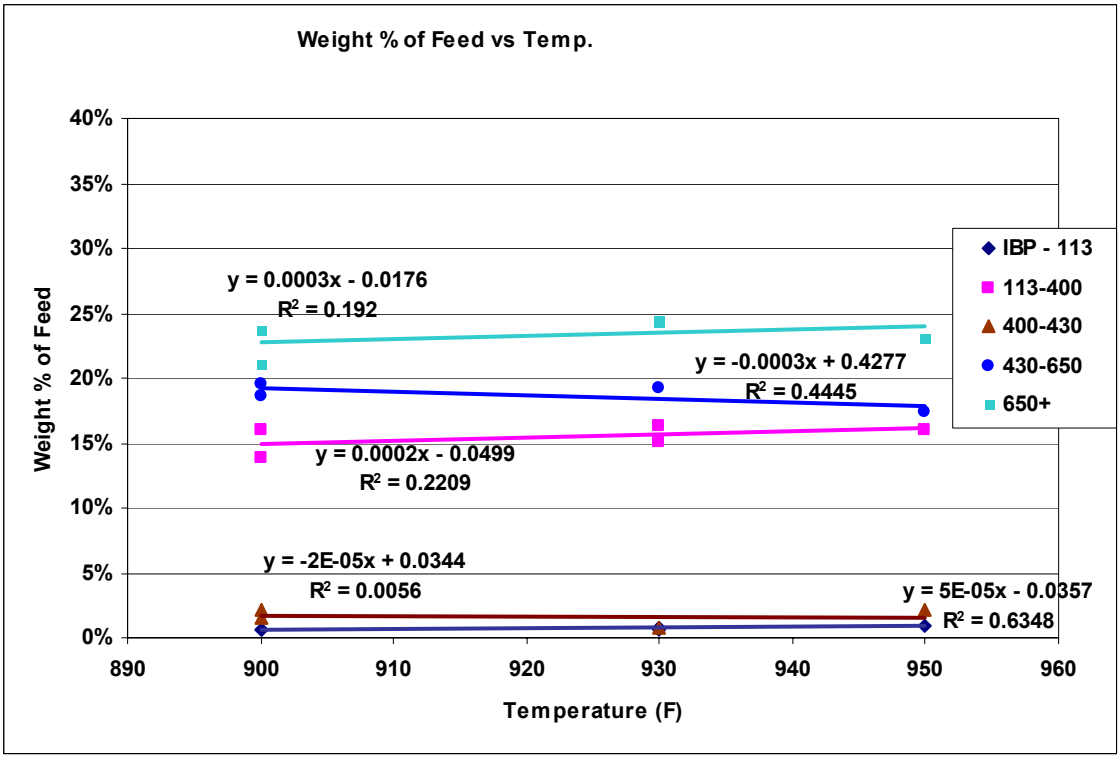

Figure 67: PU Distillation at 40psig with bottom temperatures of 900F and 930F

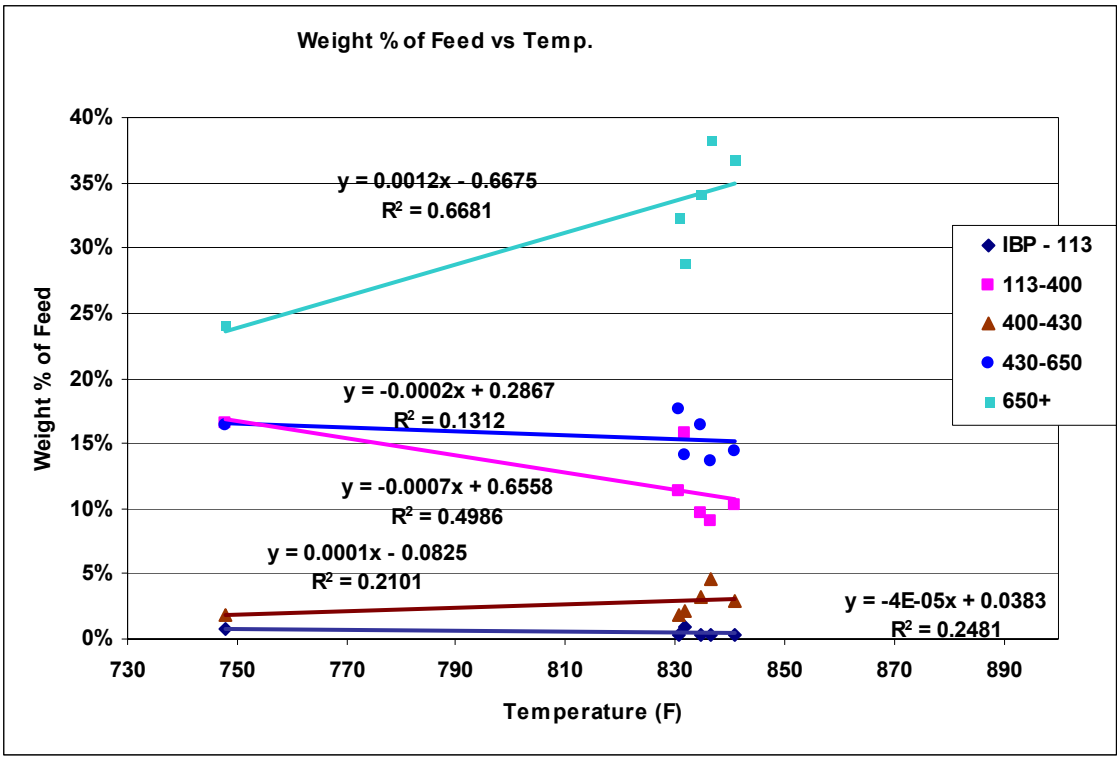

Figure 68: PU Distillation at 15psig with average overhead temperatures

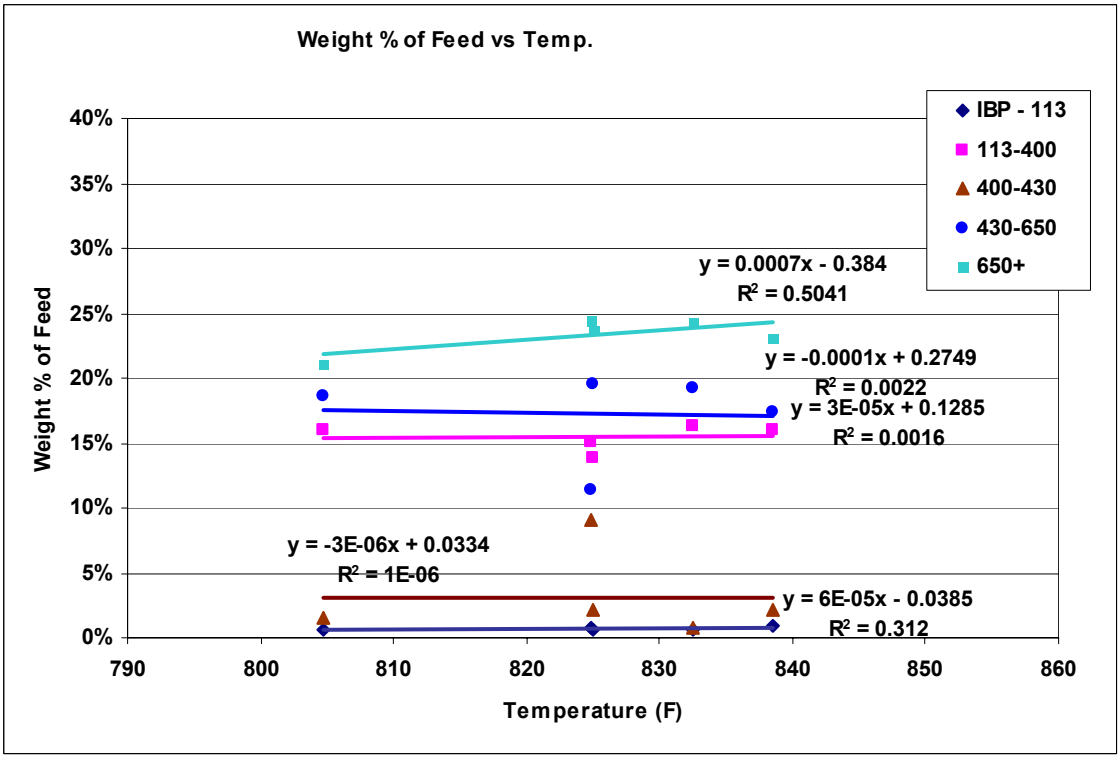

Figure 69: PU Distillation at 40psig with average overhead temperatures

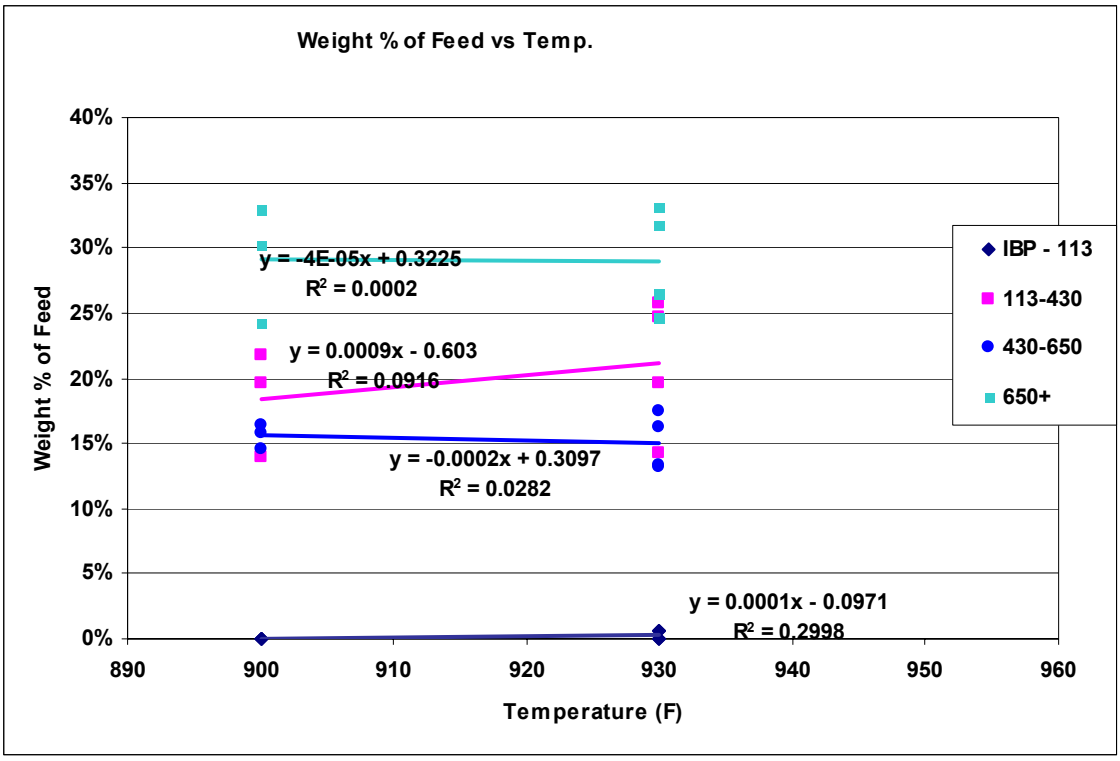

Figure 70: PU Sim. Distillation at 15psig with bottom temperatures of 900F and 930F

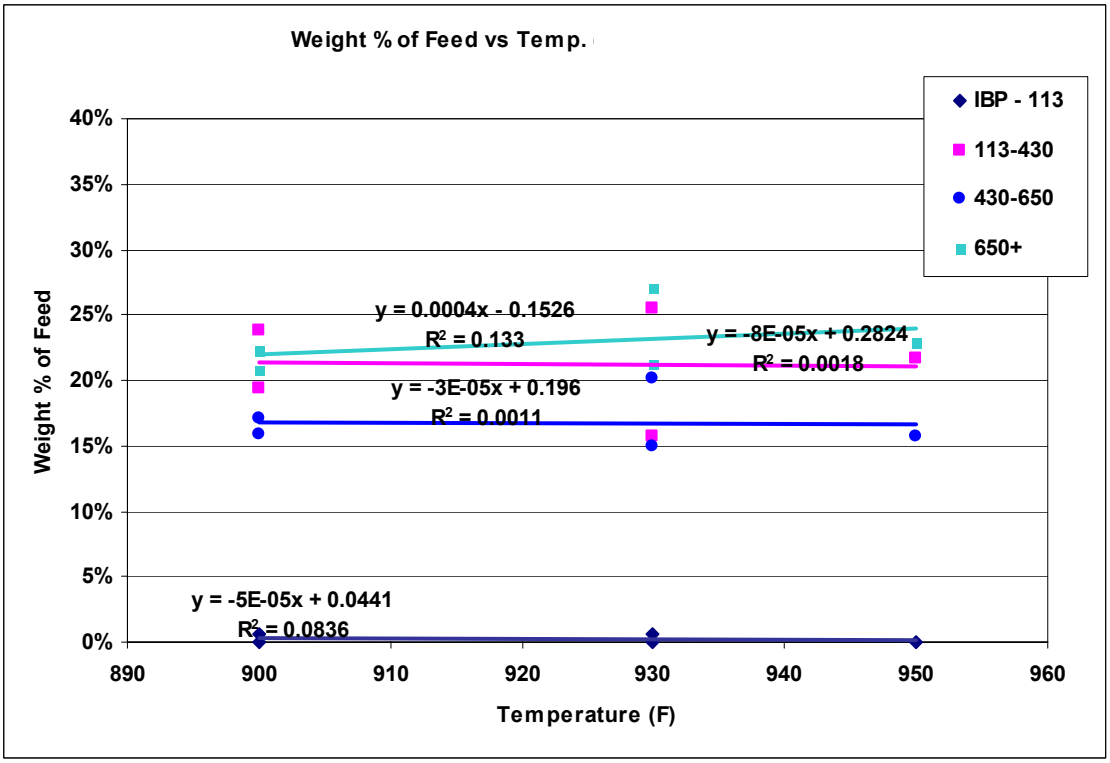

Figure 71: PU Sim. Distillation at 40psig with bottom temperatures of 900F and 930F

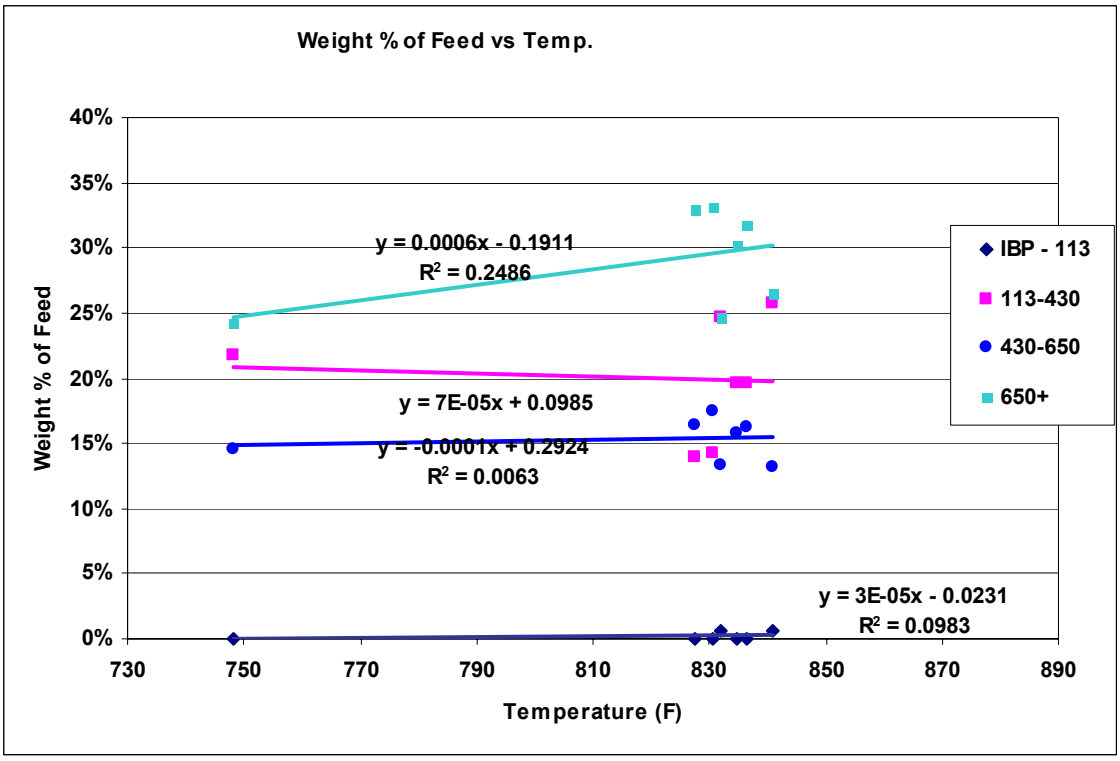

Figure 72: PU Sim. Distillation at 15psig with average overhead temperatures

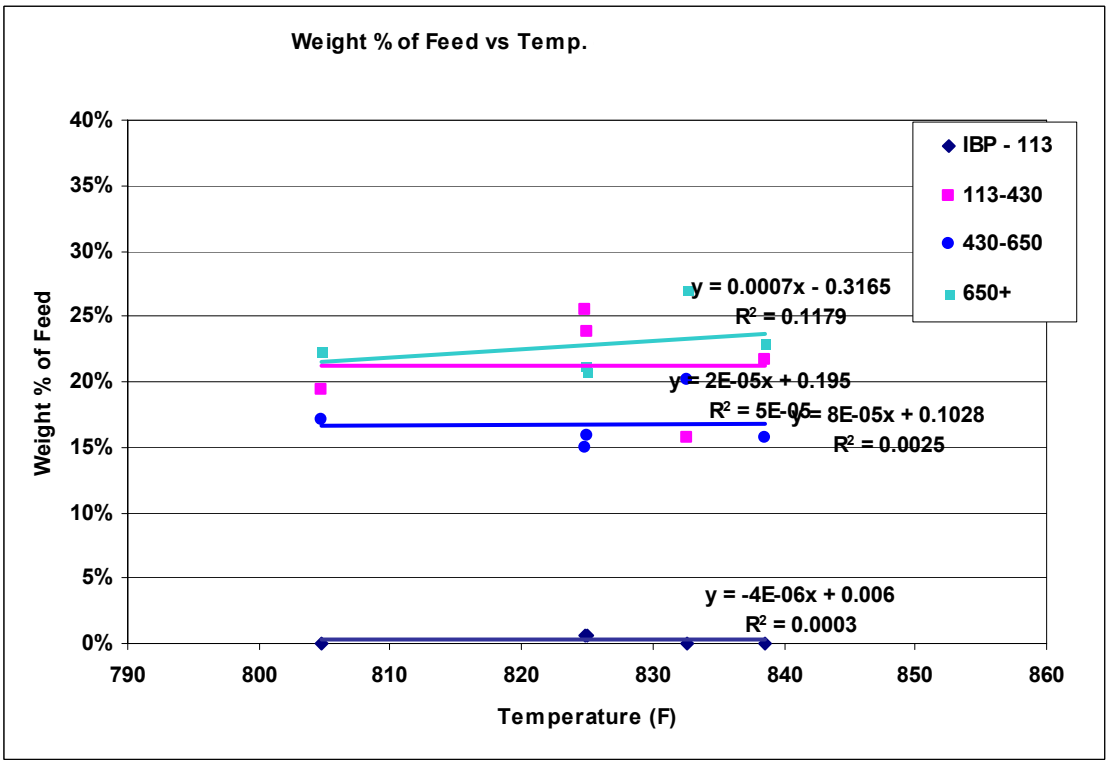

Figure 73: PU Sim. Distillation at 40psig with average overhead temperatures

The slopes of the distillation data plots in Figure 66 through Figure 73 are represented in the matrixes below. Most of the resids had similar trends for both the bottom and overhead temperatures. Using the Suncor resid as a reference, it is seen that the correlations were quite consistent among each resid group.

PU Distillation **The weight % of feed vs. temperature curve slopes**

+	Positive slope
-	Negative slope
0	y = 0

Bottom Temperature

Sample	IBP - 113	113 - 400	400 - 430	430 - 650	650+
CHV	-	-	+	-	+
MAR	+	-	+	+	-
PET	-	-	-	-	+
CIT	-	-	-	-	+
EQU	Only One Data Available				
SUN	-	+	-	+	-

Table 37: PU Bottom temperature at 15

Sample	IBP - 113	113 - 400	400 - 430	430 - 650	650+
CHV	+	+	-	-	+
MAR	+	+	+	-	+
PET	-	-	+	-	+
CIT	+	+	+	-	+
EQU	+	+	+	+	+
SUN	+	+	+	-	+

Table 38: PU Bottom temperature at 40 psig

Overhead Temperature

Sample	IBP - 113	113 - 400	400 - 430	430 - 650	650+
CHV	-	-	+	-	+
MAR	+	+	-	-	+
PET	-	-	-	-	+
CIT	-	-	-	-	+
EQU	Only One Data Available				
SUN	-	+	-	+	-

Table 39: PU Overhead Temperature at 15 psig

Sample	IBP - 113	113 - 400	400 - 430	430 - 650	650+
CHV	+	+	-	+	+
MAR	+	+	+	-	+
PET	-	+	+	+	+
CIT	+	+	+	-	+
EQU	+	+	+	+	+
SUN	+	+	+	-	+

Table 40: PU Overhead Temperature at 40 psig

As with the distillation data, the slopes of the Sim Dis data in Figure 70 through Figure 73 were incorporated into the matrices in below. Again, using the Suncor resid as a reference, the correlations among each resid group are quite consistent.

PU Simulation Distillation **The weight % of feed vs. temperature curve slopes**

+	Positive slop
-	Negative slop
0	y = 0

Bottom Temperature

Sample	IBP - 113	113 - 430	430 - 650	650+
CHV	+	+	-	-
MAR	0	-	+	+
PET	0	+	-	+
CIT	0	+	-	+
EQU	Only One Data Available			
SUN	0	-	-	-

Table 41: PU Sim Dis at bottom temperature (15 psig)

Sample	IBP - 113	113 - 430	430 - 650	650+
CHV	-	-	-	+
MAR	-	-	-	+
PET	+	-	-	+
CIT	+	+	-	+
EQU	0	+	-	+
SUN	0	-	-	+

Table 42: PU Sim Dis at bottom temperature (40 psig)

Overhead Temperature

Sample	IBP - 113	113 - 430	430 - 650	650+
CHV	+	-	+	+
MAR	0	+	-	+
PET	0	+	-	+
CIT	0	+	-	+
EQU	Only One Data Available			
SUN	0	-	-	-

Table 43: PU Sim Dis at overhead temperature (15 psig)

Sample	IBP - 113	113 - 430	430 - 650	650
CHV	-	+	+	+
MAR	-	-	+	+
PET	-	-	-	+
CIT	+	+	-	+
EQU	0	+	+	+
SUN	0	-	-	+

Table 44: PU Sim Dis at overhead temperature (40 psig)

To ensure that the similarities between the bottom and overhead temperatures were not restricted to the pilot unit (3ft drum); the 6ft PUAF distillation and simulation distillation data were analyzed at both the bottom and average overhead temperatures for the different boiling cuts at 15 psig and 40 psig. The resulting slopes are represented the matrixes in the tables below for the PUAF distillation data, and that of the PUAF Sim Dis data is on the next page. Using the Suncor resid as a reference, it is seen that the correlations were consistent among each resid group.

PUAF Distillation **The weight % of feed vs. temperature curve slopes**

+	Positive slope
-	Negative slope
0	y = 0

Bottom Temperature

Sample	IBP - 113	113 - 400	400 - 430	430 - 650	650+
CHV	-	-	+	-	+
MAR	+	-	+	-	+
PET	-	-	-	-	+
CIT	-	-	-	-	+
EQU	-	+	-	+	+
SUN	-	-	+	-	+

Table 45: PUAF Bottom temperature at 15 psig

Sample	IBP - 113	113 - 400	400 - 430	430 - 650	650+
CHV	+	-	+	-	+
MAR	+	+	-	+	-
PET	+	-	-	-	+
CIT	+	+	+	-	+
EQU	+	+	+	-	+
SUN	+	+	-	-	+

Table 46: PUAF Bottom temperature at 40 psig

Overhead Temperature

Sample	IBP - 113	113 - 400	400 - 430	430 - 650	650+
CHV	+	-	+	-	+
MAR	+	-	+	-	+
PET	-	-	-	-	+
CIT	+	-	-	-	+
EQU	-	+	-	+	+
SUN	-	-	+	-	+

Table 47: PUAF Overhead temperature at 15 psig

Sample	IBP - 113	113 - 400	400 - 430	430 - 650	650+
CHV	-	-	+	-	+
MAR	+	+	-	+	-
PET	-	-	+	-	+
CIT	-	-	-	-	+
EQU	+	+	+	-	+
SUN	+	+	-	-	+

Table 48: PUAF Overhead temperature at 40 psig

PUAF Simulation Distillation **The weight % of feed vs. temperature curve slopes**

+	Positive slope
-	Negative slope
0	y = 0

Bottom Temperature

Sample	IBP - 113	113 - 430	430 - 650	650+
CHV	+	+	-	-
MAR	-	-	-	-
PET	-	+	-	-
CIT	+	+	+	-
EQU	-	+	+	-
SUN	+	-	+	-

Table 49: PUAF Sim Dis Bottom temperature (15 psig)

Sample	IBP - 113	113 - 430	430 - 650	650+
CHV	+	-	+	-
MAR	Only one data point			
PET	+	+	-	-
CIT	+	+	+	-
EQU	+	+	-	-
SUN	-	+	-	-

Table 50: PUAF Sim Dis Bottom temperature (40 psig)

Overhead Temperature

Table 16c: 15 psig

Sample	IBP - 113	113 - 430	430 - 650	650+
CHV	-	+	-	-
MAR	-	-	-	-
PET	-	+	-	-
CIT	+	+	+	-
EQU	-	+	+	-
SUN	+	-	+	-

Table 51: PUAF Sim Dis Overhead temperature (15 psig)

Table 16d: 40 psig

Sample	IBP - 113	113 - 430	430 - 650	650+
CHV	-	+	+	-
MAR	Only one data point			
PET	+	+	-	-
CIT	-	+	+	-
EQU	+	+	-	-
SUN	-	+	-	-

Table 52: PUAF Sim Dis Overhead temperature (40 psig)

Both the PU and PUAF distillation and simulated distillation data indicated that the feed and overhead temperatures would exhibit similar trends at the same pressure. This observation reduces the work of having to repeat analyzing data at both the bottom and overhead temperatures.

3. ***Distillation:*** *Feed Rate Analysis*

A feed rate of 1200g/hr was used for all of the resids run in the 3ft pilot unit, therefore the effect of changes in the feed rate on the distillation data could not be analyzed. On the contrary, the 6ft pilot unit was run at different flow rates ranging from 1200g/hr to 4800g/hr. For brevity, only the Chevron PUAF samples at both 15psig and 40psig will be discussed.

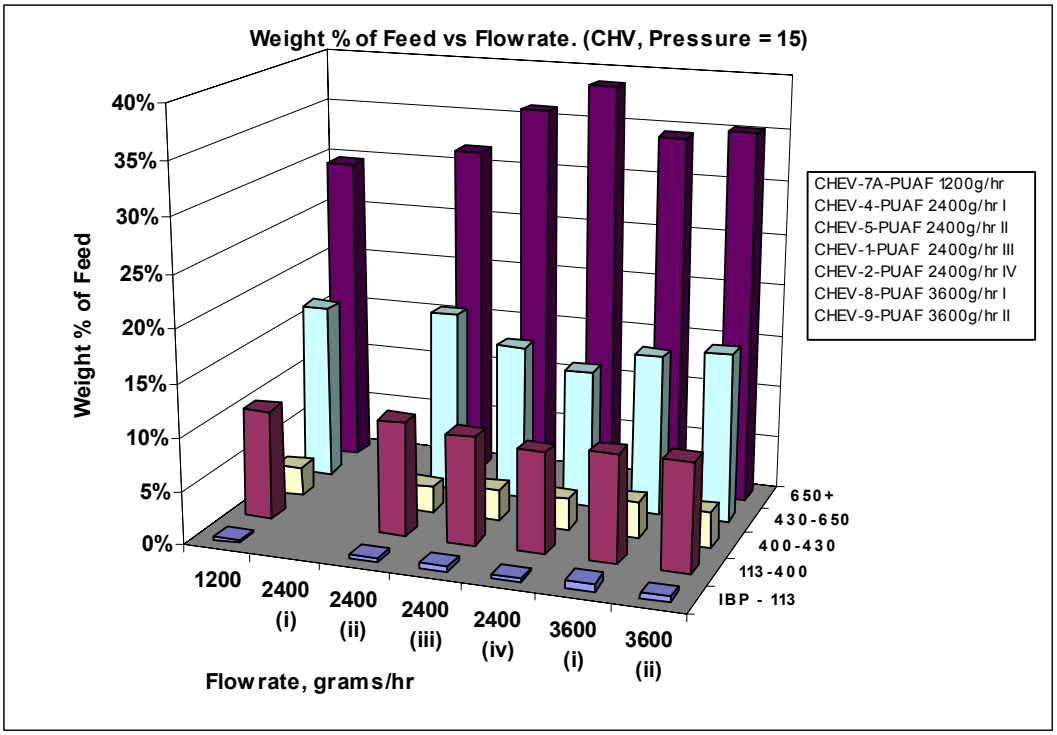

Figure 74: Flow rate analysis of Chevron PUAF samples at 15psig

In Figure 74 above, the 650+^{o}F cut had the highest weight percent of feed, followed by the 430-650^{o}F cut, then the 113-400^{o}F cut and 400-430^{o}F cut. The IBP-113^{o}F had the least weight percent of feed. This trend was the same for the 1200 g/hr, 2400 g/hr and 3600 g/hr flow rates.

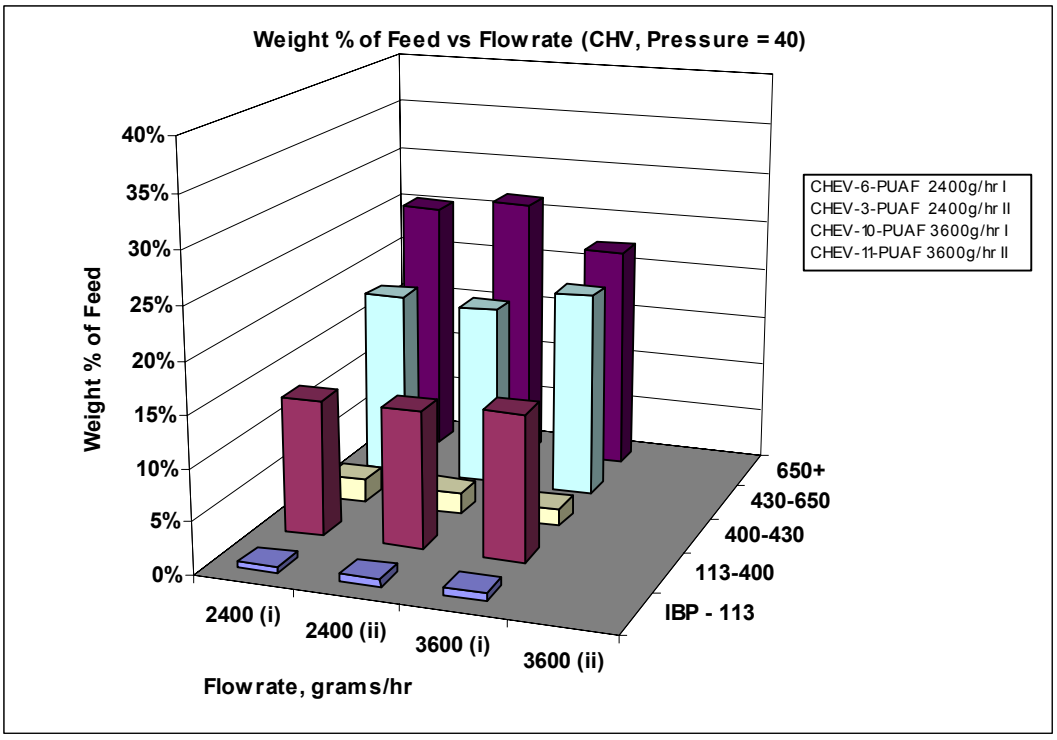

Figure 75: Flow rate analysis of Chevron PUAF samples at 40psig

Again in Figure 75, at 40psig, the 650+°F cut had the highest weight percent of feed, followed by the 430-650°F cut, then the 113-400°F cut and 400-430°F cut. The IBP-113°F had the least weight percent of feed. This trend was the same for the 2400 g/hr and 3600 g/hr flow rates.

In conclusion, it has been observed that changing the flow rate does not affect the distribution of the weight percent of feed in the different temperature cuts.

The effect of the changing the flow rates on the PiONA components at the different DHA temperature cuts will be analyzed in the DHA section of the report.

4. ***Detailed Hydrocarbon Analysis (DHA)***

As stated previously, the overall outcome of the DHA analysis is to be able to predict what type of PiONA component would be dominant at a certain temperature and pressure, and how a change in the temperature and pressure would affects its production.

DHA analyses were conducted for both the PU and PUAF liquid sub products. The effect of temperature and pressure on the mass percent will be discussed for each type of PiONA component at the three cuts. For brevity, only the results for the chevron resid will be discussed.

In general, it is observed that the IBP-113^{o}F cut has the highest mass percent of paraffin, followed by the 113-400^{o}F and then the 400-430^{o}F, for the Chevron runs.

At 15 psig, the 113-400^{o}F cut has the highest amount of Iso-paraffin followed by the IBP-113^{o}F, then the 400-430^{o}F. The same trends were seen when the pressure is raised to 40psig.

Regardless of pressure, the lowest temperature cut (IBP-113^{o}F) contained the largest amounts of olefins.

The middle temperature cut (113-400^{o}F) contained the largest amount of naphthene, while the 400-430^{o}F cut contained the smallest amount of naphthene.

The most aromatics for the Chevron runs were found in the 400-430^{o}F cut followed by the 113-400^{o}F cut then the IBP-113^{o}F cut.

The majority of the oxygenate present in the Chevron samples were in the IBP-113^{o}F cut. There were no traces of oxygenates in the 400-430^{o}F cut.

PiONA plots were also constructed for the Marathon, Petrobras, Citgo, Equilon and Suncor liquid samples, These are provided in the appendix. The effects of temperature and pressure on the mass percent of each PiONA component have been complied into a matrix form. The order of decreasing mass percent (%) of component is from 1 to 3. A key is provided below to interpret the DHA tables

1	**Highest mass percent of component**
2	
3	**Lowest mass percent of component**

DHA PU TEMPERATURE ANALYSIS

900F		CHEVRON			MARATHON			PETROBRAS			CITGO			EQUILON			SUNCOR		
		IBP-113	113-400	400-430	IBP-113	113-400	400-430	IBP-113	113-400	400-430	IBP-113	113-400	400-430	IBP-113	113-400	400-430	IBP-113	113-400	400-430
Paraffin	15 psig	1	2	3	No samples were run			No samples were run			1	3	2	No samples were run			1	2	3
	40 psig	1	2	3	1	2	3	1	2	3	1	3	2	1	2	3	1	2	3
Iso-Paraffin	15 psig	2	1	3	No samples were run			No samples were run			2	1	3	No samples were run			2	1	3
	40 psig	2	1	3	2	1	3	2	1	3	2	1	3	2	1	3	2	1	3
Olefin	15 psig	1	2	3	No samples were run			No samples were run			1	2	3	No samples were run			1	2	3
	40 psig	1	2	3	1	2	3	1	2	3	1	2	3	1	2	3	1	2	3
Naphthenes	15 psig	2	1	3	No samples were run			No samples were run			2	1	3	No samples were run			2	1	3
	40 psig	2	1	3	2	1	3	2	1	3	2	1	3	2	1	3	2	1	3
Aromatics	15 psig	3	2	1	No samples were run			No samples were run			3	2	1	No samples were run			3	2	1
	40 psig	3	2	1	3	2	1	3	2	1	3	2	1	3	2	1	3	2	1
Oxygenates	15 psig	1	2	3	No samples were run			No samples were run			No Oxygenates present			No samples were run			1	2	3
	40 psig	1	2	3	1	2	3	1	2	3	No Oxygenates present			1	2	3	1	2	3

Table 53: DHA PU Temperature Analysis at 900F

For the 900°F feed temperature at 15psig and 40psig, the IBP-113°F cut had a high concentration of paraffin, olefin, and oxygenates, followed by iso-paraffins and naphthenes in medium amounts, while aromatics are in minimal proportions. The 113-400°F cut for all six resids had high quantities of iso-paraffins and naphthenes. For the Chevron, Marathon, Petrobras, Equilon, and Suncor resids, the 113-400°F cut had medium amounts of paraffin, olefins, aromatics, and oxygenates. In the Citgo resid, the 113-400°F cut had paraffin in minimal proportions. The 400-430°F cut, for most of the resids, had a high concentration of aromatics and contained small amounts of paraffin, iso-paraffins, olefins, naphthenes, and oxygenates. The Citgo resid had medium amounts of paraffin present in the 400-430°F cut and no oxygenates present in any of the temperature cuts.

930F		CHEVRON			MARATHON			PETROBRAS			CITGO			EQUILON			SUNCOR		
		IBP-113	113-400	400-430	IBP-113	113-400	400-430	IBP-113	113-400	400-430	IBP-113	113-400	400-430	IBP-113	113-400	400-430	IBP-113	113-400	400-430
Paraffin	15 psig	1	2	3	No samples were run			No samples were run			1	3	2	1	2	3	1	2	3
	40 psig	1	2	3	1	2	3	1	2	3	1	3	2	1	2	3	1	2	3
Iso-Paraffin	15 psig	2	1	3	No samples were run			No samples were run			2	1	3	2	1	3	2	1	3
	40 psig	2	1	3	2	1	3	2	1	3	2	1	3	2	1	3	2	1	3
Olefin	15 psig	1	2	3	No samples were run			No samples were run			1	2	3	1	2	3	1	2	3
	40 psig	1	2	3	1	2	3	1	2	3	1	2	3	1	2	3	1	2	3
Naphthenes	15 psig	2	1	3	No samples were run			No samples were run			2	1	3	2	1	3	2	1	3
	40 psig	2	1	3	2	1	3	2	1	3	2	1	3	2	1	3	2	1	3
Aromatics	15 psig	3	2	1	No samples were run			No samples were run			3	2	1	3	2	1	3	2	1
	40 psig	3	2	1	3	2	1	3	2	1	3	2	1	3	2	1	3	2	1
Oxygenates	15 psig	1	2	3	No samples were run			No samples were run			No Oxygenates present			1	2	3	1	2	3
	40 psig	1	2	3	1	2	3	1	2	3	No Oxygenates present			1	2	3	1	2	3

Table 54: DHA PU Temperature Analysis at 930F

The 930°F feed temperature at 15psig and 40psig, the IBP-113°F cut had a high concentration of paraffin, olefin, and oxygenates, followed by iso-paraffins and naphthenes in medium amounts, and aromatics in minimal proportions. The 113-400°F cut for all six resids had high quantities of iso-paraffins and naphthenes. For the Chevron, Marathon (40psig), Petrobras (40psig), Equilon, and Suncor resids, the 113-400°F cut had medium amounts of paraffin, olefins, aromatics, and oxygenates. In the Citgo resid, the 113-400°F cut had paraffin in minimal proportions. The 400-430°F cut, for most of the company resids, had a high concentration of aromatics and contained small amounts of paraffin, iso-paraffins, olefins, naphthenes, and oxygenates. The Citgo resid had medium amounts of paraffin present in the 400-430°F cut and no oxygenates present in any of the temperature cuts. No samples were run at 15 psig for Marathon and Petrobras.

950F		CHEVRON			MARATHON			PETROBRAS			CITGO			EQUILON			SUNCOR		
		IBP-113	113-400	400-430	IBP-113	113-400	400-430	IBP-113	113-400	400-430	IBP-113	113-400	400-430	IBP-113	113-400	400-430	IBP-113	113-400	400-430
Paraffin	15 psig	No samples were run			No samples were run			No samples were run at 950F			1	3	2	No samples were run at 950F			No samples were run		
	40 psig	1	2	3	1	2	3				No samples were run						1	2	3
Iso-Paraffin	15 psig	No samples were run			No samples were run						2	1	3				No samples were run		
	40 psig	2	1	3	2	1	3				No samples were run						2	1	3
Olefin	15 psig	No samples were run			No samples were run						1	2	3				No samples were run		
	40 psig	1	2	3	1	2	3				No samples were run						1	2	3
Naphthenes	15 psig	No samples were run			No samples were run						2	1	3				No samples were run		
	40 psig	2	1	3	2	1	3				No samples were run						2	1	3
Aromatics	15 psig	No samples were run			No samples were run						3	2	1				No samples were run		
	40 psig	3	2	1	3	2	1				No samples were run						3	2	1
Oxygenates	15 psig	No samples were run			No samples were run						No Oxygenates present						No samples were run		
	40 psig	1	2	3	1	2	3				No samples were run						1	2	3

Table 55: DHA PU Temperature Analysis at 950F

No Petrobras and Equilon samples were run at 950°F. No samples were run at 15psig for Chevron, Marathon and Suncor, and no samples were run at 40psig for Citgo. At 40psig, the IBP-113°F cut had a high concentration of paraffin, olefin, and oxygenates in the Chevron, Marathon and Suncor resids, followed by iso-paraffins and naphthenes in medium amounts, and aromatics in minimal proportions. The 113-400°F cut for Chevron, Marathon and Suncor had high quantities of iso-paraffins and naphthenes, and paraffins, olefins, aromatics, and oxygenates in medium amounts. The 400-430°F cut for Chevron, Marathon and Suncor had a high concentration of aromatics and contained small amounts of paraffins, iso-paraffins, olefins, naphthenes, and oxygenates. The Citgo resids, at 950F, were run at 15psig. Its IBP-113°F cut had high quantities of paraffin, and olefin, medium amounts of iso-paraffins and naphthenes, and minimal amounts of aromatics. The 113-400°F cut had minimal amounts of paraffin, and contained mostly iso-paraffins and naphthenes, and at the 400-430°F cut, had mostly aromatics present. The Citgo resid had no oxygenates present at 15 psig.

PiONA plots were constructed using the PUAF data for all six resids. The effects of temperature and pressure on the mass percent of each PiONA component were complied into a matrix form. The order of decreasing mass percent (%) of component is labeled from 1 to 3. The key used in interpreting the PU DHA data allows applies to the PUAF DHA data.

DHA PUAF TEMPERATURE ANALYSIS

900F		CHEVRON			MARATHON			PETROBRAS			CITGO			EQUILON			SUNCOR		
		IBP-113	113-400	400-430	IBP-113	113-400	400-430	IBP-113	113-400	400-430	IBP-113	113-400	400-430	IBP-113	113-400	400-430	IBP-113	113 - 400	400 - 430
Paraffin	15 psig	1	2	3	3	1	2	1	2	3	1	2	3	1	2	3	-	-	-
	40 psig	1	2	3	2	1	3	1	2	3	1	2	3	1	2	3	-	-	-
Iso-Paraffin	15 psig	3	1	2	2	1	3	2	1	3	2	1	3	2	1	3	-	-	-
	40 psig	2	1	3	2	1	3	2	1	3	2	1	3	2	1	3	-	-	-
Olefin	15 psig	1	2	3	1	2	3	1	2	3	1	2	3	1	2	3	-	-	-
	40 psig	1	2	3	1	2	3	1	2	3	1	2	3	1	2	3	-	-	-
Naphthenes	15 psig	2	1	3	2	1	3	2	1	3	2	1	3	2	1	3	-	-	-
	40 psig	2	1	3	2	1	3	2	1	3	2	1	3	2	1	3	-	-	-
Aromatics	15 psig	3	2	1	3	2	1	3	2	1	3	2	1	3	2	1	-	-	-
	40 psig	3	1	2	3	1	2	3	2	1	3	2	1	3	1	2	-	-	-
Oxygenates	15 psig	1	2	3	1	2	3	1	2	3	1	2	3	1	2	3	-	-	-
	40 psig	1	2	3	1	2	3	1	2	3	1	2	3	1	2	3	-	-	-

Table 56: DHA PUAF Temperature Analysis at 900F

Since PUAF DHA has not been run on most of the Suncor sample, it is not analyzed in the matrix. Petrobras, Citgo, and Equilon exhibited identical trends. These three resids contained large amounts of paraffin, olefins, and oxygenates at the IBP-113°F cut, mostly iso-paraffins and naphthenes in the 113-400°F cut, and predominantly aromatics in the 400-430°F cut. The Chevron resid showed almost the same trends, but the IBP-113°F cut contained minimal amounts of iso-paraffins at 15 psig. The 113-400°F cut had iso-paraffins in high concentrations and the 400-430°F cut had average amounts of iso-paraffins. The Marathon 113-400°F cut had large quantities of paraffins, iso-paraffins, and naphthenes.

930F		CHEVRON			MARATHON			PETROBRAS			CITGO			EQUILON			SUNCOR		
		IBP - 113	113 - 400	400-430	IBP - 113	113 - 400	400 - 430	IBP - 113	113 - 400	400 - 430	IBP - 113	113 - 400	400 - 430	IBP - 113	113 - 400	400-430	IBP-113	113 - 400	400 - 430
Paraffin	15 psig	1	2	3	3	1	2	1	2	3	1	2	3	-	-	-	1	2	3
	40 psig	-	-	-	-	-	-	1	2	3	1	2	3	-	-	-	-	-	-
Iso-Paraffin	15 psig	3	1	2	2	1	3	2	1	3	3	1	2	-	-	-	2	1	3
	40 psig	-	-	-	-	-	-	2	1	3	3	1	2	-	-	-	-	-	-
Olefin	15 psig	1	2	3	1	2	3	1	2	3	1	2	3	-	-	-	1	2	3
	40 psig	-	-	-	-	-	-	1	2	3	1	2	3	-	-	-	-	-	-
Naphthenes	15 psig	2	1	3	2	1	3	2	1	3	2	1	3	-	-	-	2	1	3
	40 psig	-	-	-	-	-	-	2	1	3	2	1	3	-	-	-	-	-	-
Aromatics	15 psig	3	2	1	3	2	1	3	2	1	3	2	1	-	-	-	3	2	1
	40 psig	-	-	-	-	-	-	3	2	1	3	2	1	-	-	-	-	-	-
Oxygenates	15 psig	1	2	3	1	2	3	1	2	3	1	2	3	-	-	-	1	2	3
	40 psig	-	-	-	-	-	-	1	2	3	1	2	3	-	-	-	-	-	-

Table 57: DHA PUAF Temperature Analysis at 930F

The PUAF DHA has not been run on most of the Equilon samples at 930°F so it is not analyzed in the matrix. The Petrobras and Citgo resid exhibited similar trends with the exception of the iso-paraffin production. At both 15 and 40 psig, the IBP-113°F cut contained iso-paraffin in minimal amounts for Citgo, and average amounts for Petrobras. No PUAF DHA data is available for Chevron, Marathon and Suncor at 40 psig.

The majority of the resids had identical correlations at both 15 psig and 40 psig, for the different bottom temperatures. Based on the available data, a general trend can be seen in which the IBP-113°F consisted primarily of paraffins, olefins and oxygenates. The 113-400°F cut had predominantly iso-paraffins and naphthenes, and the 400-430°F cut had a high concentration of aromatics present.

Detailed Hydrocarbon Analysis (DHA): Feed Rate Analysis

The effects of changing feed rates and pressure on the mass percent of each PiONA component were constructed for all the resids and have been condensed into a matrix format. The key below can be used to decipher the matrix and are labeled 1 to 3 in order of decreasing mass percent (%) of component.

1	**Highest mass percent (%) of component**
2	
3	**Least mass percent (%) of component**

No samples were run at 1200 g/hr for all the six PUAF company resids. Chevron, Equilon and Suncor resids were not run at 2400g/hr.

In general, Marathon, Petrobras, and Citgo had identical trends for iso-paraffins, olefins, naphthenes, aromatics, and oxygenates. The IBP-113°F cut for Petrobras and Citgo consisted primarily of paraffin, while high quantities of paraffin were in the 113-400°F cut for the Marathon resid.

		CHEVRON			MARATHON			PETROBRAS			CITGO			EQUILON			SUNCOR		
		IBP - 113	113-400	400-430	IBP - 113	113 - 400	400 - 430	IBP-113	113 - 400	400 - 430	IBP-113	113 - 400	400-430	IBP - 113	113-400	400 - 430	IBP-113	113 - 400	400-430
Paraffin	15 psig	NO SAMPLES WERE RUN AT 2400 g/hr			3	1	2	1	2	3	1	2	3	NO SAMPLES WERE RUN AT 2400 g/hr			NO SAMPLES WERE RUN AT 2400 g/hr		
	40 psig				3	1	2	1	2	3	1	2	3						
Iso-Paraffin	15 psig				2	1	3	2	1	3	2	1	3						
	40 psig				2	1	3	2	1	3	2	1	3						
Olefin	15 psig				1	2	3	1	2	3	1	2	3						
	40 psig				1	2	3	1	2	3	1	2	3						
Naphthenes	15 psig				2	1	3	2	1	3	2	1	3						
	40 psig				2	1	3	2	1	3	2	1	3						
Aromatics	15 psig				3	2	1	3	2	1	3	2	1						
	40 psig				3	2	1	3	2	1	3	2	1						
Oxygenates	15 psig				1	2	3	1	2	3	1	2	3						
	40 psig				1	2	3	1	2	3	1	2	3						

Table 58: DHA PUAF Flow Rate Analysis at 2400g/hr

		CHEVRON			MARATHON			PETROBRAS			CITGO			EQUILON			SUNCOR		
		IBP - 113	113-400	400-430	IBP - 113	113 - 400	400 - 430	IBP-113	113 - 400	400 - 430	IBP-113	113 - 400	400-430	IBP - 113	113 - 400	400 - 430	IBP - 113	113 - 400	400-430
Paraffin	15 psig	1	2	3	3	1	2	1	2	3	1	2	3	1	2	3	1	2	3
	40 psig	1	2	3	No samples were run			1	2	3	1	2	3	1	2	3	No samples were run		
Iso-Paraffin	15 psig	3	1	2	2	1	3	2	1	3	2	1	3	2	1	3	2	1	3
	40 psig	2	1	3	No samples were run			2	1	3	2	1	3	2	1	3	No samples were run		
Olefin	15 psig	1	2	3	1	2	3	1	2	3	1	2	3	1	2	3	1	2	3
	40 psig	1	2	3	No samples were run			1	2	3	1	2	3	1	2	3	No samples were run		
Naphthenes	15 psig	2	1	3	2	1	3	2	1	3	2	1	3	2	1	3	2	1	3
	40 psig	2	1	3	No samples were run			2	1	3	2	1	3	2	1	3	No samples were run		
Aromatics	15 psig	3	2	1	3	2	1	3	2	1	3	2	1	3	2	1	3	2	1
	40 psig	3	1	2	No samples were run			3	2	1	3	2	1	3	2	1	No samples were run		
Oxygenates	15 psig	1	2	3	1	2	3	1	2	3	1	2	3	1	2	3	1	2	3
	40 psig	1	2	3	No samples were run			1	2	3	1	2	3	1	2	3	No samples were run		

Table 59: DHA PUAF Flow Rate Analysis at 3600g/hr

No samples were run at 3600g/hr and 40psig for both Marathon and Suncor resids. At a flow rate of 2400g/hr and 3600g/hr, the Marathon resids produced identical trends for all cuts at 15 psig. The Petrobras, Citgo and Equilon resids produced similar trends. The Chevron resid produced similar trends with Petrobras, Citgo and Equilon with the exception of the iso-paraffin production at 15 psig and aromatics production at 40 psig. At 15 psig, the IBP-113^{o}F cut had minimal amounts of paraffin present, while at 40 psig, the 113-400^{o}F cut had high amounts of aromatics.

		CHEVRON			MARATHON			PETROBRAS			CITGO			EQUILON			SUNCOR		
		IBP-113	113-400	400-430	IBP - 113	113 - 400	400 - 430	IBP-113	113 - 400	400 - 430	IBP-113	113 - 400	400-430	IBP - 113	113 - 400	400 - 430	IBP - 113	113-400	400 - 430
Paraffin	15 psig	NO SAMPLES WERE RUN AT 4800 g/hr			3	1	2	NO SAMPLES WERE RUN AT 4800 g/hr			NO SAMPLES WERE RUN AT 4800 g/hr			NO SAMPLES WERE RUN AT 4800 g/hr			NO SAMPLES WERE RUN AT 4800 g/hr		
	40 psig				No samples were run														
Iso-Paraffin	15 psig				2	1	3												
	40 psig				No samples were run														
Olefin	15 psig				1	2	3												
	40 psig				No samples were run														
Naphthenes	15 psig				2	1	3												
	40 psig				No samples were run														
Aromatics	15 psig				3	2	1												
	40 psig				No samples were run														
Oxygenates	15 psig				1	2	3												
	40 psig				No samples were run														

Table 60: DHA PUAF Flow Rate Analysis at 4800g/hr

No samples were run at 4800g/hr for Chevron, Petrobras, Citgo, Equilon and Suncor resids, none were run for Marathon at 40 psig. At a feed rate of 4800g/hr and 15 psig, the Marathon resids produced identical trends with 2400g/hr and 3600g/hr for all cuts at 15 psig.

In conclusion, by comparing the Petrobras and Citgo resids at 15 psig and 40 psig (2400g/hr and 3600g/hr) and Marathon resids at 15 psig (2400g/hr, 3600g/hr, and 4800g/hr), it is observed that changing the feed rate does not affect the concentration of each PiONA component at the different temperature cuts.

5. Sulfur Analysis

The weight percent of sulfur was plotted for the liquid, gas, water and coke fractions for the resids at 15 psig and 40 psig and at feed temperatures of 900°F and 930°F. The sulfur analysis has only been run for the 3ft pilot unit drum and the analysis for the 6ft pilot unit drum is still pending. For brevity, only the Chevron sulfur data obtained using the 0.25 inch coil in the 3ft pilot unit will be displayed.

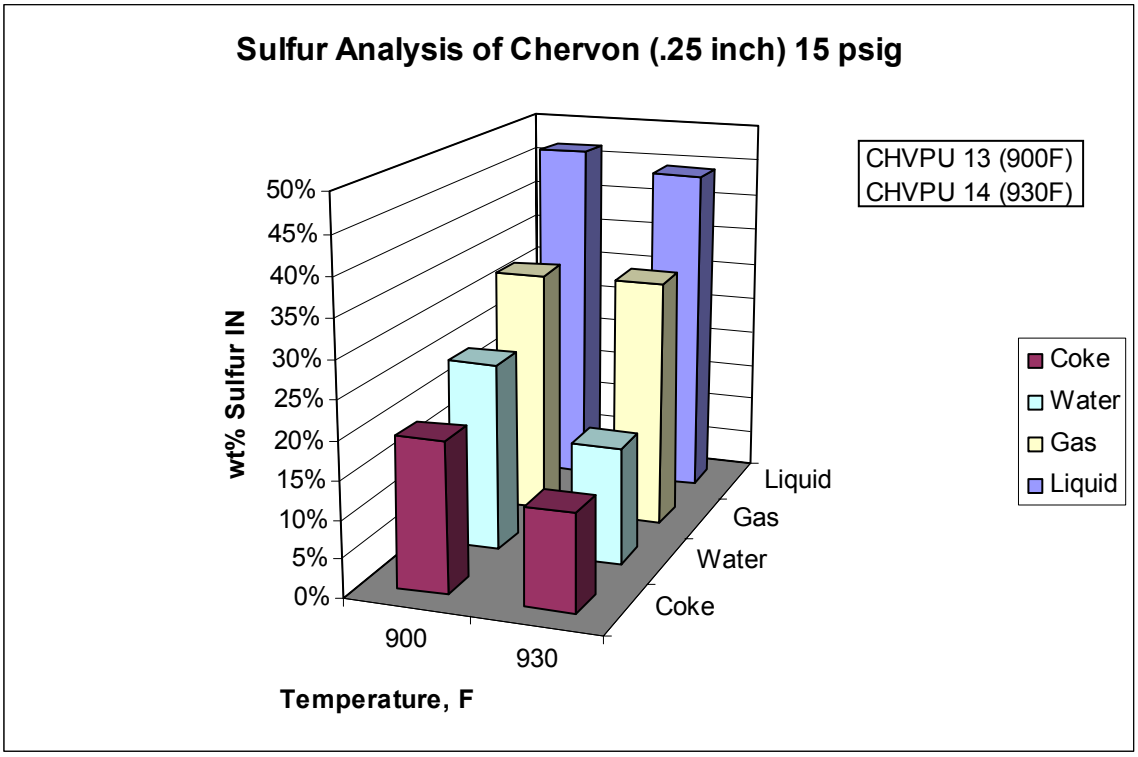

Figure 76: PU Sulfur Analysis at 15 psig

From Figure 76, it is observed that the liquid cut contained the largest amount of sulfur and the coke cut contained the smallest amount of sulfur. These trends were observed at both 900°F and 930°F.

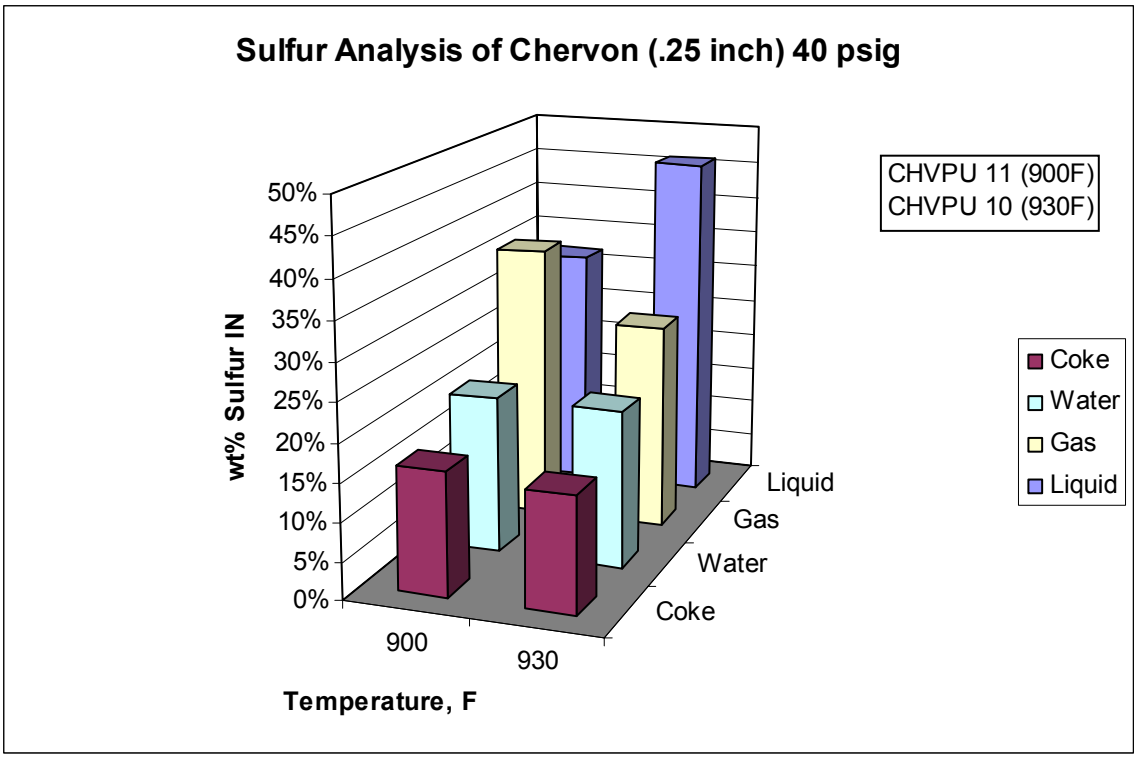

Figure 77: PU Sulfur Analysis at 40 psig

Figure 77 shows that at 930°F the liquid cut contained the largest amount of sulfur and the coke cut contained the smallest amount of sulfur. At 900°F, the gas cut contained largest of the sulfur present followed by the liquid cut.

The effects of temperature and pressure on the weight percent of sulfur contained in the liquid, gas, water and coke cuts were constructed using only sulfur data that was available, the results have been condensed into a matrix format. The key below can be used to decipher the matrix and are labeled 1 to 4 in order of decreasing weight percent (%) of sulfur in.

1	**Highest weight percent (%) Sulfur IN**
2	
3	
4	**Lowest weight percent (%) Sulfur IN**

PU SULFUR ANALYSIS 0.25 inch

0F

	CHEVRON				MARATHON				PETROBRAS				CITGO				EQUILON				SUNCOR			
sure	Liquid	Gas	Water	Coke	Liquid	Gas	Water	Coke	Liquid	Gas	Water	Coke	Liquid	Gas	Water	Coke	Liquid	Gas	Water	Coke	Liquid	Gas	Water	Coke
sig	1	2	3	4	No samples were run				No samples were run				3	2	4	1	No samples were run				1	2	4	3
sig	2	1	3	4	2	1	4	3	1	2	3	4	3	2	4	1	3	2	4	1	2	1	4	3

Table 61: PU Sulfur Analysis (0.25 inch coil) at 900F

0F

	CHEVRON				MARATHON				PETROBRAS				CITGO				EQUILON				SUNCOR			
sure	Liquid	Gas	Water	Coke	Liquid	Gas	Water	Coke	Liquid	Gas	Water	Coke	Liquid	Gas	Water	Coke	Liquid	Gas	Water	Coke	Liquid	Gas	Water	Coke
sig	1	2	3	4	No samples were run				No samples were run				1	3	4	2	2	3	4	1	1	2	4	3
sig	1	2	3	4	1	3	4	2	1	2	3	4	1	3	4	2	2	3	4	1	2	1	4	3

Table 62: PU Sulfur Analysis (0.25 inch coil) at 930F

0F

	CHEVRON				MARATHON				PETROBRAS				CITGO				EQUILON				SUNCOR			
sure	Liquid	Gas	Water	Coke	Liquid	Gas	Water	Coke	Liquid	Gas	Water	Coke	Liquid	Gas	Water	Coke	Liquid	Gas	Water	Coke	Liquid	Gas	Water	Coke
sig	No samples were run				No samples were run				No samples were run				2	3	4	1	No samples were run				No samples were run			
sig					2	3	4	1					No samples were run								1	2	4	3

Table 63: PU Sulfur Analysis (0.25 inch coil) at 950F

Table 61, Table 62 , and Table 63 show the PU sulfur analysis data at 900°F, 930°F and 950°F respectively. From comparing the tables, there are fluctuations in the amount of sulfur produced for each cut at the different temperatures and pressures. No conclusive remarks can be made until the sulfur analysis is run for the 6ft pilot unit (PUAF) drum and the resulting trends are compared with that of the 3ft pilot unit (PU) drum.

6. Density Analysis

The density in API was plotted for five temperature cut, IBP-113°F, 113-400°F, 400-430°F, 430-650°F, and 650+°F, at pressures of 15 psig and 40 psig and bottom temperatures of 900°F and 930°F. For brevity, only the Chevron density data for both the 3ft and 6ft pilot unit will be discussed.

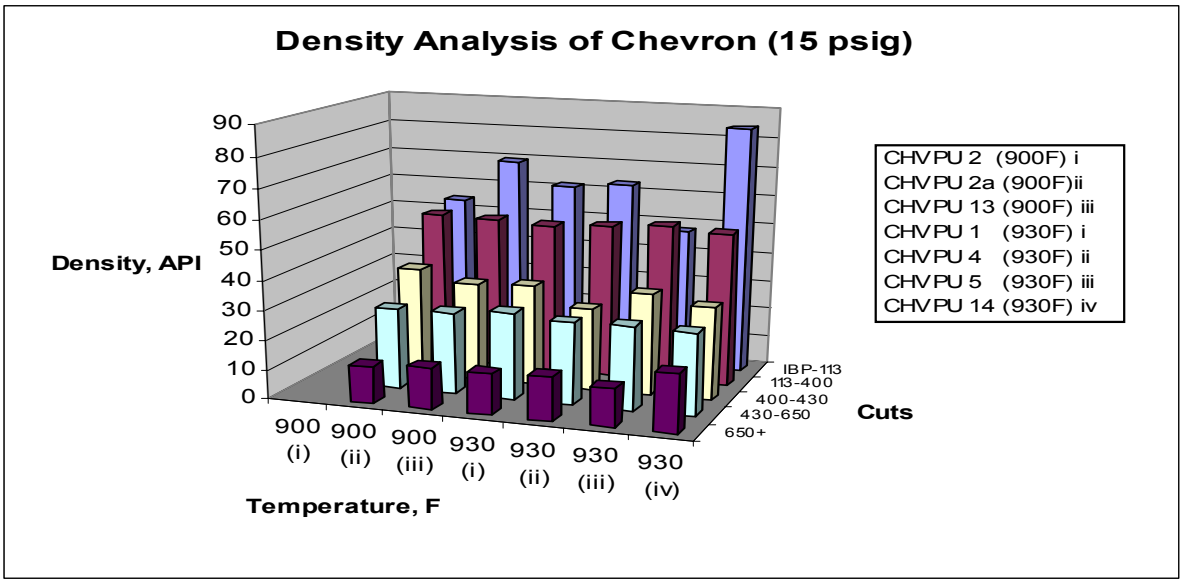

Figure 78: PU Chevron Density Analysis at 15 psig

From Figure 78, it is observed that the density API, decreases as the boiling point cuts increases. These trends were observed at both 900°F and 930°F.

7. Conclusions

The distillation and simulated distillation data showed similar trends at the same pressure for both feed and overhead temperatures. This reduces the amount of analytical work required. It was observed that changing the feed rate, 1200 to 3600 gm/hr did not affect the distribution of the weight % of feed in the different temperature coils nor did it affect the concentration of each PiONA component at the different temperature cuts. Although still on progress, the overall outcome of the DHA analysis is to be able to predict what type of PiONA component would affect its production. Based on the preliminary analysis conducted, this goal appears achievable.

8. Future work

Distillation of the PUAF Samples will continue as well as running of the DHA analysis on the incomplete and new samples upon completion of the DHA analysis, the 6890 will be converted to sulfur analysis using the PFPD. This analysis will be conducted on the liquid samples that have recently been analyzed for DHA Analysis. A linear regression analysis will be introduced to compare the average overhead temperature with the bottom temperature for each individual resid, and then adding a feedstock parameter to make a correlation between all six resids. The detailed liquid analysis data generated be Equilon will be reviewed and the trends compared to that currently being generated. The RON values will be observed and compiled to the work preformed in Phase I.

E. FOAMING STUDIES

1. Foam density determination/Time of collapse

This section deals with the foam density determination and also compares the time of collapse for different resides for different type of antifoam injection types.

a) *Chevron - Overhead injection*

The Chevron 5 run was used to establish a value for the foam density in the first phase of the foaming studies. As shown in Figure 79, a foam column 54 inches in height with a density of approximately 0.1 gm/cm existed after one hour. Since the height continued to grow, antifoam was injected continuously (100,000 cSt-5% AF in sun diesel) after 71 minutes of coking and wasn't stopped until the 121 minute mark. As shown in Figure 80, by 90 minutes the foam height was suppressed 14 inches. A total of 1.4 cc of antifoam had been injected. After another 44 minutes of antifoam injection (2.5 additional cc's) the foam height was suppressed an additional 10 inches for a total suppression of 24 inches, as shown in Figure 81. This suppression can also be seen on the density versus elapsed time plot shown in Figure 82 through Figure 87. For these runs, based on what was being collapsed, a good number for foam density is less than 0.1 gm/cc to 0.2 gm/cc.

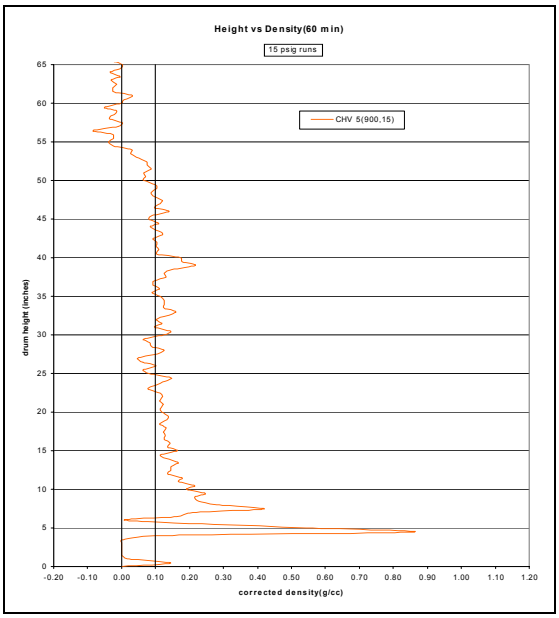

Figure 79 - Chevron Anti-Foaming Runs – Height vs. Density (Temperature and Pressure Effects on Foaming)

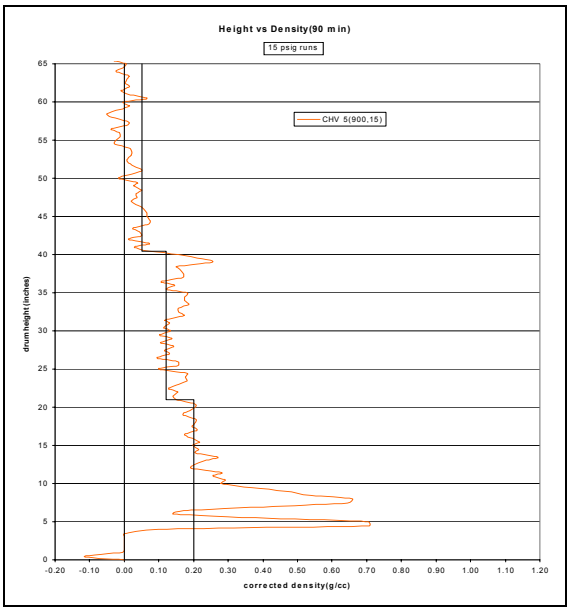

Figure 80 - Chevron Anti-Foaming Runs – Height vs. Density (Temperature and Pressure Effects on Foaming)

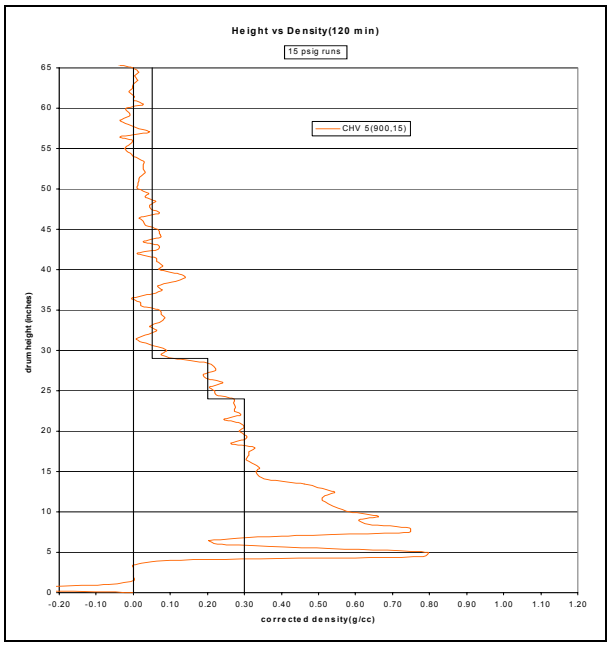

Figure 81 - Chevron Anti-Foaming Runs – Height vs. Density (Temperature and Pressure Effects on Foaming)

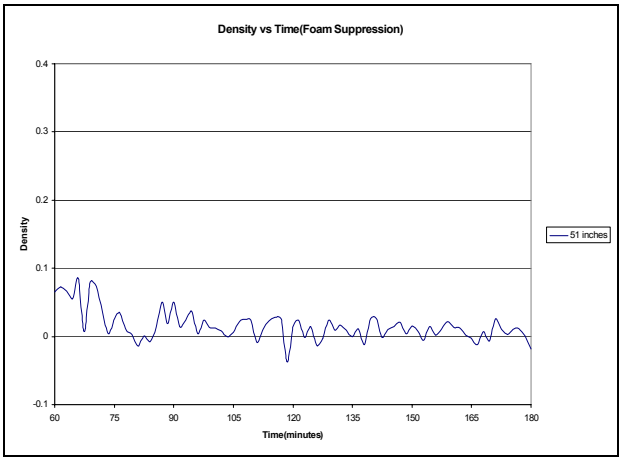

Figure 82 - Chevron Anti-Foaming Runs – Density vs. Time (Foam Suppression)

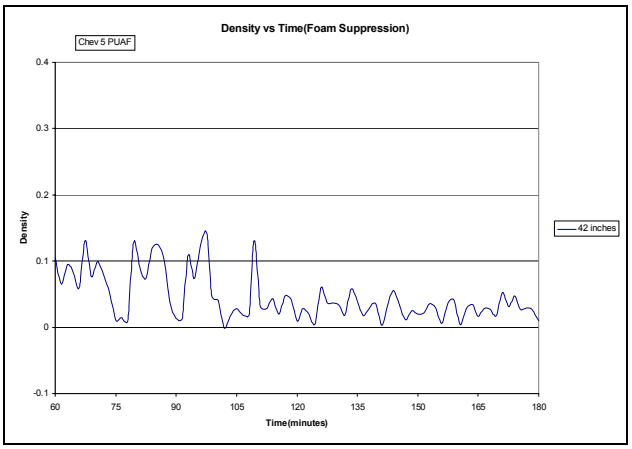

Figure 83 - Chevron Anti-Foaming Runs – Density vs. Time (Foam Suppression)

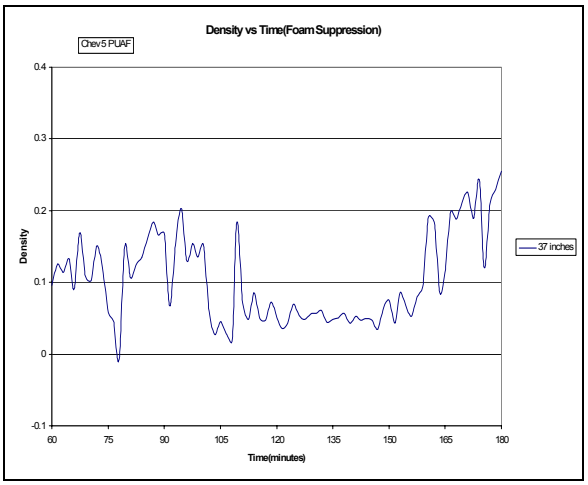

Figure 84 - Chevron Anti-Foaming Runs – Density vs. Time (Foam Suppression)

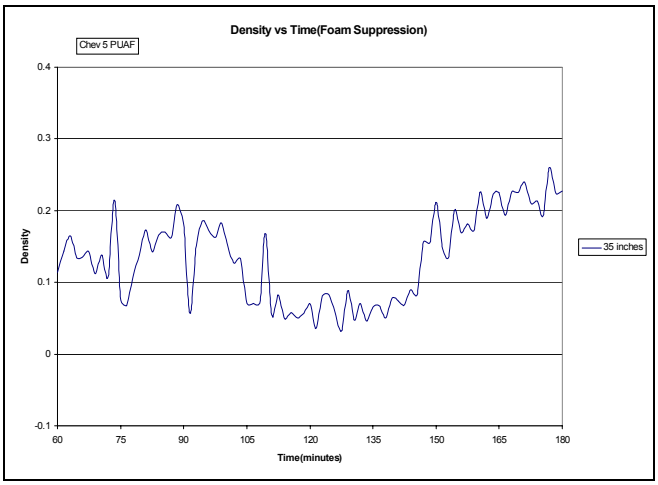

Figure 85 - Chevron Anti-Foaming Runs – Density vs. Time (Foam Suppression)

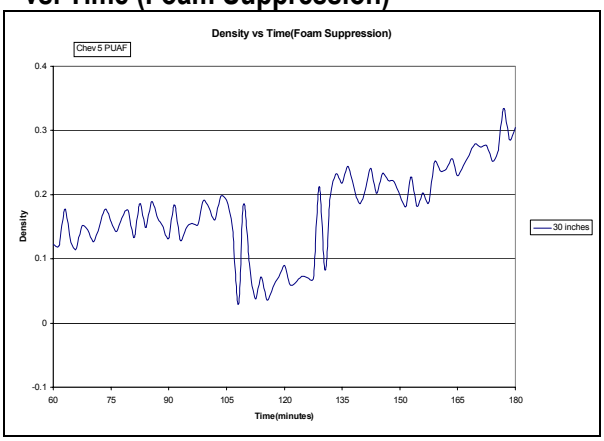

Figure 86 - Chevron Anti-Foaming Runs – Density vs. Time (Foam Suppression)

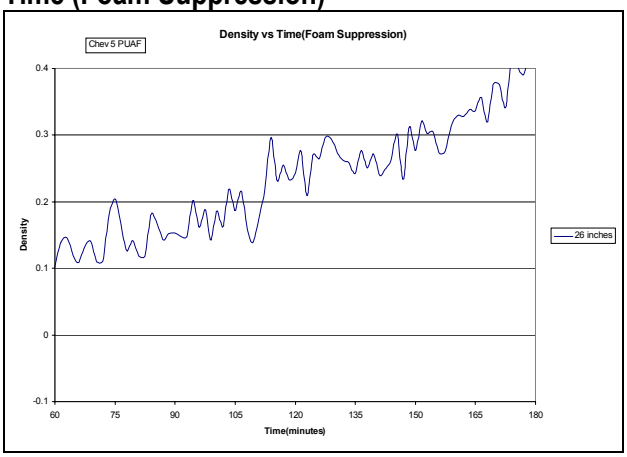

Figure 87 - Chevron Anti-Foaming Runs – Density vs. Time (Foam Suppression)

b) *Petrobras – Feedline injection*

Feed line injection of antifoam was used for the Petrobras tests. As shown in Figure 88 the collapse of a foam column with a 0.2 gm/cc density was instantaneous using 100,000 cSt antifoam (30 ml/AF/70 sun diesel) ml same as observed in the refinery when antifoam is injected. The collapse occurred between two gamma traces that were 1.5 minutes apart.

The injection sequence is shown in Figure 89. In this test, foam injection began 25 minutes into the run using overhead injection. Injection overhead continued for approximately 20 minutes without any effect. At that point, injection was switched to the feed line. Collapse was seen 8 minutes later after injecting another 1.8 cc's of antifoam. This suppression can also be seen on the density vs. elapsed time plot shown in Figure 90 through Figure 95. For this run, based on what is being collapsed, 0.1 gm/cc to 0.2 gm/cc is still a good number for foam density. Tests continued with feed line injection of antifoam until a new injection system was installed that will be able to pump carrier fluids overhead at a higher rate.

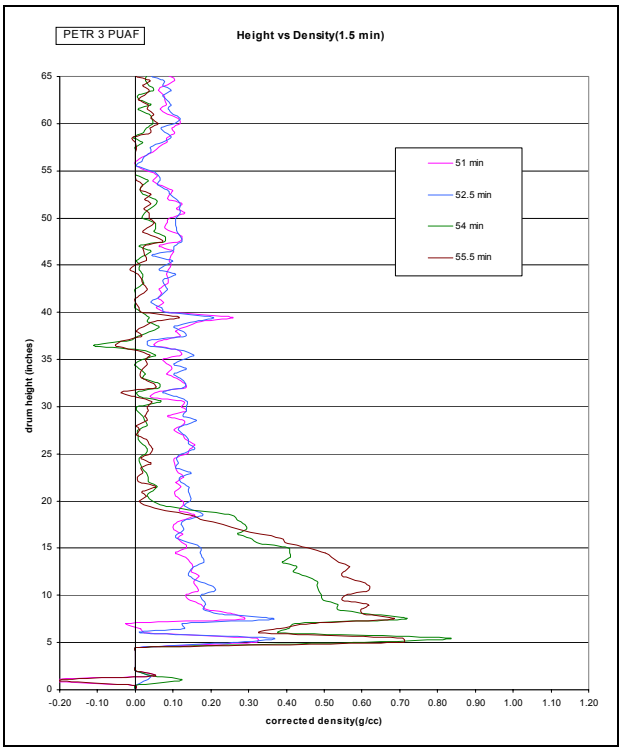

Figure 88 - Petrobras Anti-Foaming Runs – Height vs. Density (Temperature and Pressure Effects on Foaming)

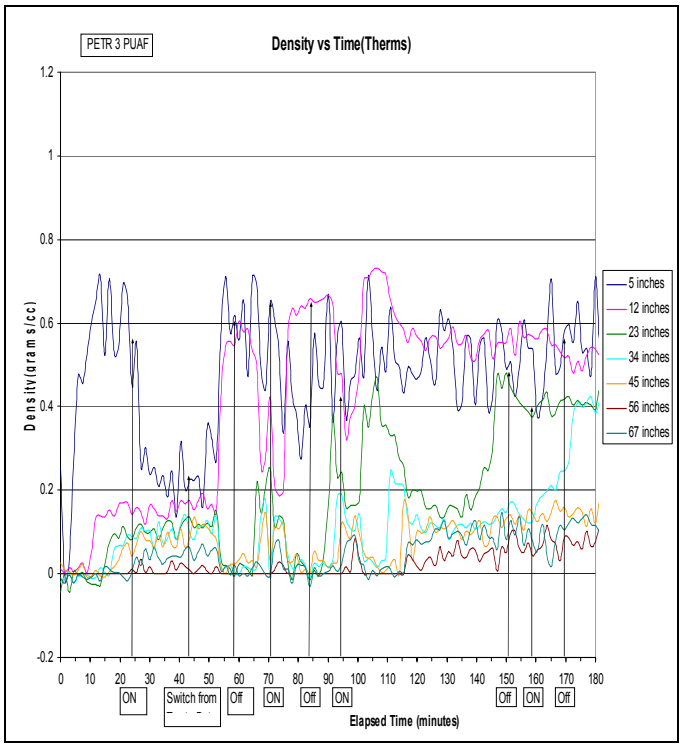

Figure 89 - Petrobras Anti-Foaming Runs – Density vs. Time (Foam Suppression)

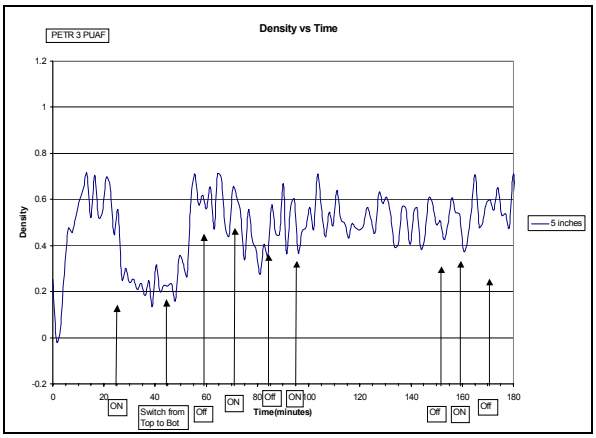

Figure 90 - Petrobras Anti-Foaming Runs – Density vs. Time (Foam Suppression)

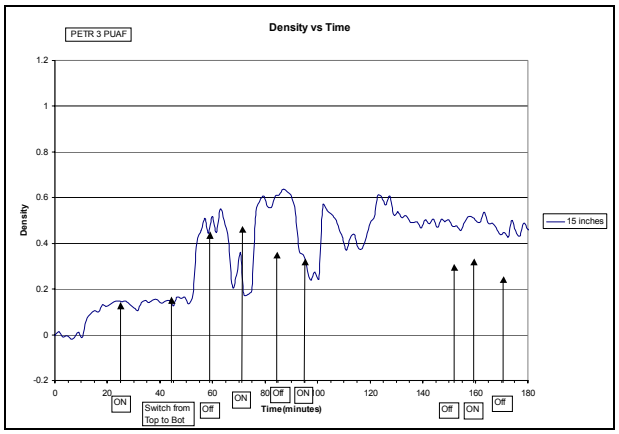

Figure 91 - Petrobras Anti-Foaming Runs – Density vs. Time (Foam Suppression)

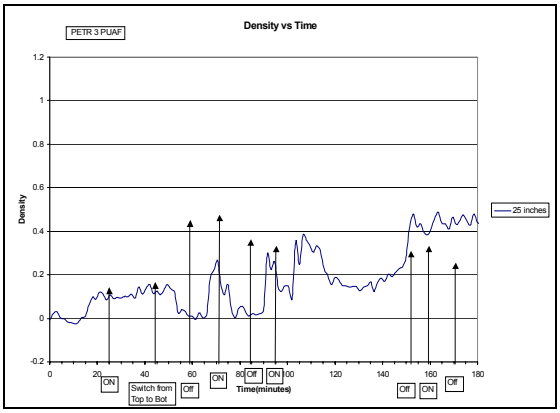

Figure 92 - Petrobras Anti-Foaming Runs – Density vs. Time (Foam Suppression)

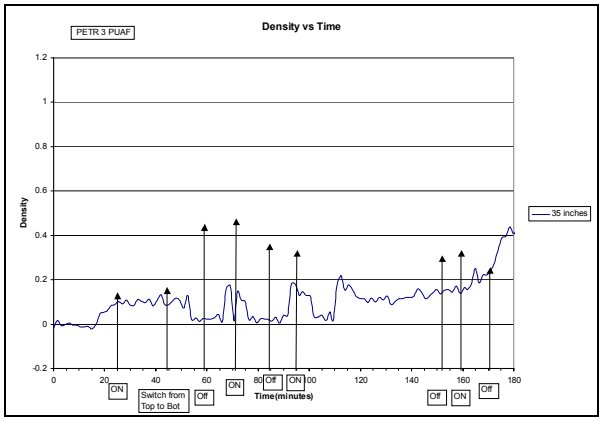

Figure 93 - Petrobras Anti-Foaming Runs – Density vs. Time (Foam Suppression)

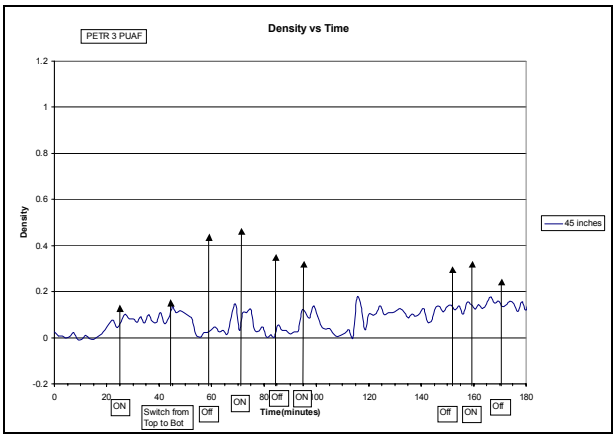

Figure 94 - Petrobras Anti-Foaming Runs – Density vs. Time (Foam Suppression)

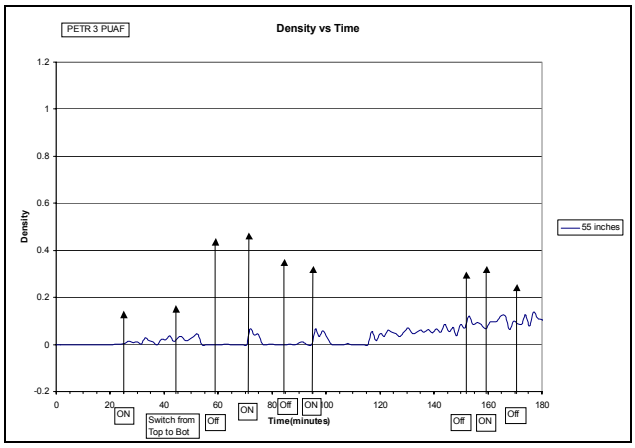

Figure 95 - Petrobras Anti-Foaming Runs – Density vs. Time (Foam Suppression)

2. Comparison of Antifoam Injection Techniques

Five runs were made to examine different approaches of injecting antifoam. Antifoam was mixed with the feed, injected in the feed line and injected overhead. For overhead injection, both low (1 ml AF/300 ml carrier) concentrations and high (30 ml AF/ 70 ml carrier) concentrations were used for the 100,000 cSt antifoam. Continuous antifoam injection was used for both the overhead and feed line injection tests.

The Suncor resid was first used to compare feed vs. overhead injection of the 100,000 cSt antifoam. These tests were conducted at a temperature of 930^{o}F, a pressure of 15 psig at a feed rate of 3600 gm/hr. In the Suncor 3 run the antifoam was injected overhead while for the Suncor 4 run the antifoam was injected in the feed. The data for these runs are presented in Figure 96 and Figure 97 as density vs. elapsed time at 5-inch intervals in the drum. Two preliminary observations can be made. First, as shown in Figure 96 the densities fluctuated wildly for the overhead injection case (antifoam injection began at the 165 minute mark) whereas as shown in Figure 97 when the antifoam is injected in the feed the fluctuations are more subdued. These fluctuations were also seen in the Suncor 2 run that was conducted in the same manner. It can also be seen that the coke produced when the antifoam is injected in the feed is denser than when it is injected overhead. This will be discussed in more detail later. Other tests need to be conducted before any firm conclusions are drawn.

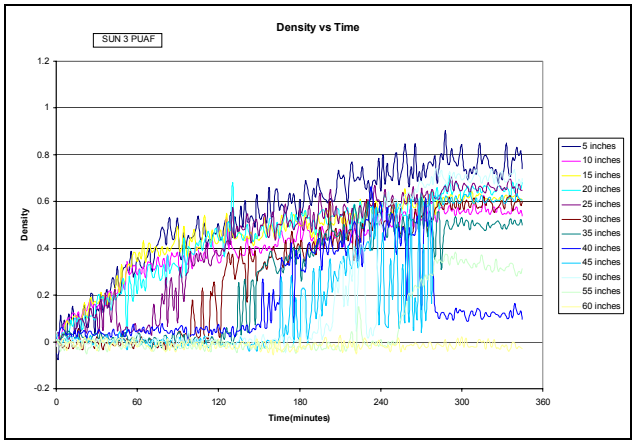

Figure 96 - Suncor Anti-Foaming Runs - Density vs. Time (Overhead Injected Antifoam)

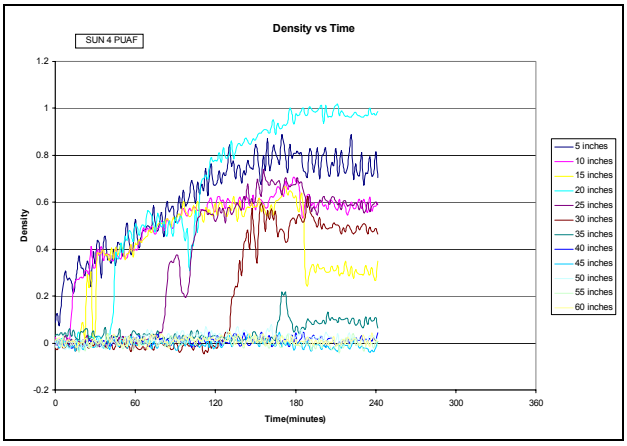

Figure 97 - Suncor Anti-Foaming Runs - Density vs. Time (Feed Injected Antifoam)

Comparison of the five runs is shown in Figure 98. Figure 98 shows that no foaming was occurring when the antifoam was injected in the feed or in the feed line. It was noted that there is a much smaller fluctuation in the density (+/- 0.05 gm/cc) at a given height in the drum when antifoam is injected in the feed or feed line whereas when no antifoam is injected, the contents in the drum are much more reactive with density swings of +/- 0.3 gm/cc going from liquid to gas sinusoidally. Injection of antifoam at low concentrations (close to commercial rates) did not control the foaming very well. It must be kept in mind that based on earlier discussions it appears that the antifoam is being carried out of the drum. However, when a high concentration of the 100,000 cSt antifoam was used, the foam behaved similarly to the ones when antifoam was injected in the feed and feed line. It is anticipated that when the antifoam injection facility is modified to be able to pump more viscous carriers, the antifoam control will be the same as that observed when injected in the feed or feed lines. At this time, no explanation can be provided as to why the high concentration of (600,000 cSt) antifoam, did not perform as well as the 100,000 cSt high concentration antifoam. Additional runs are planned.

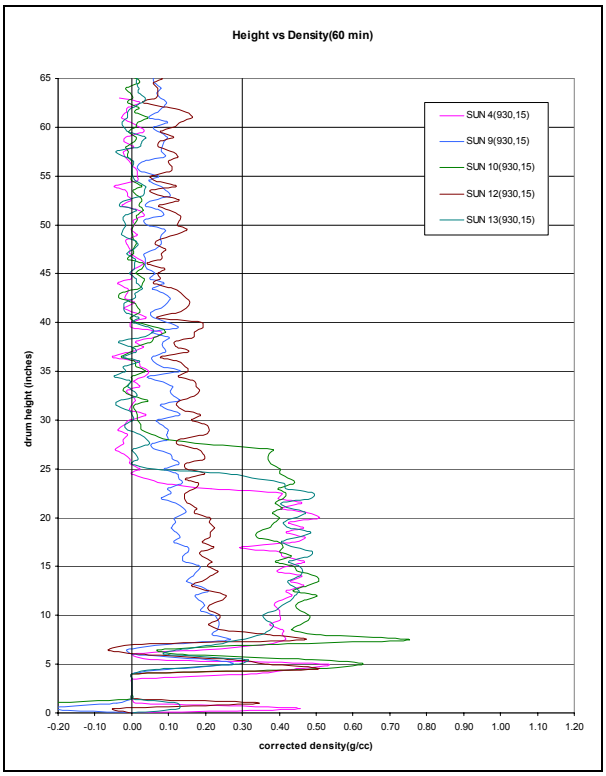

Figure 98 - Comparison of Density traces for all 5 runs after 60 minutes of coking

3. Antifoam Optimization Studies

The antifoam optimization studies began with the resid from Petrobras. Eight tests were conducted: four tests were conducted with different antifoam/carrier concentrations using the 100,000 cSt antifoam; two tests were conducted to compare continuous overhead to continuous feedline injection; and 2 tests were conducted with the 600,000 cSt antifoam to compare its effectiveness to the 100,000 cSt antifoam. The amount of antifoam used for each run is shown in Table 64. In general, the contents in the drum were allowed to foam until the drum was two-thirds full before antifoam was injected. Injection continued until the column was knocked back to one-half the drum height. Since scans are taken every 1.5 minutes, rigorous control could not be applied using this procedure.

Table 64 - Antifoam Injection Quantities

Run #	AF Mixture	Injection											Total Injected
		1	2	3	4	5	6	7	8	9	10	11	
Petrobas 9	30/70	4.639	2.876	2.928	7.930	3.472							21.845
Petrobas 10	3/70	0.852	0.401										1.253
Petrobas 11	0.3/70	0.031	0.025	0.046	0.052	0.057							0.211
Petrobas 12	0.03/70	0.006											0.0057
	0.3/70		0.076	0.100	0.037	0.105	0.028						0.346
	3/70							1.491	0.593	0.213	0.380	0.355	3.032

The first antifoam optimization test was conducted using a 30/70 antifoam/carrier mixture. Antifoam was injected 5 times during the run. As shown in Figure 99 through Figure 101, the antifoam was injected on an as-needed basis for a period of 3 to 4 minutes with the amount of antifoam varying from 3.3 to 5.4 grams. In each case, the foam was collapsed. As shown in Figure 102, antifoam was injected later in the run at the 148 minute mark providing a smaller collapse.

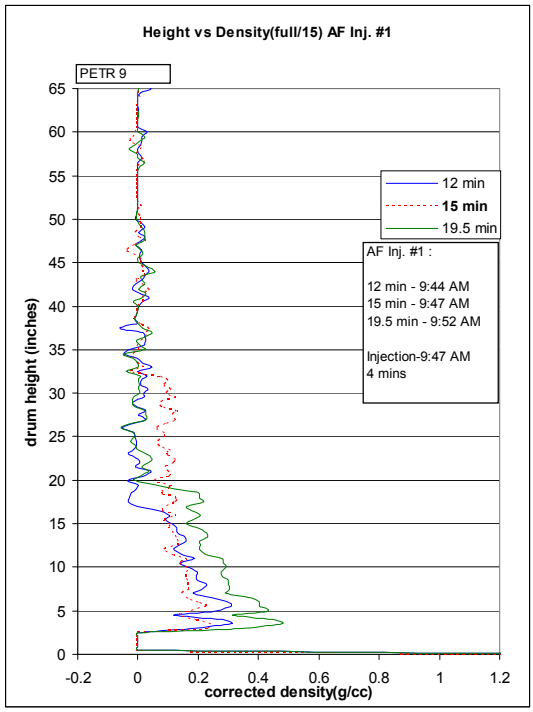

Figure 99 - PETR 9 – Antifoam Injection Response #1 After 15 Minutes of Coking

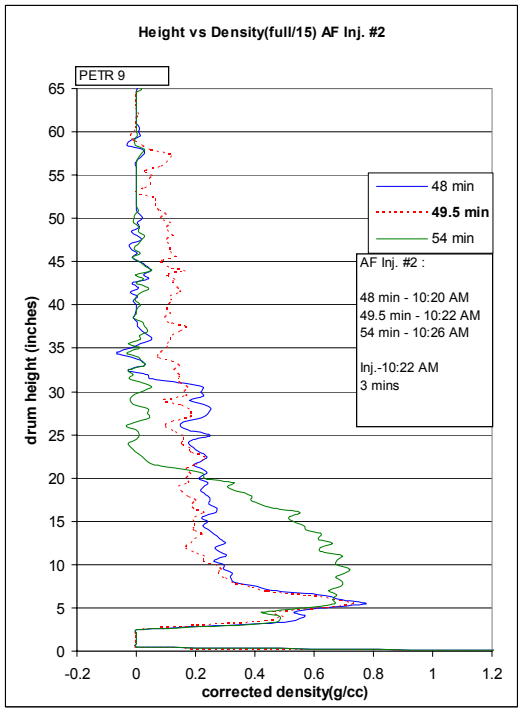

Figure 100 - PETR 9 – Antifoam Injection Response #2 After 50 Minutes of Coking

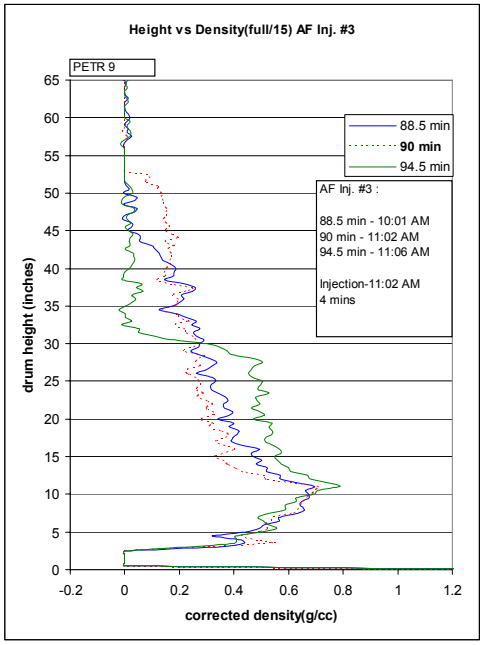

Figure 101 - PETR 9 – Antifoam Injection Response #3 After 90 Minutes of Coking

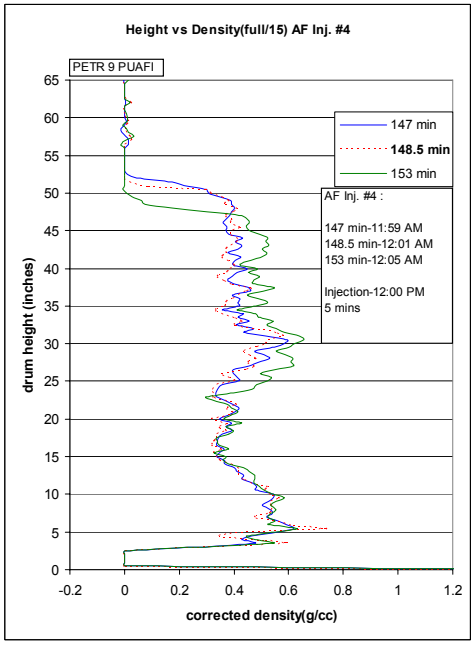

Figure 102 - PETR 9 – Antifoam Injection Response #4 After 148 Minutes of Coking

The second run was conducted using an antifoam/carrier mixture of 3/70. Injections to collapse the foam were only carried out twice as shown in Figure 103 and Figure 104, but effectively in each case. The first injection utilized 0.99 grams of antifoam while the second injection utilized 0.46 grams. No other injections were required to control the foam even though the contents foamed for the first 60 minutes.

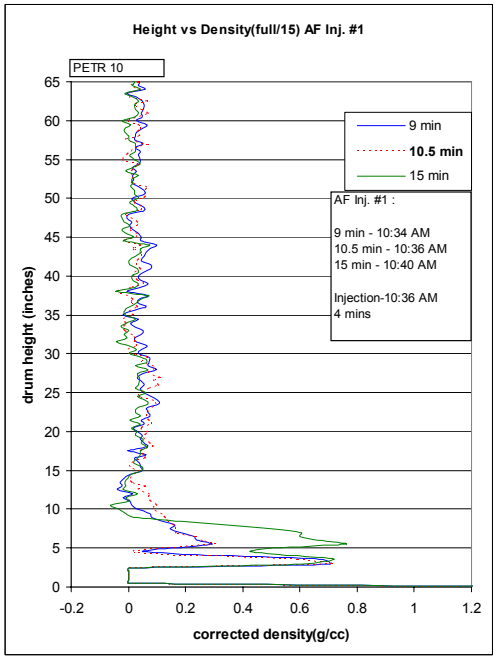

Figure 103 - PETR 10 – Antifoam Injection Response #1 After 10 Minutes of Coking

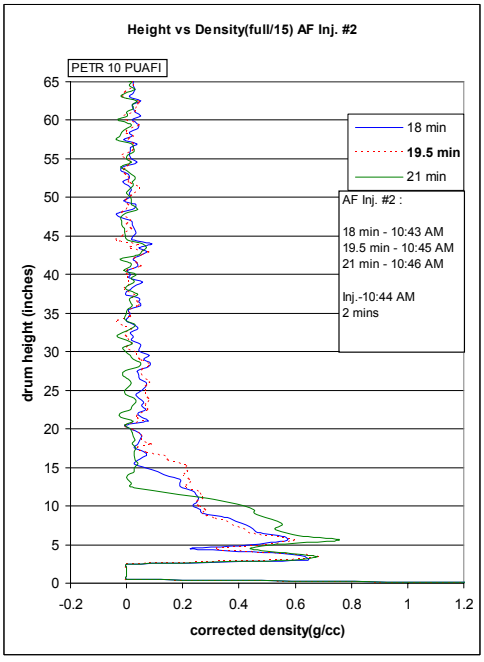

Figure 104 - PETR 10 – Antifoam Injection Response #2 After 20 Minutes of Coking

In the third run, an antifoam/carrier mixture of 0.3 to 70 was used. Five injections were utilized as shown in Figure 105 through Figure 109. Very little antifoam was used each time, 0.02 to 0.06 grams; however, in each case collapse was effective.

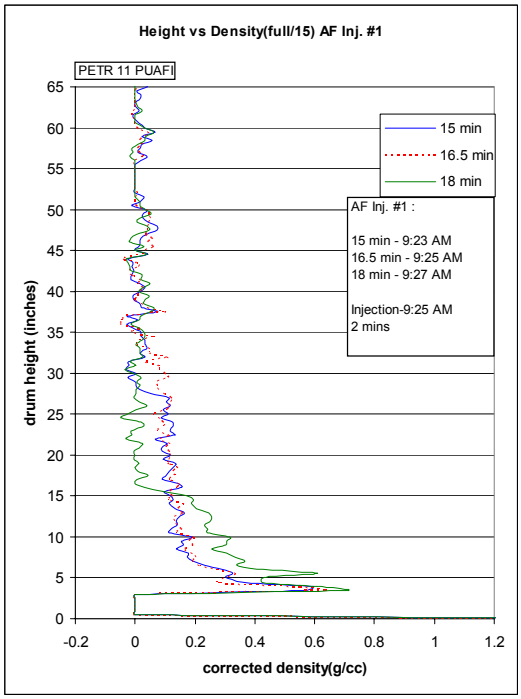

Figure 105 - PETR 11 – Antifoam Injection Response #1 After 16 Minutes of Coking

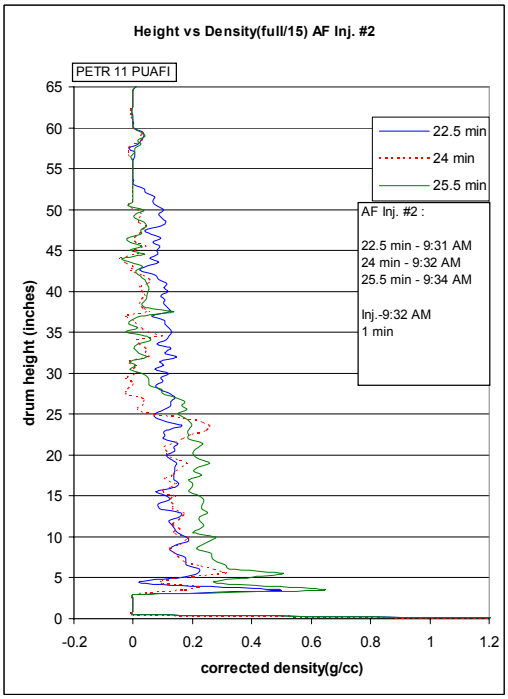

Figure 106 - PETR 11 – Antifoam Injection Response #2 After 24 Minutes of Coking

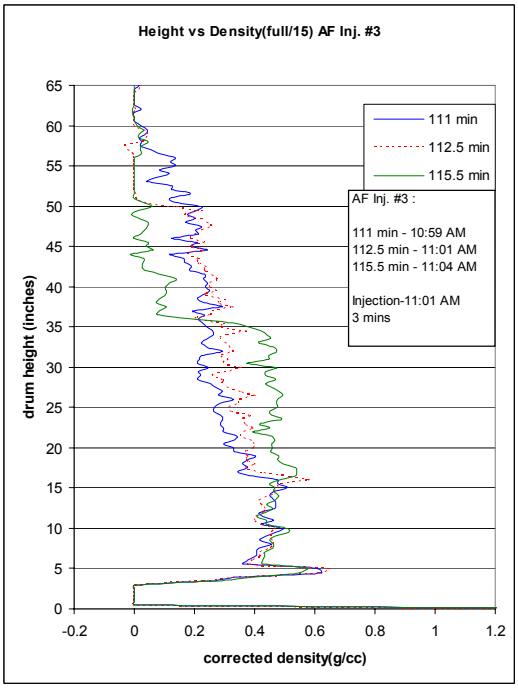

Figure 107 - PETR 11 – Antifoam Injection Response #3 After 112 Minutes of Coking

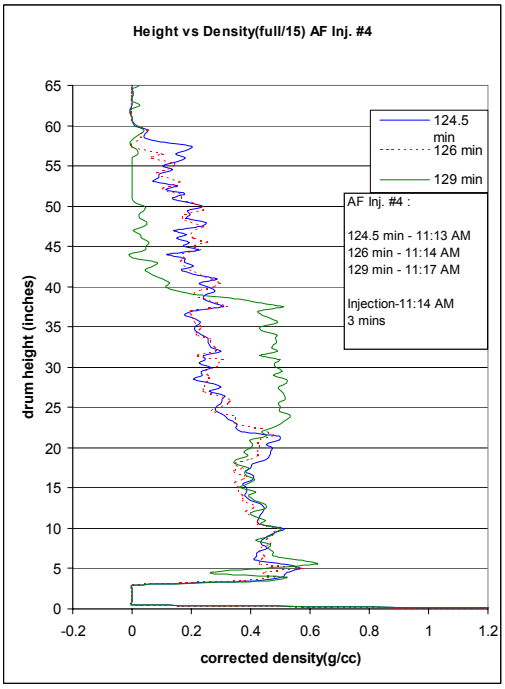

Figure 108 - PETR 11 – Antifoam Injection Response #4 After 126 Minutes of Coking

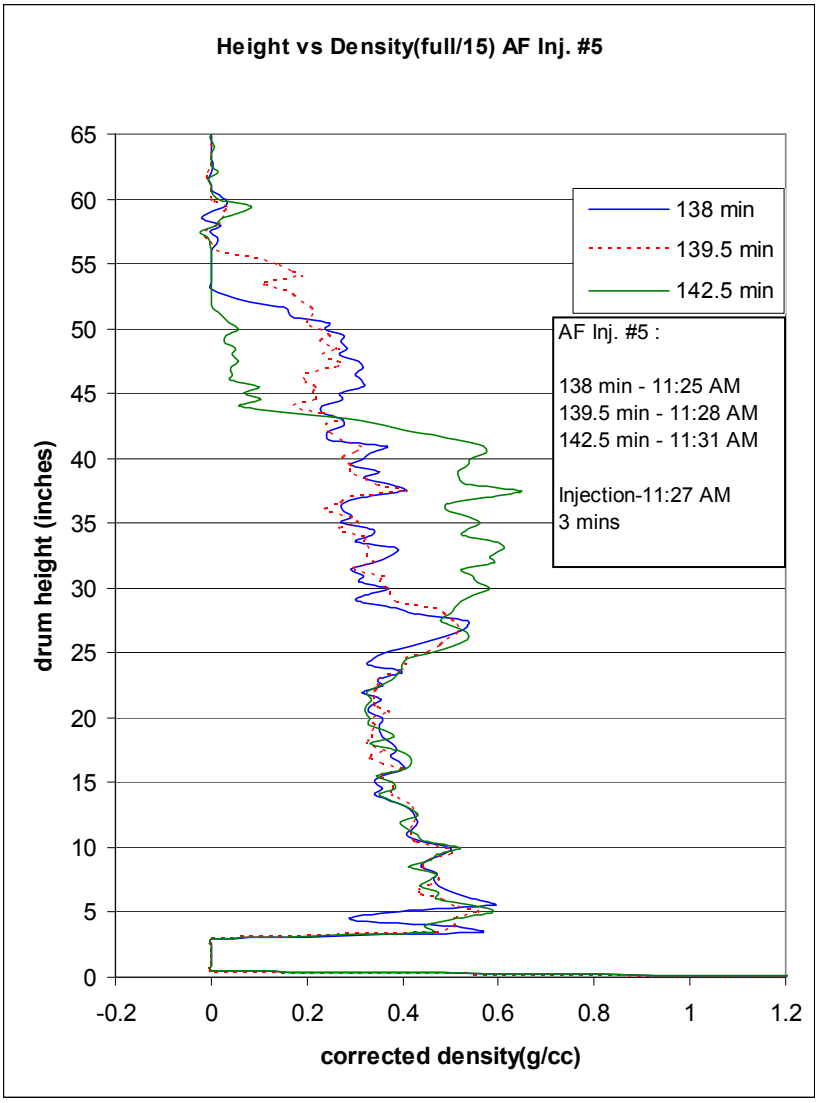

Figure 109 - PETRO 11 Antifoam Injection #5 Response After 139 Minutes of Coking

The final run was with an antifoam/carrier mixture of 0.03/70. This concentration was not effective in collapsing the foam. As a result, the antifoam/carrier was switched to 0.3/70 and the test continued.

4. Impact of Antifoam on Coke Density

Comparison of the gamma traces showed the density to increase with an increase in antifoam/carrier concentration. A similar trend in coke density was observed with the Suncor resid.

5. Continuous vs. Feedline Injection

Petrobras 13 and 14 were run to compare continuous overhead injection to continuous feedline injection using the 100,000 cSt antifoam. For these tests, antifoam was injected for 2 minutes and then shut off for 8 minutes. This injection procedure was repeated throughout the run. Plotted in each figure are 5 density traces, each at a different height in the drum. 2 traces are from the top of the drum while 3 traces are from the bottom of the drum. Note that as the foam is collapsed (decrease in density in upper two traces) there is a corresponding increase in the density at the bottom of the drum. Note the cyclical nature of the events. Better control was observed with feedline injection for the first 80 minutes; however, after that it was necessary to inject the antifoam overhead to control foaming. No explanation as to why this was necessary can be provided at this time. Further insight may be gained once the liquid and coke samples from this run are analyzed.

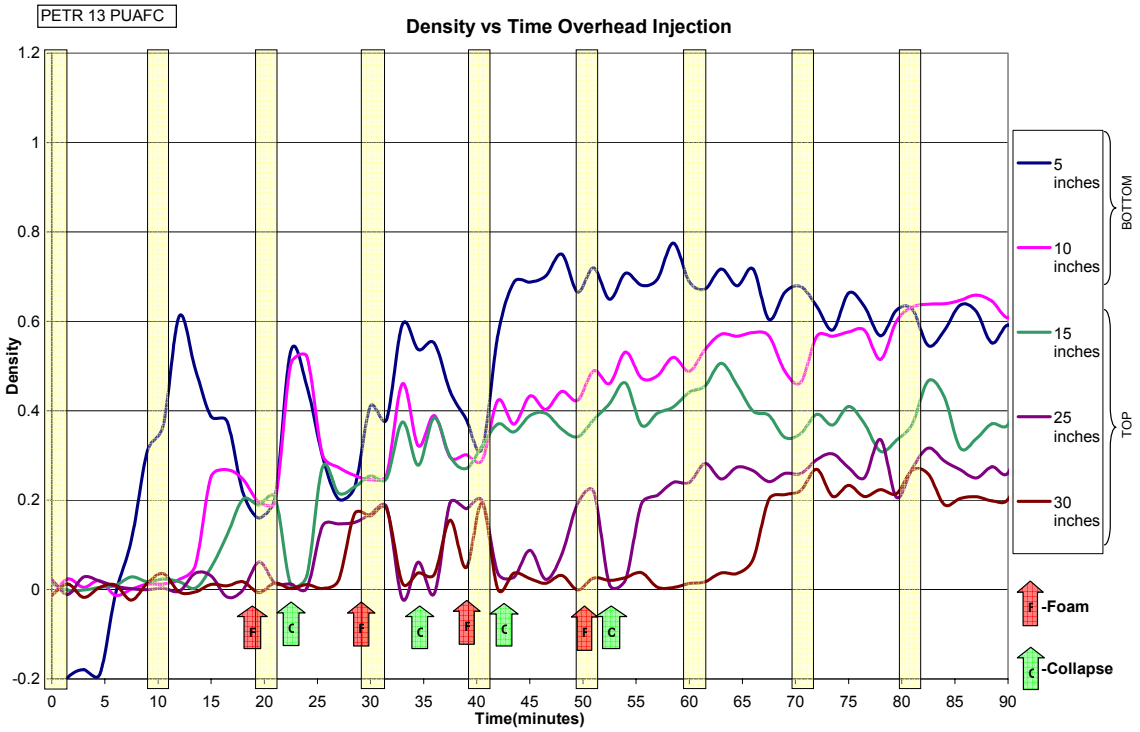

Figure 110 - Continuous Overhead Antifoam Injection For PETR 13 Run

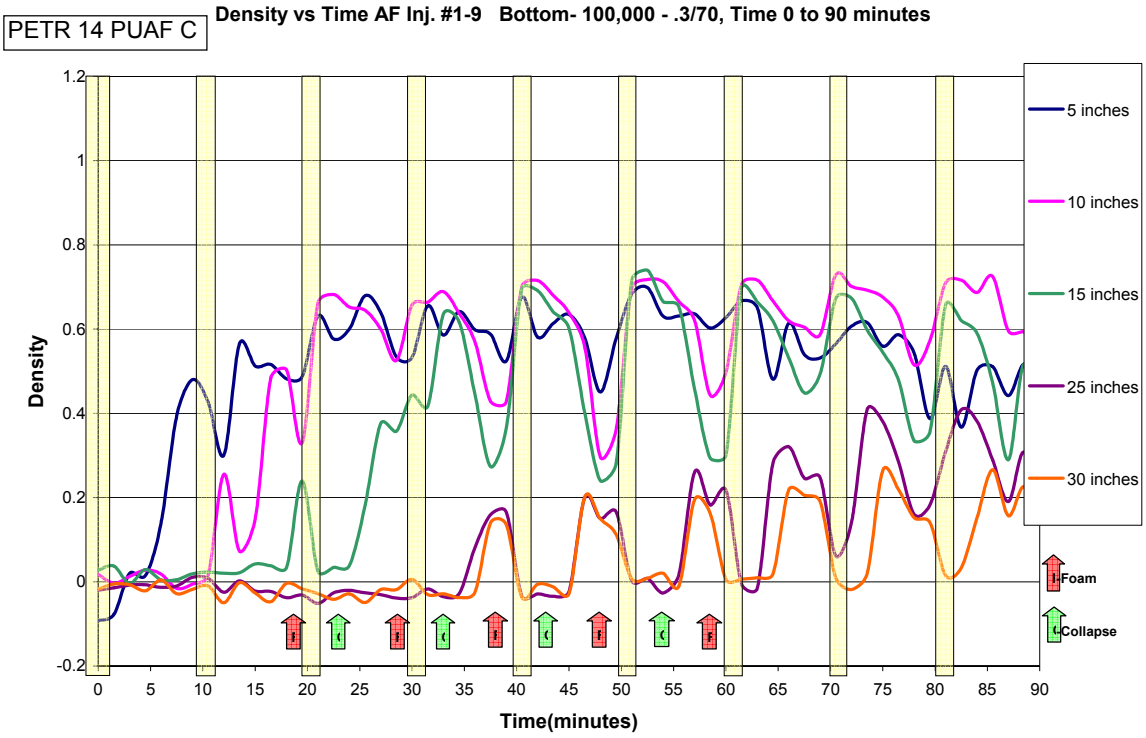

Figure 111 - Continuous Feedline Antifoam Injection for PETR 14 Run

A series of optimization tests was conducted to compare the effectiveness of the 600,000 cSt antifoam to the 100,000 cSt antifoam. The first test was begun using an antifoam/carrier concentration of 0.12/70 mixture which is less than what is used commercially. As shown in Figure 112, suppression was obtained early in the run, but the injection period was 18 minutes rather than the 2 to 3 observed for the 100,000 cSt antifoam. Within minutes of shutoff, the drum began foaming again. From fear of foaming over, and the inability to process the data on the fly, we switched to the 100,000 cSt antifoam to suppress the foaming.

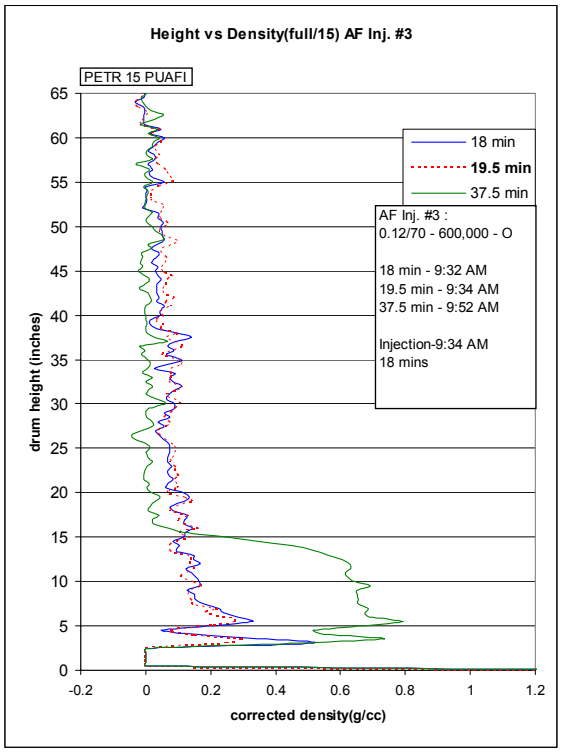

Figure 112 - PETR 15 – 600,000 cSt Antifoam Injection Response #1 After 18 Minutes of Coking

6. Time to Rise and Time to Collapse

It would be useful to have some sort of correlation between feed characteristics and overall foaming tendency in a coke drum. It has been hypothesized for years that feeds with higher levels of naphthenic acids will foam more severely. Correlations of foaming tendency with acid number, napthenate content by FTIR and asphaltene content will be undertaken. Asphaltene content is a feed parameter that is likely to correlate to foam stability.

Ranking foaming tendency will be attempted using one or more of the following objective indicators:

1. Total amount of defoamer used.
2. Total number of defoamer injections during a run, i.e. injection frequency
3. Speed of foam reappearance after defoamer injection (sort of a corollary of 2)
4. Time to formation of first foam front

Hopefully, more than one of these criteria will give the same rankings, which will build some confidence in the objective ranking. Subjective judgment of those who ran the tests will also be used to see if the subjective judgment generally agrees with the objective criteria. Comparisons will be made only across runs using similar defoamer injection methods.

Three resids have been studied, Petrobras, Chevron and Equilon. The data from these runs are plotted as density at a given height in the drum vs. time. Continuous Feedline and continuous overhead injection for the Chevron Resid using the 100,000 cSt antifoam is compared in Figure 114 and Figure 115. Note that after injection, the foam collapsed but within a short period of time foaming resumed. Figure 116 and Figure 117 show the results for collapsing the foam when a 600,000 cSt antifoam is used at an equivalent concentration to the 100,000 cSt antifoam. Note that the time to rise was a lot longer than when the 100,000 cSt antifoam was used. This observation provides support that at equivalent concentrations, fewer injections of antifoam would be required.

Continuous Feedline injection was utilized with the Equilon resid. As shown in Figure 118, little foaming was observed with this resid. Note that when continuous injection was used there appears to be an increase in the coke density. It would be interesting to conduct similar tests, but with increasing cm concentrations of antifoam to see if it compacts the coke density as discussed in the previous section. This study is in its early stages. Additional results will be presented in future reports.

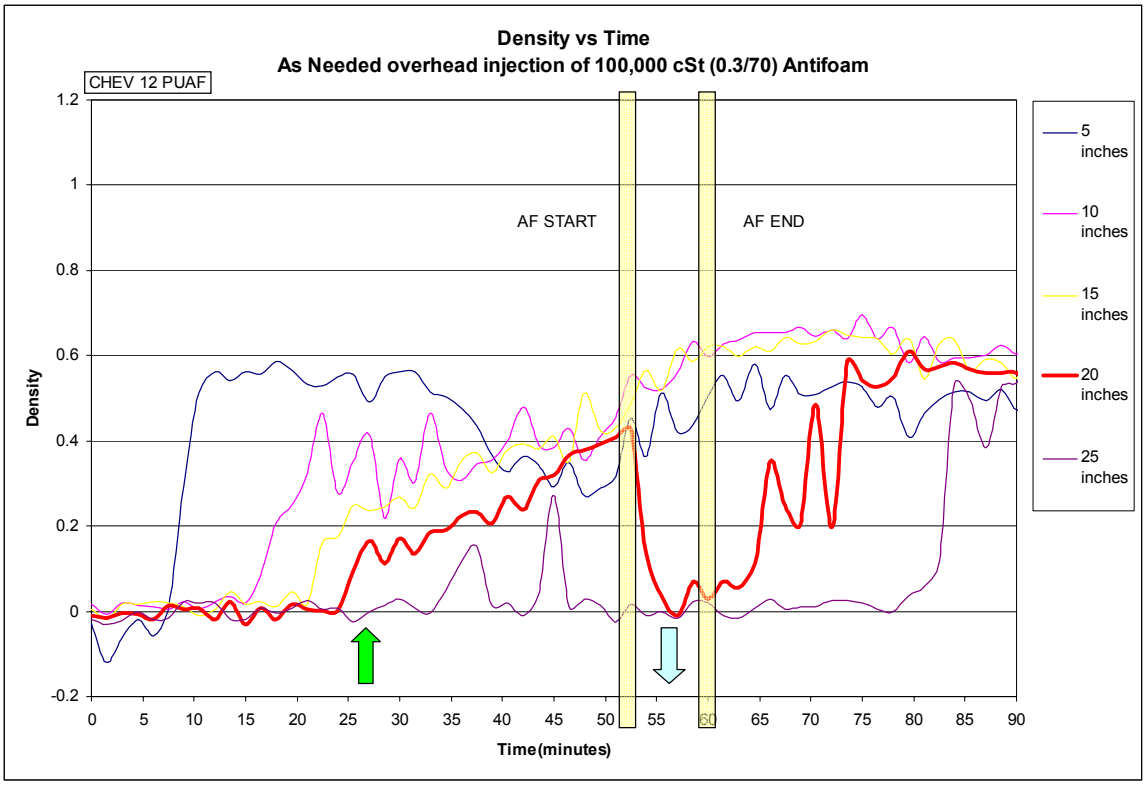

Figure 113 - Rise and Collapse of Foam for CHEV 12 PUAFI

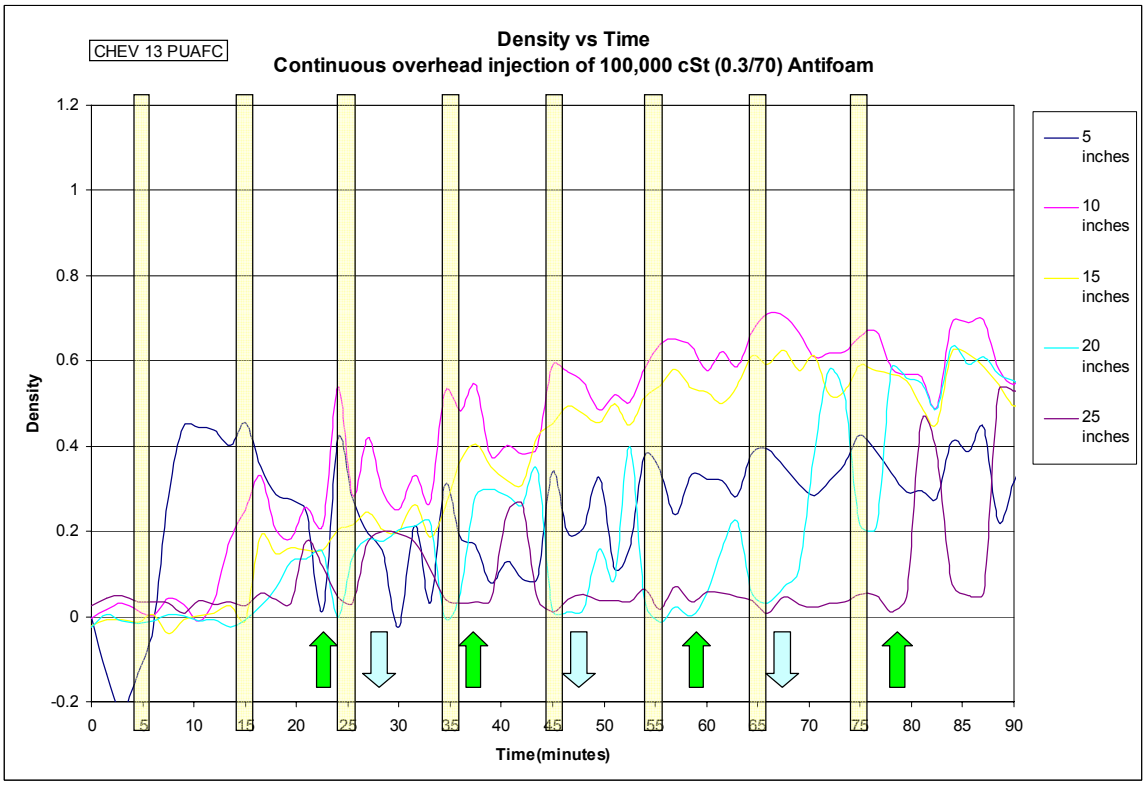

Figure 114 - Rise and Collapse of Foam for CHEV 13 PUAFC

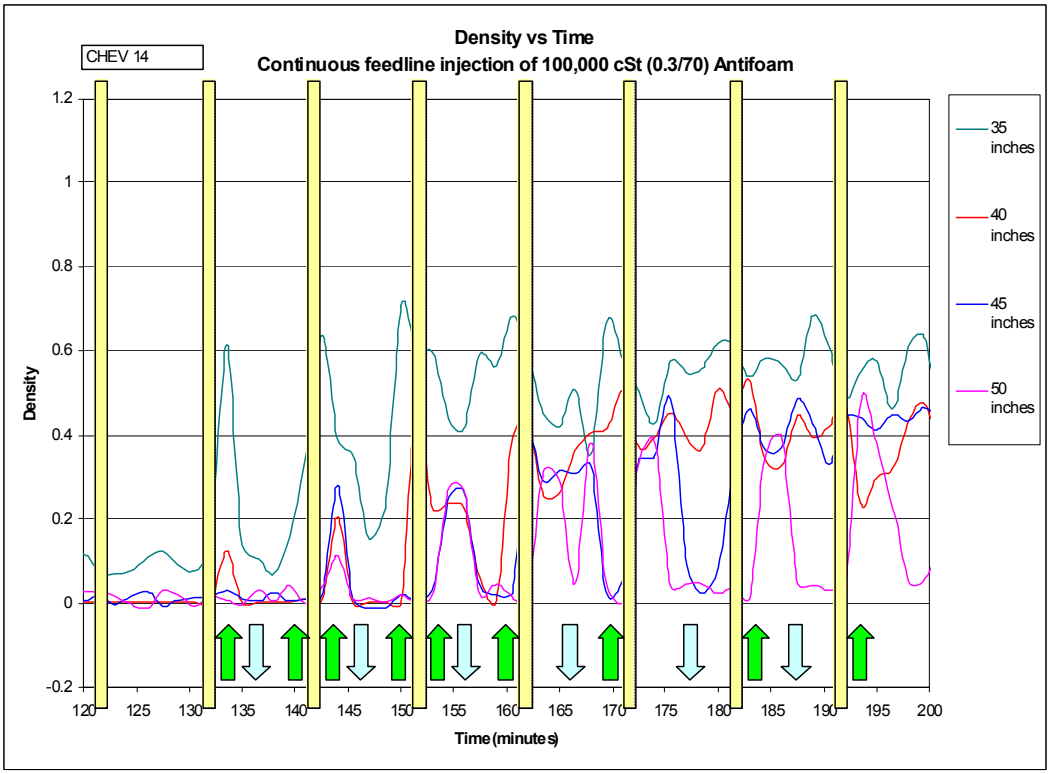

Figure 115 - Rise and Collapse of Foam for CHEV 14 PUAFC

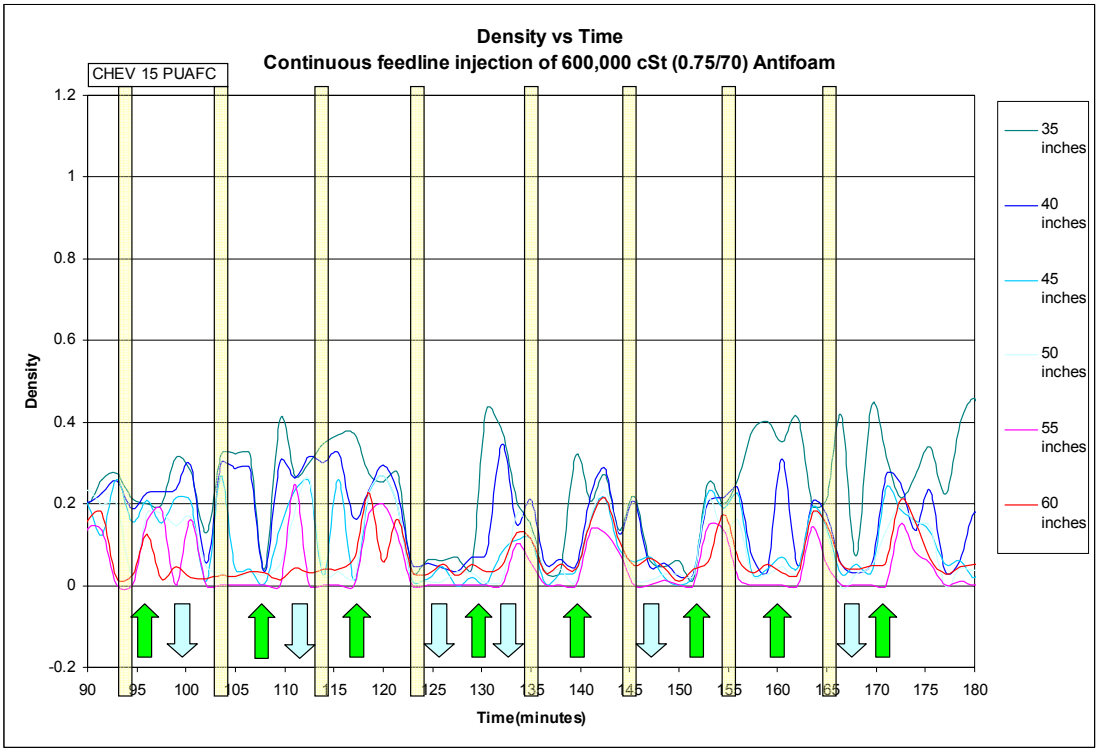

Figure 116 - Rise and Collapse of Foam for CHEV 15 PUAFC

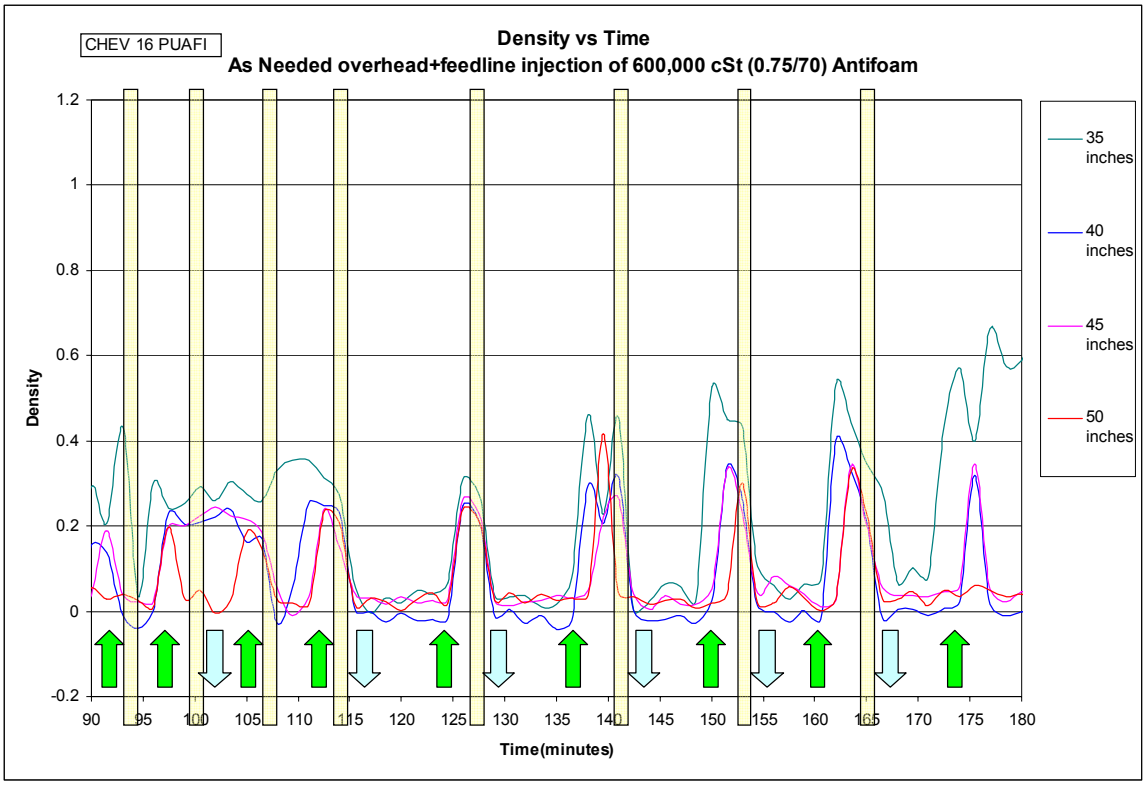

Figure 117 - Rise and Collapse of Foam for CHEV 16 PUAFI

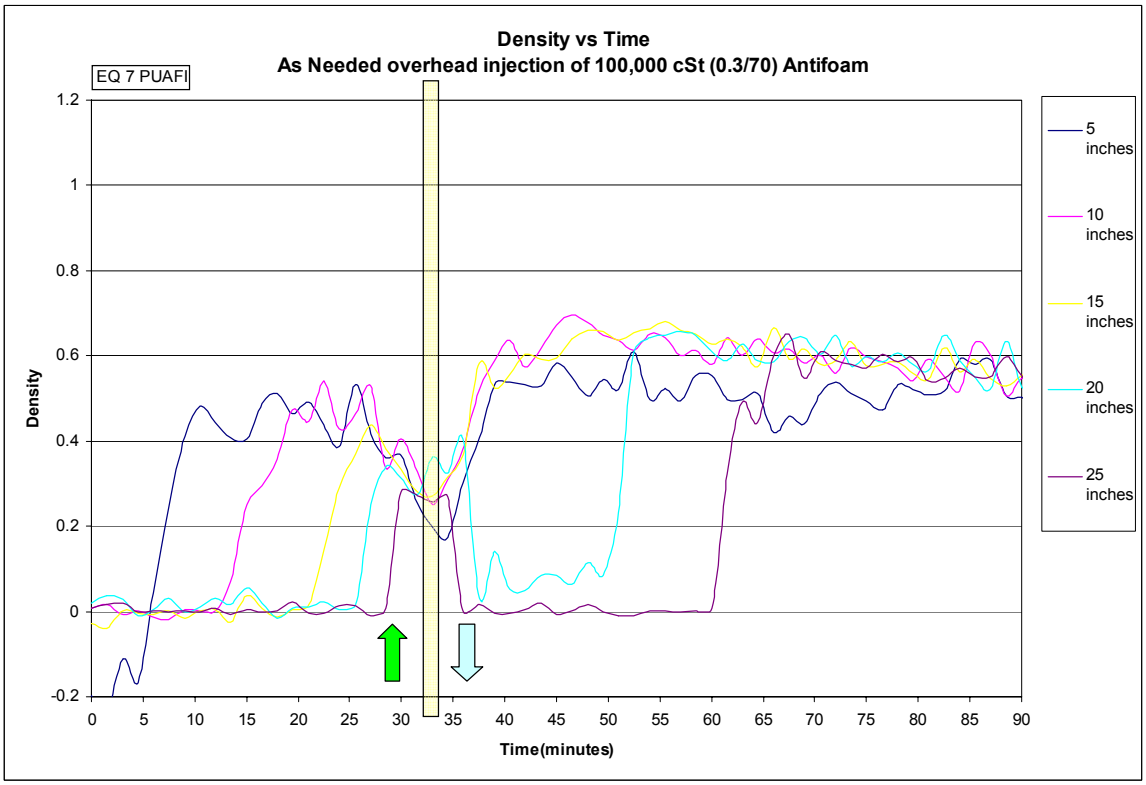

Figure 118 - Rise and Collapse of Foam for EQU 7 PUAFI

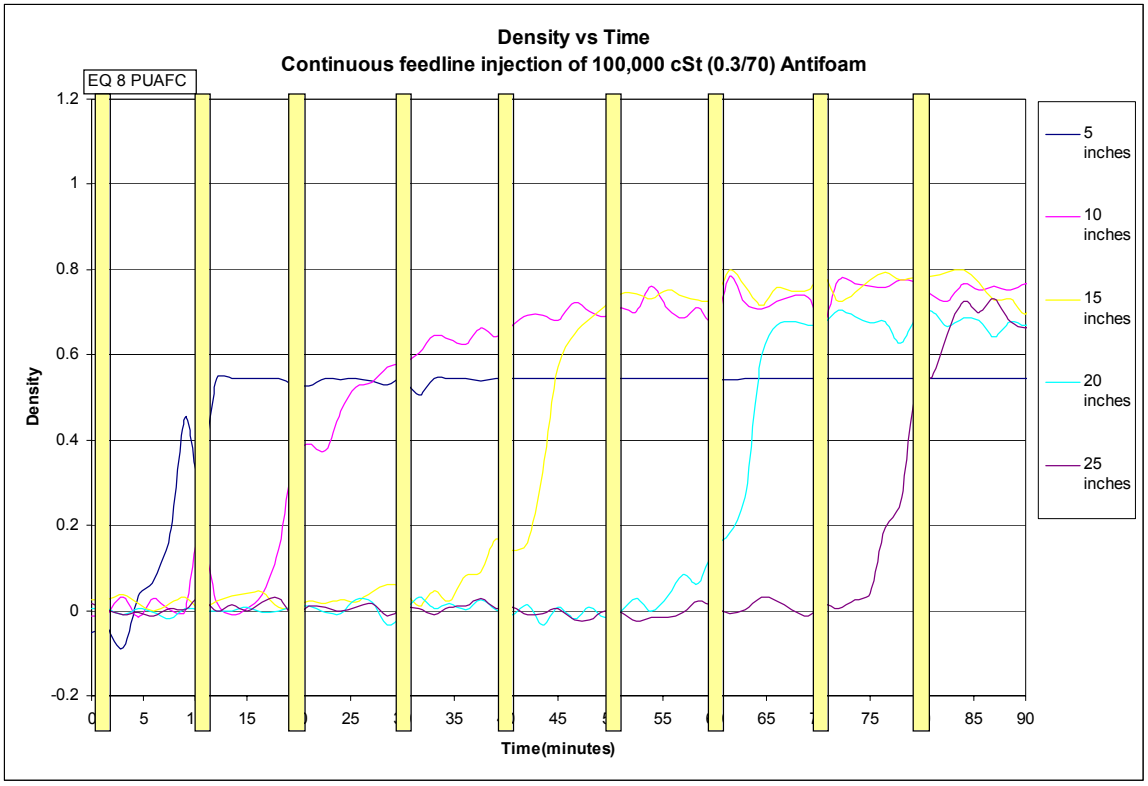

Figure 119 - Foam was not observed during EQU 8 PUAFC

7. Quantification of Bubbly Liquid and Foam Layers

Different runs are considered to depict the build up of coke, bubbly liquid and foam layers with time. The data of resid density at different heights inside the drum is provided by the Gamma Densitometer. At each antifoam injection, a plot of drum height (inches) versus corrected density (gm/cc) depicts the foam volume collapse at that particular antifoam injection. Based on the density values the height of coke, bubbly liquid and foam layer is calculated. The basic criteria for density values for coke is in the range of 0.56(gm/cc) to 0.6(gm/cc) and above, bubbly liquid layer is in the range of 0.35(gm/cc) to 0.45(gm/cc) and foam is in the range of 0.2(gm/cc) to 0.35(gm/cc). Operator's observation during the run is taken into consideration. Respective drum height of coke, bubbly liquid and foam layer are plotted against time to show the build up of these layers with coking time. It indicates the foaming characteristic of resids with coking times. The studies of type and method of antifoam used can be enhanced by observing the formation of these layers with time. The following plots show the collapse of foam during that particular antifoam injection. The data is plotted before the antifoam injection, at injection and after injection to determine the foam volume collapse and efficacy of antifoam during that injection. Similarly the densities and drum heights of coke, bubbly liquid layer and foam are calculated for Chevron, Equilon and Petrobras runs.

CHEV 12 PUAFI was run at a temperature of 900°F, a pressure of 15 psig and at a feed rate 3600 gm/hr. This run was an as-needed overhead injection of 100,000 cSt (0.3/70) antifoam. A total of 147.25 cc of antifoam was injected during the run. The first injection of antifoam was made 53 minutes into the run and it was continued for seven minutes (see Figure 120). It is seen that the foam collapsed within 4 minutes of injection. The second injection was made 149 minutes into the run for a total time of 4 minutes (see Figure 121). The collapse of the foam can be seen at the end of the injection. The third injection of antifoam was made 169 minutes into the run for a total time of 4 minutes (see Figure 122). The foam collapse can be seen at the end of this injection. The fourth injection was made 184 minutes into the run for a total time of 3 minutes (see Figure 123). Injection # 5 was made 196 minutes into the run for a total time of 3 minutes (see Figure 124). Substantial collapse of foam was seen during this injection. There was a rise in the foam volume during injection # 6 (see Figure 125), but the foam collapsed at the end of the injection. Injection # 7 was made 237 minutes into the run for a total time of 5 minutes (see Figure 126). Around 10 inches of foam drum height collapse was seen during this injection. The last injection, injection # 8 was made 296 minutes into the run during the steam strip for a total time of 6 minutes (see Figure 127). A total of 22.75 cc of antifoam was injected during the steam strip process.

Figure 130, Figure 128 and Figure 129 show the buildup of coke, bubbly liquid and foam as a function of time for Chevron runs 12 through 14 respectively. These plots show a foam layer that is 7 to 10 inches thick. Also note for Chevron 13 where continuous overhead injection was used there was a collapse of foam for a period up to 50 minutes during the run. Being that this was a continuous overhead injection run, more antifoam was injected than what was needed. Similar results were seen when continuous Feedline injection shown in Figure 129.

This data is plotted in Figure 131 and Figure 132. For the Equilon resid the foam layer was very small and/or was not detectable as shown in Figure 131 and Figure 132.

A much thicker foam layer, approximately 20 inches was determined for the Petrobras resid as shown in Figure 133 through Figure 136.

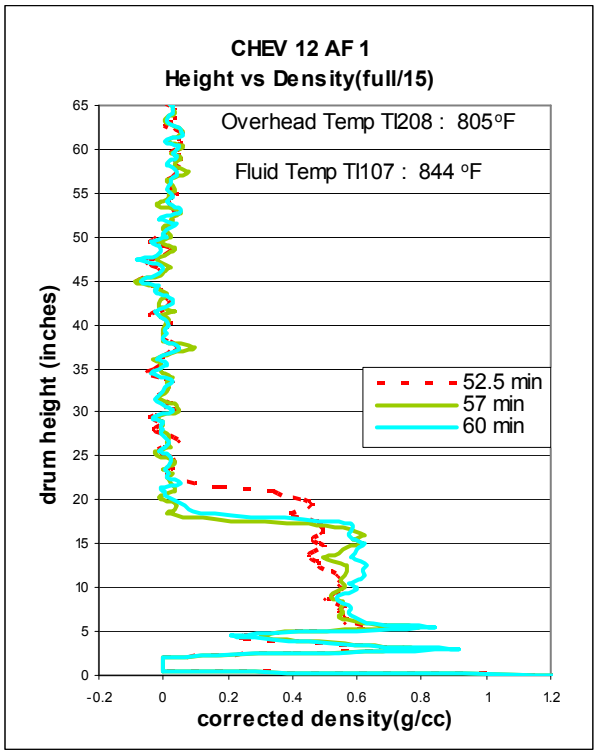

Figure 120 - Chev 12 PUAFI, Injection # 1

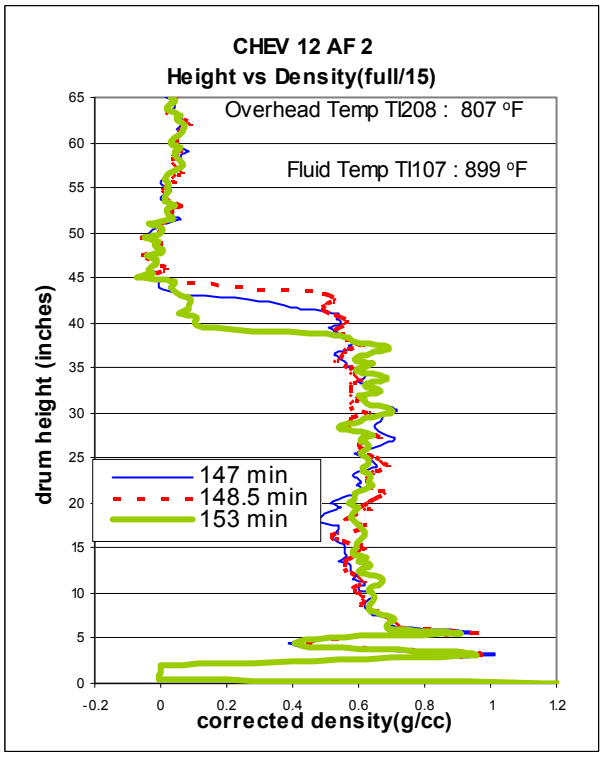

Figure 121 - Chev 12 PUAFI, Injection # 2

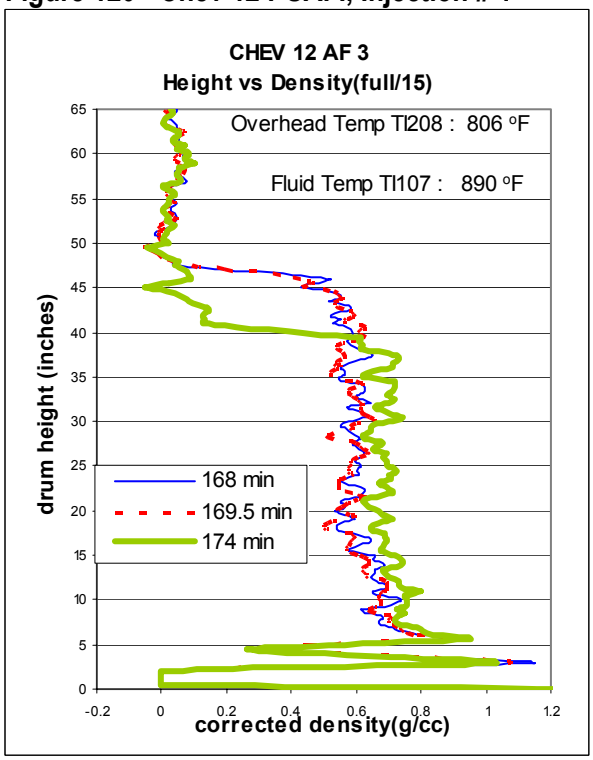

Figure 122 - Chev 12 PUAFI, Injection # 3

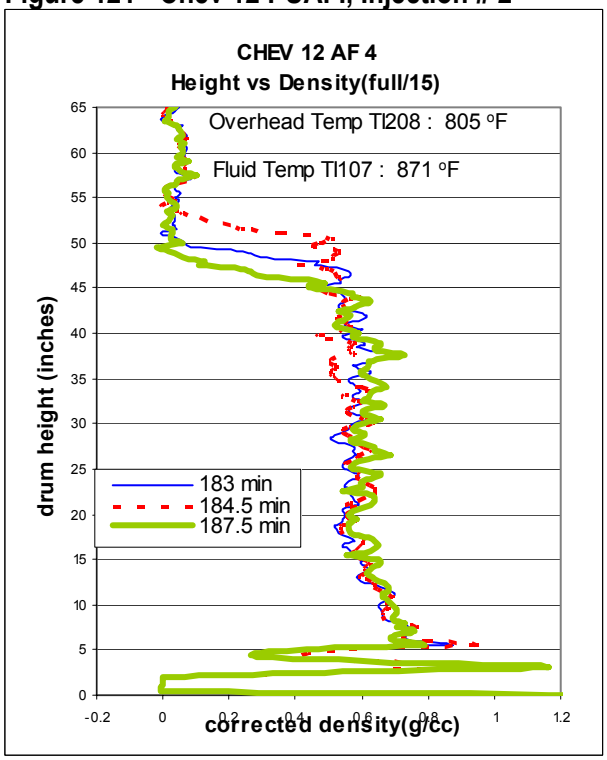

Figure 123 - Chev 12 PUAFI, Injection # 4

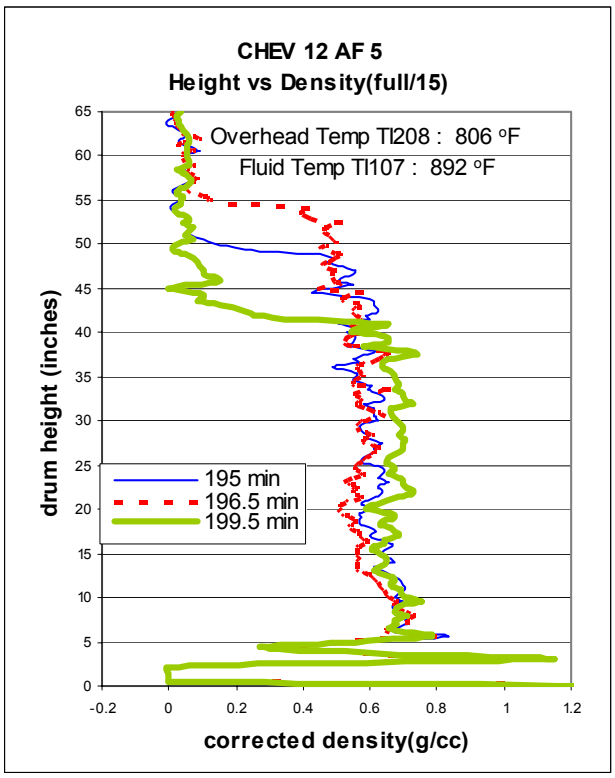

Figure 124 - Chev 12 PUAFI, Injection # 5

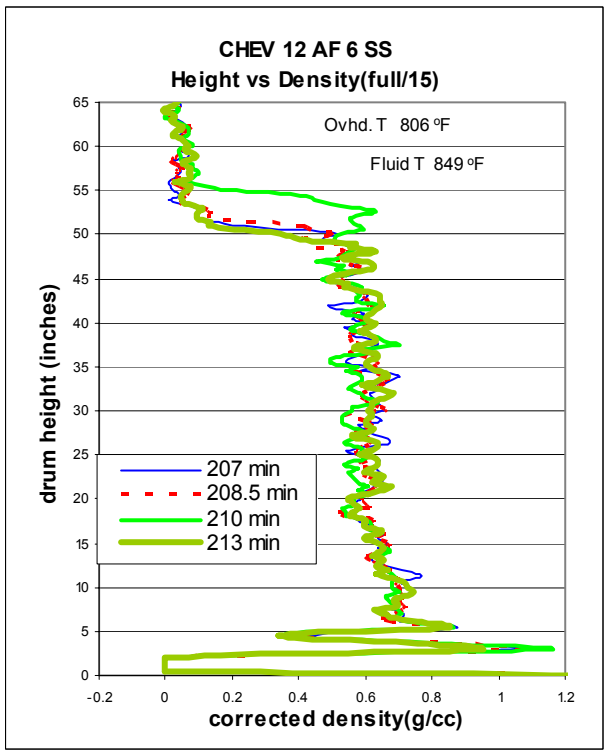

Figure 125 - Chev 12 PUAFI, Injection # 6

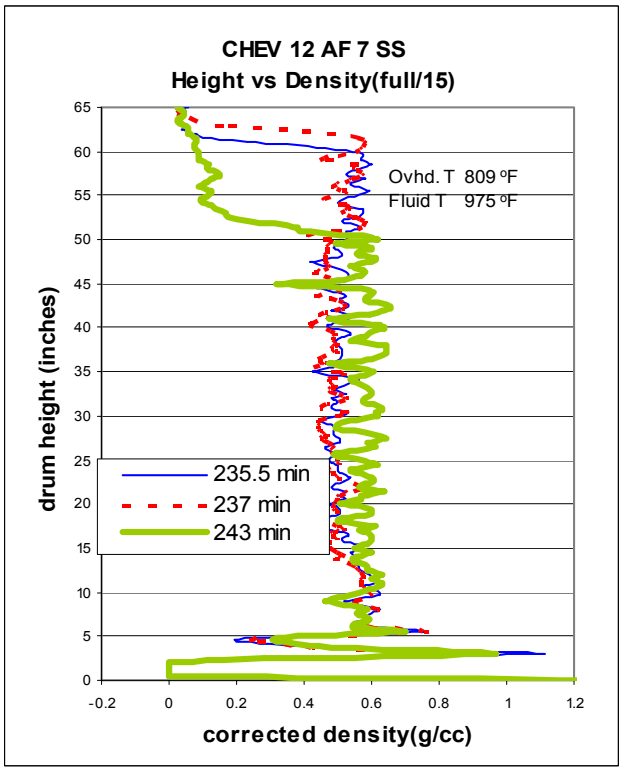

Figure 126 - Chev 12 PUAFI, Injection # 7

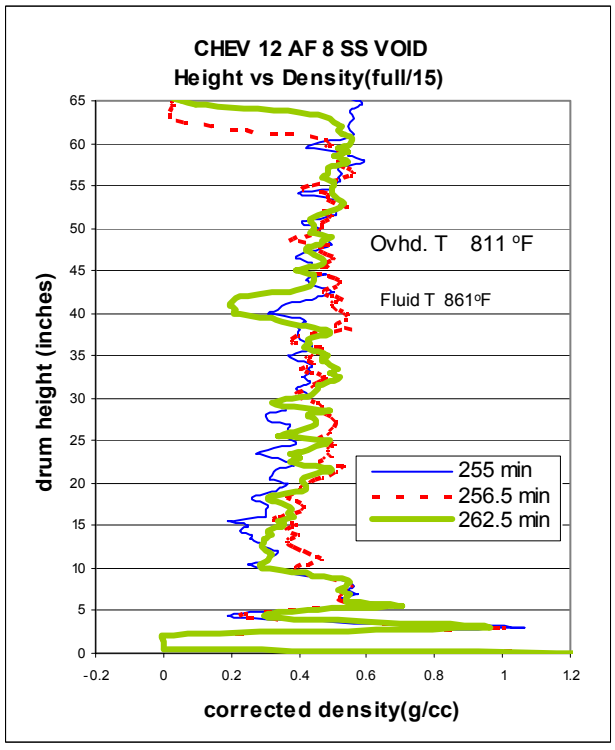

Figure 127 - Chev 12 PUAFI, Injection # 8

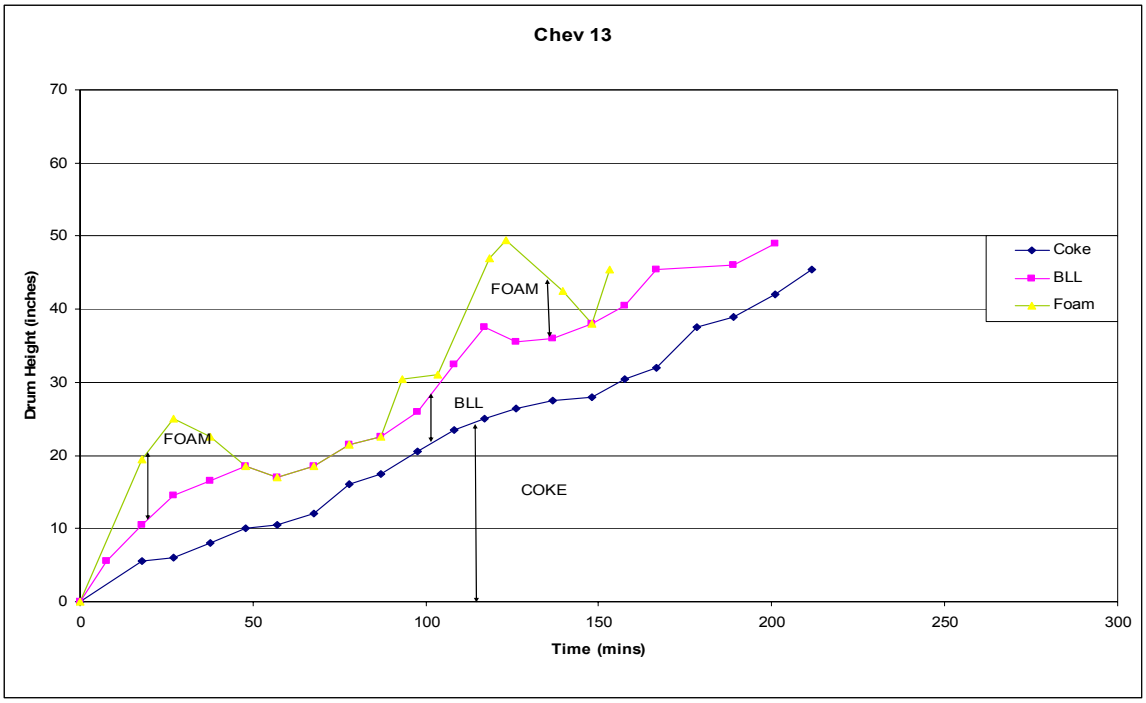

Figure 128 - Build-up of coke, bubbly liquid and foam layer with coking time for CHEV 13 PUAFC

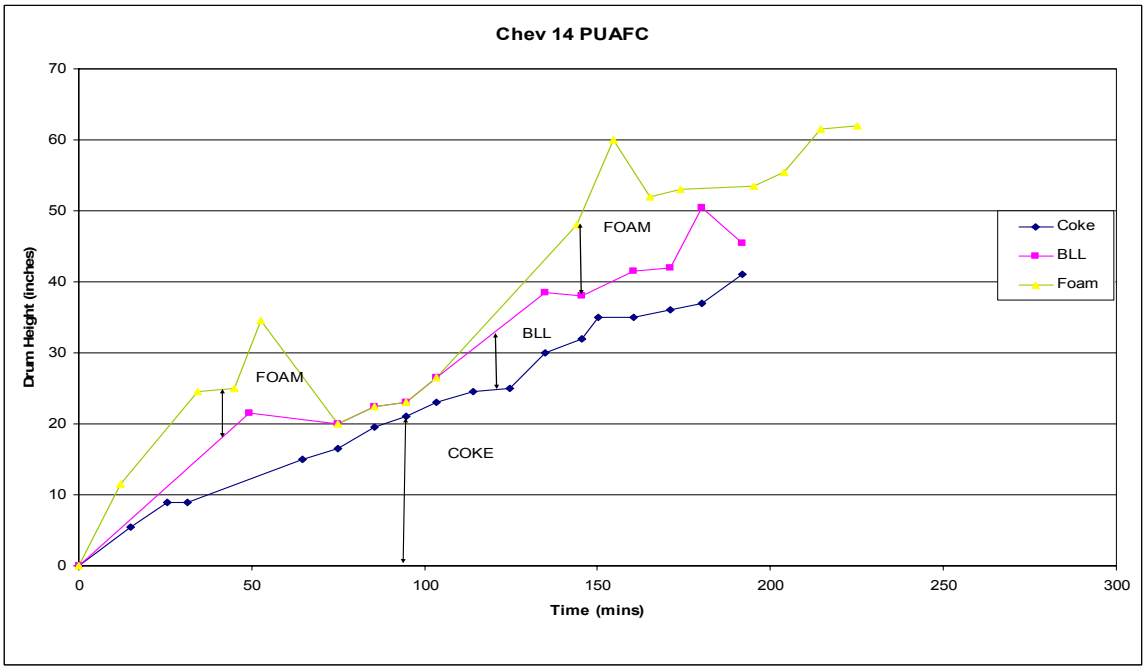

Figure 129 - Build-up of coke, bubbly liquid and foam layer with coking time for CHEV 14 PUAFC

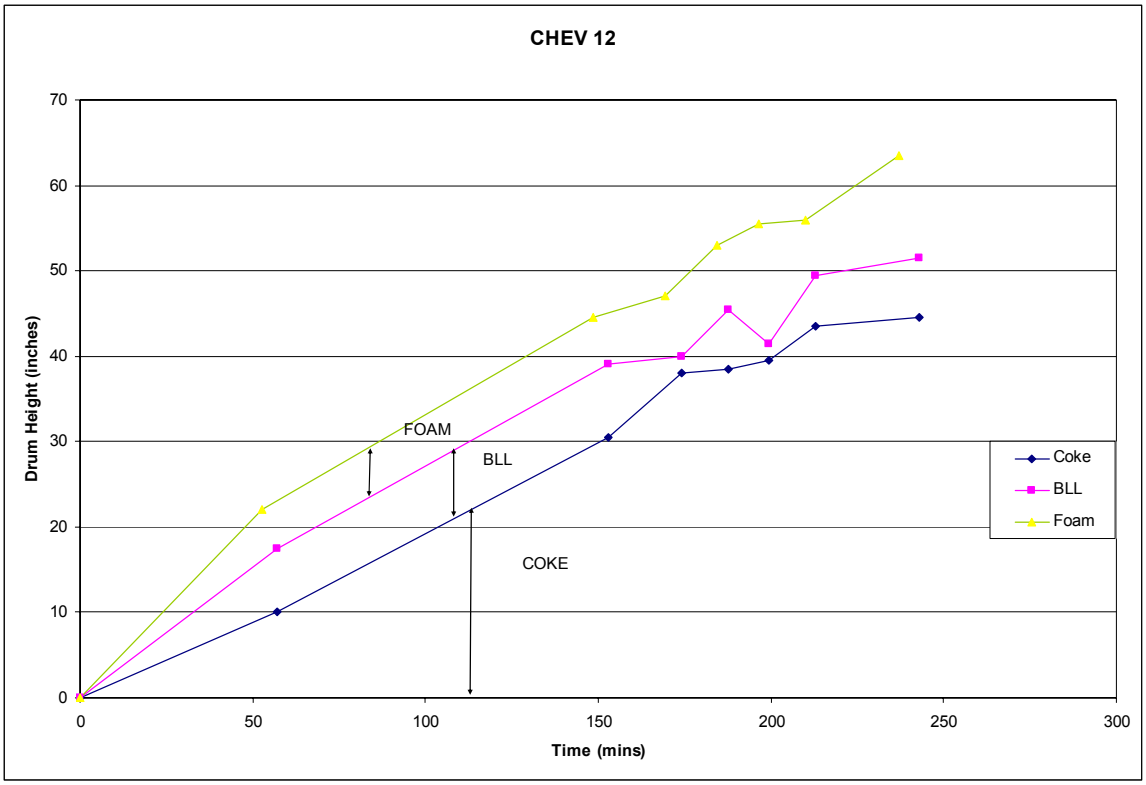

Figure 130 - Build-up of coke, bubbly liquid and foam layer with coking time for CHEV 12 PUAFI

Equilon Runs:

EQU 5 run was carried out at a temperature of 930°F, a pressure of 40 psig and a feed rate of 3600 gm/hr, whereas EQU 6 run was carried out at a temperature of 900°F, a pressure of 40 psig and a feed rate of 3600 gm/hr. EQU 5 was an as-needed overhead injection of 100,000 cSt (30/70) antifoam and EQU 6 was an as-needed feedline injection of 100,000 cSt (30/70) antifoam. As can be seen in Figure 61, Equilon required more heat input to the feedline to attain the higher temperature and the overhead temperature was very high compared to EQU 6. Run EQU 6 required less heat input to the feedline but the overhead temperature dropped remarkably thereby stripping more during the steam strip.

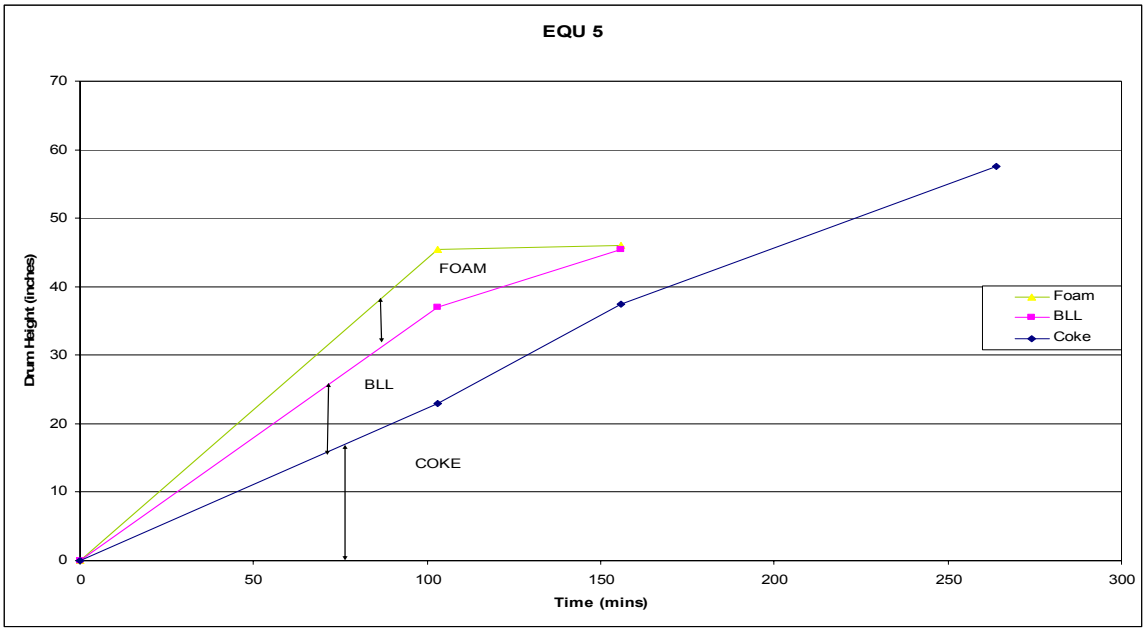

Figure 131 - Build-up of coke, bubbly liquid and foam layer with coking time for EQU 5 PUAFI

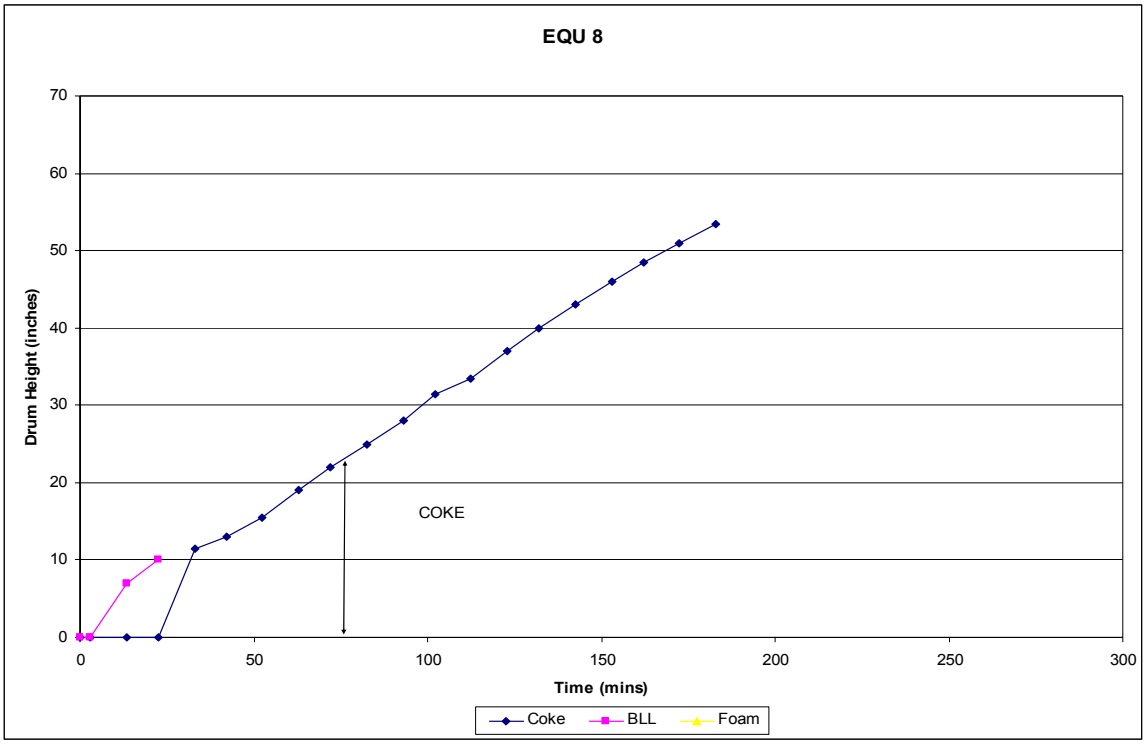

Figure 132 - Build-up of coke, bubbly liquid and foam layer with coking time for EQU 8 PUAFC

Runs PETR 3 and PETR 13 were carried out at a temperature of 900°F, a pressure of 15 psig and a feed rate of 3600 gm/hr. PETR 3 was an as-needed overhead+feedline injection of 100,000 cSt (30/70) antifoam, whereas PETR 13 was a continuous overhead injection of 100,000 cSt (0.3/70) antifoam. As can be seen in Figure 64, PETR 3 required less heat input to the inlet coil, and had a warmer overhead temperature. PETR 13 on the other hand required more heat input to the inlet coil and had a comparatively cooler overhead temperature. The fluid and the furnace skin temperature were the same for both the runs.

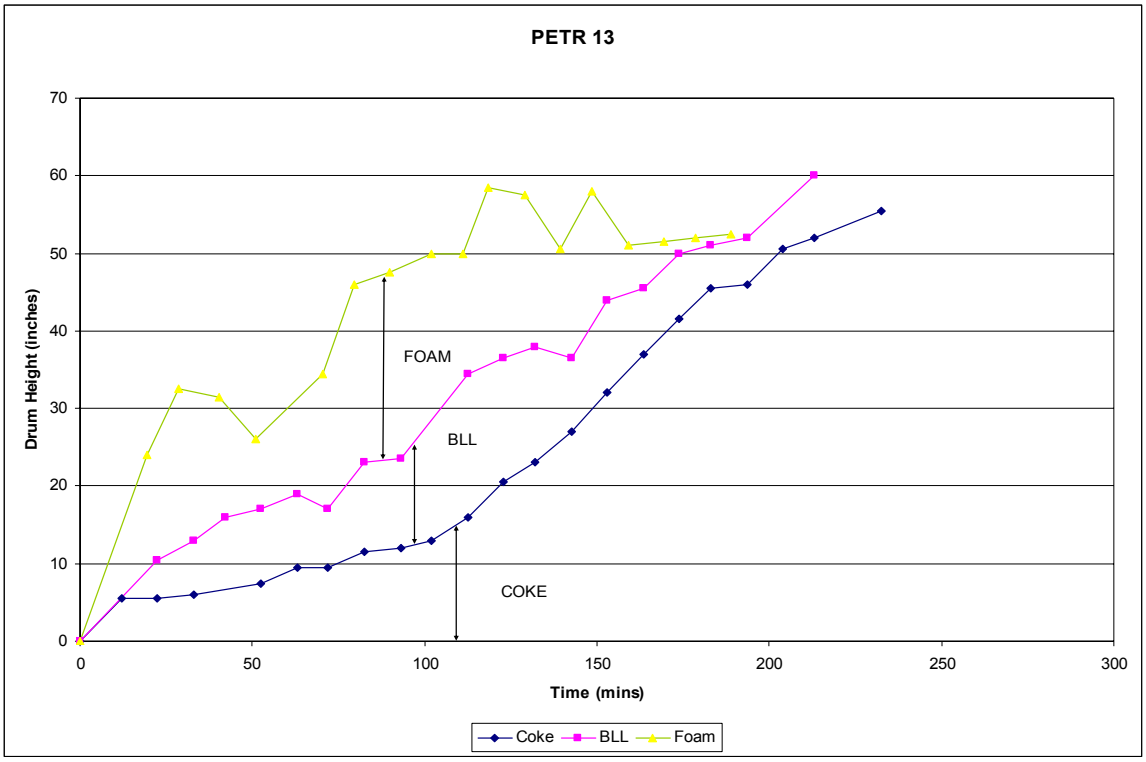

Figure 133 - Build-up of coke, bubbly liquid and foam layer with coking time for PETR 13 PUAFC

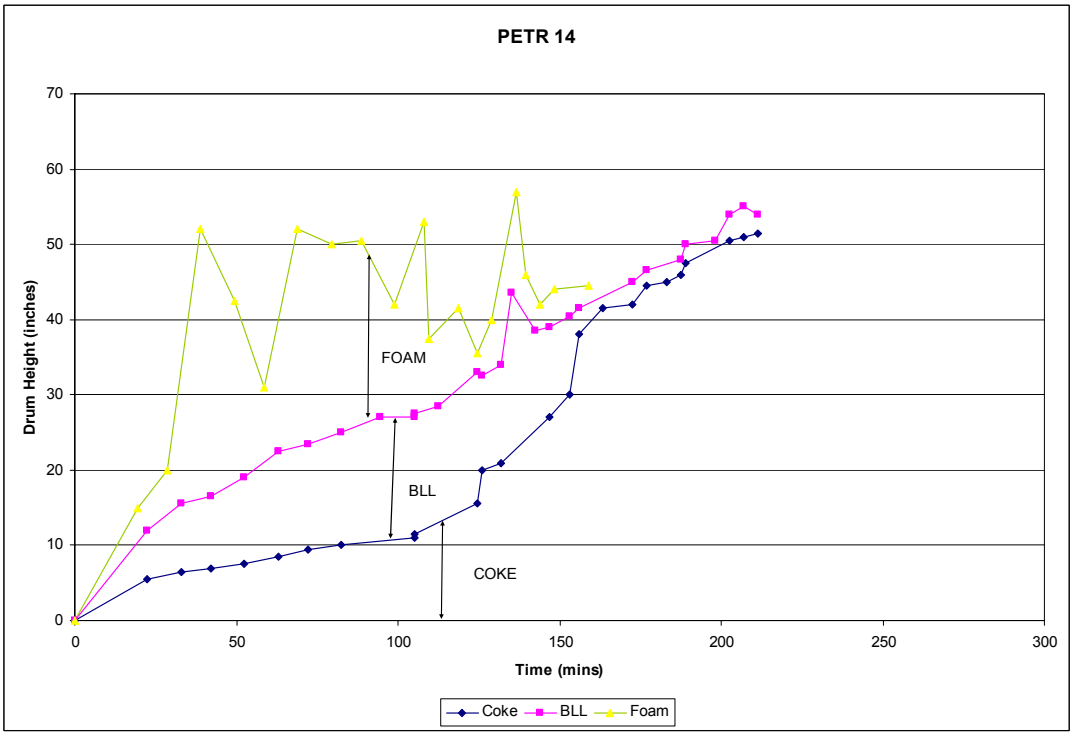

Figure 134 - Build-up of coke, bubbly liquid and foam layer with coking time for PETR 14 PUAFC

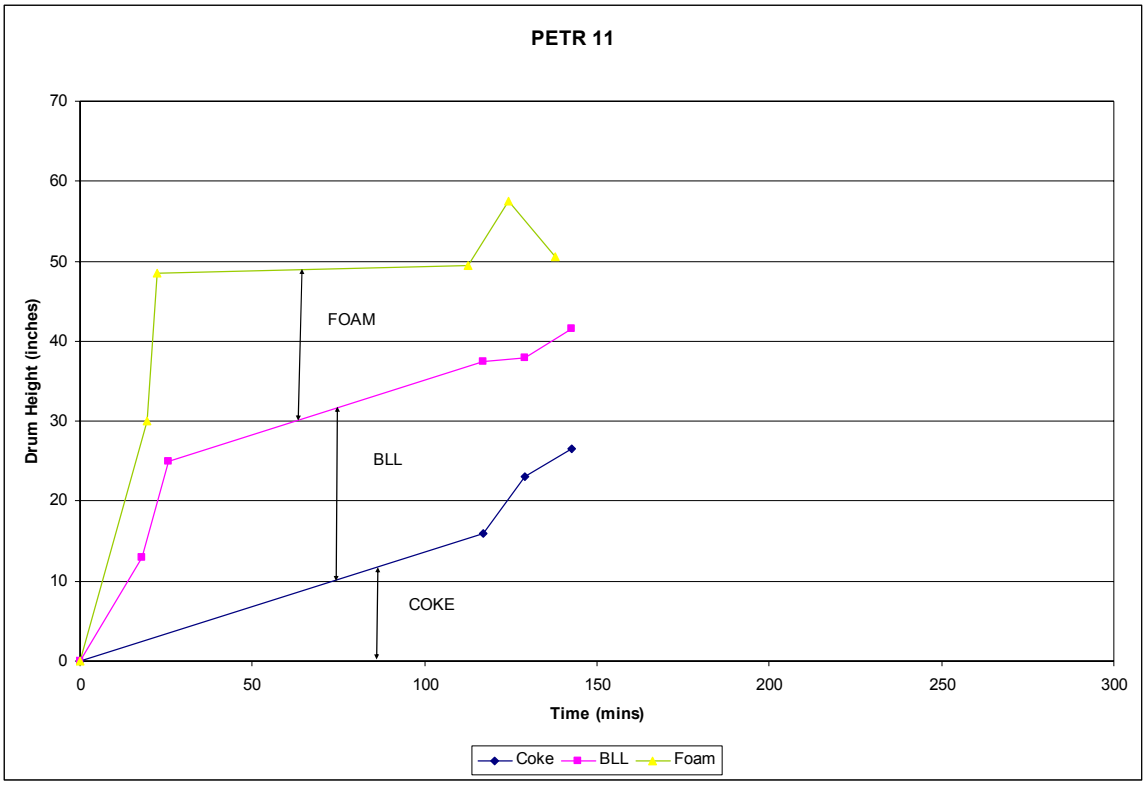

Figure 135 - Build-up of coke, bubbly liquid and foam layer with coking time for PETR 11 PUAFI

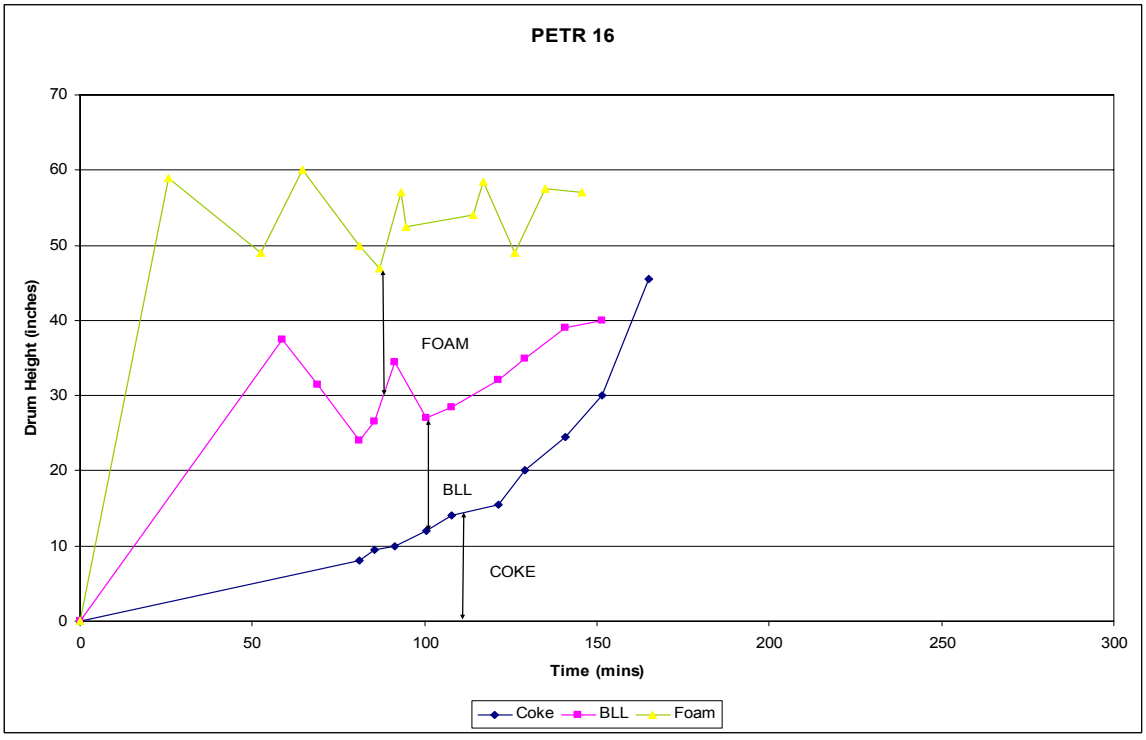

Figure 136 - Build-up of coke, bubbly liquid and foam layer with coking time for PETR 16 PUAFI

8. Para Metric Studies

The number of Pilot unit Antifoam runs conducted for each resid is tabulated in Table 65. Feedstock properties for each of the used resids are provided in Table 66.

Table 65 – Pilot Unit Antifoam Runs Considered by Resid

Resid	# of runs
Chevron	10
Citgo	12
Equilon	7
Suncor	12
Petrobras	12
Marathon	7
Total	60

Table 66 – Resid Properties

Resid	API	NMR	Structure	C7 Asphaltenes wt%	MCRT wt%	C7 Asphaltenes/MCR	Morphology	
		Saturate/aromatics					Proposed	Observed
Chevron	5.7	2.4	Napthenic	8.75	20.25	0.43	Sponge	Sponge/Shot
Marathon	10.3	2.8	Paraffinic	2.35	16.25	0.14	Sponge	Sponge
Petrobras	6.5	2.4	Paraffinic	8.56	21.77	0.39	Sponge	Sponge
Citgo	4.6	1.9	Napthenic	15.27	25.74	0.59	Shot	Sponge/Shot
Equilon	0.5	2.3	Intermediate	24.60	29.4	0.84	Shot	Shot
Suncor	2.9	2.5	Aromatic	12.97	21.15	0.61	Shot	Shot

Table 66 gives the proposed morphology of the coke based on the rule of thumb, if the value of the C7+Asplatenes/MCR > 0.5 then the resid forms shot coke. The observed morphology agrees with the rule of thumb. From Table 66 it is also observed that the Napthenic structured resids made a mixture of shot and sponge coke, Paraffinic resids made pure sponge coke, Aromatic resids made pure shot coke, while Intermediate structured resids made a mixture of Agglomerated and Large BB shot coke.

In this study, the coke morphology of each resid will be discussed separately later in the report.

Coke Morphology

i) Data Analysis:

The morphology of coke that is produced can be broadly classified as Sponge coke, Shot coke and Needle coke. In the foaming studies only Sponge coke and Shot coke are observed. The morphology study is aided by the use of data from the gamma densitometer that is plotted in three different ways.

a) Height vs Density plotted over set time period,
b) Height vs Time for a given density in the coke drum, and
c) Density vs Time plotted for a set height in the coke drum.

In the study of Pilot unit test runs, the data is analyzed by a new method of plotting. The data is plotted by picking the highest height in the column at which the resid (foam/liquid/coke) has a certain density. This height trace for given density is plotted with respect to time for a given test run.

Approximation: Height of the column for a given density is picked up only if two consecutive points (each varying by ½ in) below it, has value greater than the given density.

The plots given below show the highest height trace for a given density through out the test run. Both if the test runs are conducted at same operating conditions (930, 15, 3600 g/hr). Marathon test run made sponge coke and the Citgo test run made shot coke.

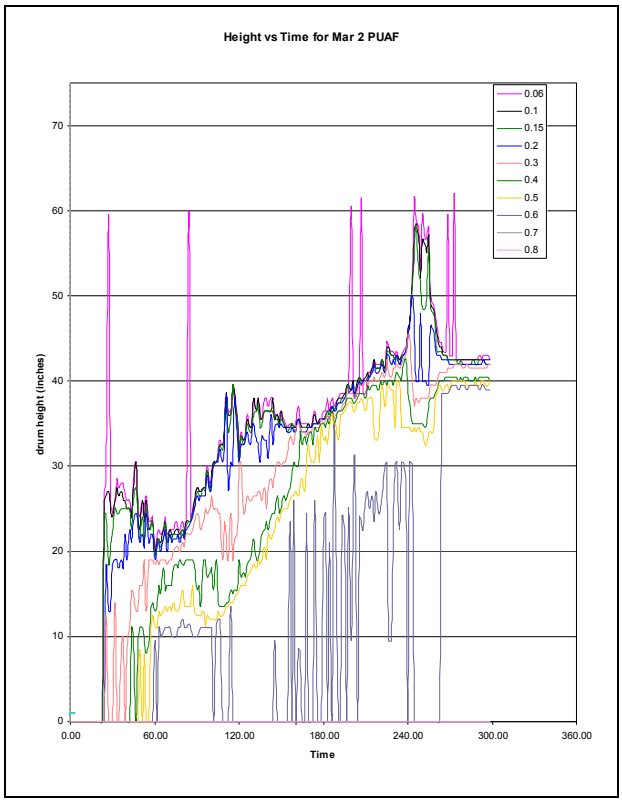

Figure 137 - Marathon Anti-Foaming runs – Height vs. Time (Sponge coke from Mar 2 PUAF)

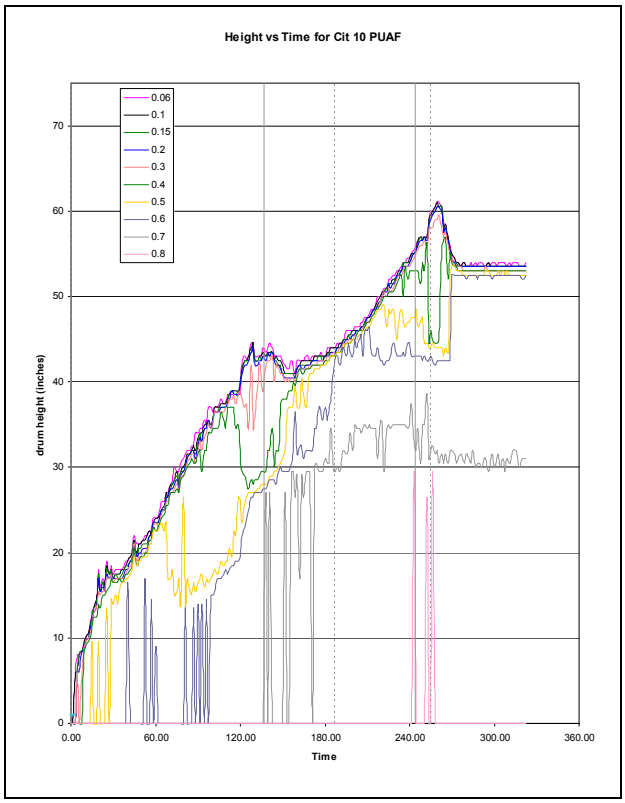

Figure 138 - Citgo Anti-Foaming Runs – Height vs. Time (shot coke from Cit 10 PUAF)

(i) Sponge coke

Sponge coke is named after its sponge like structure, generally made by low asphaltenic feeds (in this study where the asphaltenic content is < 24 wt %), and resids that have a value of C7+Asphaltenes/MCR <0.5. It is soft and can be easily crushed. The density of Sponge coke is generally less than that of shot coke because the structure of sponge coke is more porous than that of shot coke. Figure 139 and Figure 140 gives the digital photos of sponge coke formed from Petrobras and Marathon resids. Figure 3 gives the CT scan of the sponge coke made by Petrobras resid, which clearly shows the tree structured coke formation.

Literature review shows that sponge coke is formed at low temperature, higher pressure and low superficial velocities as the environment at these conditions is not turbulent. Petrobras and Marthon resids made pure sponge coke irrespective of operating conditions as these resids are low asphaltenic. Chevron made sponge coke in the middle and top portions of the drum when the feed rate was 1200 gm/hr(superficial velocity 0.06 ft/s) and 2400 gm/hr(superficial velocity 0.11 ft/s). Citgo made sponge coke for low temperature (900°F) and feed rate of 2400 gm/hr(superficial velocity 0.11 ft/s) runs.

Figure 142 and Figure 143 shows Height vs. Time traces for these resids as a factor of density. These traces have a definite slope after the first unsteady state (foaming) period of 90-120 min, demonstrating a linear growth of the bed.

Figure 144 and Figure 145 show Height vs. Density traces for sponge coke made by Petrobras and Marathon resids respectively. It is observed that the coke formed is fairly uniform in density after the initial foaming period (0-80 min for PET 4PUAF run and 0-110 min for MAR 2 PUAF run). The densities at the bottom grew up 0.6-0.7 gm/cc and allowed the resid to coke up above the drum to almost similar density as sponge coke has a good porous structure through which the resid can pass.

Petrobras and Marathon made sponge coke throughout the drum.

Figure 139 – Photo of Sponge Coke from PETR 4 PUAF

Figure 140 – Photo of Sponge Coke from MAR 4 PUAF)

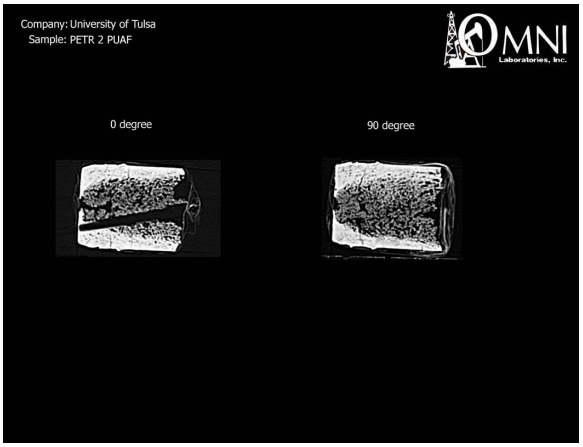

Figure 141 – CT scan of sponge coke made by Petrobras resid.

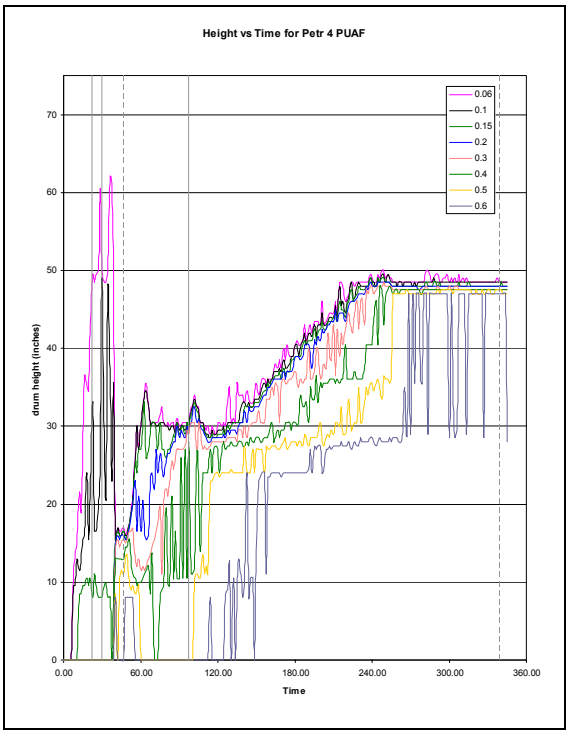

Figure 142 – Petrobras Anti–Foaming – Height vs. Time – (Sponge Coke for PETR 4 PUAF)

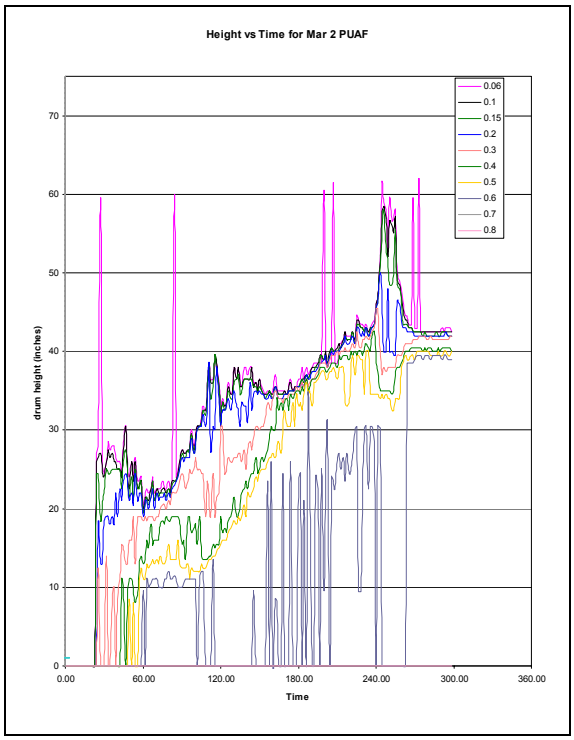

Figure 143 – Marathon Anti–Foaming – Height vs. Time – (Sponge Coke for MAR 2 PUAF)

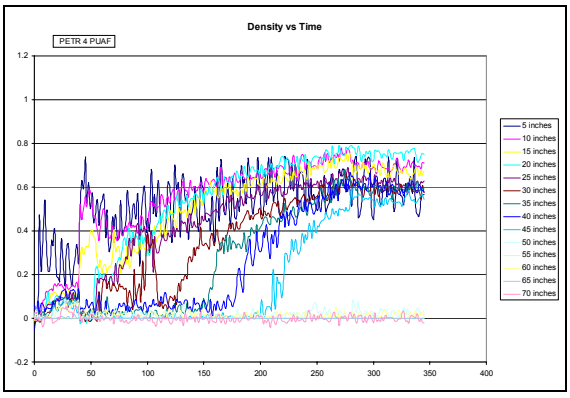

Figure 144 – Petrobras Anti–Foaming –Density vs. Time – (Sponge Coke for PETR 4 PUAF

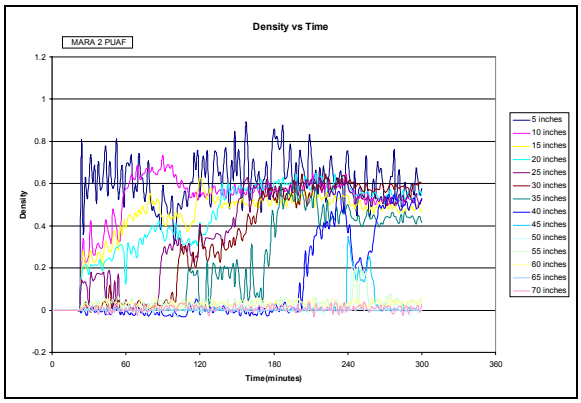

Figure 145 – Marathon Anti-Foaming – Density vs. Time – (Sponge Coke for MAR 2 PUAF)

(i) <u>Petrobras Resid:</u>

The morphology of coke for the Petrobras resid did not change with a change in operating variables. The Petrobras resid is Paraffinic and it made sponge coke as reported in the literature.

Effect of Temperature

Consider the Height vs Time plots for a given density in the coke drum, the density traces can be classified as Foam (density <0.2 gm/cc), Liquid (density >0.2 and <0.5 gm/cc) and coke (density >0.5 gm/cc) layers. Figure 146 and Figure 147 show the density traces for the Petrobras resid at the same operating conditions (40 psig, 2400 g/hr) except that the temperature is increased from 900°F to 930°F.

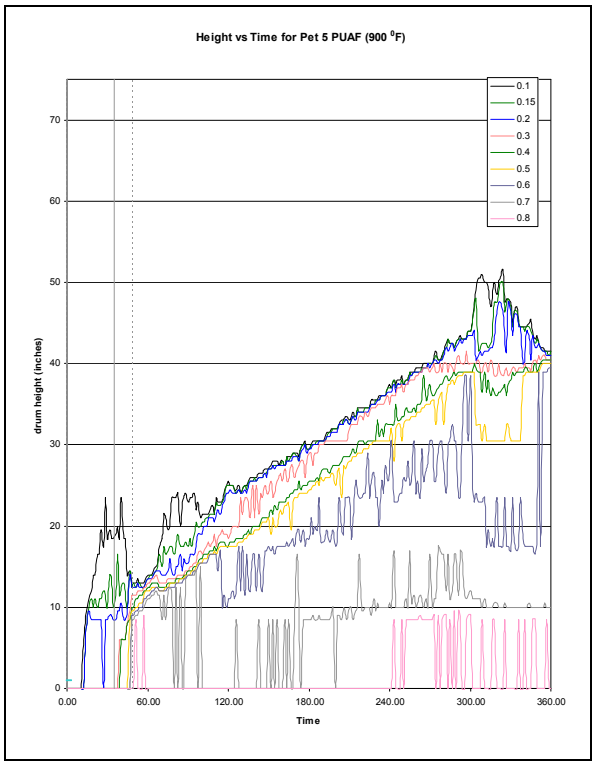

Figure 146 – Petrobras Anti-Foaming Runs – Height vs. Time (Sponge Coke from PET 5 PUAF)

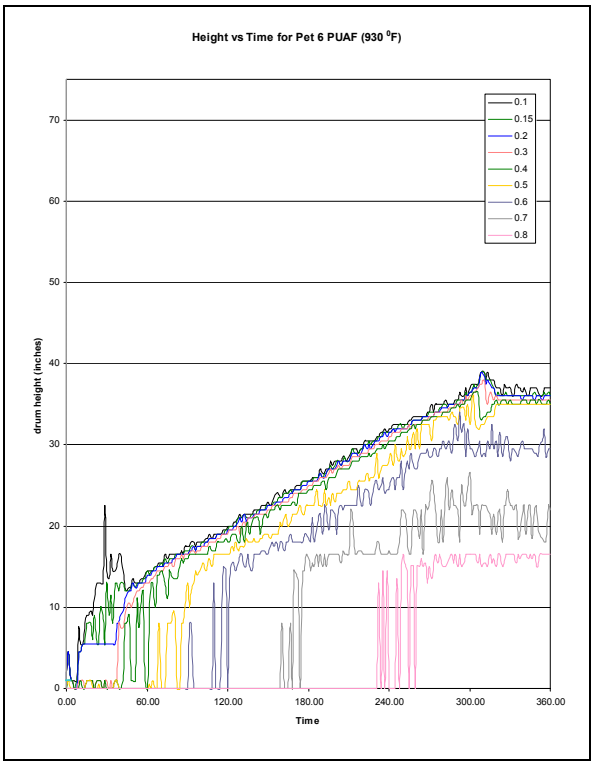

Figure 147 – Petrobras Anti-Foaming Runs – Height vs. Time (Sponge Coke from PET 6 PUAF)

For the Petrobras resid, the liquid layer (density >0.2 < 0.5 gm/cc) decreased with an increase in temperature because at higher temperatures coking occurs more rapidly.

It is observed that with increase in feedrate from 2400 gm/hr to 3600 gm/hr rate of coke growth dh/dt increased from 0.09 to 0.16 in/min.

Effect of operating conditions on coke morphology

Bulk and gamma densities were calculated for 8 Petrobras antifoam test runs which were conducted at varying operating conditions. Bulk density is obtained by dividing the weight of coke deposited in the drum with the volume occupied by the coke in the drum. Gamma density is taken from the average of the density values for last three traces of steam stripping. The average difference between Gamma density from the plots and the Bulk density is 0.13 gm/cc. The Bulk density is always greater than the gamma density.

Some of the reasons for these differences are:

1) The weight of the coke taken is the difference of initial and total weights of the drum, not the exact weight of the coke in the volume considered for calculating density, i.e. coke coating on the walls of the upper part of the drum is also added.
2) The Gamma densitometer scans the drum vertically on a straight line capturing a thin section of the coke morphology and may miss the morphology changes that can occur throughout in the coke drum.

The Coke density was found to increase with an increase in both temperature and pressure while the density was found to decrease with an increase in superficial velocity.

Effect of Feedrate:

With an increase in the feed rate, the coke density decreased. Corresponding temperature profiles for PET 2 and PET 4 are shown in Figure 148 and Figure 149 respectively. These two plots demonstrate that a lower density coke is formed when the temperature profiles are more uniformly distributed in the drum, than the case when higher density coke is formed. With an increase in feed rate a lot of foaming is observed (PET 4 test run), causing the temperatures throughout the drum to be uniform.

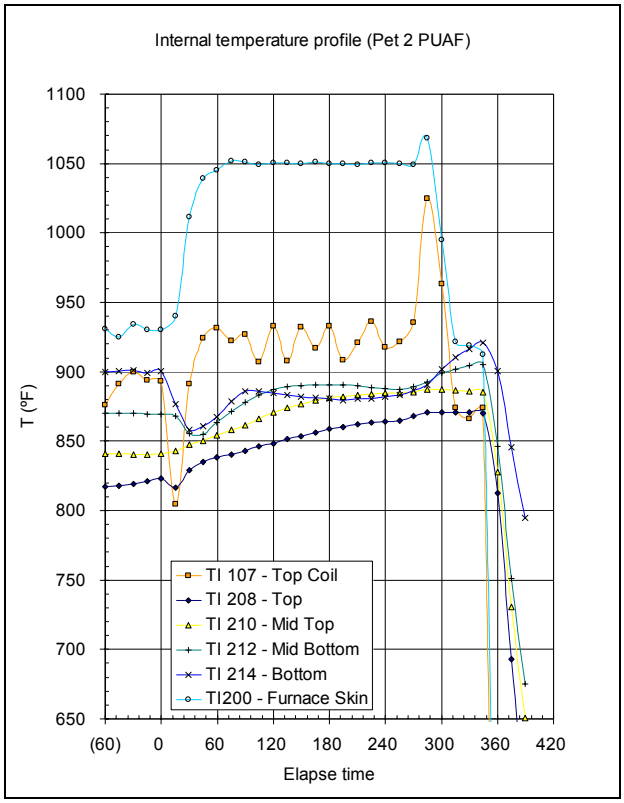

Figure 148 – Petrobras Anti-Foaming Runs – Temperature Profile (High density Sponge Coke from PET 2 PUAF)

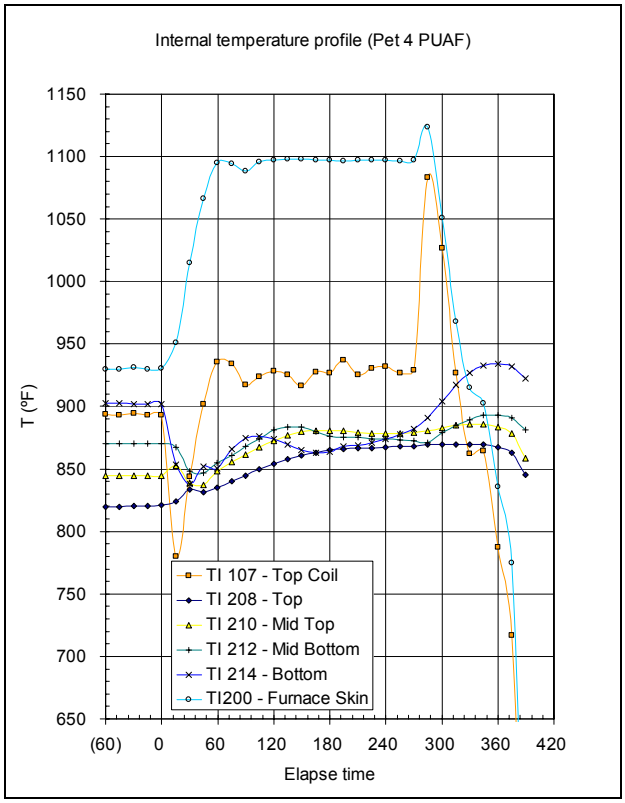

Figure 149 – Petraobras Anti-Foaming Runs – Temperature Profile (Lower Density Sponge Coke from PET 4 PUAF)

Foaming tendencies for Petrobras resid:

Increase of temperature decreased foaming as it decreases the height of liquid layer for Petrobras resid. Pressure chage did not have much impact on foaming for Petrobras resid. An increase in superficial velocity from 0.11 ft/s to 0.15ft/s increased foaming for all sets of temperature and pressure for Petrobras Resid. Temperature appears to be more dominant variable for Petrobras resid.

In the case of Petrobras resid, antifoam concentration as low as 0.3ml/70ml was effective in knocking back foam.

(ii) Marathon Resid:

The Marathon resid also made pure sponge coke irrespective of the operating conditions. This resid is also paraffinic.

Effect of Temperature

The liquid layer decreased with an increase in temperature. Figure 150 and Figure 151 show the density traces for the Marathon resid at the same operating conditions (15 psig, 2400 g/hr) with temperature increasing from 900°F to 930°F. All the 900°F had a thicker liquid layer than their 930°F counterparts. The 40 psig runs also foam more than the 15 psig runs at 900°F.

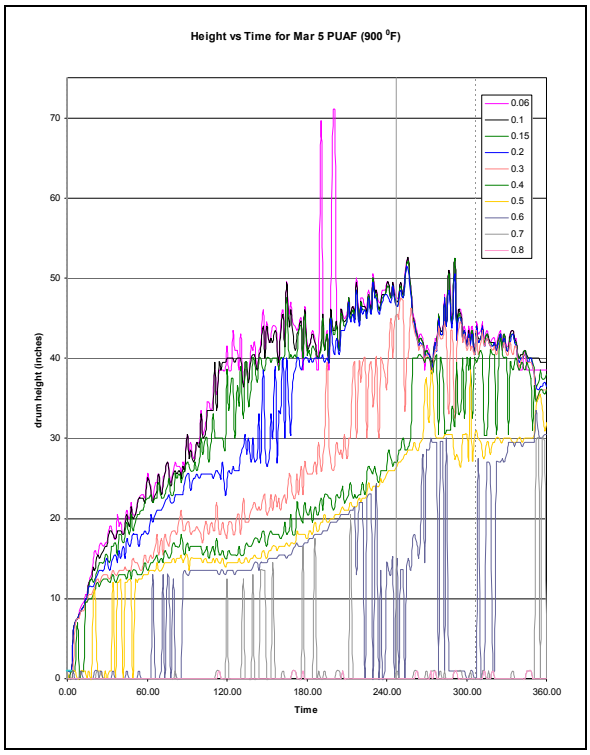

Figure 150 – Marathon Anti-Foaming runs – Height vs. Time (Sponge Coke from MAR 5 PUAF)

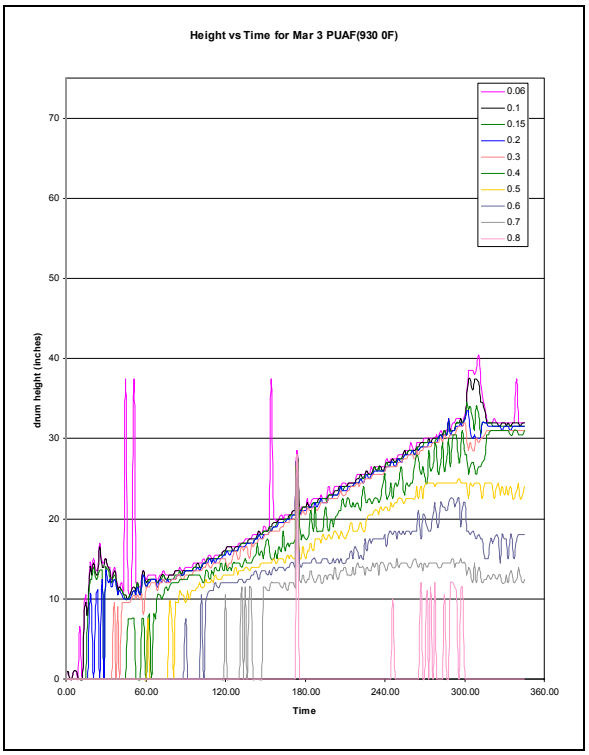

Figure 151 – Marathon Anti-Foaming Runs – Height vs. Time (Sponge Coke from MAR 3 PUAF)

It was observed that both the Marathon and Petrobras resids have nearly the same liquid layer height for a given set of temperature and pressure.

Effect of operating conditions on coke morphology

The Bulk density of Coke was found to decrease slightly with an increase in temperature at 15 psig pressure where as gamma density increased with increase in temperature. At 40 psig both bulk and gamma density increased with an increase in temperature. An increase in the pressure increased the density of the coke formed; however this observation is based on one run at each pressure. An increase in superficial velocity didn't have much impact on the density of the coke made for the Marathon resid.

For both Marathon and Petrobras resids bulk density ranged from 0.6 – 0.8 gm/cc and gamma density ranged from 0.45 -0.65 gm/cc approximately. The average difference between Bulk and gamma densities for petrobras and marathon resids are 0.13 gm/cc and 0.16 gm/cc respectively.

Effect of Feedrate:

Consider the three Marathon test runs at same operating conditions (930 ^{0}F, 15 Psig) but varying by feedrate, Mar 3 Puaf is a 2400g/hr, Mar 2 Puaf is a 3600 g/hr and Mar 4 Puaf is a 4800 g/hr test runs as shown in Figure 152 through Figure 155. An increase in superficial velocity resulted in increased foaming and also increased the slope of the bubbly liquid layer curve.

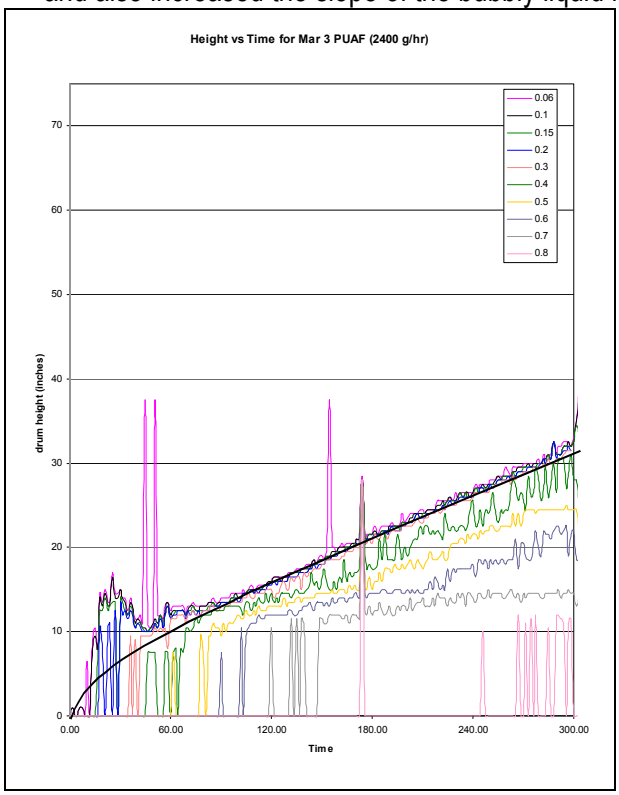

Figure 152 - Marathon Anti-Foaming runs – Height vs. Time (Sponge coke from MAR 3 PUAF)

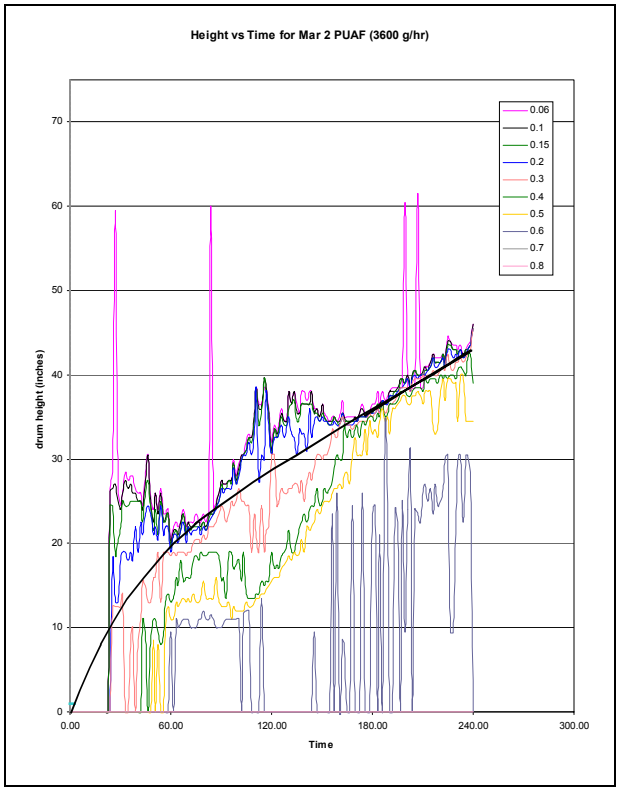

Figure 153 - Marathon Anti-Foaming runs – Height vs. Time (Sponge coke from MAR 2 PUAF)

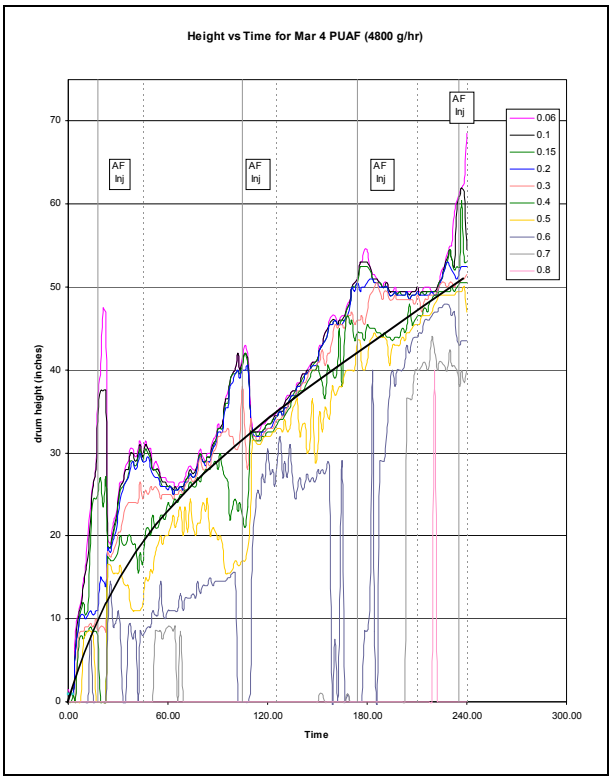

Figure 154 - Marathon Anti-Foaming runs – Height vs. Time (Sponge coke from MAR 4 PUAF)

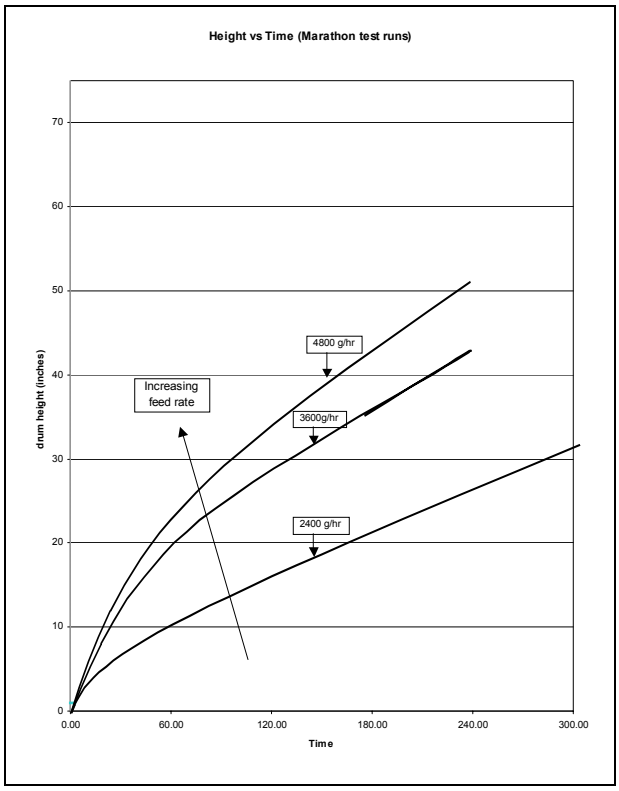

Figure 155 - Marathon Anti-Foaming runs – Height vs. Time (Sponge coke)

Foaming tendencies for Marathon resid :

Lower temperature and lower pressure caused foaming for Marathon.

An increase in temperature decreased foaming as it decreased the liquid layer for marathon resid. Pressure didn't have much impact on foaming for marathon resid. Increase in superficial velocity increased foaming. Temperature appears to be more dominant variable for this resid.

b) *Shot coke*

Coke Sizing

Coke sizing is a procedure of visually inspecting the coke to determine a percentage of the coke, which is to be considered shot coke. Great Lakes Carbon provided the procedure, and a short lesson on the analysis was provided. Generally the procedure is fairly simple. However, the inherent error is due to the fact that the analysis is subjective in that the observations can vary depending on the person performing the analysis. The procedure used for the coke sizing is as follows:

SHOT COKE DETERMINATION

1. Take the sample as prepared according to the Shot Coke Sample Preparation.

2. Take the +4 mesh fraction and separate into shot coke and sponge coke fractions. The visual guidelines for separation are described as follows:

Shot Coke includes small ball-shaped particles about 2-5 mm. diameter; individual round particles which may be bird-egg shape; lumps of bonded or agglomerated shot particles; and lumps which are of high density with shot particles or circular domains surrounded with coke. Photos of Sponge coke and Shot coke are given in Figure 156 and Figure 157.

Figure 156 – Photo of Sponge Coke from MAR 4 PUAF

Figure 157 – Photo of Shot coke from SUN 5 PUAF Bottom

3. Take the –4/+10 mesh fraction and riffle it down with the small counter-top riffler in the lab to obtain ~10-15 grams of sample. Divide the total 4/10M fraction weight by the riffled sample weight to obtain a riffle factor (R).

4. Inspect the 4/10M fraction and separate into shot and sponge coke fractions as described in step 2.

5. Due to the difficulty in identification, it is not necessary to inspect the –10M fraction for the presence of individual shot particles. In our calculation, the % shot content of the –10M fraction is assumed to be equal to that of the cumulative +10M fraction.

6. The percent shot content is calculated as follows:

$$\% \text{ Shot Content} = \frac{+4\text{M shot weight} + R^* (4/10\text{M shot weight})}{\text{Cumulative} + 10\text{M sample weight}} * 100$$

The Coke sizing is done for portions of samples from three different test runs in which the transition of sponge from shot is clearly observed. The results are given in Table 67 given below.

Table 67 Coke sizing

Sample	% Shot
CHEV 2 PUAF Bottom	95.0%
CHEV 3 PUAF Top	30.5%
CIT 7 PUAF Bottom	59.1%

Shot coke is generally made by high asphaltenic feeds and can either be made as spheres of different size or agglomerated into a hard dense mass. Agglomerated shot coke is harder to remove from the coke drum, where as the BB shot is very loosely packed and is easily removed from the drum. The density of shot coke is generally greater than the sponge coke (by a value of 0.1 - 0.3 gm/cc) as its structure is less porous. The digital photo for shot coke is shown in Figure 158 and a Boroscope photo is shown in Figure 159. The CT scan for shot coke is shown in Figure 160 and Figure 161.

Literature review shows that shot coke is formed at high temperature, low pressure and low superficial velocities as the environment at these conditions is highely turbulent. The Suncor Resid made shot coke irrespective of operating conditions as this resid is aromatic by its nature. Chevron, Citgo and Equilon made shot coke at higher temperature, lower pressure and higher superficial velocities (superficial velocities >= 0.15 ft/s).

Figure 158 – Suncor Anti-Foaming Runs – Coke Picture (SUN 5 PUAF Bottom)

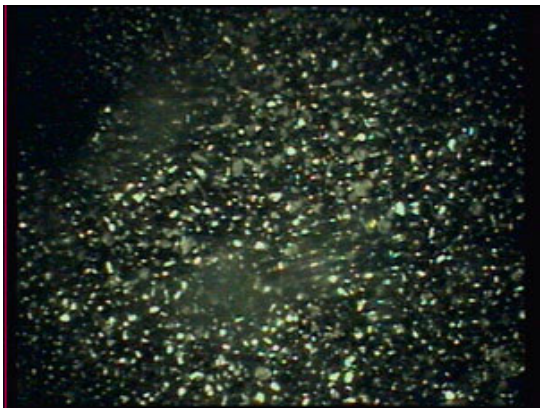

Figure 159 – Suncor Anti-Foaming Runs – Coke Picture (SUN 5 PUAF Bottom)

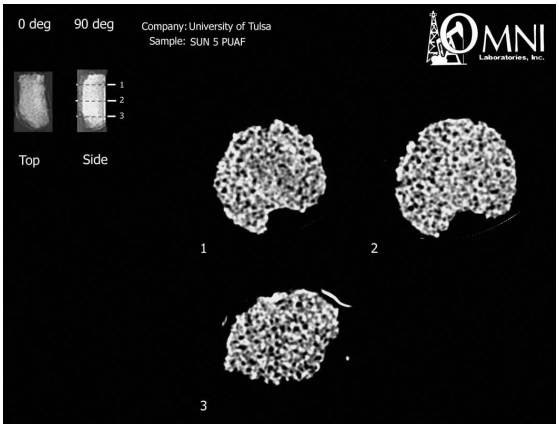

Figure 160 – Suncor Anti-Foaming Runs – CT Scan (Sun 5 PUAF Bottom)

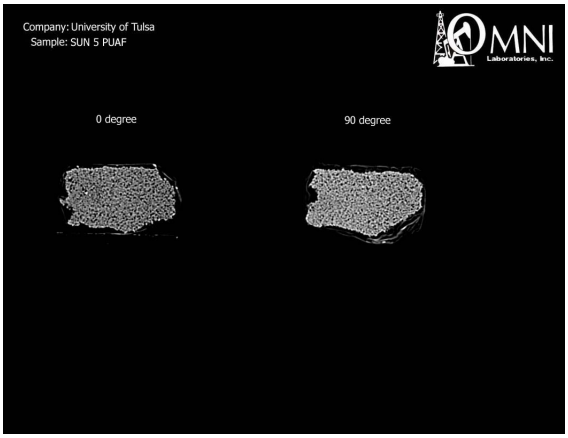

Figure 161 – Suncor Anti-Foaming Runs – CT Scan (Sun 5 PUAF Bottom)

Error! Reference source not found. and **Error! Reference source not found.** shows the Height vs. Time traces for given density for 100% Agglomerated shot coke made by Chevron and Citgo resids respectively. The characteristic feature of agglomerated shot coke traces is that the density traces until 0.5 gm/cc are knit together and after attaining a certain height they stay at that height, becoming denser until they form coke. Once the resid breaks through this agglomerated shot material the height of the coke bed begins to grow again. **Error! Reference source not found.** shows an Equilon test run, which made large BB's at the bottom, and a dense streak of agglomerated hard dense coke at the top of the BB's. **Error! Reference source not found.** shows a SUN 3 test run which made fine loose BB's throughout the drum.

Sponge vs. shot coke:

The MAR 3 run made sponge coke throughout and the EQ 1 run made shot coke. Both the test runs are at the same operating conditions (930°F, 15 psig, 2400 g/hr). Figure 162 and Figure 163 show how the densities of sponge coke and shot coke vary during a test run. Sponge coke has a good porous structure that allows the resid to continually flow through the coke as a function of time. This is shown in Figure 162 where the higher density traces follow the lower density traces (slope is nearly the same). Shot coke has a tendency to agglomerate in the drum, which is shown by Figure 163 where the lower density traces, once they reach a certain height, stay there (no growth in coke height vs time) allowing the coke below to become denser. Also for this run, when the resid breaks through this agglomerated portion, coke begins to accumulate above this layer as a function of time.

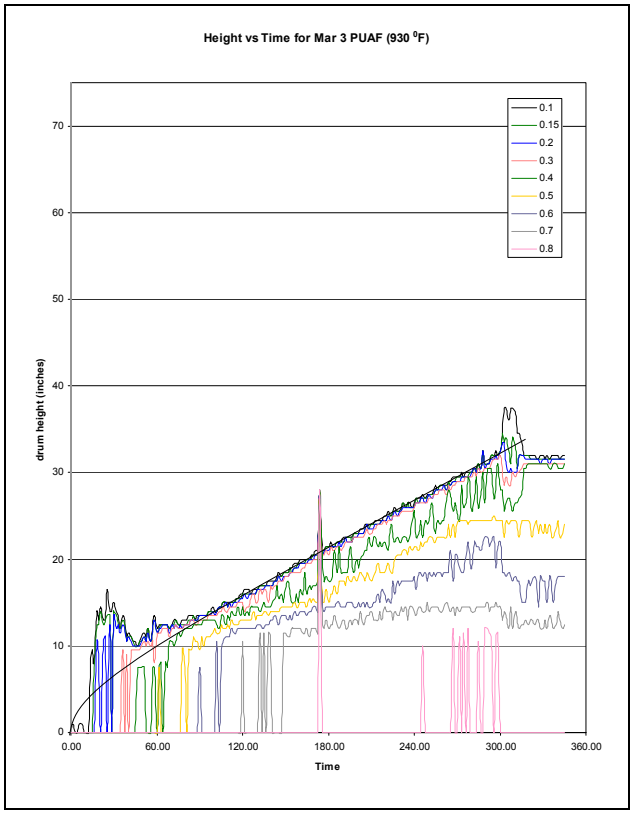

Figure 162 – Marathon Anti-Foaming runs – Height vs. Time (Sponge coke from MAR 3 PUAF)

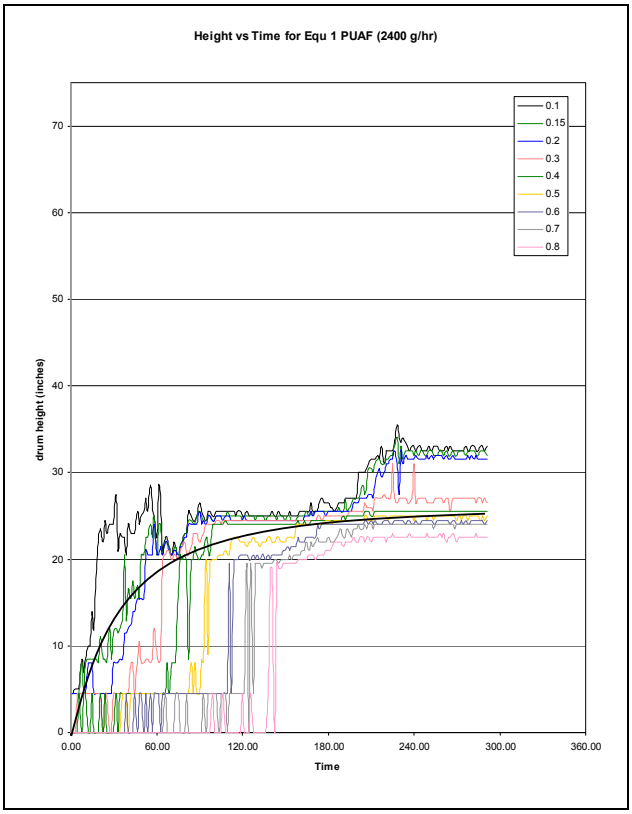

Figure 163 – Equilon Anti-Foaming Runs – Height vs. Time (Shot coke from EQ 1 PUAF)

(i) Suncor resid:

The Suncor resid made shot coke throughout the runs; however, the morphology did vary from Agglomerated shot coke to BB's with increase in temperature and decrease in pressure.

Agglomerated shot vs. BB shot

The test runs considered for this comparison are SUN 2 which made agglomerated shot coke and SUN 3 which made a fine loose BB shot. Both the test runs are at same operating conditions (930°F, 15 psig, 3600 g/hr). Figure 164 shows agglomerated shot coke, where after a period of time, the coke level after reaching certain height, just grows denser. Figure 165 shows BB shot coke which has tendency to continuously grow in height in the drum with time, similar to sponge, the only difference being a lot of fluctuations of height in the column.

Figure 166 and Figure 167 show the temperature profiles for SUN 2 and SUN 3 antifoam runs respectively. The difference in coke morphology at the same operating conditions can be explained by comparing the temperature profiles for the bottom of the drum (TI-214) shown in Figure 168 and fluid inlet temperatures (TI-107) as shown in Figure 169. The temperature in the bottom of the drum is different by about 20-30°F between SUN 3 and SUN 2 for the first two hours as shown in Figure 168. Figure 164 shows that the antifoam is injected in the beginning of the test run and the foam thus collapsed and suppressed the bottom temperature (TI-214). Figure 165 shows that SUN 3 didn't foam badly in the beginning and the antifoam was injected only in the later part of the test run, which allowed quick recovery of the bottom temperature (TI-214). The lower temperatures at the bottom of the drum allow the molten mass at the bottom to solidify into dense agglomerated coke, whereas higher temperatures at the bottom of the drum tend to vaporize or crack the molten liquid and forms BB's.

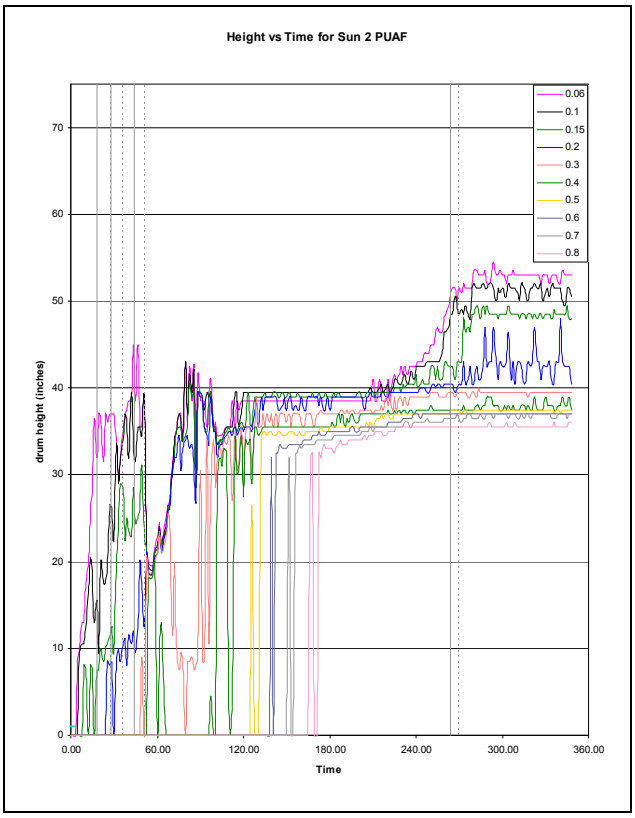

Figure 164 – Suncor Anti-Foaming Runs – Height vs. Time (Aggl Shot Coke from SUN 2 PUAF)

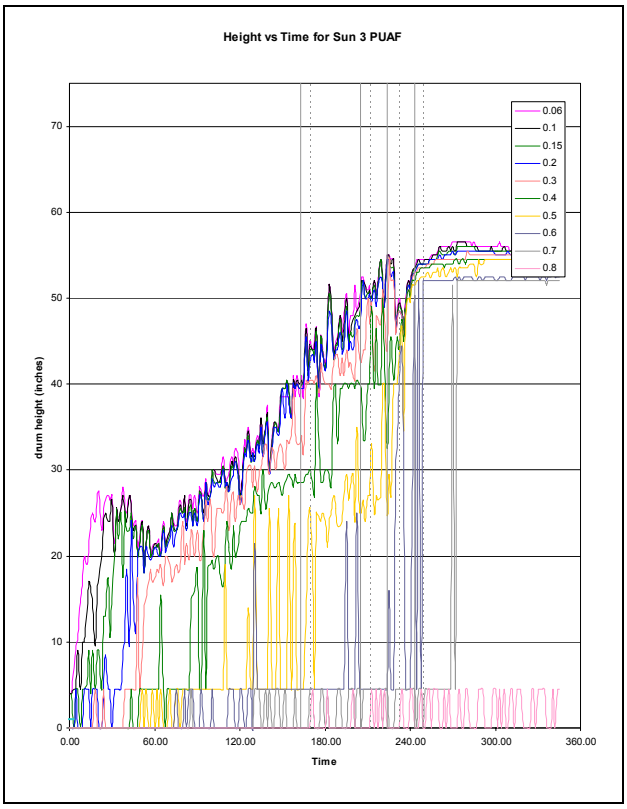

Figure 165 – Suncor Anti-Foaming Runs – Height vs. Time (BB Shot Coke from SUN 3 PUAF)

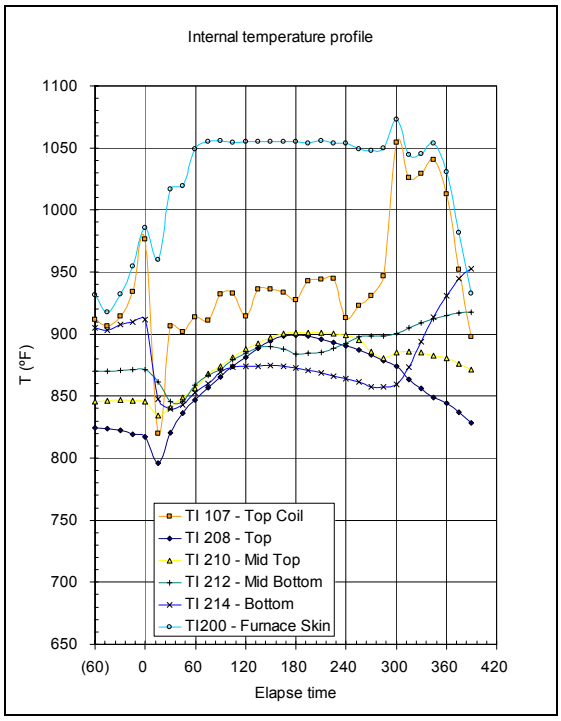

Figure 166 – Temperature Profile for SUN 2 PUAF

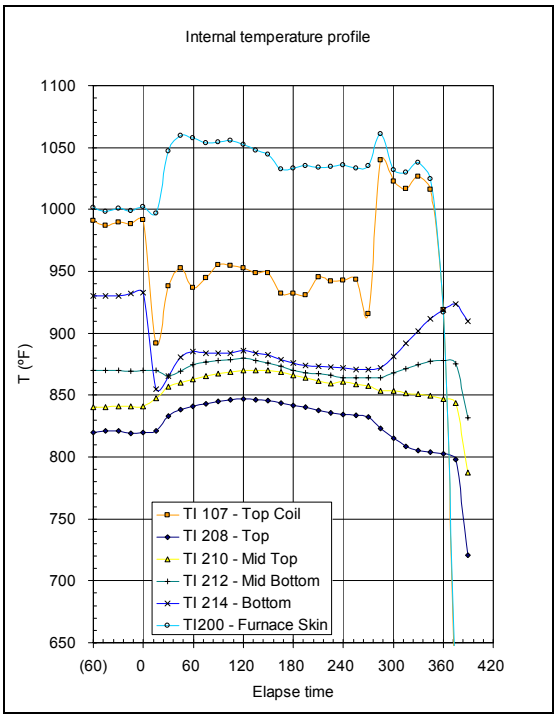

Figure 167 – Temperature Profile for SUN 3 PUAF

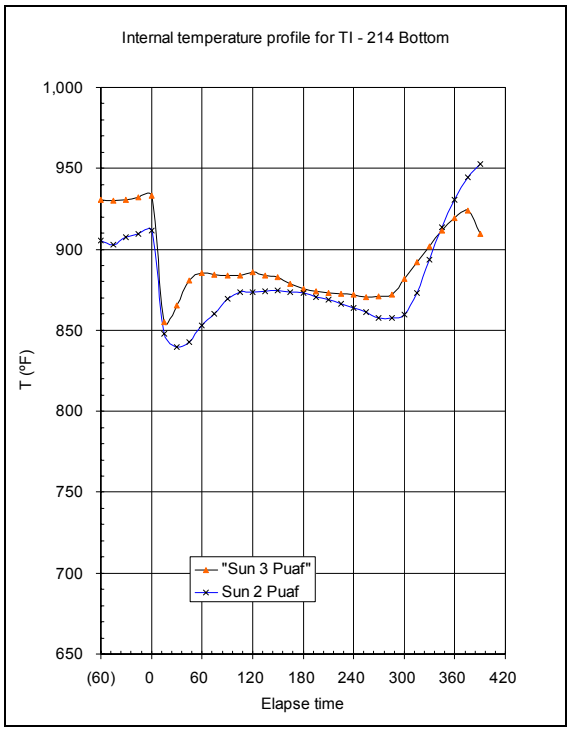

Figure 168 – TI-214 Bottom Temperature Comparison for Suncor Runs

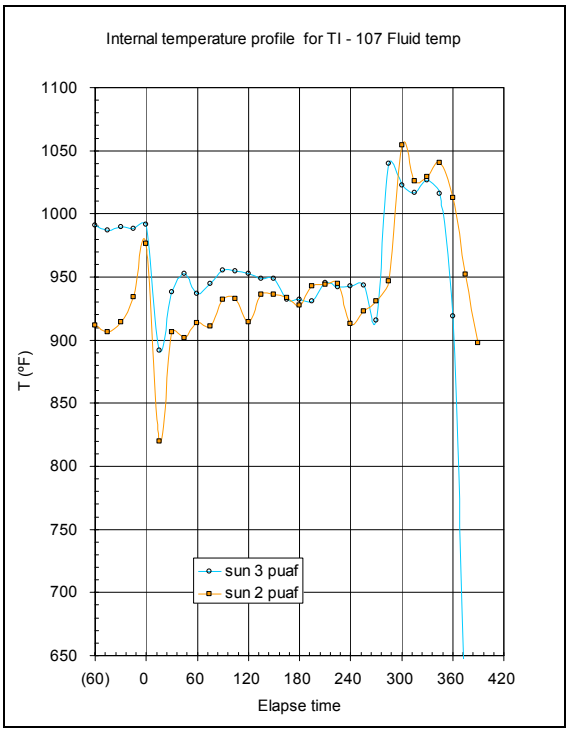

Figure 169 – TI-107 Fluid Temperature Comparison for Suncor Runs

Effect of operating Conditions on Coke Morphology:

Temperature:

With an increase in temperature from 900°F to 930°F the % of BB's formed decreased, which contradicts the rule of thumb that at higher temperature more BB's are formed. The reason could be because the two test runs are at a higher pressure (40 psig).

It was seen that there was not much of a change in the liquid layer with change in pressure or temperature. The foam layer increased with increase of temperature at 15 psig and it decreased with increase in temperature at 40 psig.

Feed rate:

Error! Reference source not found. shows the effect of increasing feed rate for Suncor runs, where the other operating conditions such as temperature (930°F) and pressure (15 psig) are the same. With an increase in feed rate from 2400 g/hr to 3600 g/hr the % of BB's formed decreased. Increase in feed rate increases the time required for the temperature to get back to the desired fluid temperature, which lowers the amount of BB's formed in the coke drum.

Effect of Antifoam injection

The amount of BB's formed increased with an increase in either the amount of antifoam used or concentration of antifoam used. For the SUN 13 run, the feed line injection resulted in complete elimination of BB's, which formed in the prior runs when the antifoam injection was overhead and possibly carried out of the drum.

Effect of operating conditions on Density of coke:

Considering the density columns, it was inferred that the increase in temperature, pressure or feed rate increases the coke density. For shot coke the discrepancy of increase in density due to increase in feed rate, from the sponge coke is due to the formation of dense agglomerated shot coke at higher feed rates.

Foaming tendencies for Suncor resid:

Increase in temperature decreased foaming for Suncor resid while an increase in pressure and superficial velocities increased foaming for Suncor resid. Pressure appears to be more dominant variable for Suncor resid.

(ii) Equilon resid:

Equilon made mixture of agglomerated shot, BB's and sponge coke. The BB's formed varied from fine BB's to small spheres of different sizes.

Effect of operating Conditions on Coke Morphology:

Temperature:

An increase in temperature from 900°F to 930°F caused the % of BB's formed to increase. Considering all the four runs higher temperature more shot coke is formed.

Both foam and liquid layers increased with increase of temperature at 15 psig and it decreased with increase in temperature at 40 psig.

Note: The observations are based on only one test run at certain set of temperature and pressures.

Pressure:

An increase in pressure eliminated the BB's and also reduced the % of shot coke formed.

Feed rate:

With an increase in feed rate from 2400 g/hr to 3600 g/hr the amount of shot coke as well as % of BB's has increased.

Effect of operating conditions on Density of coke:

Data available for the Bulk densities did not have a specific trend for either the temperature or pressure as the values didn't change much.

Foaming tendencies for Equilon resid:

The severest foaming was seen at high pressure and higher feed rate runs. Figure 170 and Figure 171 shows the Height vs. Time plots for given density for the EQ 5 and EQ 6 runs. Pressure appears to be more dominant variable for Equilon resid.

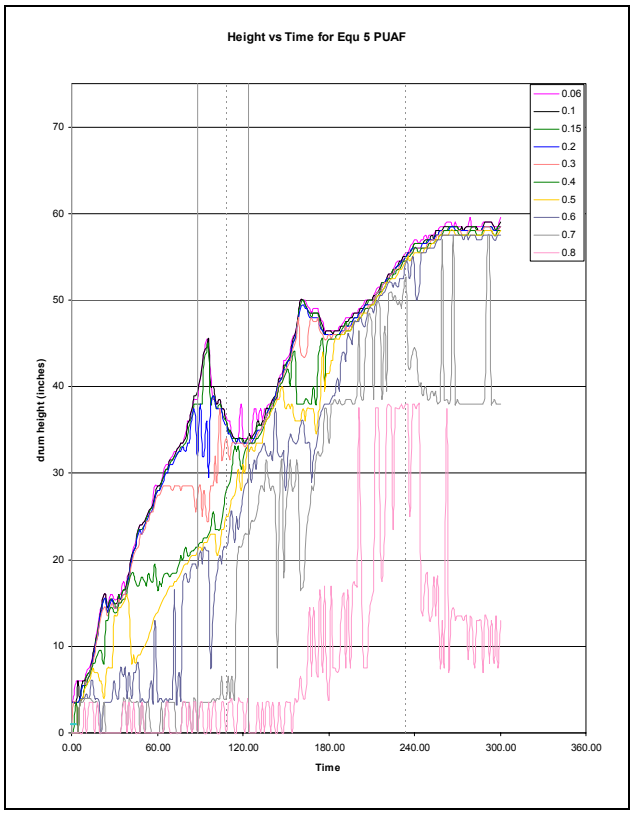

Figure 170 – Equilon Anti-Foaming Runs – Height vs. Time (EQ 5 PUAF)

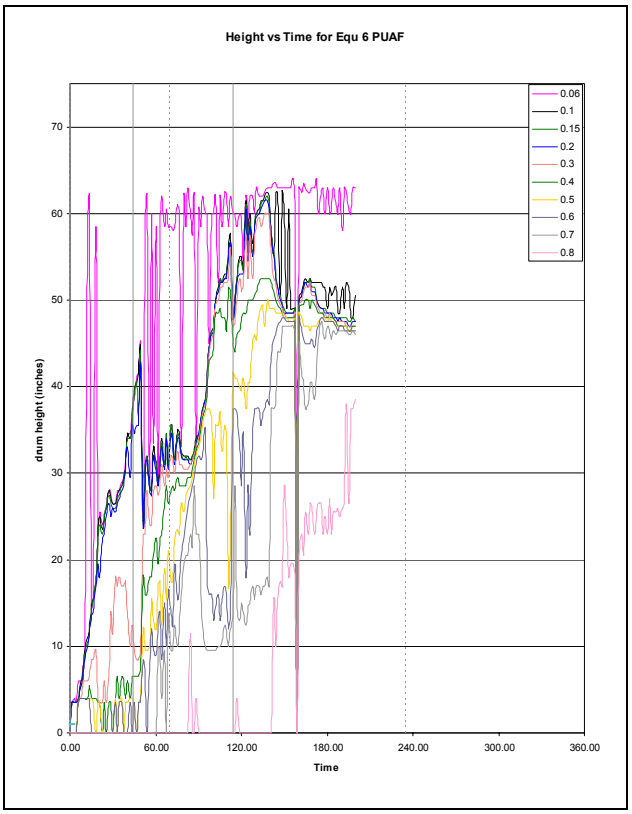

Figure 171 – Equilon Anti-Foaming Runs – Height vs. Time (EQ 6 PUAF)

(iii) Chevron resid:

Chevron made sponge coke at the top and middle portions and agglomerated shot coke in the bottom. This kind of mixture of sponge and shot coke formation might be because it is a naphthenic structured resid.

Sponge vs. shot coke:

The CHEV 6 run made 85% sponge coke while the CHEV 8 run made 100% agglomerated shot coke. Figure 172 and Figure 173 show how the densities of the sponge coke and the shot coke vary during a test run.

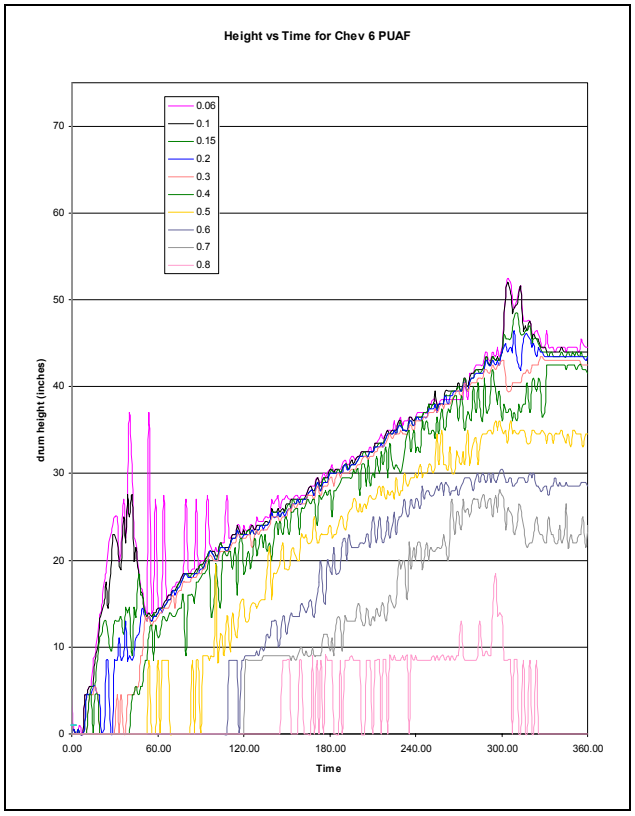

Figure 172 – Chevron Anti-Foaming Runs – Height vs. Time (Sponge Coke from CHEV 6 PUAF)

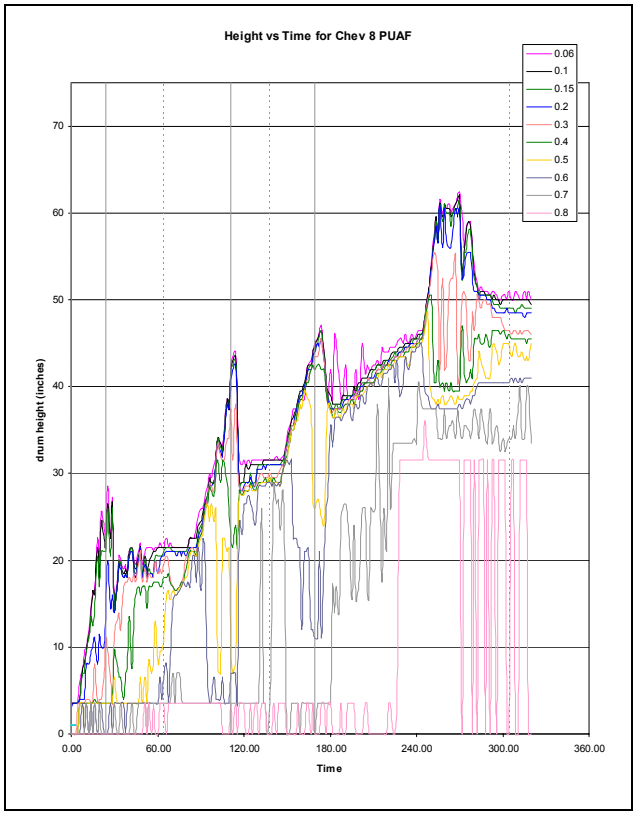

Figure 173 – Chevron Anti-Foaming Runs – Height vs. Time (Aggl Coke from CHEV 8 PUAF)

Sponge coke has a very porous structure allowing the coke height to continually increase with time, which is shown in Figure 172 where the higher density traces followed the lower density traces (slope is nearly same). Shot coke has a tendency to agglomerate in the drum, which is shown by Figure 173 where the lower density traces, once they reach a certain height, stay there allowing the coke below to become denser. Also for this run, once the resid breaks through this agglomerated portion, the coke height begins to increase on a continual basis.

Effect of operating Conditions on Coke Morphology:

Temperature:

For the 15 psig runs it was observed that an increase in temperature from 900°F to 930°F reduced the % of agglomerated shot formed. The 4 tests at higher pressure (40 psig) showed an increase in temperature from 900°F to 930°F increased the % of agglomerated shot coke formed.

The foam layer did not change much with increase in temperature and pressure. Liquid layer decreased slightly at 15 psig and quite significantly at 40 psig with an increase in temperature.

Pressure:

For thr 900°F tests it is observed that an increase in pressure from 15 psig to 40 psig reduced the % of agglomerated shot formed. At a higher temperature of 930°F, an increase in pressure from 15 psig to 40 psig increased the % of agglomerated shot coke formed.

Feed rate:

Effect of operating conditions on Density of coke:

An increase in bulk density with an increase in temperature was ran for the 2400 g/hr runs, but there was a decrease in density with an increase in temperature for the 3600 g/hr runs. A slight increase in density with an increase in pressure was seenfor all the other operating conditions. A decrease in density with an increase in feed rate except for the 900°F and 40 psig, 3600 g/hr run which foamed badly and produced a denser coke with an increase in the feed rate were seen.

Foaming tendencies for Chevron Resid:

At low superficial velocities there is not much foaming observed for the Chevron test runs. Figure 174 and Figure 175 show the Height vs. Time plots for given density for the CHEV 8 and CHEV 10 runs respectively. The lower temperature runs were the worst foamers when the Chevron resid was used. Also of the two runs considered below the higher pressure run was worst foamer. Pressure appears to be dominant variable for chevron resid.

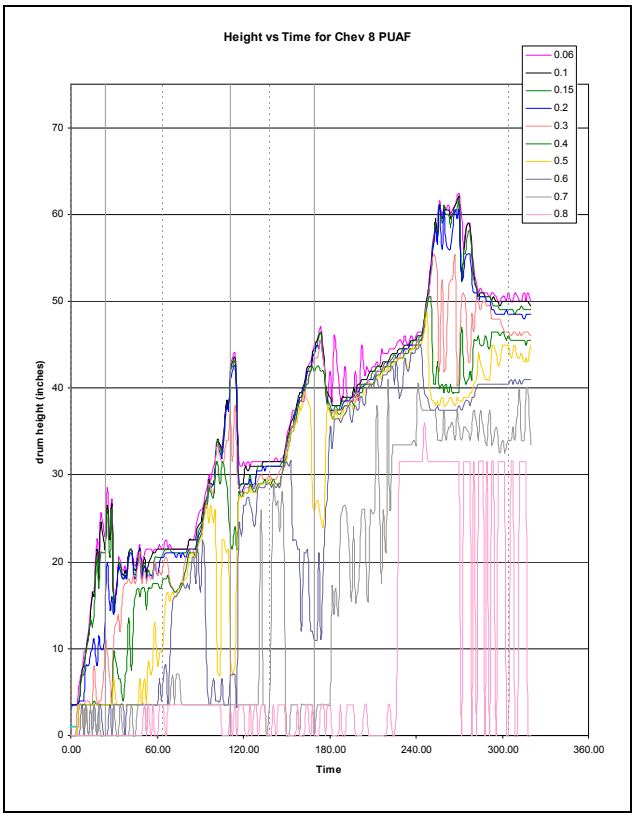

Figure 174 – Chevron Anti-Foaming runs – Height vs. Time (CHEV 8 PUAF)

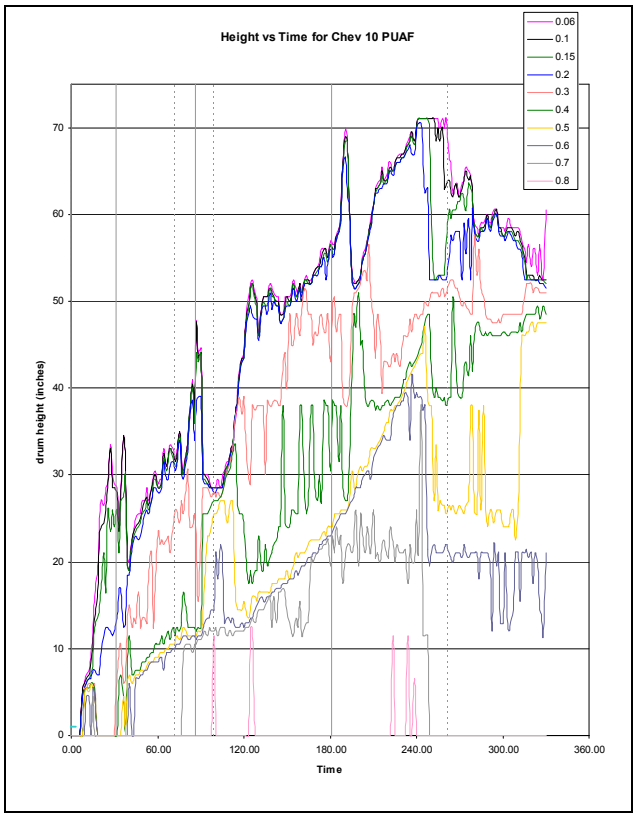

Figure 175 – Chevron Anti-Foaming Runs – Height vs. Time (CHEV 10 PUAF)

(iv) Citgo resid:

The Citgo resid made agglomerated shot coke with some portions of BB's at either high temperatures or higher feed rate(superficial velocities >= 0.15 ft/s). The Citgo resid also made sponge coke at low temperature and lower feed rate runs. This kind of mixture of sponge and shot coke formations might be because it is a naphthenic structured resid.

Sponge vs. shot coke:

The CIT 8 run made 100% sponge coke while CIT 11 made 100% agglomerated shot coke. Figure 176 and Figure 177 show how the densities of sponge coke and shot coke vary during a test run.

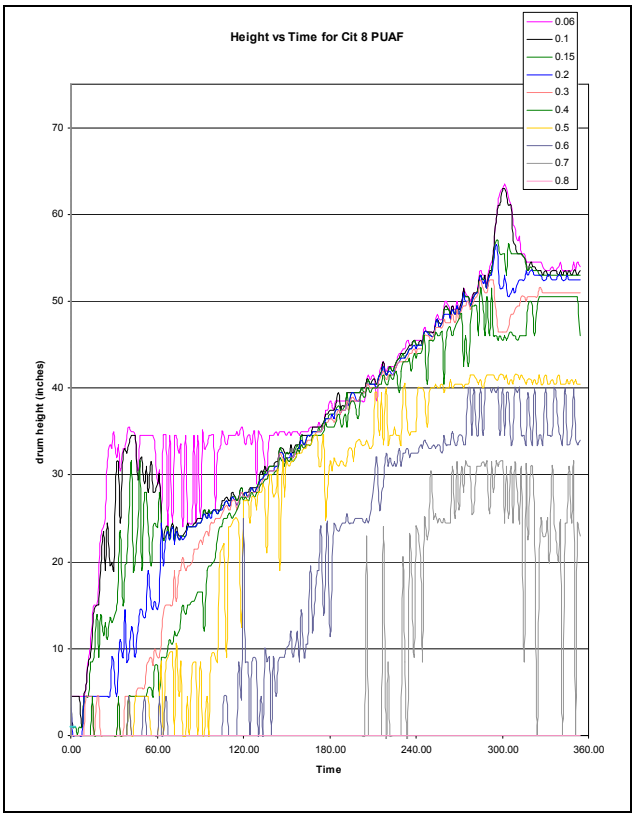

Figure 176 – Citgo Anti-Foaming runs – Height vs. Time (Sponge Coke from CIT 8 PUAF)

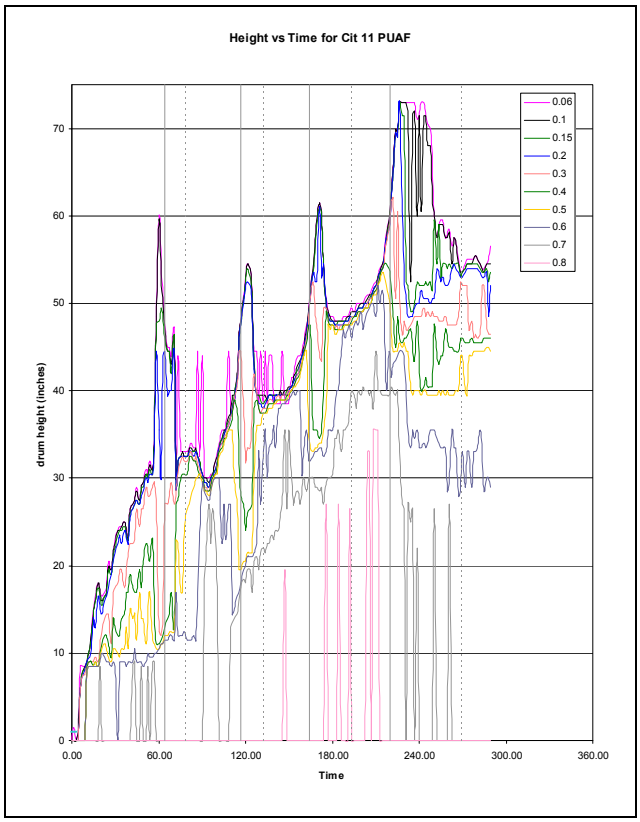

Figure 177 – Citgo Anti-Foaming runs – Height vs. Time (Aggl Coke from CIT 11 PUAF)

Sponge coke has a porous structure that allows the coke height to continually grow as a function of time, which is shown in Figure 176 where the higher density traces followed the lower density traces (slope is nearly same). Shot coke has a tendency to agglomerate in the drum, which is shown by Figure 177 where the lower density traces, once they reach a certain height, stay there allowing the coke below to become denser. Note though that the agglomerated shot was formed after each antifoam injection. Also for this run, when the resid breaks through this agglomerated portion, the coke height begins to grow again.

Effect of operating Conditions on Coke Morphology:

Temperature:

At low pressure (15 psig) and low flowrate (2400 g/hr) an increase in temperature from 900°F to 930°F increased the % of both agglomerated shot and BB's. At low pressure and higher feed rates (15 psig and 3600 g/hr respectively), an increased in temperature increases the % of BB's. At a higher pressure (40 psig) the coke morphology didn't change with an increase in temperature; however the morphology changed from sponge coke to shot coke when the feed rate was increased from 2400 to 3600 g/hr.

Both foam and liquid layers decreased with with increase of temperature at 15 psig and they did not change much with increase in temperature at 40 psig.

Pressure:

At lower feed rates (2400 g/hr) and lower temperature (900°F) where sponge coke is also formed, an increase in pressure from 15 psig to 40 psig reduced the % of agglomerated shot formed, increasing the sponge coke %. At higher temperature (930°F) run times are not equal to make any observation. The higher feed rate (3600 g/hr) runs foamed badly and the run times were shorter to make any comparisons.

Feed rate:

Increasing the feed rate makes more shot coke for any given set of temperature and pressure.

Effect of operating conditions on Density of coke:

An increase in bulk density was seen with an increase in temperature except for one run which was less than 3 hrs. An increase in density was seen with an increase in pressure for all operating conditions. Feed rate change didn't have a specific trend on the density of coke formed.

Foaming tendencies for Citgo Resid:

At low superficial velocities when Citgo resid made sponge coke, an increase in temperature decresed foaming and temperarute appeared to be the more dominant variable. When test runs having feedrate of 3600 gm/hr were considered, Cit 9 and Cit 11 runs were the worst foamers. Figure 174 and Figure 175 show the Height vs. Time plots for given density for the Cit 9 and Cit 11 runs respectively. The lower temperature runs were the worst foamers when the Citgo resid was used. Also of the two runs considered below higher pressure run was worst foamer. Pressure appears to be dominant variable for Citgo resid.

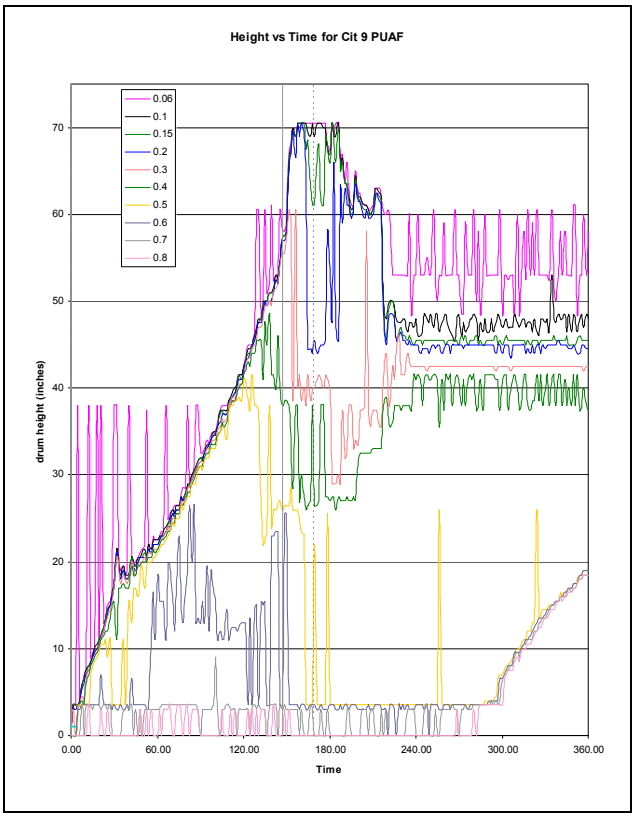

Figure 178 – Citgo Anti-Foaming runs – Height vs. Time (Cit 9 PUAF)

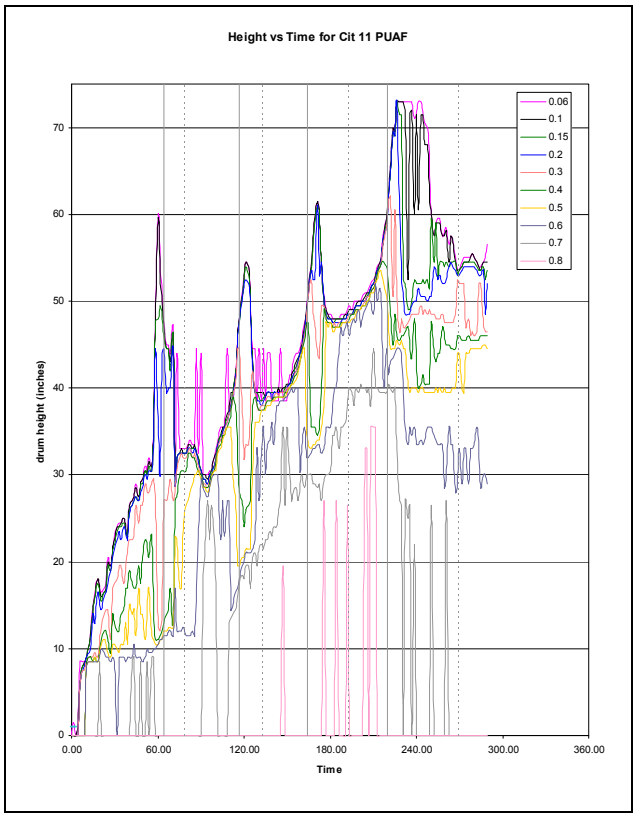

Figure 179 – Citgo Anti-Foaming Runs – Height vs. Time (Cit 11 PUAF)

9. Conclusions

Foam Densities typically have values less than 0.2gm/cc. However, values as high as 0.35 gm/co were observed. Feedline injection was found to be as effective as overhead injection. An optimum antifoam concentration exists.

Foam and bubbly liquid layers were quantifiable. Little or no foam layer was observed in the Equilon run. The Chevron runs had foam layers 7 to 10" thick while the Petrobras runs had foam layers as thick as 20". The time to rise using the 600,000 cSt antifoam was a lot longer when the 100,000 cSt antifoam was used. This observation provides support that at equivalent concentrations, fewer injections, or less antifoam. Increasing concentrations of antifoam were found to increase coke density.

Paraffinic structured resids made Sponge Coke, Aromatic resids made Shot coke, Napthenic resids made mixture of shot and sponge coke and Intermediate structured resids made mixture of agglomerated and large BB's. On a resid basis, the Petrobras and Marathon resids made completely sponge coke irrespective of the operating conditions, the Suncor resid made shot coke irrespective of operating conditions, while the Equilon resid made mix of sponge, agglomerated shot and different sized BB's.

Petrobras and Marathon resids which made pure sponge coke have nearly same liquid layer and foam layer heights for a given set of temperature and pressure. With an increase in temperature the liquid layer decreased for the resids which make sponge coke. The rate of coke growth (dh/dt) with an increase in feedrate, was found to be comparable for the Petrobras (0.09-0.16 in/min) and Marathon resids (0.1-0.13). Foaming tendencies decreased with increase in temperature for pure sponge coke making resids (Petrobras and Marathon). Temperature appears to be the more dominant variable than pressure for foaming in case of sponge making resids. For both Petrobras and Marathon resids bulk density ranged from 0.6 – 0.8 gm/cc and gamma density ranged from 0.45 -0.65 gm/cc approximately. The average difference between Bulk and gamma densities for Petrobras and Marathon resids are 0.13 gm/cc and 0.16 gm/cc respectively. The density (both bulk and gamma densities) increased with an increase in temperature and pressure for sponge coke making resids.

Shot coke is formed because of more asphaltenes and turbulent conditions. An increase in temperature and/or superficial velocity increases the shot coke formation while an increase in pressure decreases shot coke formation. Agglomerated shot coke was noticed to form when it took longer to attain the desired operating temperature or after antifoam was injected. An increase in either the amount or concentration of antifoam caused an increase in percentage of BB's formed for the Suncor resid. For resids which made only shot coke (Suncor and Equilon) the foam layer increased with an increase in temperature at 15 psig and decreased with an increase in temperature at 40 psig. An increase in pressure increased foaming for both resids and pressure appears to be dominant variable for shot coke making resids. The liquid layer did not change much for the Suncor resid.

Two of the resids, Chevron and Citgo, made variable morphologies. Both resids produced more sponge coke at low superficial velocities but more shot coke at higher superficial velocities. Foam and liquid layers were a function of operating conditions as was the density.

68 tests have been conducted with the pilot unit using the in-house resids. Studies were first conducted to determine the extent of antifoam carrying over during overhead injection using water. These studies indicated that some of the antifoam was carried over into the liquids when injected from overhead. However, the very low recovery of silicon indicates that most of the injected antifoam remained in the drum. More antifoam would be carried over during the coking process because the superficial velocity of the HC vapor is larger. Studies were also conducted to establish what was causing the fluctuations in the fluid in the furnace tube. By recording temperatures as a function of distance from coil inlet to outlet, it was

hypothesized that an increase in vaporization of the fluid causes more irregularities in the flow pattern and temperature profile. When both recycle and antifoam were injected, it was noticed that the furnace had to be fired harder to achieve the desired operating temperature as compared to when only resid is injected.

Antifoam injection studies were run using both a low viscosity 100,000 cSt (0.3 ml AF/ 70 ml diesel) and a high viscosity 600,000 cSt (0.75 ml AF/ 70 ml diesel) antifoam. In some of the tests, antifoam was injected continuously (2 min ON and 8 min OFF) while in others it was injected on as-needed basis (observation of foam determines the injection time). Antifoams were injected in the drum overhead, through the feedline, and mixed with the resid in the feed bucket. During the experiments, temperatures at the inlet to furnace coil, the fluid temperature, the furnace skin temperature, the overhead temperature and the temperature inside the coke drum near the bottom were measured. From test to test, variations were seen in the overhead temperature and the furnace coil temperatures. In general, injecting antifoam on a continuous basis reduces the overhead temperature, while injecting antifoam in the feedline requires the furnace to be fired harder to get the fluid to the desired temperature.

A partitioning study was conducted on the samples taken during the pilot unit tests in which oil and water samples were collected from the lights and heavies tank. More analytical results are needed for silicon in the liquid products but the tentative conclusion is that silicon from the antifoam injected overhead tends to carry over to the hydrocarbon liquids, while the silicon injected from the feedline tends to break down and end up in the decant water.

A detailed liquid analyses study was initiated in June 2003. This study is looking at 160 liquid samples generated in the first phase of study and those currently being generated in the continuation phase. The samples are being distilled and simulated distillation, detailed hydrocarbon analyses and sulfur analyses are run on each cut. The overall outcome of the study is to be able to predict what type of PiONA component, sulfur, etc. would be dominant at a certain temperature and pressure, and how a change in the temperature and pressure would affect its production.

Foaming runs were begun in June 2002. The first series of foaming tests were conducted using the Suncor resid to establish the differences between overhead, feed and feed line injection. The second series of tests were run using six in-house resids to gain an understanding of how pressure and temperature affect foaming as well as the impact of feed rate. This data was integrated with the results obtained during the first phase of study.

In general, the lower the temperature and pressure, and the higher the feedrate, the worse the foaming. This was especially true for the Marathon, Petrobras, and Chevron resid. However, Equilon & Citgo foamed worse at higher pressure.

Nine antifoam optimization tests using the resid from Petrobras showed that injection of higher concentrations of antifoam/unit of carrier uses more antifoam than is required to effectively control foaming; however, the time between injection is longer and a denser coke is made. When large quantities of diesel are injected as the carrier, foaming appeared to be enhanced. Foaming resulted in uniform temperature profiles in the drum and when the temperatures in the drum were fairly uniform throughout, pure shot or a uniform sponge was made.

Continuous overhead and feed line injection are effective at controlling foaming throughout the run. Feed line injection with an antifoam/carrier concentration of 0.3/70 was only effective at controlling foaming on a continuous basis for the first 80 minutes whereas the 30/70 concentration was effective throughout the run. The 0.3/70 mixture was also the optimum AF concentration for controlling foaming overhead. It was also found that when 100,000 cSt and 600,000 cSt antifoams are used at equivalent concentrations, foam control is comparable; however, the time to rise was longer for the 600,000 cSt antifoam..

Two approaches were developed to quantify foam, liquid and coke heights. These approaches are being compared to test data to determine which technique, or a combination the techniques, works best.

10. Future Work

Work on processing the antifoam runs will continue to determine the coke bubbly liquid and foam layers. During some of the continuous injection runs, foam suppression was observed for significant amounts of time. Similar tests will be conducted on other resids for the resids that exhibit extended suppression additional tests with recycle and at refinery conditions will continue. As additional runs are made, the temperature data will be processed to determine the effect of antifoam on overhead and coil temperature and the foaming tendencies based on resid characteristics.

F. FOAMING MODEL

1. Theoretical Discussion

a) *Foams and Foam Model Development*

Foams are agglomerations of gas bubbles separated from each other by thin liquid films. They belong to the colloidal system comprising of gas dispersed in liquid. A very large majority of industrial processes require the injection of materials known as antifoams to inhibit the foam growth because the foam formation and continuous growth is sometimes undesirable in chemical processes leading to fouling in equipment. Antifoams such as silica particles dispersed in carrier oil such as mineral oil are important from the standpoint of controlling and inhibiting foam. Consequently foam models that can predict how the foam-antifoam interaction will affect the foam is going to be very important as it will provide insight to rapid foam control whenever required and also optimum antifoam requirements for doing so. Presented here is the theory of a foam model that predicts foam volumes both in the presence and absence of antifoam emulsions.

b) *Experimental Setup*

A common laboratory procedure for evaluation of antifoam emulsions is the dynamic foam rise test. Generally the aqueous surfactant is kept in a graduated cylinder and gas bubbles are produced by passing air or nitrogen through a frit at the bottom of the cylinder. In the experimental setup described in the literature [2], the foaming solution comprised of SDS (sodium dodecyl sulfate) in distilled water. The commercial antifoams that were used consisted of hydrophobic silica dispersed in silicone oil and the material was emulsified with a mixture of nonionic surfactants. The antifoam emulsion was weighed in a freshly prepared SDS solution that was added to a graduated cylinder. Humidified nitrogen was introduced through an ace glass pore, ASTM 25-50 μm glass frit attached to the glass tube and suspended down the center of the cylinder. The gas flow rate was controlled by a Matheson 8420 mass flow controller.

c) *Description of the Model*

The model foam conceptualized here consisted of the elements shown in Figure 180. The gas entered the liquid phase in the form of “primary bubbles”. Also the liquid phase comprised of the antifoam emulsion droplets. The foam phase was present above the liquid phase. The primary bubbles in the liquid phase were assumed to collect the antifoam emulsion droplets by heterocoagulation. On entering the foam phase these primary bubbles were assumed to coalesce with neighboring primary bubbles leading to the formation of “secondary bubbles”. The model requires the following input parameters: R_P, R_S, R_E, V, G, Q for predicting the foam volumes.

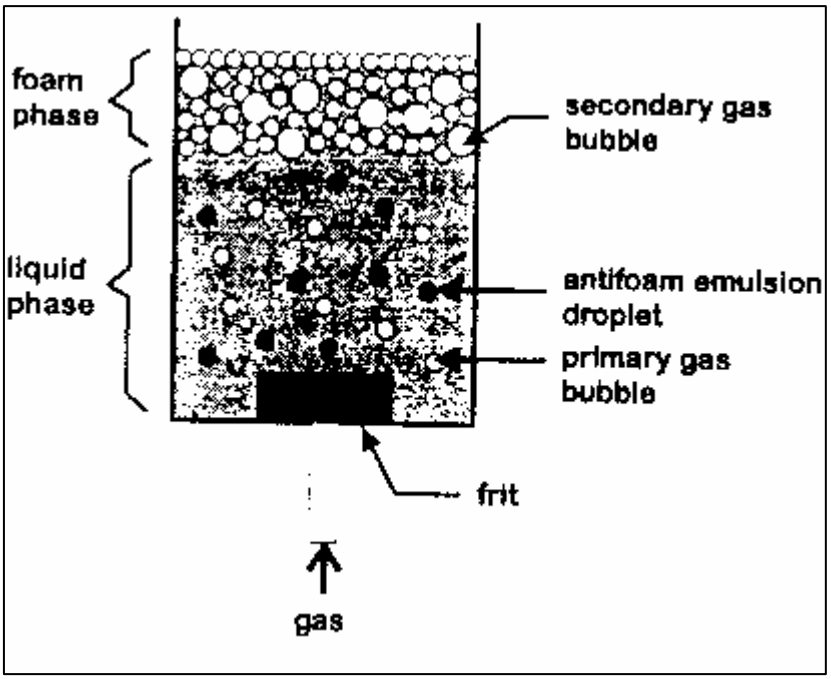

Figure 180 - Schematic Diagram showing the different elements of the Model

Primary bubble radius is given by R_P, Secondary bubble radius is given by R_S, the antifoam emulsion droplet radius is given by R_E, V stands for the total volume of liquid phase, G stands for the volume fraction of gas in the liquid phase and Q stands for the volumetric flow of gas into the cylinder. According to the literature [1], the model uses the values of the input parameters described above to calculate certain quantities eventually leading to the calculation of the number of antifoam emulsion droplets (δ) and the rate of foam rise or fall given by S(t). Once S(t) and δ are calculated, the expression for S(t) which is a function of time (t) is substituted in the integral $\int S(t)dt$ and integrated for the time period required to get the foam volumes for different times (t). The time period chosen for doing the integrations will be explained in a later portion of this report. The quantities that are calculated, the different equations involved and the methodology for doing the model calculations are outlined as follows:

The number concentration of primary bubbles in the liquid phase is given by

$$B = 3G/4\Pi R_P^3$$

Once B is calculated, utilizing the input parameters R_P, R_S, V, g (which is the total number of groups in the liquid phase can be calculated) by

$$g = R_P^3 BV/R_S^3$$

Alternately, g can be interpreted as the number of primary bubbles divided by the number of primary bubbles required to produce a secondary bubble.

The concentration of antifoam emulsion droplets at time t is given by

$$E(t) = E_O \exp(-K_S f B t)$$

where

E_O = initial antifoam concentration,

Factor $K_S = (R_P + R_E)[(1/R_P) + (1/R_E)]2kT/3\acute{\eta}$

T = temperature

k = Boltzmann constant

$\acute{\eta}$ = viscosity of the antifoam

f = adjustable coagulation efficiency factor cited in the literature [1] (a value of 20,000 has been cited)

Thus after the calculation of the factor K_S from model input information and run operating conditions and the choosing of a suitable value for the adjustable factor f, the concentration of antifoam emulsion droplets E(t) can be determined for various times(t). The calculation of the initial antifoam concentration E_O from existing antifoam injection data will be explained later in the report. The average residence time of bubbles in the liquid phase, (z) is given by z = GV/Q. The z value determined from model inputs G, V, Q go into the calculation of the number of antifoam emulsion droplets (δ) that heterocoagulate with the primary bubbles.

The number of antifoam emulsion droplets δ according to literature, is given by

$$\delta = [E(t-z) - E(t)]V$$

E(t-z) is basically the antifoam emulsion concentration at time (t-z) and hence can be determined by replacing t by (t-z) in the expression for E(t) outlined earlier. Hence E(t-z) is given by $E(t-z) = E_O \exp[-K_S fB(t-z)]$ where E_O = initial antifoam concentration as before. After the successful calculation of δ, utilizing the value of g determined previously, the rate of foam rise or fall, S(t) can be calculated as

$S(t) = [1-1/g]^{\delta}$. The foam volume V(t) is given by $V(t) = \int S(t)dt$ integrated for the particular time period. The choice for the limits of the integral evaluated is explained in the latter portion of the report. It has to be remembered while calculating S(t) that S(t) is a function of time (t) as because the expression for S(t) involves δ which itself is a function of time (t). Thus as can be seen, the model tries to predict what the foam volume is going to be at different times at different run conditions. The following flowchart explains the sequence in which the different quantities are calculated leading to the final determination of foam volumes for various times (t):

LITERATURE CITED:

[1] "A *model of foam growth in the presence of antifoam emulsion*" by Robert Pelton, 1996.

[2] "*A theory for foam growth kinetics in the presence of antifoam emulsion*" by R.H. Pelton, E.D. Goddard, 1986.

2. Preliminary Predictive Results

The calculations were done for CIT 9, CIT 11 and PETR 4 runs and the following plots show the comparison between the Model predicted and the Actual foam volumes obtained from run data:

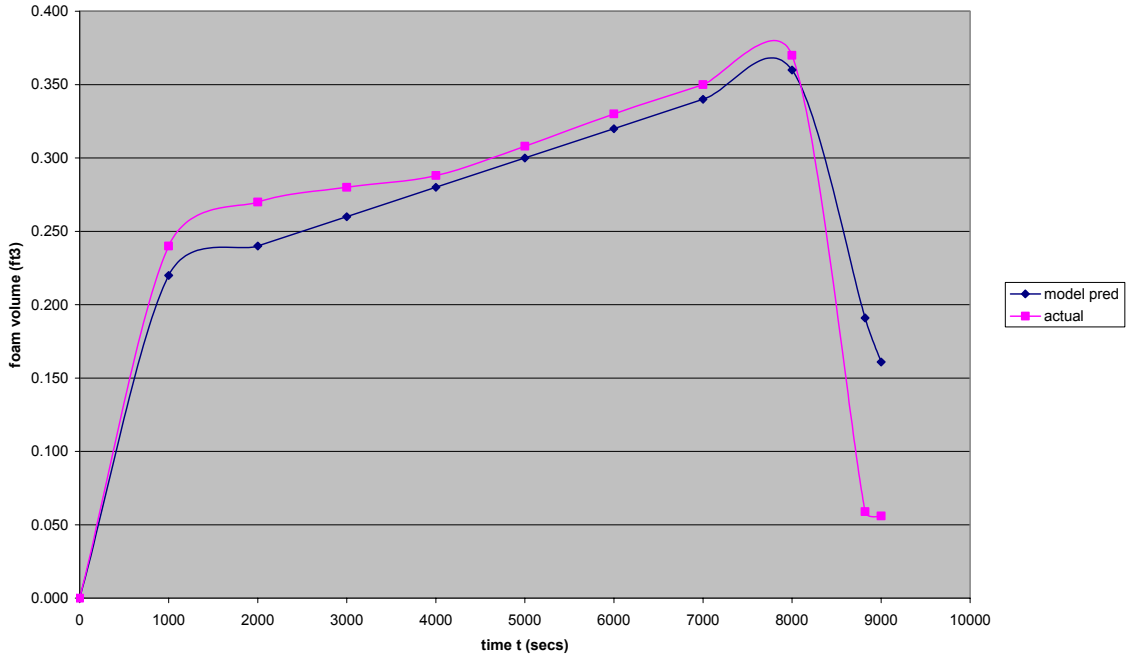

Figure 181 - Comparison between foam volumes, model predicted and actual run data for CIT 9

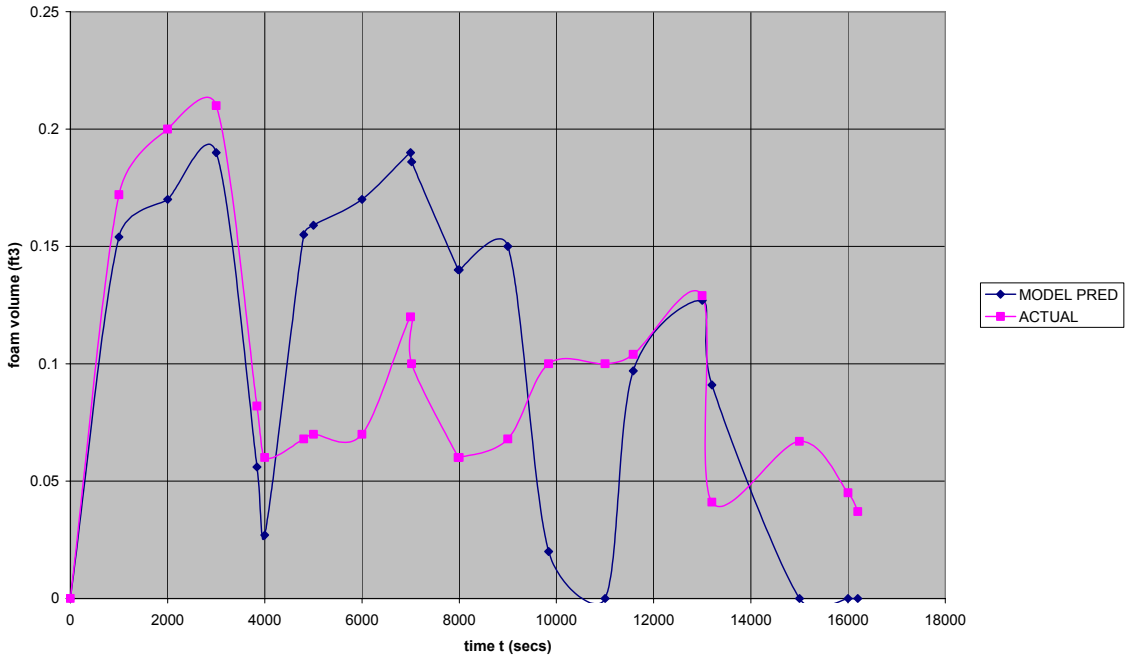

Figure 182 - Comparison between foam volumes, model predicted and actual run data for CIT 11

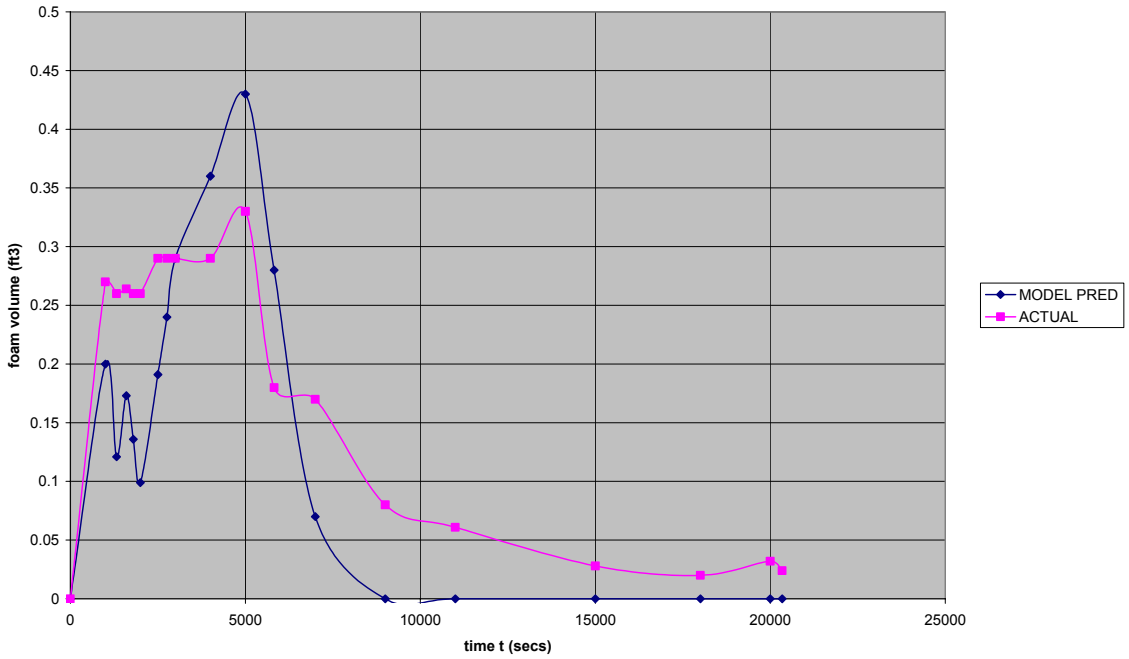

Figure 183 - Comparison between foam volumes, model predicted and actual run data for PETR 4

The foam model, in general, predicts a foam volume rise when there is no antifoam interaction and a foam volume collapse when there is antifoam interaction.

Antifoam interaction between the foam and the antifoam starts when the antifoam is injected into the system. The antifoam is basically responsible for collapsing the foam after its initial build up.

3. Conclusions

A foaming model was developed based on work by Pelton and Goddard. The model predicts foam volumes both in the presence and absence of antifoam emulsions. The model was tested on three data sets, Citgo 9, Citgo 11 and Petrobras 4. The predictions are very good for the 3 runs investigated. The model, apart from predicting foam volumes for various times during the run, predicts the foam collapse taking place at antifoam injection and thereafter. The model is able to predict possible foam over tendencies for particular runs like Petrobras 4 and in general predicts a foam volume increase before an antifoam injection.

4. Future Work

In order to match the actual run foam volumes with the model predicted ones and to increase the efficacy of the foam model, three areas require further study. The first will examine the effect of changing some of the adjustable input parameters like bubble radius on the results for the foam volumes, the second one will result in having a better understanding of how the antifoam is interacting with the foam and helping deplete the foam, while the third will introduce an antifoam efficiency into the model (%) that will help in understanding the efficiency of the antifoam being used for the respective runs.

G. PROCESS STUDIES

1. Recycle Test Runs

Studies using recycle, Suncor runs 14, 15 (5% RC), 16 (10% RC) and SUNC 17 (15% RC- industry conditions), were carried out in the month of September/October 2003. The Suncor 14 run was carried out at a temperature of 900 ^{o}F, a pressure of 15 psig and a feed rate of 2400 gm/hr. Suncor 14 used as-needed overhead injection of 100,000 cSt (0.3/70) antifoam. The Suncor 15 run which contained 5% recycle in the feed was carried out at a temperature of 900 ^{o}F, a pressure of 15 psig and a feed rate of 2400 gm/hr. Figure 184 shows the comparison of temperature profiles for the Suncor 14 and 15 runs. As can be seen, Suncor 15 required more heat input to the feedline and the overhead temperature was comparatively warmer. Suncor 14 required less heat input to the feedline and had a cooler overhead temperature. The Suncor 16 run, which contained 10% recycle in the feed, was carried out at a temperature of 900 ^{o}F, a pressure of 15 psig and a feed rate of 2400 gm/hr. **Error! Reference source not found.** shows the comparison of temperature profiles for Suncor 14 and 16 runs. As can be seen, Suncor 16 required around 40-50 degrees of more heat input to the feedline compared to Suncor 14. The overhead temperature for Suncor 16 was higher compared to Suncor 14. SUNC 17 (15 % RC) was run at industry conditions, at a temperature of 928^{o}F, and a pressure of 38 psig; however a feed rate of only 2400 gm/hr was used. **Error! Reference source not found.** shows the comparison of temperature profiles for Suncor 14 and 17 runs. As can be seen, SUNC 17 required around 50-60 degrees more heat input to the feedline compared to SUNC 14. Note though that the fluid temperature was 28° F higher for SUNC 17 compared to SUNC 14. SUNC 14 made a void of 5 inches in the drum whereas SUNC 15 (5% RC), SUNC 16 (10% RC) and SUNC 17 (15% RC) runs showed good steam strip behavior. Comparison of Suncor runs 14, 15, 16 and 17 show that as the amount of recycle in the feed increases, the heat input to the furnace increases to maintain the same operating temperature of 900 ^{o}F as shown in Figure 185. Under the same conditions of pressure and temperature, a less dense coke was also made when recycle was used. The SUNC 17 (15% RC) run was made at industry conditions, that is, at a temperature of 928 ^{o}F and a pressure of 38 psig. The feed rate was 2400 gm/hr. In this run, the coke formed at the bottom of the drum was denser and the morphology began to change. The lower part of the drum was a mix of what looked like sponge and agglomerated shot. Another run is planned under the same conditions, but at a higher feed rate of 3600gm/hr. It is postulated that the higher feed rate will have an additional effect on the morphology, possibly changing more of it to sponge. Significant stripping was observed in the run without recycle. A void was also produced. These effects were not observed in the runs where recycle was used.

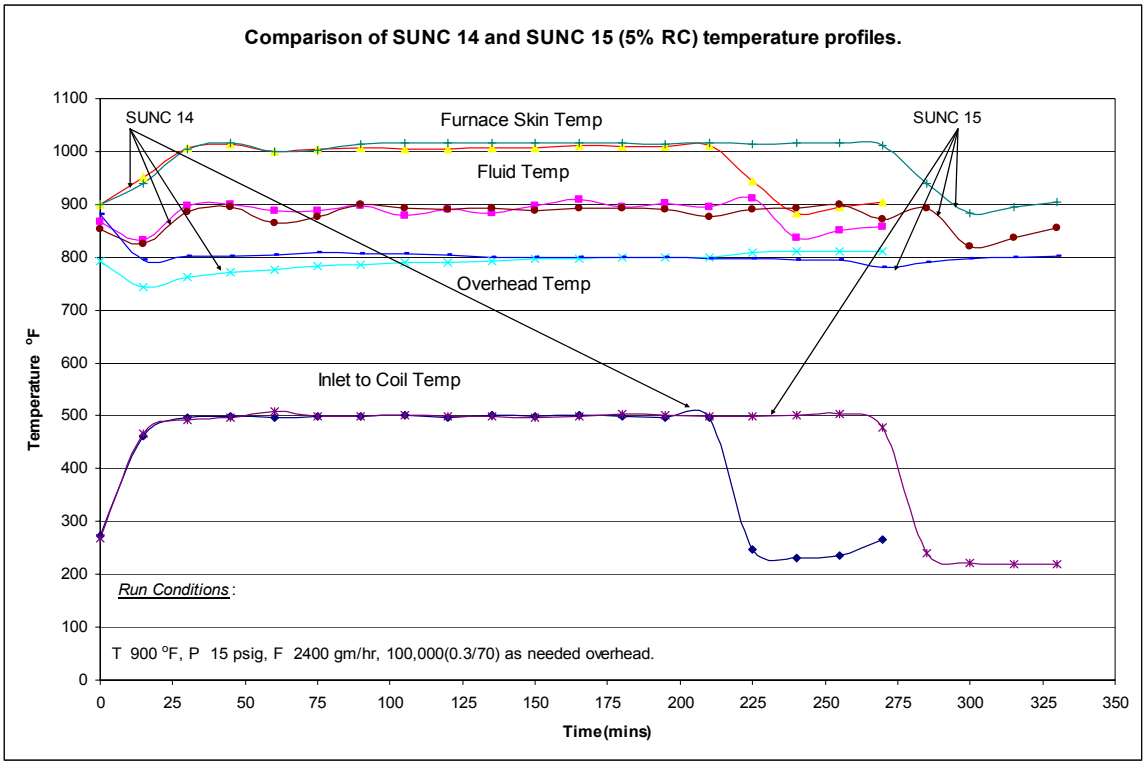

Figure 184: Temperature profiles for SUNC 14 PUAFI and SUNC 15 (5% RC) PUAFI runs.

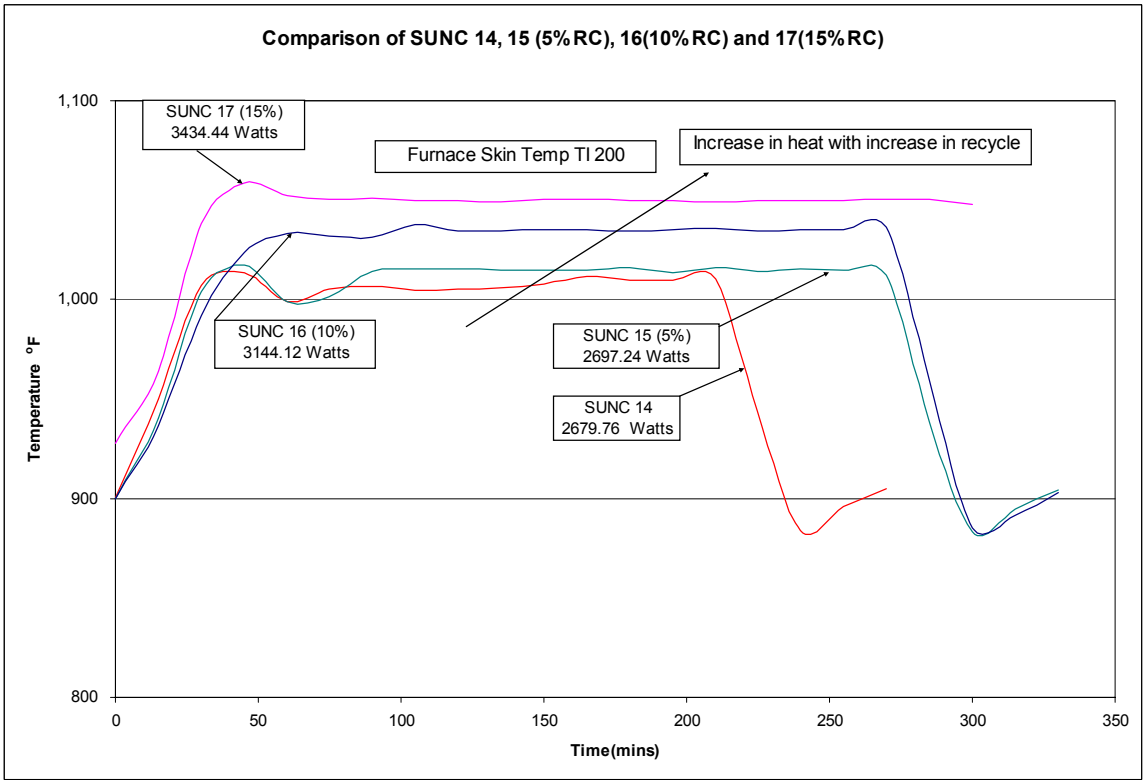

Figure 185: Furnace Skin Temperature for SUNC 14, 15, 16 and 17.

a) *Conclusions:*

Preliminary observation suggests that overhead injection of antifoam lowers the overhead temperature. Further observation indicates that lower overhead temperature results in more material being stripped from the drum because of the slower reactions taking place. Feedline injection requires more heat input to the feedline to maintain equivalent fluid temperatures compared to the overhead injection of antifoam. The coking time for a particular run can be affected by the foaming characteristics of that particular resid. If the foam is too high in the drum, it affects the run length as there is a possibility of overhead lines getting clogged with time. Foam, if not controlled within a reasonable amount of time, is hard to control during the rest of the run. During antifoam injection a sudden rise of foam is observed. This property can be attributed to diesel flashing inside the coker drum. It is seen that the runs using higher viscosity 600,000 cSt (0.75/70) antifoam take longer for the foam to re-appear compared to runs using the lower viscosity 100,000 cSt (0.3/70) antifoam. Steam strip plots for Equilon indicate that the reduced run temperature strips the unreacted resid out of the drum. In terms of minimizing the loss of mass in the coker drum during steam strip, it is observed that asphalitic (Equilon) resids operate best at a temperature of 930 ^{o}F and a pressure of 40 psig whereas paraffinic (Petrobras) resids operated well under all conditions tested. With the addition of recycle to the feed, it is observed that the heat input requirement is higher compared to runs with no recycle.

b) *Future Work:*

It has been observed that during runs with continuous injection of antifoam, there is a suppression of foam for a substantial amount of time after an hour into the run. Hence injecting antifoam during this time does not serve the purpose. Thus a revised method will be designed for continuous injection of antifoam. Equilon runs will be carried out at a temperature of 930 ^{o}F and a pressure of 40 psig to observe the steam strip behavior. Further studies will be conducted on the effect of antifoam on overhead and coil temperatures and the foaming tendencies based on resid characteristics.

2. Effect of Diesel on Overhead Temperature

Temperature profiles for the pilot unit typically show a drop in the overhead temperature when antifoam is introduced at the top of the drum. The question is whether this temperature drop is due to the foam being knocked back, displacing the hot resid back to the bottom of the drum, or to quenching from the diesel carrier added at the top of the drum.

Figure 186 through Figure 191 show the temperature profiles at the top and bottom of the drum for runs EQ 4 PUAF, EQ 7 PUAF, and EQ 8 PUAF. All three runs were at 900°F, 15 psig, and 3600 g/hr. Run EQU 4 had no antifoam injection, while EQU 7 had intermittent antifoam injection (0.3/70 concentration, 100,000 cSt) and EQU 8 had continuous injection (0.3/70 concentration, 100,000 cSt). Both the runs with antifoam injection showed a significant temperature reduction at the top of the drum as compared to the case with no antifoam injection, whereas the temperature profile at the bottom of the drum looked nearly the same in every case.

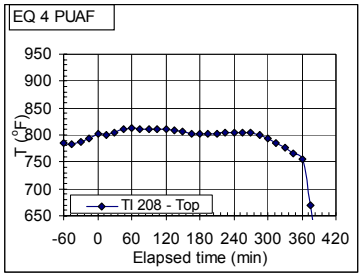

Figure 186 - Temperature vs. time at drum top, run EQ4 PUAF

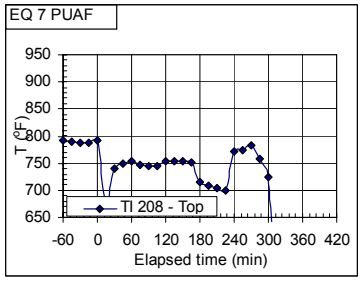

Figure 187 - Temperature vs. time at drum top, run EQ7 PUAF

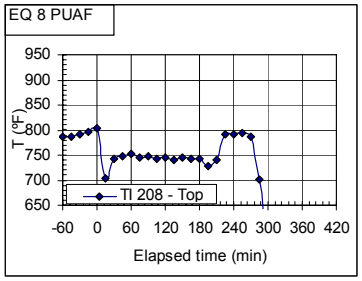

Figure 188 - Temperature vs. time at drum top, run EQ8 PUAF

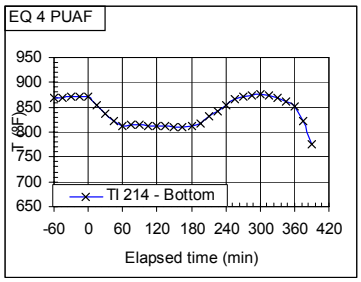

Figure 189 - Temperature vs. time at drum bottom, run EQ4 PUAF

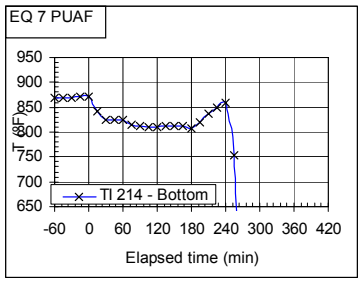

Figure 190 - Temperature vs. time at drum bottom, run EQ7 PUAF

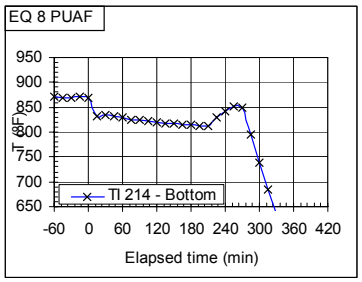

Figure 191 - Temperature vs. time at drum bottom, run EQ8 PUAF

Run EQU 7 had a total of 66 g of diesel added with the antifoam, while run EQU 8 had a total of 95 g of diesel added with the antifoam. Assuming that the diesel has a mean heat of vaporization of 180 Btu/lb, an average boiling temperature of 540°F, and a heat capacity of 0.65 Btu/lb/°F, a rough estimate can be made of the cooling provided by the diesel injection. The calculated cooling for run EQU 7 is ~70

Btu and the cooling for run EQU 8 is ~100 Btu. This amount of cooling, if introduced instantaneously to the bed, could lower the bed temperature by as much as 15-20(F (assuming a heat capacity for the bed material of 0.5 Btu/lb/(F). In the case of run EQU 8, where this material was introduced slowly over 3 hours, the bed temperature effect from the diesel ought to be negligible. For run EQU 7, however, the antifoam injections were made in several large doses. Table 68 shows the antifoam injection rates for EQU 7 along with the estimated temperature drop, based on the above assumptions and the estimated bed mass as a function of time. It can be seen that the first antifoam injection causes a significant temperature drop, because the mass of the material in the bed is rather small. Subsequent antifoam injections have much smaller effects. Figure 187 shows the large temperature drop at the top of the bed from the first antifoam injection, followed by a temperature recovery and then a relatively stable profile. The results are consistent with this analysis, although it should be noted that the initial temperature drop for run EQU 7 (~100°F) is significantly larger than predicted. It can be concluded that most of the temperature drop observed following antifoam addition is probably the result of the hot foam moving to the bottom of the bed, although the initial antifoam addition probably contributes some toward this cooling due the thermal effect of the diesel carrier addition.

Table 68 - Bed cooling for run EQU 7 PUAF

Run Time (hrs)	Total Inj. Amt. (g)	diesel injected (lb)	est. cooling (Btu)	estimated bed temp. drop (F)
0:33	23.2	0.051	24.8	28
1:38	8.6	0.019	9.2	4
2:01	17.4	0.038	18.5	6
2:24	8.6	0.019	9.2	2
2:37	8.6	0.019	9.2	2

3. Steam Stripping Studies

Gamma densitometer traces before and after steam stripping show the loss of mass from the coke bed due to the stripping steam. This loss of mass is due to the volatile matter that is stripped from the coke. Figure 192 show the gamma densitometer trace for run SUN 6 PUAF. It can be seen that there is a notable loss of material, mostly between 6 and 12 inches bed height, just below the layer of agglomerated shot at the top of the bed. This loss of material resulted in the bed slumping by approximately 2 inches. For most runs where shot agglomeration occurred, the loss of material from steam stripping occurs primarily below the agglomerated shot section. For runs that made sponge coke, the loss of material is often more uniformly distributed, as illustrated in Figure 193 for run PETR 5 PUAF. Note that this run also showed some slumping of the bed following steam stripping. On the other hand, run PETR 9 PUAF, shown in Figure 194, had significant bed compaction from steam stripping, resulting in the bed slumping by nearly 5 inches. This slumping actually caused an increase in the coke bed density, mostly at the bottom of the bed but to a lesser extent in the middle of the bed (between 30 and 35 inches bed height). There are also some runs such as CIT 7 PUAF, shown in **Error! Reference source not found.**, which show some loss of material but no slumping of the bed, and runs such as SUN 1 PUAF, shown in **Error! Reference source not found.**, which show very little loss of material from steam stripping.

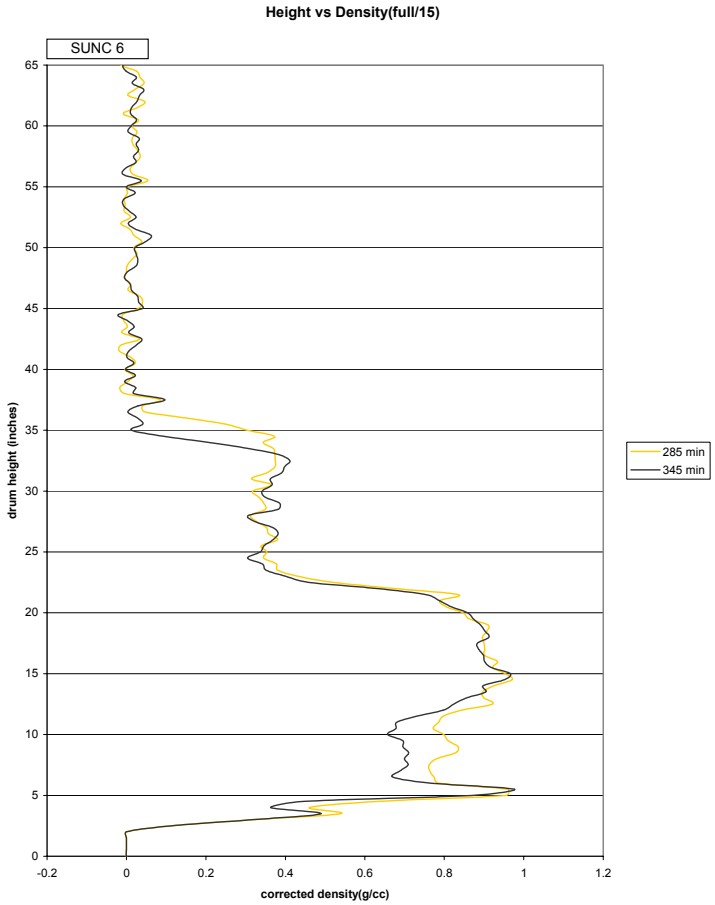

Figure 192 - Gamma densitometer traces for run SUN 6 PUAF before and after steam stripping

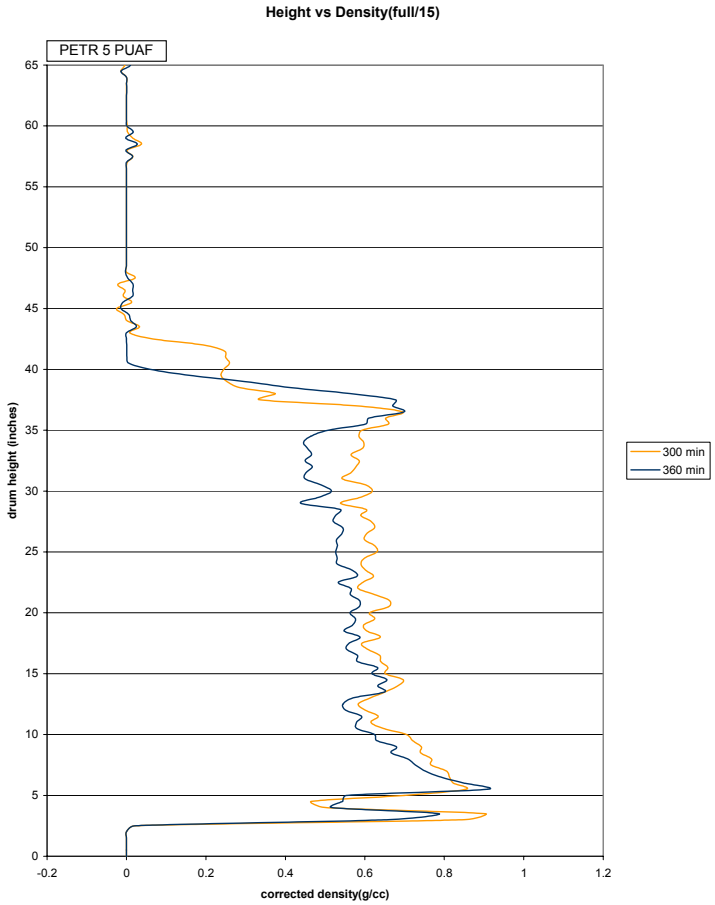

Figure 193 - Gamma densitometer traces for run PETR 5 PUAF before and after steam stripping

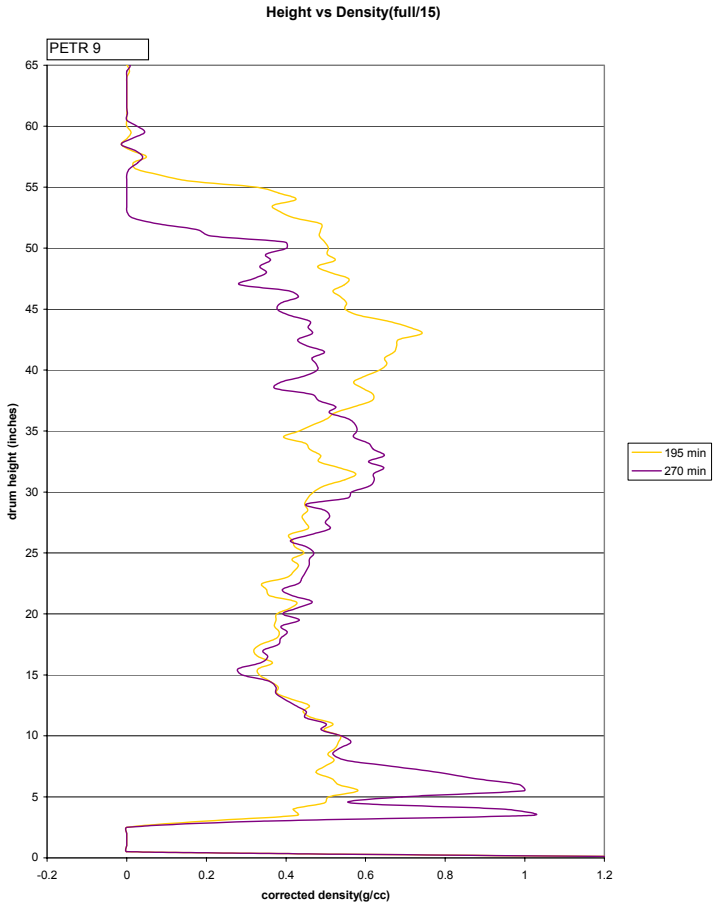

Figure 194 - Gamma densitometer traces for run PETR 9 PUAF before and after steam stripping

A definite tendency toward more material loss for lower temperatures and higher flow rates was observed.

Gamma densitometer plots illustrating the steam stripping effects for runs PETR 8-10 and EQU 7-8 are shown in the following figures. The Equilon gamma scans shown in Figure 197 and **Error! Reference source not found.** show that a great deal of material has been stripped out of the bed by steam stripping. These scans can be compared to EQU 4 PUAF, shown in **Error! Reference source not found.**; all three runs were made at 900°F, 15 psig, and 3600 g/hr. The loss of material is somewhat less for EQU4. This can be attributed to the higher temperature at the top of the bed for this run, due to the absence of antifoam usage, as discussed above in Figure 186 to Figure 188. Apparently the low overhead temperatures (~750°F) experienced in runs EQU 7 & 8 did not result in complete conversion to coke for these reaction times (2.75 hrs for EQU 7 and 3 hrs for EQU 8).

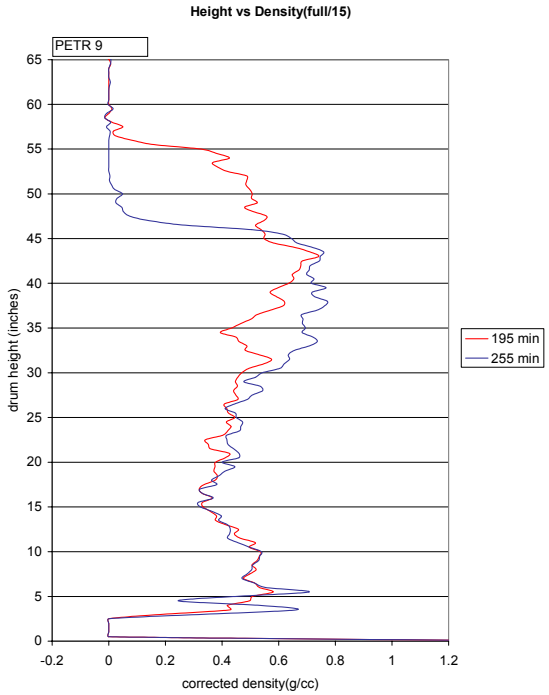

Figure 195 - Gamma densitometer traces for run PETR 9 PUAF before and after steam stripping

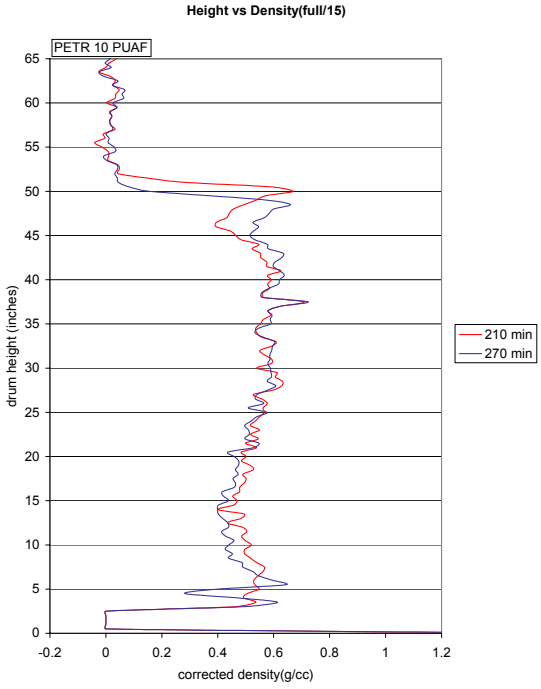

Figure 196 - Gamma densitometer traces for run PETR 10 PUAF before and after steam stripping

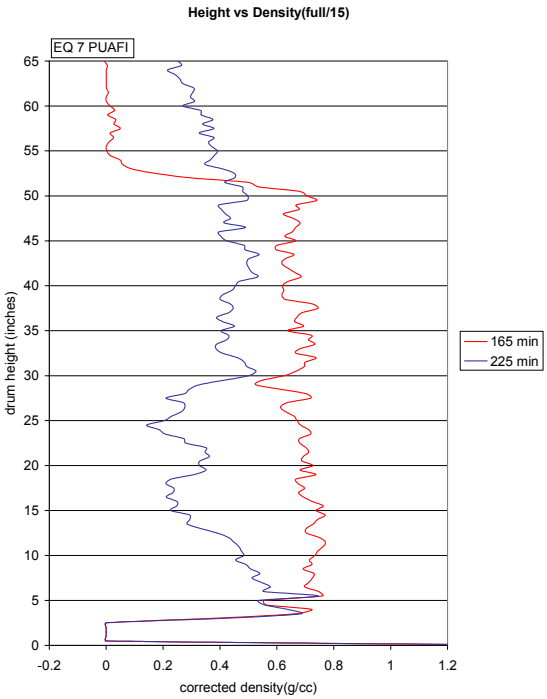

Figure 197 - Gamma densitometer traces for run EQU 7 PUAF before and after steam stripping

4. Conclusions

Preliminary observation suggests that overhead injection of antifoam lowers the overhead temperature. Further observation indicates that lower overhead temperature results in more material being stripped from the drum because of the slower reactions taking place. Feedline injection requires more heat input to the feedline to maintain equivalent fluid temperatures compared to the overhead injection of antifoam. The coking time for a particular run can be affected by the foaming characteristics of that particular resid. If the foam is too high in the drum, it affects the run length as there is a possibility of overhead lines getting clogged with time. Foam, if not controlled within a reasonable amount of time, is hard to control during the rest of the run. During antifoam injection a sudden rise of foam is observed. This property can be attributed to diesel flashing inside the coker drum. It is seen that the runs using higher viscosity 600,000 cSt (0.75/70) antifoam take longer for the foam to re-appear compared to runs using the lower viscosity 100,000 cSt (0.3/70) antifoam. Steam strip plots for Equilon indicate that the reduced run temperature strips the unreacted resid out of the drum. In terms of minimizing the loss of mass in the coker drum during steam strip, it is observed that asphaltic (Equilon) resids operate best at a temperature of 930°F and a pressure of 40 psig whereas paraffinic (Petrobras) resids operated well under all conditions tested. With the addition of recycle to the feed, it is observed that the heat input requirement is higher compared to runs with no recycle.

A rough estimate was made of the cooling of the drum due to injection of the diesel antifoam carrier. Calculations show that most of the temperature drop observed following antifoam addition is probably the result of the hot foam moving to the bottom of the bed, although the initial antifoam addition probably contributes some toward this cooling due to the thermal effect of the diesel carrier addition.

5. Future Work

It has been observed that during runs with continuous injection of antifoam, there is a suppression of foam for a substantial amount of time after an hour into the run. Hence injecting antifoam during this time does not serve the purpose. Thus a revised method will be designed for continuous injection of antifoam. Equilon runs will be carried out at a temperature of 930°F and a pressure of 40 psig to observe the steam strip behavior. Further studies will be conducted on the effect of antifoam on overhead and coil temperatures and the foaming tendencies based on resid characteristics.

Further study will be done on stripping of material from the bed during the steam strip process. An attempt will be made to correlate the amount of material stripped with overhead temperature, feedstock type, antifoam injection, and other pertinent variables.

H. QUENCHING STUDIES

Discussed below are the pilot unit process studies regarding coke cooling and foaming during coking. Coke cooling was analyzed in three different ways: (1) by looking at its temperature profiles, (2) by looking at its cooling rates for the cases when the coke bed is cooled with nitrogen and with the furnace door closed or opened, and when the coke bed is quenched with water, and (3) by observing some general trends from the coke bed cooling rates. The foaming issue was analyzed by looking at the drum temperature profiles during coking and observing differences between profiles with and without foaming taking place. The effect of foaming on the type of coke produced is also addressed. Unless otherwise specified, most of the studies are related to the 6 foot drum.

1. Cooling Temperature Profiles

In this section, cooling of the coke bed was looked into by analyzing the drum temperature profiles after steam stripping was completed to see how different coke beds cooled as a function of thermocouple height in the drum. In general, the coke beds were either cooled using nitrogen or water. For the first case the furnace door was either left closed after the run ended or it was opened after steam stripping ended.

a) *Open Furnace Door*

To see how the coke bed temperature varied at each thermocouple height as a function of time for the case when the furnace door was opened, we plotted CHV 3 PUAF as shown in Figure 198 below.

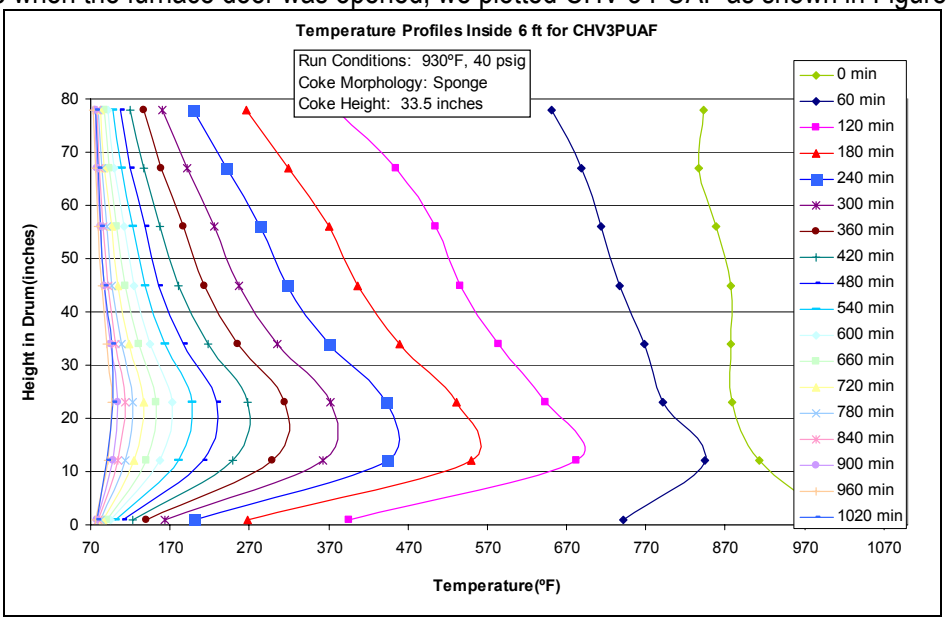

Figure 198 - Cooling Temperature Profiles as a Function of Thermocouple Heights for a Chevron Run Allowed to Cool for 17 Hours

From the figure it can be seen that the temperature profiles of the coke bed decrease unsteadily as cooling time progresses until the temperature profile of the entire drum is almost vertical, that is – the entire

coke bed reaches room temperature. It is seen too, that most of the cooling takes place during the first few hours after the furnace door is opened and after that the cooling is more uniform and steady.

Another observation made from the temperature profiles plotted as a function of thermocouple height is that regardless of the amount of coke produced, the conditions at which the run was operated, and the coke morphology produced, the profiles looked very similar as long as the cooling procedure was the same. To illustrate this, see Figure 199 below which corresponds to a run made in the 3 foot drum.

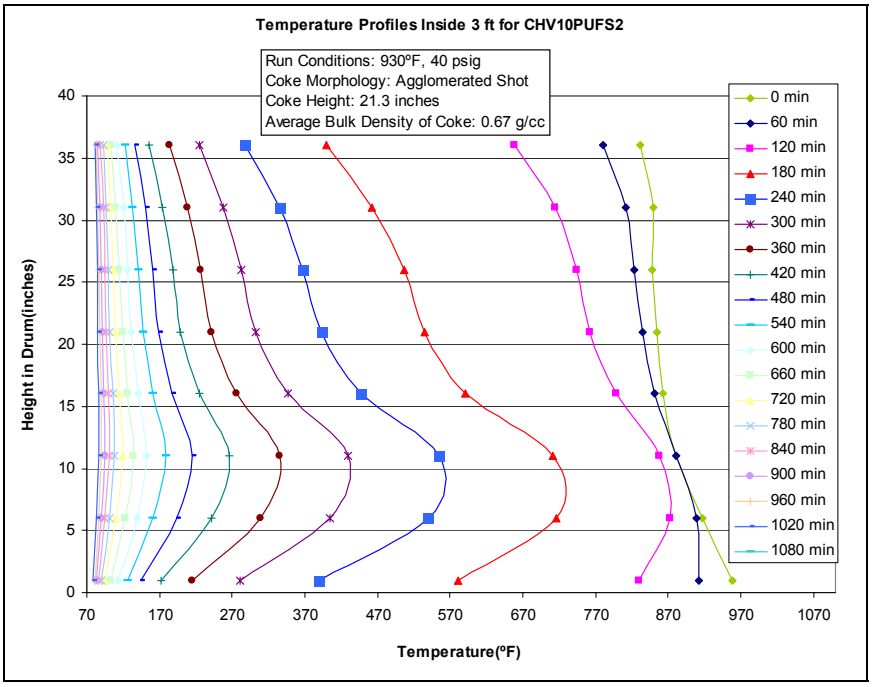

Figure 199 - Cooling Temperature Profiles as a Function of Thermocouple Heights for a Chevron Run Allowed to Cool for 17 Hours

From the figure it is seen that the profiles indicate that the furnace door was opened and that the same pattern of cooling occurs; large temperature drop in the beginning and a more uniform and steady cooling afterwards.

b) *Closed Furnace Door*

In contrast, when the furnace door was left closed after the run ended, as was the case with CIT3 PUAF and a few other runs, the drum temperature profiles decreased more steadily but much slower than when the furnace door was opened after steam stripping for an hour.

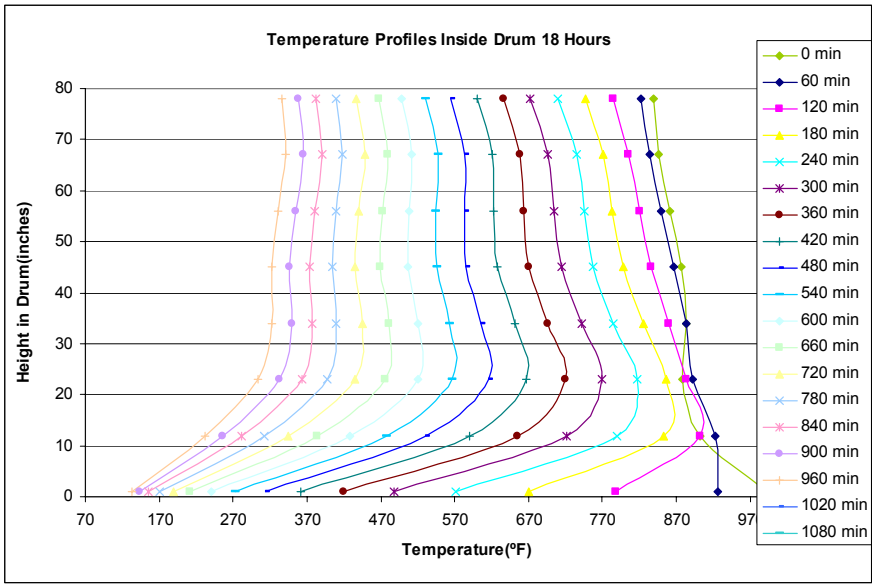

Figure 200 - Cooling Temperature Profiles as a Function of Thermocouple Heights for a Citgo Run Allowed to Cool for 16 Hours

As shown in Figure 200 above, it was observed that from 3:41 pm (the time when steam stripping ended) until 8:00 am next day, the drum cooled only to approximately 170ºF. This shows that there is a significant difference in the cooling profiles when the furnace door is left closed and when the door is opened after the run is over. This is to be expected because when the furnace door is left closed, cooling of the coke bed takes place solely due to the continuous flow of Nitrogen which is only about 0.5 SCFH; on the other hand, when the furnace door is opened a great deal of the cooling takes place due to free convection resulting from the exposure of the drum to air. This issue will be discussed further in a later section.

c) *Water Quenching*

As mentioned earlier, a third procedure used to cool the coke bed was to quench the coke bed with water after one hour of steam stripping. Plotting the cooling temperatures as a function of thermocouple heights in the drum revealed a third type of temperature profiles. As can be seen in Figure 201 below, a run that was quenched with water shows drastic cooling during the entire cooling period especially in the bottom part of the drum.

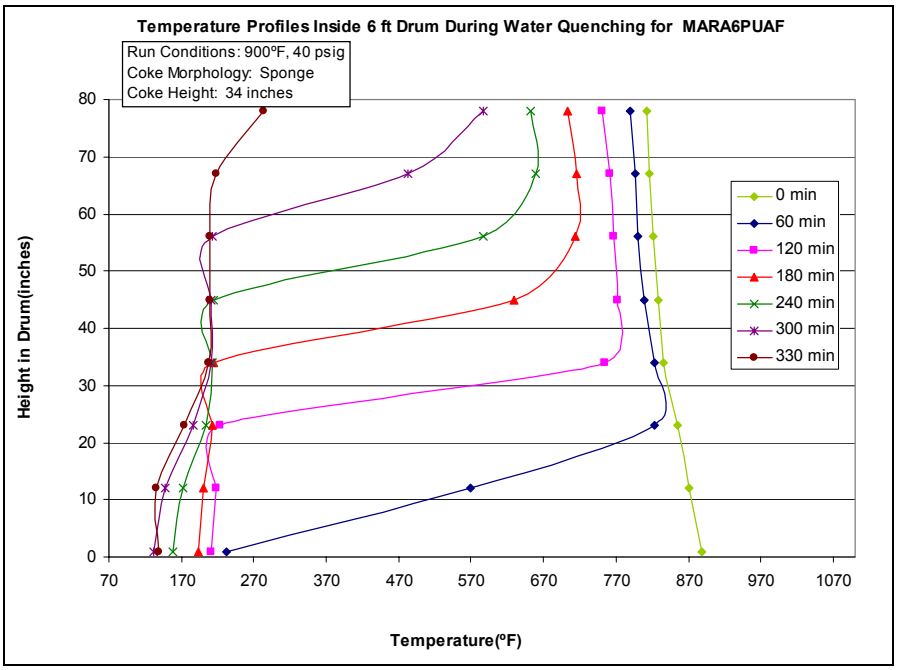

Figure 201 - Cooling Temperature Profiles as a Function of Thermocouple Heights for a Marathon Run Allowed to Cool for 5 Hours

From the discussion above, it was seen that as long as the cooling procedure used between runs was the same the cooling profiles of the coke bed were very similar. However, the rates at which each individual run cooled were different for each run and this is due to the individual properties of the coke produced in a test run, different coke morphologies, and different run conditions. This issue is discussed next.

2. Cooling Rates

The rates at which the coke beds cooled were analyzed and grouped by coke morphology and/or coke density and by run conditions. To analyze the rates at which coke cooled for different runs, the cooling temperature data was plotted as a function of time for zones or sections of the coke bed that had similar morphologies. The runs were grouped by coke morphology/density, run pressure and run temperature, and coke particle size. The focus of the studies was on the open furnace door case and the water quenching case.

a) *Open Furnace Door*

(i) Coke Morphology/Density/Particle Size Effects

A typical plot of cooling rates for a run cooled with the furnace door opened is shown in Figure 202 below. Different resids showed different cooling rates and a few are shown next.

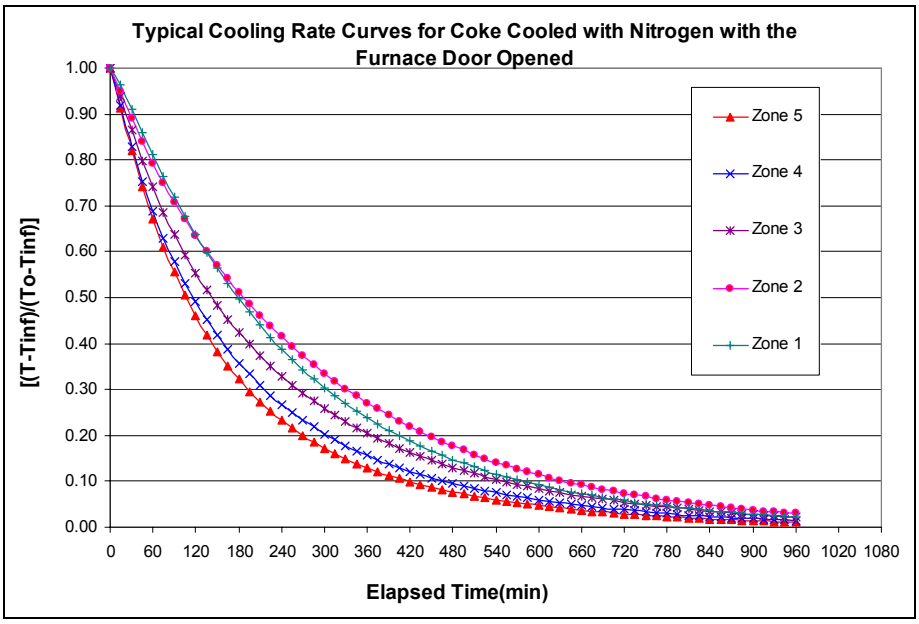

Figure 202 – Typical Cooling Rate Curves of Coke Cooled with Nitrogen and with Furnace Door Opened

To study the effect of coke morphology effects on the cooling rates the following morphologies were used: hard sponge and soft sponge, agglomerated shot, and BB shot surrounded by agglomerated shot. The sizes of the BB shot pellets varied and for one of the resids the effect of particle size was addressed. For the Chevron resid, sponge coke cooled faster than shot coke and, with a few deviations, this observation was repeatedly observed for the other resids as well.

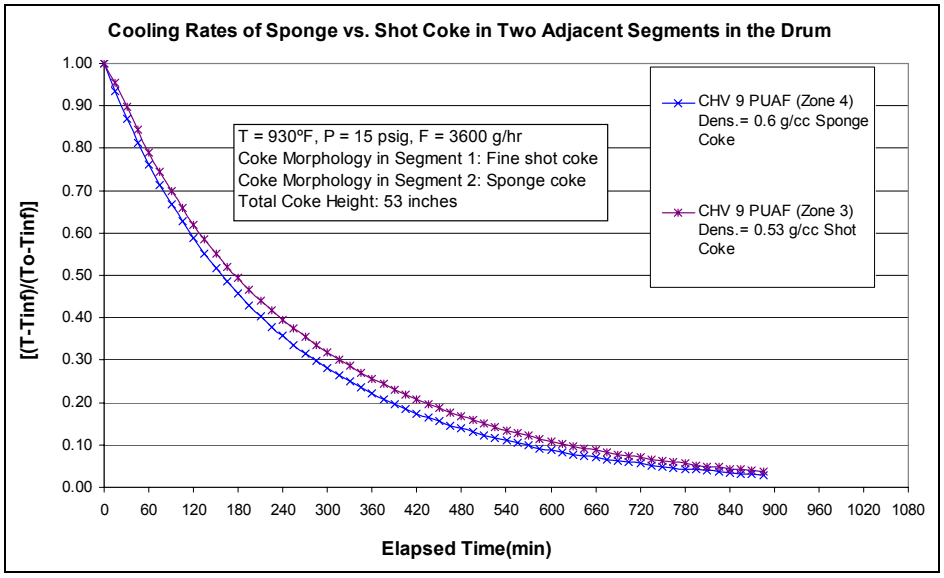

Figure 203 - Effect of Coke Morphology on Cooling Rates for Chevron

This observation was to be expected because as its name itself indicates, sponge coke has a very porous microstructure with walls and pores of various sizes. Shot coke on the other hand, has ribbon-like

anisotropic domains arranged in concentric patterns to form shot-like coke which is much more compact in structure than sponge coke. For that reason, it is expected that the more porous structure will cool faster than the more compact structure, shot coke.

Because coke morphology is closely linked to coke density it was seen that sometimes sponge coke did not cool faster than shot coke as anticipated. An explanation for that behavior is that the denser coke, regardless if it is sponge or coke, will take longer to cool than the less dense coke. This observation is illustrated in Figure 204 below.

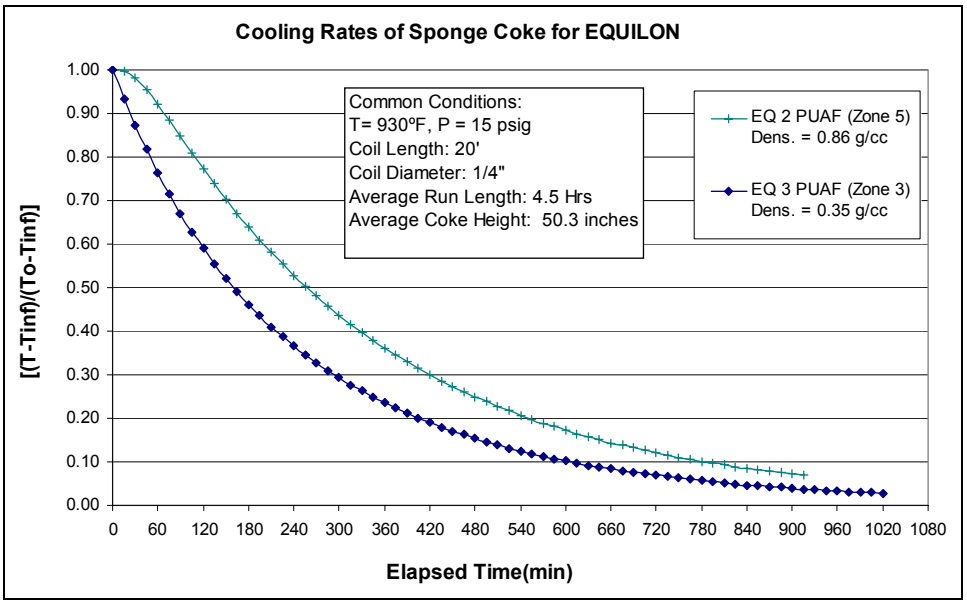

Figure 204 - Effect of Coke Density on Cooling Rates for Equilon

Notice in the figure how the denser sponge coke takes longer to cool compared to the less dense coke of the same morphology.

As mentioned previously, for one of the resids (Equilon), another observation made was that even though the coke morphology produced between two runs was agglomerated shot coke with BB's, the denser coke cooled much faster than the less dense coke. This again is the opposite of what had been seen earlier and therefore another plausible explanation was in line, see Figure 205 below.

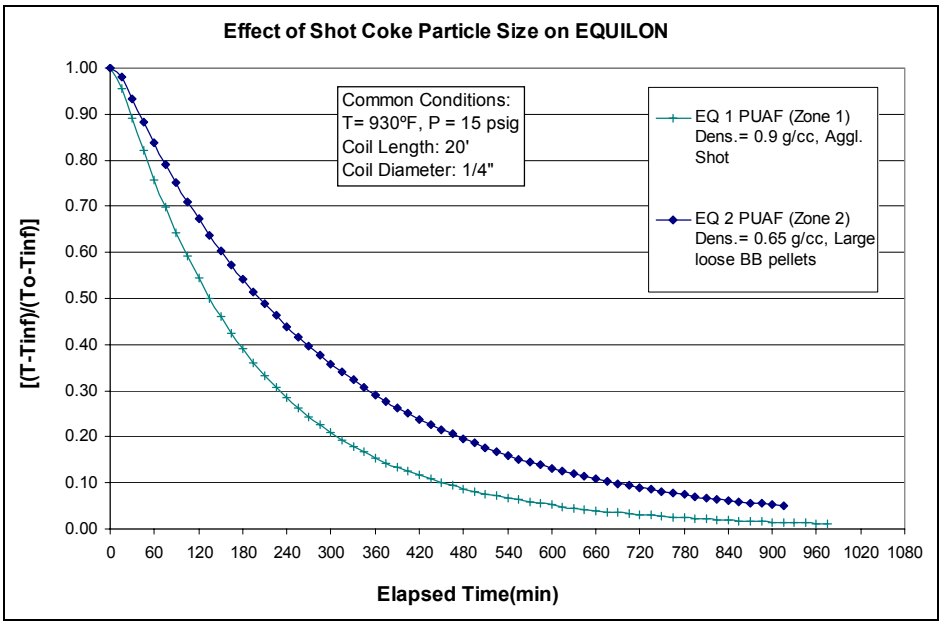

Figure 205 - Effect of Coke Particle Size on Cooling Rates for Equilon

A closer look at the morphologies produced by these runs revealed that even though the morphology was the same for both runs, the sizes of the coke particles were dramatically different. While for one run the shot spheres were very small and clustered, the other run produced large, loose, BB-like shot pellets. The large BB pellets, though with a smaller density, cooled much slower than the agglomerated shot particles of a much denser nature. An explanation for why the large BB pellets cooled much slower than the compact shot particles can be given by taking into account the microstructure of the BB pellets. Figure 206 below shows a microscopic view of one of the pellets. It is speculated that because of the large size of these pellets, the heat inside the pellet is retained longer and it takes longer to cool them.

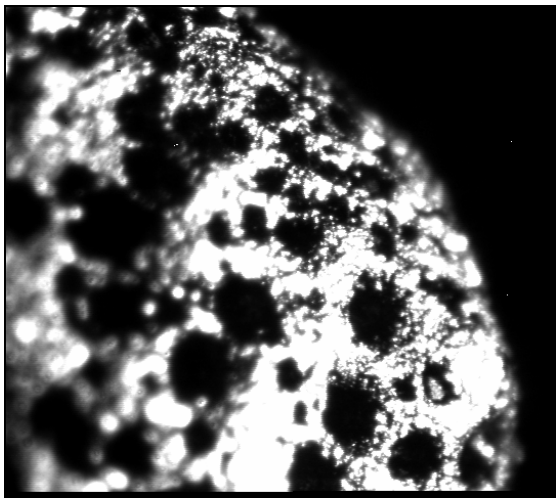

Figure 206 - Photo of a Microscopic View of a Large BB Pellet

From these considerations, it is reasonable to say that when a general trend does not hold for a certain comparison, there may be other variables affecting the way a certain coke morphology with a certain density cools which causes it to deviate from the established trend.

(ii) Pressure Effects

In the studies of the 6 foot drum it was consistently observed that the 15 psig runs made coke morphologies than were less dense the 40 psig runs. Based on that observation and by knowing the densities at each coke zone in the drum, it was possible to conclude that in general the lower pressure runs have higher cooling rates because they produce less dense morphologies. This observation is shown in Figure 207 and Figure 208.

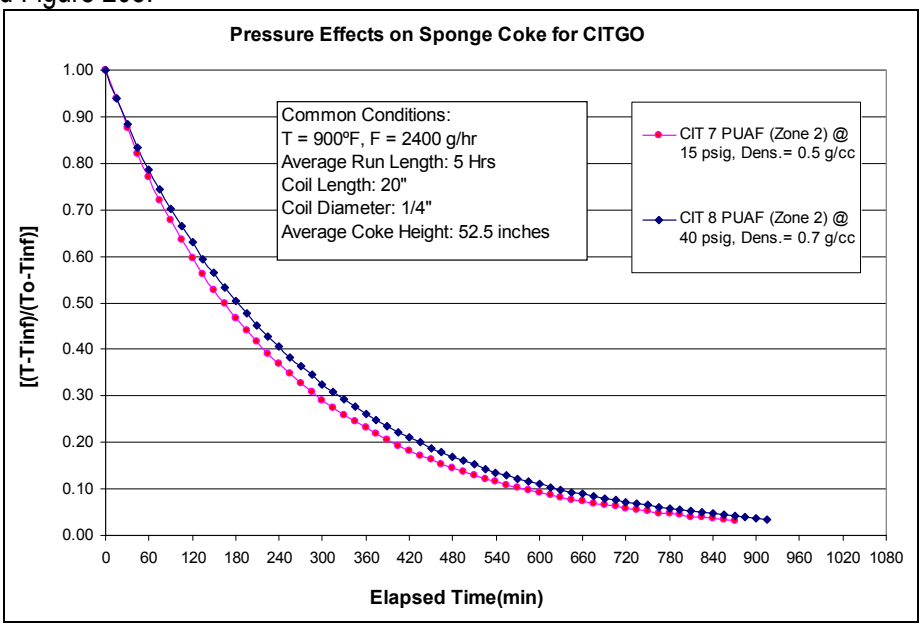

Figure 207 – Effect of Pressure on Cooling Rates of Sponge Coke for Citgo Resid

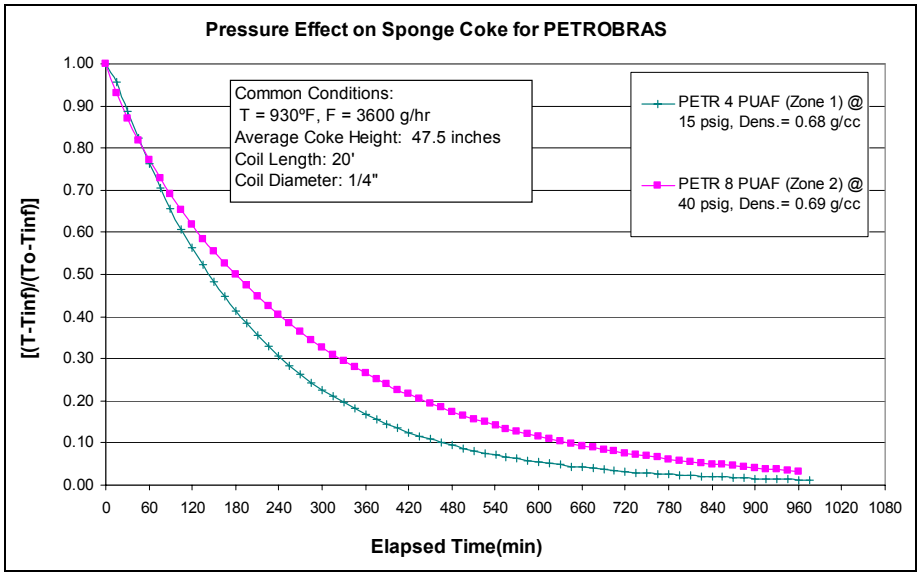

Figure 208 - Effect of Pressure on Cooling Rates of Sponge Coke for Petrobras Resid

In summary, lower pressure runs tended to make lower density coke morphologies compared to the higher densities produced by high pressure runs. Because of this, in general, the lower pressure coke cools faster than the higher pressure coke. Deviation from this trend might be due to the permeability and porosity as well as particle size of the coke morphology involved.

(iii) Temperature Effects

A consideration of the temperature effects on the cooling rates for the different resids available showed that there was no apparent correlation between temperature and the rate at which the coke cooled. Citgo and Equilon did not have any runs available for the temperature studies. Chevron, Marathon, Petrobras and Suncor did have some runs available, but because of the inconsistency of the results it was not possible to draw any conclusions. The difficulty in establishing a general trend for temperature and cooling rates was, once again, a proof that run temperature may not have a direct or indirect effect on coke cooling rates.

(iv) Open Furnace Door After Quenching

In addition to analyzing the cooling rates of coke when it was cooled with nitrogen and with the furnace door opened, and those for when the coke bed was cooled with water, the effect of opening the furnace door, after quenching was over, was also analyzed. It was found that cooling the coke bed with the furnace door opened after the bed had been quenched with water, increased the rate at which that bed cooled compared to cooling the bed with the furnace door opened without quenching it. As the next figure shows, there is a sharp difference between the cooling rates for each situation.

In Figure 209 below, it is seen that cooling the drum with water first, and then turning the oven on for a while, and after that cooling the drum with the door opened, significantly altered the cooling rates of the coke bed. This observation was made upon comparing a run that had been water-cooled first and then heated back up and allowed to cool by free convection, with a run that was simply cooled by free convection. Both runs were initially at a temperature of around 900ºF.

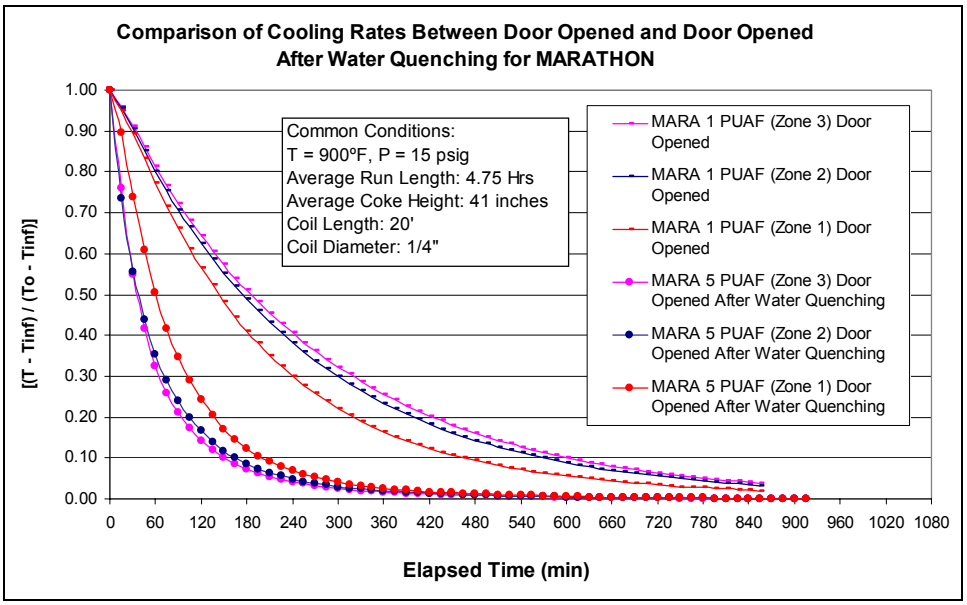

Figure 209 - Comparison of Cooling Rates between a Run with Furnace Door Opened After Steam Stripping and a Run with Furnace Door Opened After Water Quenching

The behavior of the cooling rates between these two cases can be explained by surmising that during water quenching, which is done at very high rates, the structure of the coke bed is substantially altered. If this is the case, the coke mass may have more flow channels and less molten material which would allow the coke bed to cool much faster than a coke bed that has not been water quenched at all. Also, it is possible that more volatiles are stripped out and that the drum contents are not uniformly heated. A confirmation that this might be the case was seen when analyzing an issue with steam stripping for a few runs. This issue will be addressed in a later section.

3. Cooling Trends

From what was discussed the trends observed during cooling were:

- Sponge coke cools faster than shot coke. Any deviation from this trend might be related to the density of the individual coke morphology.
- High density coke cools slower than low density coke regardless of the coke morphology. Deviations from this trend could be linked to particle size, and coke properties.
- Lower-pressure runs tend to produce lower density coke which in turn cools faster than the higher density coke produced by the higher-pressure runs.
- No apparent trend between coke cooling rates and run temperature appears to exist.

4. Overhead vs. Bottom Drum Quench

The water quenching procedure was added recently in the project and only a few runs operated in the pilot unit were quenched with water. As the procedure is improved, more runs are now being quenched and in different ways. At this point, nine runs were quenched with water. All the runs produced sponge coke, except for the Chevron run, and were operated under different conditions. The water injection rates

and volumes were also different for each run. For the majority of the quenched runs the water was injected at the bottom of the drum – that is, the water was injected at the feed line. In order to see how different the cooling rates would be if water were injected at a different point, water was injected overhead for two of the nine runs. Looking at each individual run showed that during water cooling the cooling rates behave completely different from those discussed in the previous subsections.

For the cases when the water was injected from the bottom of the drum, the temperature of the bottom thermocouple decreases drastically upon contact with the water. This thermocouple is located at the thick metal piece of the drum and thus the rapid cooling is explained. When water quenching starts, the coke mass is extremely hot and once water comes in contact with it steam is formed and it causes the temperature of the coke located just above to increase slightly before it starts to drop slowly but steadily. Now, considering zone by zone, above the bottom thermocouple, it is observed from the plots that the water first percolates through the channels and pores of the coke in one zone until it fills the entire coke mass; by that time the large drop in temperature is seen. After this large drop in temperature, very little cooling takes place. While water is cooling that zone, since it comes into contact with a very hot coke mass it vaporizes and the vapor rises to the next zone. The vapor initiates the cooling process of the new zone and when water reaches that zone and fills its channels and pores, the temperature again drops abruptly. This phenomenon repeats itself during the time water is being injected until the coke bed is filled with water and cold enough that no more steam forms.

On the other hand, when water is injected overhead, cooling of the coke bed is very unsteady. It was seen that despite using a very large quantity of water and injecting it at very high flow rates, the cooling is not significant and it takes a much longer time to quench. By comparing both plots, there seems to be an optimum water flow rate above which much of cooling is not accomplished. It appears that beyond that optimum flow rate more steam is produced instead and very little cooling takes place. From these observations, it is evident that injecting the quench water from the bottom of the drum is much more effective and time saving in achieving cooling of the coke bed than injecting the water overhead. However, analysis of water samples to find metal traces in the water may show advantages or disadvantages of both types of injection. If the longer procedure (overhead injection) contains fewer metals it might be more feasible to use it than the shorter procedure (bottom injection) because of less environmental constraints. In other words, there may exist an economic versus environmental issue and it must be addressed and taken into consideration when choosing the best procedure to use.

5. Conclusions

From the cooling studies it was observed that different coke morphologies have different cooling rates. Sponge coke seems to cool faster than shot coke. The density of the coke affects the way it cools; denser coke in general cools slower than a less dense coke morphology. Particle size and structure also have an effect on cooling rates. Large, loose BB shot coke pellets seem to take longer to cool than smaller, more clustered particles. Run pressure also seemed to have an effect on the way the produced coke bed cooled. The lower pressure runs in general produced less dense coke morphologies, which in turn cooled faster than the denser morphologies produced by the higher-pressure runs.

Cooling temperature profiles of coke reveal the cooling procedure used. Cooling the coke bed with nitrogen and with the furnace door opened is more effective than cooling it with the door shut. When cooling the coke bed with the furnace door opened a large temperature drop takes place in the first few hours and then the drop is more uniform and less dramatic until the bed is at approximately room temperature. When cooling the coke bed with the furnace door shut the cooling is very uniform and the coke bed is only at approximately at 170ºF after about 18 hours of cooling. For most of the runs the cooling profiles look similar as long as the coke bed is cooled by the same cooling procedure. The cooling rates however, are different for each run.

Water quenching seems to be the most effective way to cool the coke bed at a relatively short period of time. Several factors such as water injection rate, injection time, total amount of water injected and injection point have an effect on the way a certain coke bed cools. Injecting the water from the bottom of the drum is more effective than injecting it overhead.

6. Future Work

Pilot unit runs will continue to be quenched as part of the experimental program, mostly by bottom quenching, and these runs will be used to further validate the quenching model.

I. QUENCHING MODELS (OVERHEAD & FEEDLINE)

1. Convective Cooling Modeling

a) Lumped-Heat-Capacity Model

As already discussed, in the initial stages of the project drum cooling was achieved by flowing nitrogen through the coke bed and letting the drum cool enclosed in the ceramic material or by exposing it to free convection. In order to see how predictable the cooling rates were as a function of time, two models were developed. One model was based on a lumped-heat-capacity method in which the coke bed was assumed to be a lumped mass at a "uniform" initial temperature. Calculation of the Biot number, *Bi*, yielded 0.15 which is within the acceptable limits for the method to be applicable – that is Bi < 0.1. The lumped-heat-capacity approach involved assuming that the temperature of the coke was only a function of time, thus lacking spatial resolution. This approach simplified the energy balance in the spatial and time domain to an energy balance in the time domain only. Using this simplified analysis the convective heat flux Q, from the coke drum to the environment equals the rate of change of internal energy of the coke – that is

$$h_{air} A_{surface} \left(T_{\infty} - T\right) = m_{coke} C_P \frac{dT}{dt} \cong m_{coke} C_P \frac{\Delta T}{\Delta t} \qquad \textbf{(1)}$$

The following assumptions were made: (1) the wall surface temperature is the same as that of the coke bed (2) a given thermocouple reading represents the temperature of the zone it is located in, (3) the surface temperature of the drum is constant, (4) the drum wall thickness is negligible, and (5) the external heat transfer coefficient, h_{air} and T_{∞} do not change with time.

Once the assumptions were made and the needed data were gathered, the predicted temperatures were calculated using the following equation:

$$T^{t+\Delta t} = T^{t} + \frac{h_{air} A_{surface} \left(T_{\infty} - T^{t}\right)}{m_{coke} C_{Pcoke}} \Delta t \qquad \textbf{(2)}$$

The heat capacities estimated for the coke were around 0.5 Btu/ºF-hr for sponge coke and 0.6 Btu/ºF-hr for shot coke. Such values were in agreement with a few literature values of approximately 0.45 Btu/hr-ºF. Plotting the predicted temperatures against the measured or real values showed that the method was indeed satisfactory in roughly predicting how a certain coke morphology would cool as a function of time; see Figure 210 below for illustration.

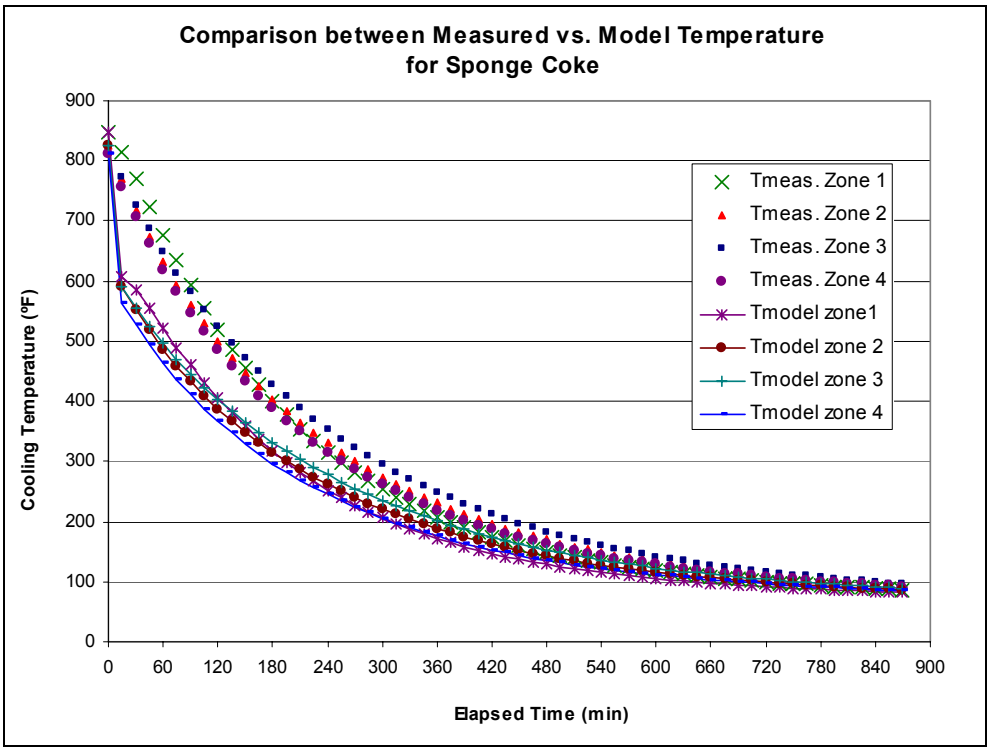

Figure 210 - Comparison between Measured and Predicted Temperature by Using the Lumped-Heat-Capacity Model (MARA 7 PUAF – Sponge Coke)

b) Cooling Rate Correlations

A second way of modeling the cooling rates for the case when the coke bed was cooled with nitrogen and with the furnace door opened was to average the cooling rates of different runs that were operated under very similar conditions and that produced similar coke morphologies and then use a curve fit to model the experimental data. Using this procedure it was found that an exponential curve fit predicts the cooling of the coke bed well. The equations found for sponge and shot coke morphologies are given in the Table 69 below.

Table 69 - 6 foot Drum Cooling Rate Correlations - Temperature

Sponge Coke (Furnace Door Opened) = $T_\infty + (T_{0average} - T_\infty)*Exp(-0.0039*t)$

Shot Coke (Furnace Door Opened) = $T_\infty + (T_{0average} - T_\infty)*Exp(-0.0036*t)$

where: $T_{0average} = \frac{\sum_{i=1}^{n} T_{0i}}{n}$ with i = 1, ….., n thermocouples inside the coke bed and

T_{0i} = temperature reading from thermocouple i at t = 0 min

T_∞ = room temperature

For both morphologies the exponential fit seemed to give a fair representation of the temperature of the coke at a specified cooling time. The next two plots show how well the exponential curve fitted the data.

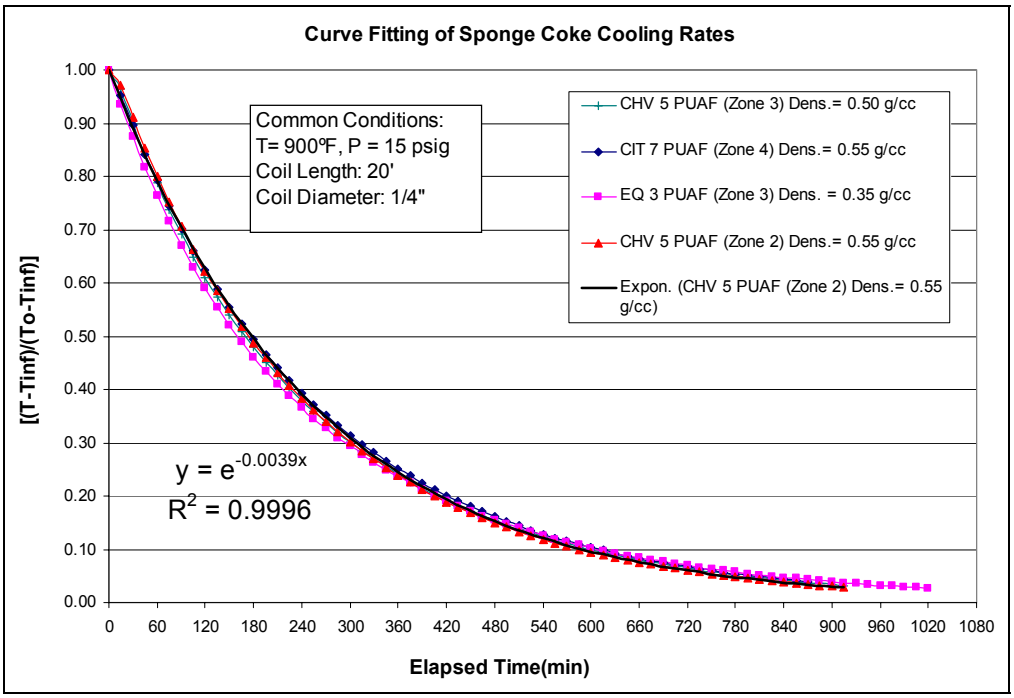

Figure 211 - Individual Resid Cooling Rate Correlation for Sponge Coke

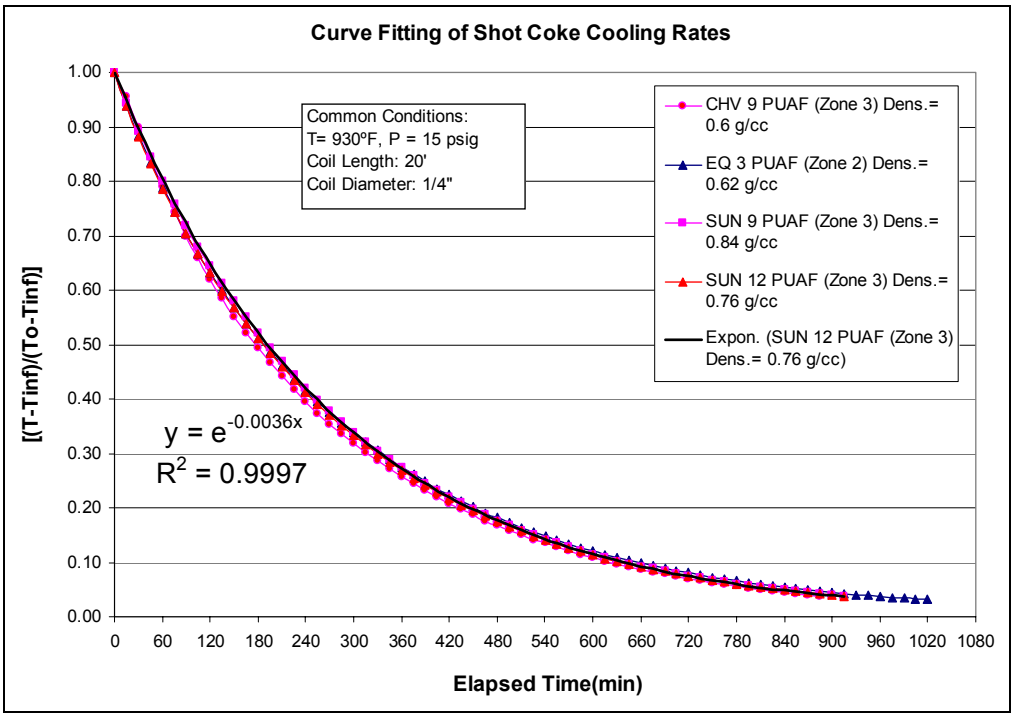

Figure 212 - Individual Resid Cooling Rate Correlation for Shot Coke

2. Quench Model

An attempt to correlate the cooling rates of coke, cooled with water, to time of water injection was also made. For this analysis four runs were available; one Chevron run, two Marathon runs, and one Petrobras run. The two Marathon runs produced sponge coke and were operated at 900ºF and 15 psig or 40 psig, respectively. One run produced a fairly uniform-density sponge coke whereas the other run produced sponge coke that varied substantially in density from bottom to top of the drum. The water injection rates and volumes were also different for each run. The Chevron run was operated at 930ºF and 40 psig and produced shot coke that was very uniform in density. Looking at each individual run showed that during water cooling the cooling rates behave completely different from the ones already discussed.

This data showed that when water is injected in the bottom of the drum the temperature of the bottom thermocouple decreases drastically upon contact with the water. This thermocouple is located at the thick metal piece of the drum and thus the rapid cooling is explained. When water quenching starts, the coke mass is extremely hot and once water comes in contact with it steam is formed and it causes the temperature of the coke located just above to increase slightly before it starts to drop slowly but steadily.

Considering zone by zone, it was observed that the water first percolates through the channels and pores of the coke in one zone until it fills the entire coke mass; by that time the large drop in temperature is seen; after that very little cooling takes place. While water is cooling that zone, since it comes into contact with a very hot coke mass it vaporizes and the vapor rises to the next zone. The vapor initiates the cooling process of the new zone and when water reaches that zone and fills its channels and pores, the temperature again drops abruptly. This phenomenon repeats itself during the time water is being injected until the coke bed is water filled and cold enough that no more steam forms.

For the modeling of these cooling rates an attempt was made to predict how coke cooled as a function of injection time. The model involved dividing the coke bed into one-inch differential elements of coke and performing energy balances on each segment for different possibilities of liquid water or steam entering or leaving the differential element of the coke bed. Since experimental temperature data was only available at some heights in the coke bed, it was necessary to use a fifth order polynomial to predict the temperature at every inch of coke at time = zero for every run that was quenched with water.

The energy balance done on each differential element includes a heat conduction term, a term accounting for the vaporization of water, a term for the heat transfer from water to coke, as well as a term for the time change in energy of the coke. The scope of the model was to duplicate the measured temperatures by using literature values of heat capacity and thermal conductivity of the coke and then to adjust the heat transfer coefficient and coke porosity to best fit the given data.

The energy balance on the coke takes the following form:

$$\rho C_{p,c} \frac{\partial T_c}{\partial t} = (ha_i)(T_w - T_c) + k \frac{\partial^2 T_c}{\partial x^2}$$

where T_c is the coke temperature, T_w is the temperature of the water or steam, k is the thermal conductivity of the coke, h is the convective heat transfer coefficient, a_i is the interfacial area per unit volume of the coke bed, ρ is the coke density, and $C_{p,c}$ is the heat capacity of the coke. The energy balance on the water is

$$-\frac{1}{A}\frac{\partial\left(\dot{m}_w \hat{H}_w\right)}{\partial x} - (ha_i)(T_w - T_c) = \rho_w C_p \frac{\partial T_w}{\partial t}$$

where $\dot{m}_w$ is the mass flow rate of water, $\hat{H}_w$ is the heat capacity of the water or steam per unit mass, and A is the cross-sectional area of the coke bed. These coupled equations were solved in an Excel

spreadsheet, with the additional assumptions that: (1) the coke and water are in thermal equilibrium when liquid water is present (since the heat transfer coefficient is much larger for liquid water than for steam); (2) the accumulation term for the steam is negligible (the water accumulation is non-zero only if $T = \underline{T_{sat}}$); and (3) the porosity, heat capacity and thermal conductivity of coke are uniform throughout the coke bed.

After setting up a routine that calculated the temperatures for each differential element for every one fifth of a minute of water injection, a plot showing the comparison between the model and the measured values was made.

The model developed worked very well in predicting the temperatures as a function of injection time for each zone. Some differences were obviously found as a theoretical model was being used to duplicate measured values. These differences are more than likely a result of assuming the same porosity, same heat capacity, and same thermal conductivity throughout the coke bed in the calculations. To get a more accurate fit to the data, it may be necessary to use different values for these parameters at different coke locations, as the coke bed is not uniform.

Although the coke bed is usually quenched from the bottom in refinery operations, quenching is occasionally done from overhead as an emergency backup, when the bottom inlet becomes plugged. For such cases, it is important to know from a safety standpoint how quickly the bed will cool. Therefore, a model for overhead quenching is of practical importance.

Work is now underway to modify the existing bottom quench model to satisfactorily describe overhead quenching. Overhead quenching is by its nature much more difficult to model than bottom quenching, because the water introduced does not initially flow through the bed, but will penetrate downward some distance into the bed before vaporizing and reversing direction to exit in the overhead line as steam. The key to successfully modeling this situation will be determining a heat transfer coefficient that will predict the rate of vaporization of the water and the rate of cooling of the coke in the top section of the bed.

3. Conclusions

A lumped heat capacity model was developed for the cooling of the coke drum by free convection to the surrounding air with the furnace door open. The heat capacities estimated for the coke were around 0.5 Btu/ºF-hr for sponge coke and 0.6 Btu/ºF-hr for shot coke. These values are in agreement with a few literature values of approximately 0.45 Btu/hr-ºF. Plotting the predicted temperatures against the measured or real values showed that the method was satisfactory in roughly predicting how a certain coke morphology would cool as a function of time.

Convective cooling rates were also correlated by averaging the cooling rates of different runs that were operated under very similar conditions and that produced similar coke morphologies and then using a curve fit to model the experimental data. Using this procedure it was found that an exponential curve fit predicts the cooling of the coke bed well.

A quench model was developed to predict temperature profiles when the coke bed is cooled by flowing water from the bottom. The model divides the coke bed into one-inch segments of coke and performs energy balances over the coke and steam or water on each segment. The model uses literature values of heat capacity and thermal conductivity of the coke and adjusts the heat transfer coefficient and coke porosity to best fit the given data. The model works very well in predicting the temperatures as a function of injection time for each zone. Some slight differences between the model and experimental data are probably due to assuming the same coke properties (porosity, heat capacity, and thermal conductivity) throughout the coke bed.

4. Future work

The current working model for bottom quenching will be modified to predict overhead quenching. Key modifications will include an accounting of bed penetration, estimation of heat transfer coefficient, and flow reversal. A few more overhead quenching runs will be made to allow testing of the overhead quench model once its development is complete. The results will be distributed as a topical report.

7. Technology Transfer / Administrative Issues

A. REPORTS

B. COMMITTEE AND COMMITTEE MEETINGS

At the first Advisory Board Meeting three committees were formed and the committee members elected a Chair. For the continuation JIP, discussions will be held at the Advisory Board Meeting regarding election of new chairs or reappointment of the old chairs as well as members of the committees. An updated chart, including only current members that attend the meetings, is shown in Table 70. In addition to the committee chair, a TU representative is on each committee. The first committee deals with the coker facilities and its operation, the second deals with process dynamics and modeling, while the third deals with technology transfer and commercialization issues. Please contact Mrs. Dorinda Alexander at The University of Tulsa if your company wishes to add other members to the committees.

Two committee meetings were held; one at the October 2002 Advisory Board Meeting and one at the May 2003 ABM. The minutes from theses meeting are provided in Appendix B. Several meetings were also held with Baker Petrolite to discuss the foaming tests.

Table 70 - Committee Organization

	Coker Facility & Operation	Process Dynamics & Modeling	Technology Transfer & Commercialization
Industry Chair	Chris Paul GLC	Shri Goyal Shell	James Blevins ChevronTexaco
TU Representative	Michael Volk	Keith Wisecarver	Michael Volk
DOE Representative		Betty Felber	Betty Felber
Members	Robert Bell ChevronTexaco	Marcos Sugaya Petrobras	Michael Zetlmeisl Baker Petrolite
	Leo Brown Exxon Mobil	Richard Lee KBC Advanced Tech	Richard Lee KBC Advanced Tech
	Paul Ellis PetroCarbon	Fred Hill Marathon-Ashland	Michael McGrath Foster Wheeler
	Chris Eppig ExxonMobil	Joseph Stark Baker Petrolite	Shri Goyal Shell
	Larry Kremer Baker Petrolite	Mike McGrath Foster Wheeler	
	Mitch Moloney ExxonMobil		
	Michael Zetlmeisl Baker Petrolite		

C. WEB SITE

The address for the Delayed Coking Web Site is http://www.tudcp.utulsa.edu. The web site has become a useful tool to welcome visitors and tell them about the JIP. It is segmented such that visitors can gain general information while the "Members Only" site contains confidential information generated in the JIP. There is a reading room, applications, a tour of the facility, a place to meet the personnel, JIP news, experimental data from the three cokers, models and correlations, and a discussion board.

During the year, significant postings and updates were made to the entire web site. The delayed coking website was redesigned, following consultation with users of the site to make it even easier for our members to locate resources and download data. A new "deliverables" area was created to allow simpler access to research information and to provide and easier way of location run data. Several improvements were made after receiving user feedback.

D. FUTURE MEETINGS

A tentative date for the tenth Advisory Board meeting is Wednesday and Thursday, May 19th-20th, 2004. The meeting will be held at the University of Tulsa in ACAC. The meeting on the 19th will begin at 1 pm and adjourn at 5 p.m. A social is planned that evening in the Presidents Lounge from 5 to 9 p.m. The meeting on the 20th will begin at 8 a.m. and adjourn at 2:30 p.m.

E. BUDGET/CASH FLOW ANALYSIS

A combined budget and cash flow analysis for a three and one third-year period beginning June 1, 2002 and ending September 30, 2005 is given in Table 71. Included are the actual income and expenses for the period beginning June 1, 2002 and ending September 30, 2002 and a forecast for October 2002 through September 2005.

Table 71 -Three Year Cash Flow Analysis

	Pre-Award June02-Sep. 02 Actual	FY 2003 Oct. 02-Sep. 03 Actual/Budget	FY 2004 Oct. 03-Sep. 04 Budget	FY 2005 Oct. 04-Sep. 05 Budget	Total
Income					
Industry	$375,914	$500,313	$385,346	$90,490	$1,352,063
DOE	$0	$340,000	$340,000	$340,000	$1,020,000
TU	$0	$42,756	$19,096	$9,996	$71,848
Total Income	**$375,914**	**$883,069**	**$744,442**	**$440,486**	**$2,443,911**
Expenses					
Salary, IDC, Fringe	$98,387	$585,711	$539,638	$501,090	$1,724,826
Supplies	$17,766	$73,423	$70,000	$70,000	$231,189
Equipment	$0	$6,575	$5,000	$5,000	$16,575
ABM Meetings	$1,396	$2,197	$7,130	$9,299	$20,022
Travel	$483	$5,664	$11,500	$12,000	$29,647
Consulting	$0	$1,340	$0	$0	$1,340
Analytical	$12,470	$64,428	$98,000	$87,500	$262,398
Outside Services	$5,944	$9,963	$0	$0	$15,907
Contingency	$0	$3,000	$10,000	$10,000	$23,000
Tuition	$11,450	$72,212	$21,616	$9,996	$115,274
Total Expenses	**$147,897**	**$824,512**	**$762,884**	**$704,885**	**$2,440,178**
Cash Flow	**$228,017**	**$58,557**	**($18,442)**	**($264,399)**	**$3,733**
Cumulative Cash Flow	**$228,017**	**$286,574**	**$268,132**	**$3,733**	

Even though two Phase 1 members were lost, income and expenditures have not been changed nor have the deliverables been altered. The lost membership fees are being offset by utilizing industry supported students.

1. Minutes from May 2003 ABM Meeting

a) *Facilities Committee Meeting Minutes*

FUNDAMENTALS OF DELAYED COKING – COKER FACILITY AND OPERATION COMMITTEE MEETING MINUTES

DATE: May 22, 2003

LOCATION: Gallery Room, University of Tulsa

MEMBERS IN ATTENDANCE WERE: Chris Paul (GLC), Mike Siskin (ExxonMobil), Chris Eppig (ExxonMobil), Leo Brown (ExxonMobil) Larry Kramer (Baker-Petrolite), Mike Zetimeisl (Baker-Petrolite), Tom Falkler (Baker-Petrolite), Jim Blevins (ChevronTexaco), Robert Bell (ChevronTexaco), Betty Felber (DOE-NPTO), Marco Robles (TU), Joshua Hogue (TU), Gene Derby (TU), Manuel Barrett (TU), and Mike Volk (TU)

Minutes from Coker Facility and Operation Committee

Fifteen people were in attendance. The topics discussed during the meeting focused on foaming studies, quench studies, morphology studies, micro reactor studies and reporting of results. The items discussed for each study are provided below

FOAMING STUDIES

1. A recommendation was made to use a 1" drum for the superficial velocity studies. However, it was shown at the last meeting that this size drum would fill too quickly and could not be used.
2. It was recommended that the advantages of using a 600,000 cSt antifoam be demonstrated on several resids, one that made sponge, one that made shot and one that makes a mix by comparing the total amount of silica used.
3. Try a non-silica based antifoam.
4. For antifoam usage, present the data as grams of antifoam / gram of feed.
5. Try a gas-oil as a carrier.
6. Adjust the gamma densitometer such that it only scans over the foaming area to try and capture how quickly foam collapses.
7. Ranking Pilot Coker Feeds According to Overall Coking Tendency and
   Correlation to Feed Characteristics: It would be useful to have some sort of correlation between feed characteristics and overall foaming tendency in a coke drum. For instance, people have hypothesized for years that feeds with higher levels of naphthenic acids will foam more severely. Ranking foaming tendency from the data already generated by the JIP might be possible using one or more of the following objective indicators. The methods that we can think of include the following:

5. Total amount of defoamer used.
6. Total number of defoamer injections during a run, i.e. injection frequency
7. Speed of foam reappearance after defoamer injection (sort of a corollary of 2)
8. Time to formation of first foam front

Hopefully, more than one of these criteria will give the same rankings, which will build some confidence in the objective ranking. We can also use the subjective judgment of those who ran the tests, or at least see if the subjective judgment generally agrees with the objective criteria. Comparisons can be made only across runs using similar defoamer injection methods.

As was mentioned at the meeting on May 22, it is the naphthenate form of the naphthenic acid that is expected to aggravate foaming. Since that is the case, in addition to correlating the foaming tendency with acid number, we might want to determine naphthenate content by FTIR. We can do those determinations at Baker Petrolite.

Asphaltene content is another feed parameter likely to correlate to foam stability.

8. Have another ICP analysis done on tap water.
9. Refine/strengthen procedure used for classifying foaming

QUENCHING STUDIES

1. Look at the mass of coke per run
2. Drain the quench water from the bottom of the drum at the end of the quench. Analyze the quench water for sodium, calcium and chlorides.
3. Make duplicate runs and quench one at 40 psig and the other at 10 psig.

MORPHOLOGY STUDIES

1. Take plugs from the coke and measure permeability and porosity. CT scans should also be made.
2. Develop terminology to consistently classify the coke; such as types, crush properties, etc.
3. Once the coke is catalogued and some material is saved, the rest can be discarded.

MICRO REACTOR STUDIES

1. Conduct a few studies at 950 ^{O}F. Do not conduct an exhaustive study.

REPORTING

1. Caveat the conclusions where appropriate; such as “based on limited data”.
2. Add feed properties table to the report.

b) *Modeling Meeting Minutes*

FUNDAMENTALS OF DELAYED COKING – PROCESS DYNAMICS AND MODELING COMMITTEE MEETING MINUTES

DATE: May 22, 2003

LOCATION: Chouteau Room, University of Tulsa

MEMBERS IN ATTENDANCE WERE: Betty Felber (DOE-NPTO), Mike McGrath (Foster Wheeler), Geof Stevens (Suncor), Shrik Goyal (Shell), Zola Afonso (TU), Srikanth Yalamanchili (TU), Pradipta Chattopadhyay (TU), Ashok Pushpalayari (TU), Hamad Al-Merri (TU), and Keith Wisecarver (TU)

MINUTES FROM PROCESS DYNAMICS AND MODELING COMMITTEE

Ten people were in attendance. The topics discussed during the meeting included yield and quality correlations and the kinetic model. The details of these discussions are provided below.

YIELD CORRELATIONS

1. A comparison of yields should be made between the 6 ft. drum and the 3 ft. drum. It is possible that the higher flow rates used in the 6 ft runs may result in less gas phase cracking.
2. It may be beneficial to correlate yields with the liquid layer temperature.
3. There may be a run time effect on product yields. Perhaps the stirred-batch reactor data can be used to correct for unsteady state conditions in the first hour of the pilot unit runs.
4. The possible effect of foaming on product yields should be examined.
5. An attempt should be made to correlate delta yields with changes in operating conditions (e.g., a 5 degree increase in temperature increases liquid yields by *x* percent). These types of correlations may be more useful in industry.

QUALITY CORRELATIONS

4. VCM of coke should be correlated with operating conditions and feedstock properties.
5. Coke morphology needs to be quantified better – perhaps by visually matching with well-defined coke samples.
6. Sulfur partitioning should be studied in more detail.
7. Liquid properties to correlate include liquid subproduct yields (gasoline, diesel, and gas oil), sulfur content and API gravity of liquid subproducts, PIONA results from gasoline, aromatics and nitrogen content of diesel, and N, V, Ni, and Fe contents of gas oil.
8. Gas properties to correlate include H2S, H2, and C1 thru C4 content as well as NH3 content of decant water.

KINETIC MODEL

2. Hamad's approach looks sound. However, the model needs to account for condensation reactions as well as cracking reactions.
3. We should eventually look at tying the empirical models and correlations to the kinetic model.